JACOBS
UNIVERSITY

Analyte-Responsive Macrocyclic Host-Fluorophore Systems For Monitoring Biological Processes

by

Garima Ghale

A Thesis submitted in partial fulfillment
of the requirements for the degree of

Doctor of Philosophy
in Chemistry

Thesis Committee

Prof. Dr. Werner M. Nau (Chair)
Jacobs University Bremen

Prof. Dr. Mathias Winterhalter
Jacobs University Bremen

Dr. Andreas Hennig
BAM Federal Institute for
Materials Research and Testing

Date of Defense: 19th May 2014

School of Engineering and Science

Statutory Declaration

I, **GARIMA GHALE**, hereby declare that I have written this PhD thesis independently, unless where clearly stated otherwise. I have used only the sources, the data and the support that I have clearly mentioned. This PhD thesis has not been submitted for conferral of degree elsewhere.

Bremen, June 1, 2014

Signature _____

To my beloved Mom and Dad (Da)

"I shall be telling this with a sigh
Somewhere ages and ages hence:
Two roads diverged in a wood, and I -
I took the one less traveled by
And that has made all the difference."

Robert Lee Frost, *The road less travelled*

Table of Contents

Abstract

This thesis describes the application of systems composed of a fluorophore and macrocyclic host as a sensitive and versatile analytical method to study biological processes, in particular, transport through the lipid-bilayer biomembrane and reactions catalyzed by proteases.

While it is acknowledged that only small and hydrophobic molecules can pass through the bilayer directly and while the importance of channel proteins for selective uptake is well recognized, methods to directly and sensitively monitor these membrane transport processes remain in high demand.

In the first part of the thesis, I introduce an *in vitro* fluorescence-based biomembrane assay—the *supramolecular tandem membrane assay*—based on host–guest, macrocycle–fluorophore reporter pairs encapsulated inside liposomes. Three features make this novel method unique. First, the tandem membrane assay allows label-free continuous monitoring of translocation through the lipid bilayer or through channel-proteins, which was previously not possible. Second, the assay is economic and versatile, i.e., applicable to both, diffusion through the membrane and translocation through channel proteins of different classes of translocating biomolecules. Third, the assay allows direct access to kinetic information of analyte permeation on microsecond-to-hours time scales. As a first application of the tandem membrane assay, we applied it to the unsolved biological question, whether cationic antimicrobial peptides, in particular, protamine, can enter into the cell through an outer membrane channel protein. For the first time, conclusive experimental evidence has been provided that such antimicrobial peptides can indeed enter through bacterial channels.

Protease assays for natural or unlabelled synthetic substrates are very much sought after, but the few assays that have been developed are limited to the general detection of protease activity. In the second part of this thesis, I present the label-free fluorescence-based protease assay—the *supramolecular tandem protease assay*. This newly developed label-free method overcomes the use of covalently attached fluorescent labels in peptides by, again, employing macrocycle–fluorophore reporter pairs. The beauty of our sensitive and versatile protease assay lies not only in being able to (*i*) monitor protease activity in real-time, but also in its utility to (*ii*) profile the substrate specificity of a protease, (*iii*) to sense enzyme substrate stereoselectivity, and (*iv*) in its utility for rapid and convenient screening of inhibitors and protease–resistant peptides. Additionally, the tandem protease assay allows stepwise proteolytic degradation of an entire peptide to be easily followed as sequential changes of the fluorescence response, which led us to the idea of peptide fingerprinting through unique fluorescence profiles.

Acknowledgements

This thesis represents not only my work for the past three years as a doctoral student, but my overall experience here at Jacobs University Bremen, and it is my pleasure to thank all the people who made this thesis possible.

I am greatly indebted to my supervisor, Prof. Werner M. Nau, for his unflagging support and guidance. Eight years have passed since I started working as a first year undergraduate student in his lab and he has been inspirational and a steady influence throughout my academic career (ever since). Among many things, I am most grateful to him for believing in me and supporting me in pursuing my ideas and carrying out projects independently, for sharing with me from his immense knowledge in the field (there were times when I thought my results made no sense at all but you were always there with an explanation, with a bigger picture), for setting high scientific standards, even though at times it was very stressful, I must admit, in retrospect, I would not have taken an easy way out. Whether it was tips and tricks for an effective presentation or writing a good scientific paper, or even dealing with people, I am grateful to him, and in my opinion one simply could not ask for a better mentor!

Special thanks go to my thesis committee members, Prof. Mathias Winterhalter and Dr. Andreas Henning, for their time and effort despite their busy schedule.

I have had the great privilege to collaborate with many other wonderful research groups. I would like to acknowledge Prof. Mathias Winterhalter for collaboration on membrane project, Dr. Helge Weingart for providing OmpF samples, Prof. Roland Benz and Dr. Kozhinjampara R. Mahendran for helpful discussions pertaining to the membrane research and members of Winterhalter group, for allowing me to raid their fridge for chemicals, when I needed them urgently; Prof. Adam. R. Urbach for initiating the thermolysin project and providing us with peptides; and Prof. Nikolai Kuhnert for sharing his expertise in mass spectrometry for proteases assays.

I would also like to thank Dipl.-Ing. Kai Mettler, for bringing my scientific project to life through his spectacular animations.

For fruitful cooperation and for making our lab a great place to be in, I am grateful to all the past and current members of Nau research group, of which I would like to start by acknowledging Dr. Andreas Henning and Dr. David M. Bailey, who introduced me to enzyme assays. I would also like to thank, Dr. Maik H. Jacob, Dr. Frank Biedermaan, Dr. Mara Florea, Dr. Vanya D. Uzunova and Alexandra I. Lazar. Maik, I am thankful for your

insights, helpful discussions with membrane project and mostly for listening to my frustrations when my experiments were failing miserably (and for introducing me to David Silva novels!). Frank, I have greatly benefited from your expertise with CB8•methylviologen systems, and for initiating the “membrane diffusion project”. Your advice during my PhD and career after is greatly appreciated! Mara and Vanya, you both have been great friends and co-workers and I thank you for simply being there, giving me advice and your take on various scientific, but especially non-scientific matters. Alex, I am always thankful for your (exhaustive) feedback on my manuscripts. I now pass on the torch to you for being the oldest member of Nau lab (in terms of years spent at Nau Lab, of course!) and I hope it helps you navigate when you are stuck in your infamous “local minima”. All in all, I am grateful for all the members of Nau lab, fußball and bowling competitions, Freimarkt and birthdays with you guys will be greatly missed but dearly remembered.

I would like to take this opportunity to also thank a number of graduate and undergraduate students who have contributed to my projects. In particular, I thank Adrienne G. Lanctôt, Hannah T. Kreissl for their contribution in channel-mediated translocation project, and Nader El Danaf, I trust you will continue well what I started. I wish you all the best!

For financial support, I am thankful to Jacobs University Bremen, NanoFun Center at Jacobs University, Deutsche Forschungsgemeinschaft (DFG). For conference and workshop travel support I also thank Gesellschaft Deutscher Chemiker (GDCh) and the Robert Bosch Foundation.

When you are in a new city, your friends are your family. Kanchan, Pratik and Nivedita, you have been an invaluable support day in and day out, during all these years. Kanchan, your “satisfaction is the enemy of further success” attitude to life has always helped me realize my full potential. Sushil and Sabrina, among many other things, thank you for helping me move out of "Jacobs bubble". Thank you also Sidhant, Richa, Usha, Veneta and all other friends who have filled my life in Bremen with love, laughter and happiness! And most importantly, I owe my deepest gratitude to Kanchan and Pratik for literally saving my life!

Last but definitely not least, I am thankful to the foundation of my life – my family. My sisters, Purnima, Pratima and Mahima, you are the entertainment of my life, and even at times like these, when I am stressed out, the mere mention of your names brings back memories that make me smile and laugh! To my parents I am grateful for my life and all the things in it. You have made sacrifices without a second thought, so that I could get the best education possible. You have more confidence in me than even myself at times and you supported me for each and every decision I made, even if it meant moving four thousand

miles away from home. Knowing that my family and friends are always by my side with unwavering support, without any judgment, is what helps me face new challenges and move forward!

List of Publications

1. Ghale, G., Nau, W. M. Dynamically Analyte-Responsive Macrocyclic Host–Fluorophore Systems. *Acc. Chem. Res.* (2014) DOI: 10.1021/ar500116d.

2. Ghale, G., Lanctôt A.G., Kreissl, H.T., Jacob, M.H., Weingart, H., Winterhalter, M., & Nau, W.M., Chemosensing ensembles for monitoring biomembrane transport in real time. *Angew. Chem. Int. Ed.* **53**, 2762-2765 (2014).

3. Ghale, G., Kuhnert, N., Nau, W. M. Monitoring stepwise proteolytic degradation of peptides by supramolecular domino tandem assays and mass spectrometry for trypsin and leucine aminopeptidase, *Nat. Prod. Commun*. **7**, 343-348 (2012).

4. Ghale, G., Ramalingam, V., Urbach, A. R. & Nau, W. M. Determining protease substrate selectivity and inhibition by label-free supramolecular tandem enzyme assays. *J. Am. Chem. Soc.* **133**, 7528-7535 (2011).

5. Nau, W. M., Ghale, G., Hennig, A., Bakirci, H. & Bailey, D. M. Substrate-selective supramolecular tandem assays: Monitoring enzyme inhibition of arginase and diamine oxidase by fluorescent dye displacement from calixarene and cucurbituril macrocycles. *J. Am. Chem. Soc.* **131**, 11558-11570 (2009).

6. Hennig, A., Ghale, G., & Nau, W. M. Effects of cucurbit[7]uril on enzymatic activity. *Chem. Commun.*, 1614 -1616 (2007).

Manuscripts Submitted or in Preparation

7. Biedermann, F., Ghale, G., & Nau, W.M., A Supramolecular Fluorescence-based Method to Quantify Lipid-bilayer Membrane Permeability of Organic Compounds by Real-time Kinetics. *Manuscript in Preparation*.

Participation in Scientific Conferences

Oral Contributions

July 2011 — 2nd International Conference on Cucurbiturils, Cambridge, UK. Talk entitled: "Enzyme Assays: The Domino and Tandem Game."

July 2011 — International WE-Heraeus Workshop "Nanofluidics in Biology", Bremen, Germany. Talk entitled: "Supramolecular Tandem Membrane Assays to Monitor Porin Mediated Translocation of Cationic Peptides."

May 2011 — Molecular Life Sciences Graduate Retreat, Seefeld, Germany. Talk entitled: "A Chemosensing Ensemble to Monitor Porin Mediated Permeation of Arginine-rich Peptides into Liposomes.''

January 2011 — 4th Meeting of the North German Biophysicists, Germany. Talk entitled: "Supramolecular Tandem Assays for Cross-membrane Transport of Arginine–rich Peptides."

January 2011 — Nanofun Workshop, Clausthal (Harz), Germany. Talk entitled: "Molecular Spies for Monitoring Biological Transformations."

Poster Contributions

August 2013 — Transport Through Nanopores: From Understanding to Engineering, Bremen, Germany. G. Ghale, A.G. Lanctôt, H. T. Kreissl, M. H. Jacob, H. Weingart, M. Winterhalter and W.M. Nau, "Having an Eye on Who's Passing the Biomembrane."

August 2012 — 4th EuCheMS Chemistry Congress, Prague, Czech Republic. G.Ghale, H. Weingart, M. Winterhalter and W. M. Nau, "Monitoring Channel Protein-mediated Translocation of Arginine-rich Peptides by a Supramolecular Sensing Ensemble."

September 2010 22nd Lecture Conference of the GDCh-Division Photochemistry, Erlangen, Germany. G.Ghale, W. M. Nau, "Development of Tandem Assays For Proteases''.

August 2010 3rd EuCheMS Chemistry Congress, Nürnberg, Germany. G.Ghale and W. M. Nau, "Development of Novel Fluorescent Protease Assays."

June 2009 4th joint International Symposium on Macrocyclic & Supramolecular Chemistry, Maastricht, Netherlands. G.Ghale and W. M. Nau, "Substrate-selective Tandem Assay for Diamine Oxidase."

Additional Workshops and Seminars

November 2010 1st Hamburger MicroCal Andwendertag, Germany.

October 2010 International Workshop on Frontiers of Supramolecular Chemistry, 2009, Tianjin, China.

SUMMARY

The goal of my PhD thesis has been to design and develop novel, versatile and economic fluorescence-based assays to study biological processes. The research that I have conducted until now utilizes the concept of host-guest chemistry, such as molecular recognition by macrocyclic hosts, to develop new analytical methods. Chapter 1 describes the fundamental concepts that govern the use of a macrocyclic host and a fluorescent dye as *supramolecular chemosensors* or *reporter pairs* for assay development, followed by the introduction of host-dye complexes to monitor enzymatic transformations.

Chapter 2 describes supramolecular tandem membrane assays, a label-free fluorescence-based method that I have developed to monitor diffusion/translocation of biomolecules through lipid bilayers or channel proteins. As a proof of principle for tandem assays, the successful translocation of protamine, an arginine-rich peptide, through bacterial channel outer membrane protein F (OmpF) was investigated using *p*-sulfonatocalix[4]arene and lucigenin as reporter pair inside liposomes (section 2.1, Appendix 4.1). Moreover, the translocation of protamine was accelerated (as followed by stopped-flow experiments) by substituting wild-type OmpF with a selected mutant of OmpF and suppressed translocation adding spermine as a channel blocker. In section 2.2, this newly developed method is applied for screening the membrane permeating behaviour of more than 90 different compounds, including biologically relevant species such as drugs, peptides, and neurotransmitters. Furthermore, we demonstrated that the tandem membrane assays could be further extended to confocal imaging with fluorescence microscopy and to parallelization and high-throughput screening with microplate readers.

Chapter 3 of my thesis focuses on the development of novel fluorescence-based methods to study proteolytic transformations. During my PhD, I have designed enzyme assays for two different types of proteases: endopeptidases (thermolysin) and exopeptidases (leucine amino peptidase). Using a macrocycle cucurbit[7]uril (CB7) in combination with the fluorescent dye acridine orange (AO) as a reporter pair, we carried out an intensive study on the activity of thermolysin on enkephalin-based peptides (section 3.1 and publication 4.3).

In particular, I have derived *absolute* kinetic parameters from the fluorescence signal generated during enzymatic transformation, which then led us to the unexpected substrate-dependent exopeptidase activity of thermolysin. In addition, the utility of the assay for screening inhibitors and protease-resistant peptides was also established. This project was carried out in collaboration with Prof. Adam R. Urbach from Trinity University, USA.

In my project involving leucine amino peptidase (section 3.2, Appendix 4.2), I have demonstrated that a stepwise proteolytic degradation of an entire peptide can be followed in real-time by fluorescence, and as such, presents the possibility of peptide fingerprinting from the fluorescence pattern. Additionally, an alternative method, mass spectrometry was also used to follow a complete stepwise degradation of a peptide by leucine amino peptidase. This project was an in-house collaboration with Prof. Nikolai Kuhnert.

– Chapter 1–
Introduction

1. Introduction

This chapter is derived from the content of the following article:

1. Ghale, G., Nau, W.M., Dynamically Analyte-Responsive Macrocyclic Host-Fluorophore Systems. *Acc. Chem. Res.* **2014**, DOI: 10.1021/ar500116d.

Let me begin with a quote from Max Beerbohm, "*Mankind is divided into two great classes: hosts and guests"* (1918, Host and Guest). Similarly, supramolecular chemistry is divisible into macrocycles and guests – macrocycles or receptors that function as a host by accommodating a guest or a ligand. The modern era in supramolecular chemistry, to a large degree, commenced with the work of Pedersen, who in 1967 first reported the synthesis of crown ethers.[1-3] The past 45 years have witnessed substantial progress in the field, from the design of highly selective receptors to their applications in drug delivery,[4-6] catalysis and transport.[7-10] However, the focus of my work has been on employing these macrocyclic host•guest inclusion complexes as supramolecular chemosensors for designing and developing methods to investigate biochemical processes, more specifically for monitoring biomembrane transport and enzymatic transformations. In this chapter, I will begin by describing the underlying principles that governs the use of macrocycle•fluorescent dye complexes for analyte sensing, followed by their introduction in enzyme assays and the potential of supramolecular chemosensors for the development of novel bioanalytical method to monitor biomembrane transport and proteolytic activities.

1.1. Supramolecular Sensor Systems

Supramolecular sensors are based on the principles of host•guest chemistry, whereby the receptor or the host molecules containing a binding site for an analyte "guest" are used to signal analyte binding. The analyte recognition and binding takes place through non-covalent or supramolecular interactions, and although these interactions are individually weak, they exert a great influence on the stability of supramolecular complexes through a synergistic effect. The most significant non-covalent factors are ion–ion, ion–dipole, cation-π interactions, hydrogen bonding, π- π stacking and Van der Waals forces.[11]

Traditionally, the design of supramolecular sensors was based on "receptor-spacer-reporter" system. The method relies on a receptor – frequently a macrocycle – for molecular recognition – and a reporter for signalling, typically an indicator dye which changes its photophysical properties, preferably fluorescence.[12] While such systems have been exploited for selective sensing of inorganic ions and are advantageous in complex mixtures where high local concentration is required (e.g., cells), they suffer from several drawbacks, that include laborious synthesis, e.g., tethering of a fluorophore to the receptor, which limits the selection of receptor and indicators.[13,14]

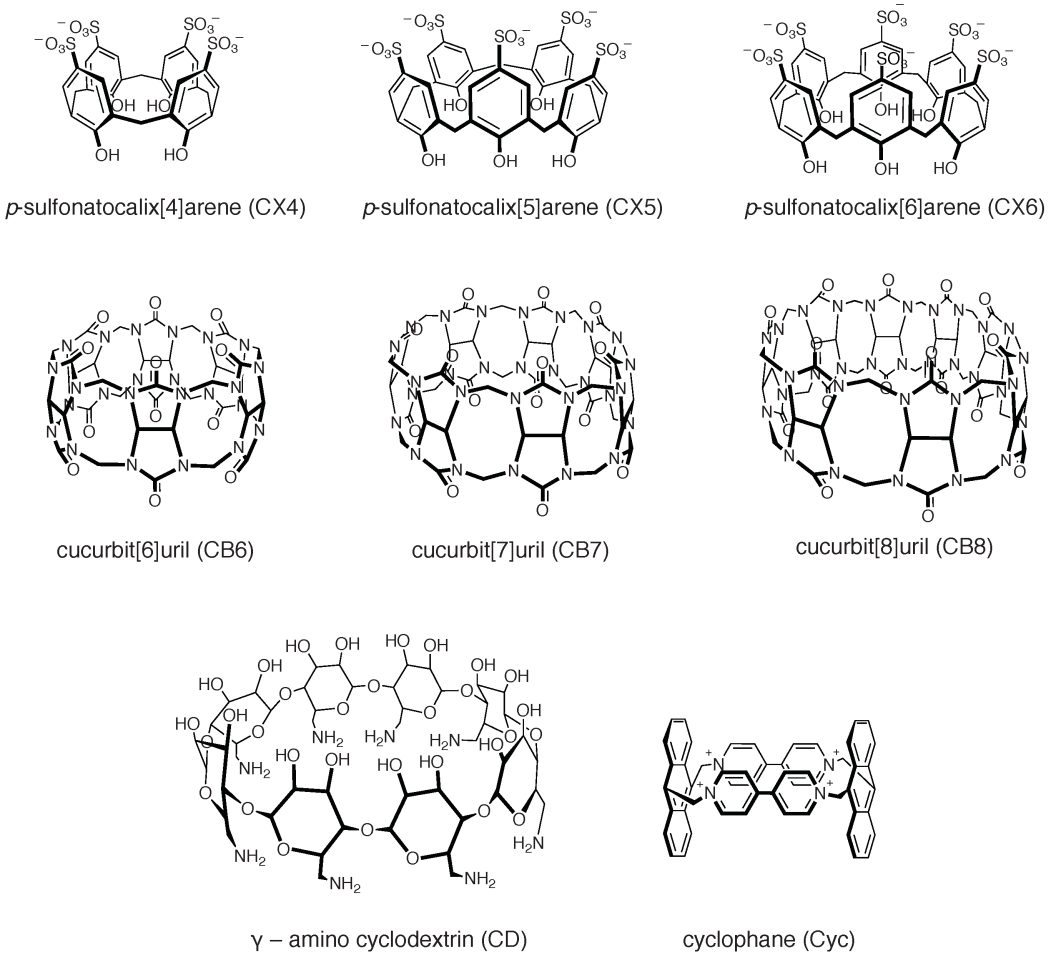

Figure 1.1: Chemical structures of macrocyclic compounds in different sizes to fit different guests. a) *p*-sulfonato calixarenes, and b) cucurbiturils are the examples of cation receptors while, c) amino-cyclodextrin and cyclophane, represents anion receptors. Adapted from ref.[15]

Indicator displacement assays (IDAs),[16-19] on the other hand, were introduced to by-pass the demanding design of chemosensors with receptor-spacer-reporter systems.[20] The

sensing principle of IDAs is based on the competition between a test substance and an indicator for the same binding site on the host. When an analyte is added to a solution containing host•indicator complex, the analyte displaces the indicator from the binding site. Upon displacement of the indicator, a change in signal is observed.

Whether it was for assessing the quality of wine from Pinot Noir grapes or determining the quantity of citrate in beverages,[16,21] indicator displacement assays have been predominantly exploited in a static fashion, namely to determine absolute analyte concentrations, or, by using combinations of several reporter pairs, to achieve a differential sensing.[22-27] In contrast, their use in biological systems, e.g., with membranes, cells, or with enzymes has been comparably less explored. This led us to the design of the so-called tandem assays, that is, dynamically analyte-responsive macrocyclic host•dye systems, in which a biological reaction or a process induces the change in analyte concentrations.[15]

1.2. Macrocycles

Macrocycles are cage-like compounds capable of accommodating guest molecules complimentary to their charge, size and shape.[2,11] The list of available macrocyclic host molecules ranges from classical crown ethers to contemporary cucurbiturils. Owing to the importance of biological analytes, my work is mostly concentrated on water-soluble macrocycles, in particular calixarenes and cucurbiturils, Figure 1.1.

The name Calixarenes (CXn) is derived from calix or chalice due to the similarity in the shape these phenol-derived macrocycles to a Greek vase calix crater.[28] Calixarenes are composed of phenolic units linked together by methylene groups and occur in different sizes, e.g., CX4, CX5 and CX6, where the numbers represent repeating phenolic units.[28-33] The structure of calixarenes is such that central π-basic cavity is capable of encapsulating guest molecules, while upper and lower rims are available for synthetic modifications to fit specific application purposes.[34] For example, the lower rim can be substituted with alkyl chains to yield calixarenes with membrane transporter properties and the upper rims can be decorated with sulfonato groups leading to highly water-soluble derivatives such as *p*-sulfonatocalixarenes.[35,36] Described as "*macrocycle with (almost) unlimited possibilities*" by Volker Böhmer,[37] calixarenes have had great impact on supramolecular chemistry with applications ranging from biomimetic recognition, to transport to catalysis.[38]

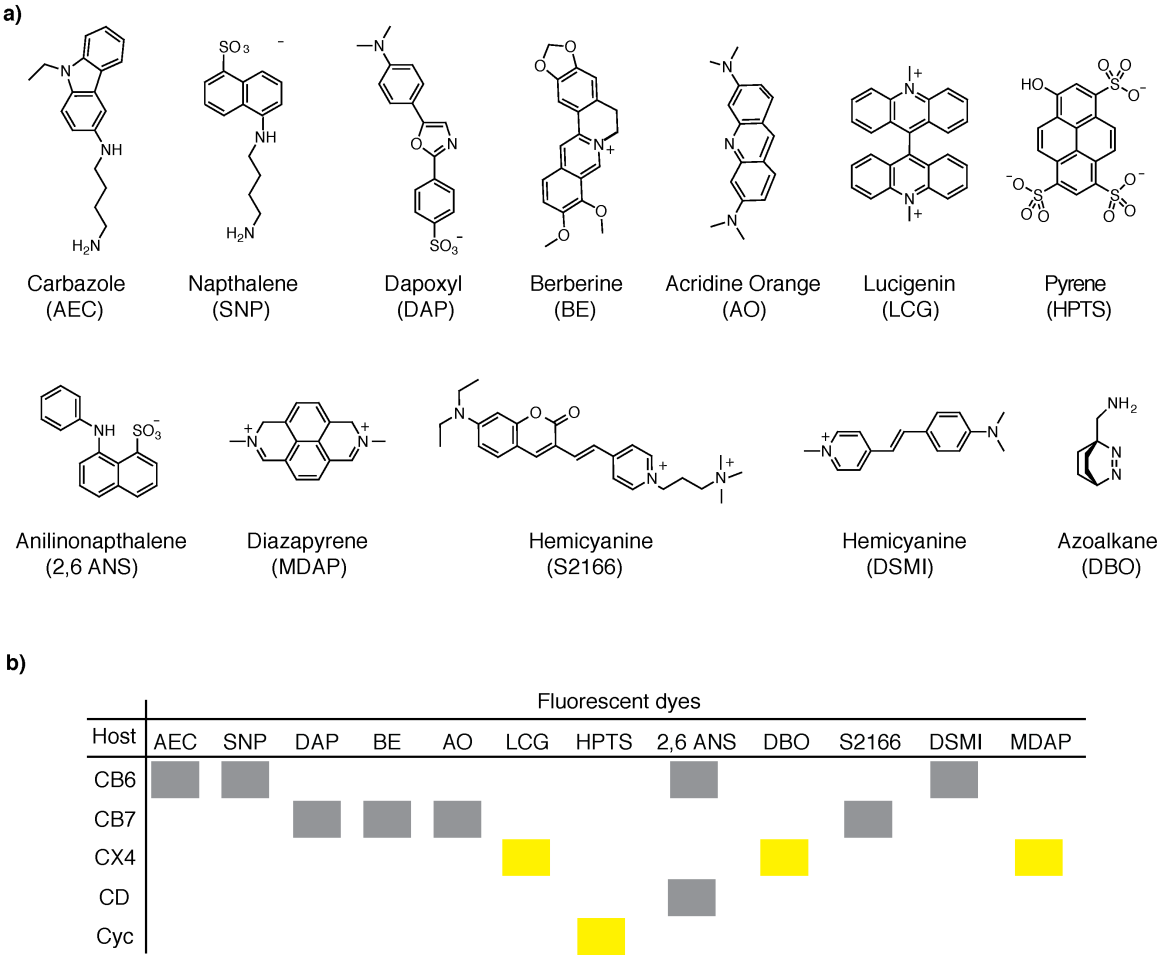

Figure 1.2: a) Chemical structures of fluorescent dyes investigated by our group as indicators. b) Matrix representation for combination of host and dye complexes suitable as reporter pairs in tandem assays are indicated by a bar, where the photophysical response upon analyte binding is color-coded (yellow: fluorescence enhancement, grey: fluorescence quenching). Adapted from ref.[15]

Unlike calixarenes, cucurbiturils (CBs) are less amenable to modifications from their parent compounds.[39,40] First synthesized by Behrend in 1905 and later synthesized and characterized by Mock in 1980s, these condensation products of glycouril and formaldehyde, are rigid, pumpkin-shaped molecules, with carbonyl portals lining the hydrophobic cavity.[41-43] Like CXn, cucurbiturils are also available in different sizes (CB5, CB6, CB7, CB8 and CB10, where numbers represent the glycouril units), out of which odd numbered homologues are water-soluble.[44-47] CBs are capable of encapsulating a wide range of aliphatic and aromatic molecules with high binding affinities and potential selectivity, making them

one of the most intensely investigated family of macrocycles in recent years. While many application of CBs are currently unfolding, CBs have already demonstrated their potential in fields as diverse as bioassays,[48-52] gas absorption or purification,[53,54] and gene transfection.[55]

My interest lies in exploiting the molecular recognition features of these macrocycles to design and develop fluorescence-based analytical methods to interrogate biochemical process. In order to do so, we first need to know how macrocycles can be combined with fluorescent dyes for generating a fluorescence signal.

1.3. Macrocycle•fluorescent Dye Sensor Systems

It has been apparent from earlier sections that macrocycles (Figure 1.1) are capable of binding and recognizing guest molecules, including fluorescent dyes (Figure 1.2a). The photophysical properties of a dye (fluorescence) changes upon formation of a macrocycle•dye complex.[56] Conversely, when the dye is displaced from the cavity, the original fluorescence of the dye is restored (1.2b and 1.3). This alteration in the photophysical characteristics of the dye upon complexation and decomplexation by a macrocycle is what makes them appealing as a "*reporter pair*" or "*chemosensing ensemble*" and is the basis of analyte detection by dye displacement. There are different mechanisms how the fluorescence of a dye is modulated by a macrocyclic host and are briefly described below.

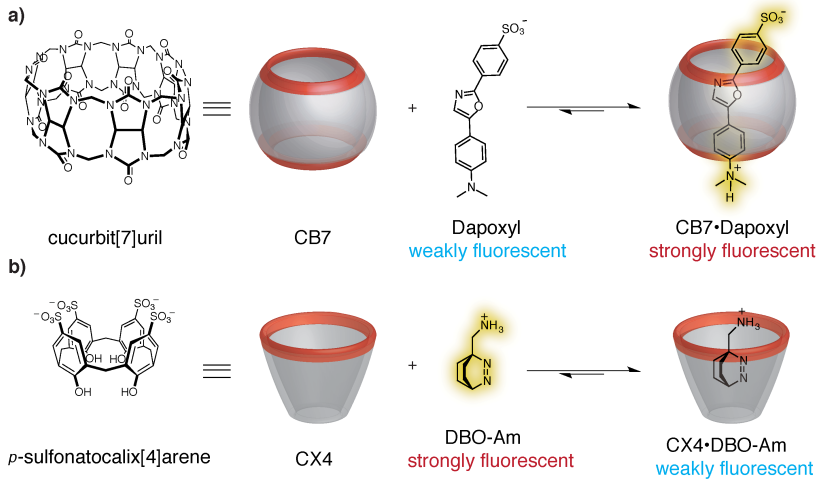

Figure 1.3: a) CB7-assisted protonation of a fluorescent dye Dapoxyl. b) Fluorescence quenching of DBO-amine by sulfonatocalixarenes.[48]

When a fluorophore is encapsulated by these nanocontainers (Figure 1.1), in most cases the photophysical properties of the dye, in particular fluorescence, is affected because, *i*) the dye is relocated into the hydrophobic environment,[57,58] *ii*) the walls of the host provides protection from solvent or quencher molecules,[47,59,60] and *iii*) the geometrical confinement of the chromophore restricts rotational and vibrational freedom.[61] In addition to the polarity and geometrical confinement of the dye, for cucurbiturils, charge-dipole interactions between the carbonyl portals and the cationic dyes, play an unquestionably dominant role in modulating photophysical properties of the dye. For example, fluorescence enhancement of dyes such as dapoxyl and acridine orange upon encapsulation by CB7 is due to the host-assisted dye protonation (Figure 1.3a).[60,62] Calixarenes with their electron-rich phenoxy rings, on the other hand, are famous for their charge-transfer induced quenching of fluorescent dyes. A pertinent example is fluorescence quenching of the azoalkane dye DBO by CX4 (Figure 1.3b).[63]

Macrocycle•fluorescent dye complexes have been extensively used for detecting the absolute concentration of analytes and for determining their binding strengths to the macrocyclic host.[64,65] What has not been pursued yet was their use as reporter pairs to follow dynamic changes in analyte concentrations. In the following section, it will be demonstrated how such host•dye complexes can be employed as versatile sensors that respond dynamically to analytes generated or depleted during enzymatic reactions.

1.4. Supramolecular Tandem Enzyme Assays

Among different available methodologies for following enzymatic reactions, fluorescence-based methods stand out due to their high sensitivity, short detection time and the possibility for continuous monitoring.[66,67] The use of fluorescently labelled substrates for assaying enzyme activity is a popular method. However, the major weakness of this method is that the labels can impede the binding of the substrate with the enzyme pocket, thus influencing the substrate reactivity.[67-69] An alternative method involves antibodies in combination with fluorescently labelled antigens.[70,71] The enzymatic reaction is carried out in presence of the antibody and the fluorescently labelled antigen. As enzymatic reaction progresses, the fluorescently tagged antigen is displaced by the product (unlabelled antigen), which leads to a

fluorescence response. This method while robust, suffers from several disadvantages, which are primarily related to the time and cost of raising antibodies.

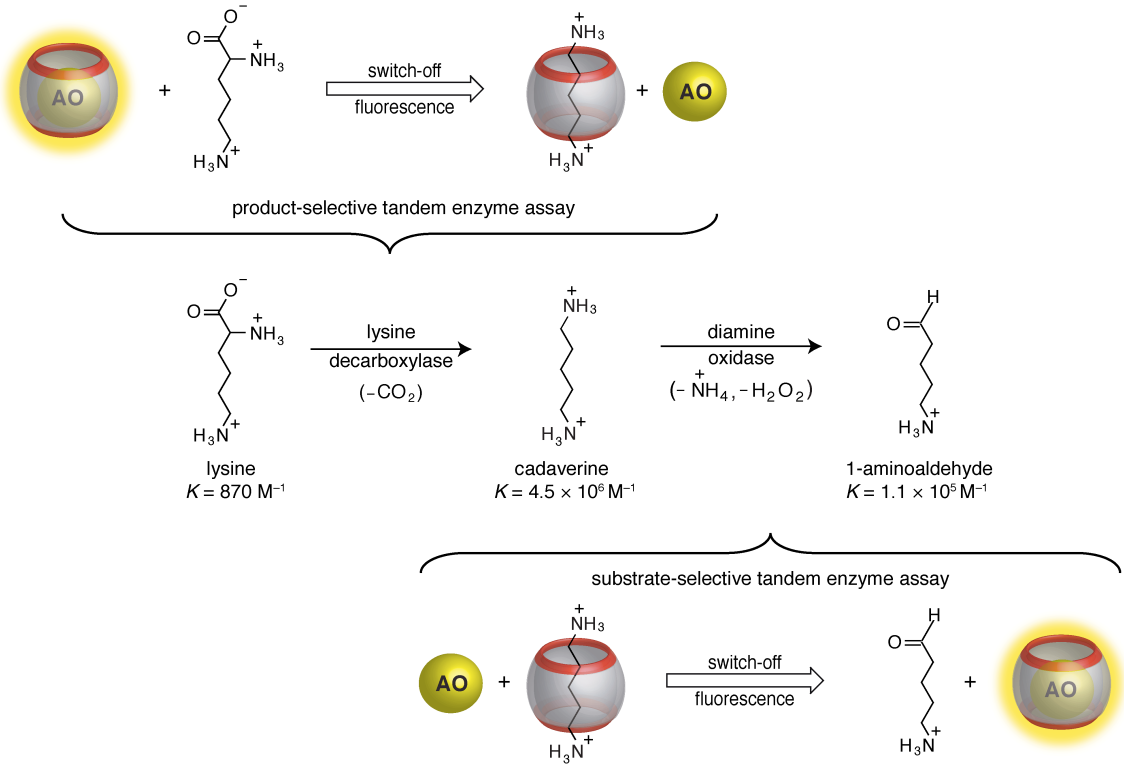

Figure 1.4: The product-selective (top) and substrate-selective variants of supramolecular tandem enzyme. The chemosensing ensemble composed of a macrocyclic host CB7 and a fluorescent dye AO ($K_{CB7 \cdot AO}$ = 2.9 × 10^5 M^{-1}).[50]

Drawing inspiration from the antibody-antigen assays, in 2007 our group introduced a versatile, economic and label-free enzyme assays – supramolecular tandem enzyme assays – where macrocycles serve as cheap and conveniently accessible antibody substitutes (Figure 1.4).[48] Since then the method has been successfully employed to investigate the activity of five different classes of enzymes.[48-52,72-75]

At the heart of supramolecular tandem assays lies the reversible and competitive binding affinity of a macrocyclic host with a fluorescent dye and an analyte, and its differential binding with the enzymatic substrate or the product (Figure 1.4). The three variants of supramolecular tandem enzyme assays are described in following sections.

1.4.1. Product-selective Supramolecular Tandem Assays. The assay setup is particularly straightforward when the product binds more strongly to the macrocycle that leads to a product-selective assay.[48,51,52,74,75] Consider an enzymatic transformation of lysine to cadaverine by lysine decarboxylase (Figure 1.4).[48] A macrocyclic host (CB7 or CX4) is chosen such that it binds weakly with the substrate (lysine), but strongly with the corresponding enzymatic product (cadaverine), allowing the complexation of the macrocyclic host with the fluorescent dye (CB7•DAP, CB7•AO and CX4•DBO). As the reaction progresses, the enzymatic product displaces the fluorescent dye from the host molecule and the enzymatic conversion is reported as an increase (fluorescence switch-on response for CX4•DBO) or decrease in the fluorescence (fluorescence switch-off response for CB7•DAP or CB7•AO) depending upon the photophysical properties of the dye. Important to note here is that using these two reporter pairs, we were not only able to monitor the activity of a single amino acid decarboxylase, but the protocol was transferrable to several decarboxylases including lysine, histidine, ornithine and tryptophan decarboxylases.[48] In contrast to antibody-based assays where a single antibody would be specific to a single antigen or product, supramolecular tandem enzyme assays constitute a very important advantage that a single reporter pair can be used to assay an entire class of enzymes which affect structurally related transformations, in this case the charge status.

1.4.2. Substrate-selective Supramolecular Tandem Assays. We can choose a macrocyclic host such that it binds to the substrate more strongly than to the enzymatic product, setting up a substrate-selective assay (Figure 1.4).[50] Although this change from a product- to a substrate-selective version may appear to be a subtle variation, it is a stand-alone feature of supramolecular tandem assays. Antibody-based assays, in particular, are entirely unsuitable for operation in a substrate-coupled mode because antibodies bind antigens with high specificity and superior affinity which leads to a very slow release kinetics. Nevertheless, given that the macrocyclic receptor binds to the substrate, we do need to consider an apparent inhibitory effect of the receptor on the enzymatic activity, due to the reduced concentration of free substrate.[76,77] However, since the absolute amount of receptor can be tuned down (low μM concentration) compared to the concentration of substrate (mM), the rate of enzymatic conversion is not significantly inhibited by the presence of the reporter pair.

As a proof-of-principle for a substrate-selective enzyme assay, consider and enzymatic oxidation of cadaverine (strong competitor) to aminoaldehyde (weak competitor) by diamine oxidase. In this scenario, before the onset of enzyme conversion, the substrate is in complexation with the host while the dye is free in solution. During the course of enzymatic transformation, i.e., as a substrate is converted to a product (weak competitor), the binding of the fluorescent dye becomes more competitive because the substrate concentration decreases. As a result, the activity of diamine oxidase is reported as a continuous increase in fluorescence because the strong competitor is diminished, allowing the fluorescent dye to be immersed in the macrocycle.

While enzyme kinetic parameters (K_M, k_{cat}) can be easily obtained from product-selective tandem assays, this can be more difficult for the substrate-selective variants due to a lag phase observed at higher substrate concentrations.[50,74] Only in special cases kinetic parameters have been determined, for example, the substrate-selective tandem enzyme assay for butyrylcholinesterase (BuChE).[78]

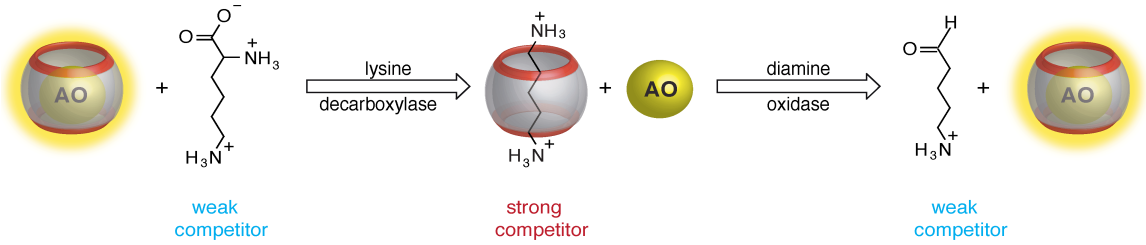

Figure 1.5: Production and the degradation of biogenic amine monitored using domino tandem assay.[50]

1.4.3. Domino Tandem Assays. By consecutively combining the product- and substrate-selective variants of tandem enzyme assays, we were able to follow a cascade of enzymatic transformations in one reaction mixture, using a single chemosensing ensemble. This new line of tandem assays is called domino tandem assay (Figure 1.5). The simplest example is the production and degradation of biogenic amines using CB7•AO as a reporter pair. First, the conversion of lysine to cadaverine by lysine decarboxylase was monitored as a fluorescence decrease due to the displacement of AO. The oxidation of cadaverine is subsequently initiated by addition of diamine oxidase to form aminoaldehyde, reflected by an increase in fluorescence signal, owing to the re-complexation of CB7 and AO.

1.5. Scope of My Thesis

If host•dye reporter pairs could be used to continuously follow the changes in concentration of either a substrate or a product (a chemical reaction), it should also be feasible to monitor the time-resolved changes in the concentration of an analyte in general. An example is the build-up of an analyte inside compartmentalized structures such as vesicles. This conceptually novel approach resulted in the development of a versatile supramolecular method to monitor biomembrane transport processes – tandem *membrane* assays (Chapter 2).[79] My motivation for exploiting supramolecular chemosensing ensembles for investigating membrane transport stemmed from the fact that fluorescence-based methods to study transport of bioorganic analytes through the lipid bilayer and channel proteins in a label-free fashion in real-time were nonexistent.[80]

The quantification of the flux of molecules across a membrane or through a channel protein has remained an experimental challenge, and, to date, only a handful of methods are available. The commonly practiced biophysical methods to monitor analyte translocation through membranes are limited to electrophysiology (which cannot readily differentiate between translocation and binding)[81] and vesicular assays with internalized pH-responsive or quenched fluorophores.[82,83] The latter have found specific fields of application, e.g., some can readily signal rupture of the membranes, but they do not allow the desirable monitoring of the translocation of biomolecular analytes with micromolar sensitivity. This limitation can be by-passed by employing fluorescently labelled analytes or lipids,[84] but this approach leads to new considerations in regard to the transferability of the results to the unlabelled analytes and to additional demands with respect to chemical synthesis.[85-87] For instance, AlexaFluo 633-labelled Tat peptide is internalized into vesicles, while the native, unlabelled peptide is not.[88]

The broad selectivity of the macrocyclic receptors, which are essentially used as cheap antibody substitutes, has presented a major advantage for assay development. Originally introduced to monitor the formation of biogenic amines by enzymatic decarboxylation of amino acids, they have subsequently been expanded into many other fields, for multiparameter sensing, for enantiomeric excess determination, for dye release from mesoporous hybrid systems and for allosteric dye release assays. My thesis explores the potential of macrocyclic host•fluorophore systems as versatile supramolecular sensors for

designing and developing innovative methods to study biological processes, in particular biomembrane transport (Chapter 2) and protease activity (Chapter3).

– Chapter 2–
Supramolecular Tandem Membrane Assays

2. Supramolecular Tandem Membrane Assays

This chapter is derived from the contents of following publications and manuscript:

1. Ghale, G., Lanctôt, A.G., Kreissl, H.T., Jacob, M.H., Weingart, H., Winterhalter, M., & Nau, W.M., Chemosensing ensembles for monitoring biomembrane transport in real time. *Angew. Chem. Int. Ed.* **53**, 2762-2765 (2014).
2. Biedermann, F., Ghale, G., & Nau, W.M., A Supramolecular Fluorescence-based Method to Quantify Lipid-bilayer Membrane Permeability of Organic Compounds by Real-time Kinetics. *Manuscript in Preparation*.
3. Ghale, G., Nau, W.M., Dynamically Analyte-Responsive Macrocyclic Host-Fluorophore Systems. *Acc. Chem. Res.* **2014**, DOI: 10.1021/ar500116d.

Supramolecular tandem membrane assays, introduced in our study, alleviate many limitations imposed by existing techniques (Chapter 1.5) by combining a fluorescent dye with a macrocyclic host as a "reporter pair" encapsulated inside liposomes, (Figure 2.1). The macrocycles in our assay are utilized as receptors for the translocated analytes, which introduces a genuine molecular recognition feature, bypassing the need for covalent fluorescent labels and increasing the sensitivity to the micromolar range.

The working principle of tandem membrane assays relies on the selective encapsulation of reporter pairs inside liposomes and the reversible interaction between the receptor and the translocated analyte (Figure 2.1). To conduct the assay, liposomes containing the host•dye reporter pair are prepared and purified, such that a subsequently added analyte affects the dye fluorescence only if it is able to enter the vesicle and to displace the dye from the macrocycle. As was the case with tandem enzyme assays, the very first step in designing tandem membrane assay involves the selection of a suitable macorcycle•fluorescent dye reporter pair.

In order to employ a macrocyclic host and a fluorescent dye as a reporter pair inside liposomes, the host and the dye has to fulfil three major criteria: (*i*) the macrocyclic host is

selected such that it shows sizable affinity with the analyte of interest, (*ii*) a fluorescent dye with a high affinity to the macrocycle and a strong fluorescence response upon complexation needed to be selected, and (*iii*) as a special consideration when working with lipid bilayers, neither the host nor the dye must dissolve in or permeate through the membrane.

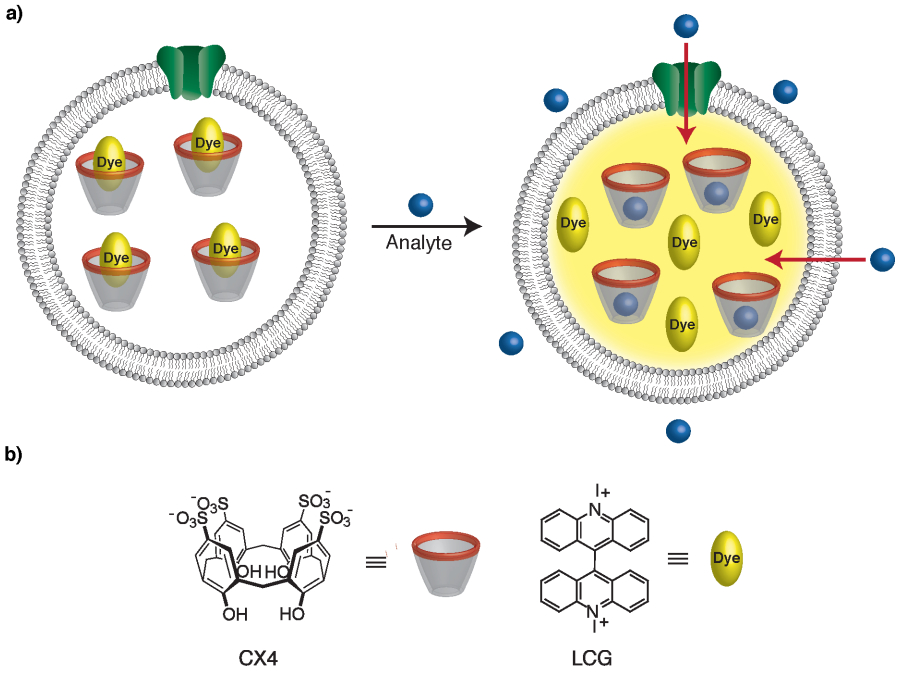

Figure 2.1.1: Working principle of a supramolecular tandem membrane assays. a) Schematic illustration of macrocyclic host•dye complexes encapsulated inside a liposome before (left) and after (right) translocation of an analyte (blue) through the lipid membrane or through the channel protein (green); the analyte binds to the macrocycle, thereby displaces the dye, which in turn becomes strongly fluorescent in its uncomplexed form. b) Chemical structures and graphical representations of the macrocyclic host *p*-sulfonatocalix[4]arene (CX4), and of the fluorescent dye lucigenin (LCG). Adapted from ref.[79]

With these considerations in mind, as a proof-of-principle in following section we have applied our method to the unsolved biological question whether cationic antimicrobial peptides such as protamine can enter into the cell through the outer membrane channel protein of gram-negative bacteria such as OmpF.

2.1. CHANNEL PROTEIN MEDIATED TRANSLOCATION OF ARGININE-RICH PEPTIDES INTO LIPOSOMES

Arginine-rich polypeptides have inspired membrane research for a decade by posing a translocation puzzle as to how such hydrophilic molecules pass through an intrinsically hydrophobic barrier.[86,89-92] On one hand it is well known that the complexes of arginine-rich peptides, e.g., with negatively charged cargoes such as DNA, can surmount the bilayer barrier.[93-95] It is also known that the uptake can be potentiated by receptors such as heparan sulphate proteoglycans.[92] Whether, on the other hand, these polycationic peptides permeate on their own or translocate through channel proteins[86,92,96,97] remains an open but crucial question in regard to their antimicrobial activity[96,97] and other putative functions.[87,94] One of these antimicrobial peptides is protamine,[96,98] which is composed of 32 amino acid residues of which 21 are arginine[95] and which I have selected to explore the capabilities of supramolecular tandem membrane assays for investigating key aspects of analyte translocation in vitro, namely into liposomes.

Considering a possible entry of protamine through channel proteins, an outer membrane protein F (OmpF) was selected. OmpF is a cation-selective, general-diffusion channel protein that is well known to allow passage of small molecules (MW < 600 Da) including many antibiotics[99,100] and also of toxins.[101] While, interaction of shorter arginine-rich peptides such as hepta– or penta–arginines with OmpF has been noted using patch clamp techniques,[102] the translocation of much larger arginine-rich peptides through OmpF has not yet been demonstrated. With protamine as an analyte of interest, my next step was to select a reporter pair fulfilling the criteria listed in above.

2.1.1. Characterization of the Reporter Pair for Biomembrane Studies

Among the known reporter pairs,[73-75,103] we found the one constituted by lucigenin (LCG) as dye and *p*-sulfonatocalix[4]arene (CX4) as macrocyclic host to fullfill the criteria for biological membrane reporter pair. Since, the fluorescence response of LCG upon complexation by CX4 was already investigated by our group for enzyme assays,[73,75] our next step was to determine the fluorescence response upon addition of analyte to the preformed host•dye reporter pair ($K_{CX4•LCG}$ = 1.03 × 10^7 M^{-1}), which was additionally used to derive the

binding constant of protamine with CX4 ($K_{CX4•protamine}$ = 1.24 × 10^9 M^{-1}). The addition of protamine to preassembled CX4•LCG complex led to a fluorescence recovery (Figure 2.1.2a &b).

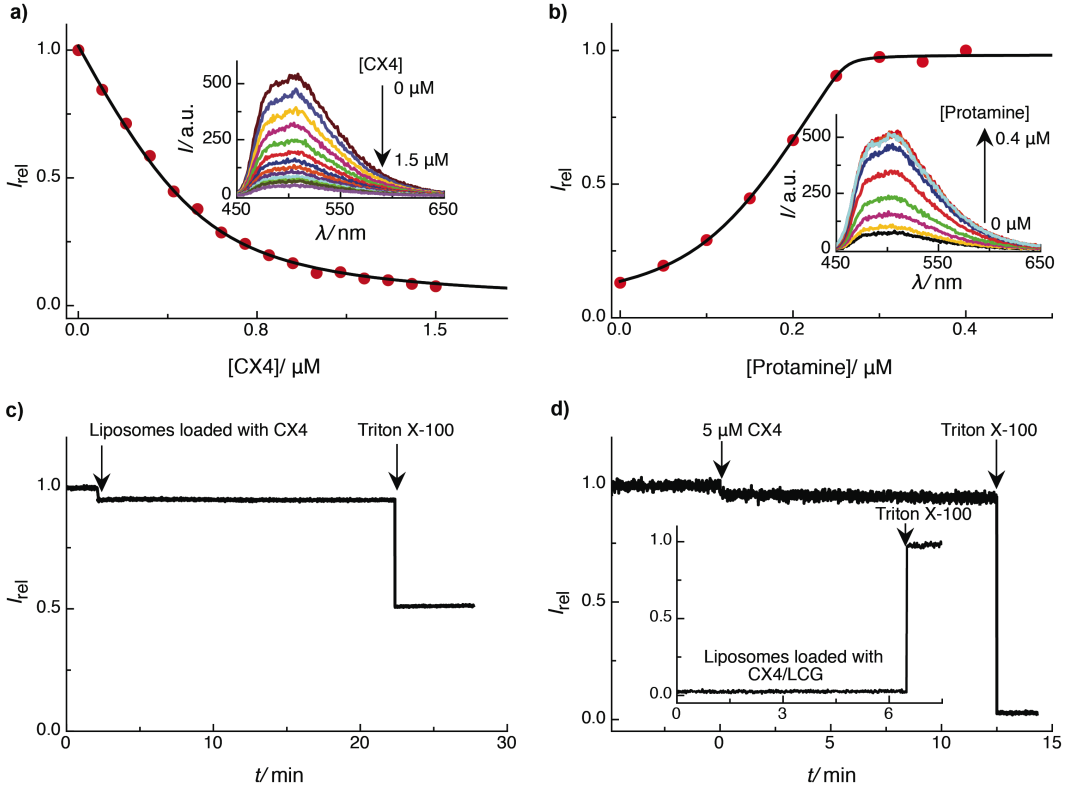

Figure 2.1.2: a) Fluorescence titration curve to determine the binding affinity of CX4 with LCG (0.5 µM). Inset: Spectral decrease in LCG fluorescence with increasing concentration of CX4. b) Competitive fluorescence displacement titration of LCG (0.5 µM) from CX4 (1 µM) by adding protamine to determine the CX4•protamine binding constant and complex stoichiometry. Inset: Full recovery of LCG fluorescence upon increasing the concentration of protamine. c) Fluorescence kinetic trace upon addition of liposomes loaded with CX4 to a 0.5 µM of LCG solution (the minor drop is due to dilution) and the subsequent rupture of the liposomes by addition of detergent, 1% Triton X-100 (t ≈ 22 min). d) Fluorescence kinetic trace upon addition of 5 µM CX4 to a solution containing LCG encapsulated in liposomes (the minor drop is due to dilution) and the subsequent liposome lysis by 1% Triton X-100 (t ≈ 12 min). Inset: Fluorescence increase upon addition of 1% Triton X-100 to CX4/LCG-encapsulated liposomes. All experiments were carried out in 10 mM sodium phosphate buffer at pH 7.0 and 25 °C with λ_{exc} = 367 nm and λ_{obs} = 500 nm. From ref.[79]

The ultimate test, however, to employ CX4•LCG for membrane translocation studies, was to check that neither CX4 nor LCG permeated through lipid bilayer. In order to confirm the membrane impermeability of both components, liposomes loaded separately with only CX4 and LCG were prepared (Figure 2.1.2). Lack of fluorescence change upon addition of a) CX4-loaded liposomes to a LCG solution (Figure 2.1.2a), and b) a CX4 solution to LCG-loaded liposomes (Figure 2.1.2b) verified the suitability of CX4•LCG as biological membrane reporter pair, because diffusion of either component through the membrane would have resulted in a strong decrease in fluorescence signal, owing to the formation of the non-fluorescent CX4•LCG complex. Nevertheless, when triton X, an effective detergent that ruptures the liposomes was added, a strong fluorescence quenching was observed, indicating the complexation of LCG by CX4, which were then no longer spatially separated.[79]

2.1.2. Monitoring the Translocation of Protamine into Liposomes

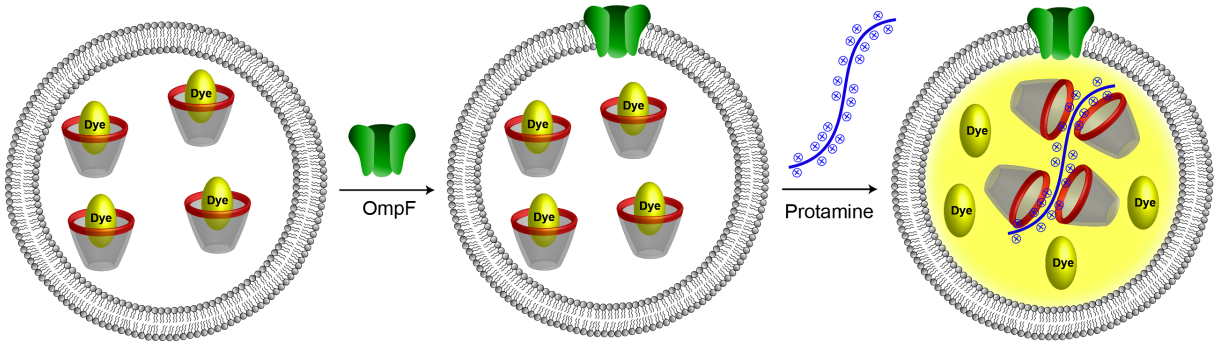

Figure 2.1.3: Spontaneous insertion of OmpF (green) into the membrane of CX4/LCG-loaded liposomes. Protamine (blue) enters the liposome through OmpF and displaces LCG from CX4 to result in a switch-on fluorescence response. The supramolecular tandem membrane assay allows monitoring of the translocation of protamine through the LCG fluorescence response. Modified from ref.[79]

For the actual membrane assays, the reporter pair was encapsulated into the liposomes, Figure 2.1.3. Direct addition of protamine to a solution of liposomes containing the reporter pair did not trigger a fluorescence response, which provided direct spectroscopic evidence that protamine did not permeate on its own through the selected lipid membrane

under our experimental conditions and the investigated time scale, i.e., up to 10 hrs (Figure 2.1.4a). Of course, since there was no fluorescence response it could also be ruled out that protamine causes any pore formation in liposomes (as independently confirmed with a conventional carboxyfluorescein assay, SI Figure 1.3), or any fusion of liposomes, which was independently confirmed by a constant size distribution (SI Figure 1.2).

However, when channel protein OmpF was administered to a solution containing both, liposomes loaded with reporter pair and protamine as an analyte in the extravesicular phase, a steep increase in fluorescence was observed (Figure 2.1.4b), implying that OmpF facilitated the uptake of polycationic peptide into the interior of the liposomes. To ensure that these critical findings were not some experimental artefacts – for example, leakage of CX4 or LCG through OmpF – control experiments were carried out (Figure 2.1.4 c & d).

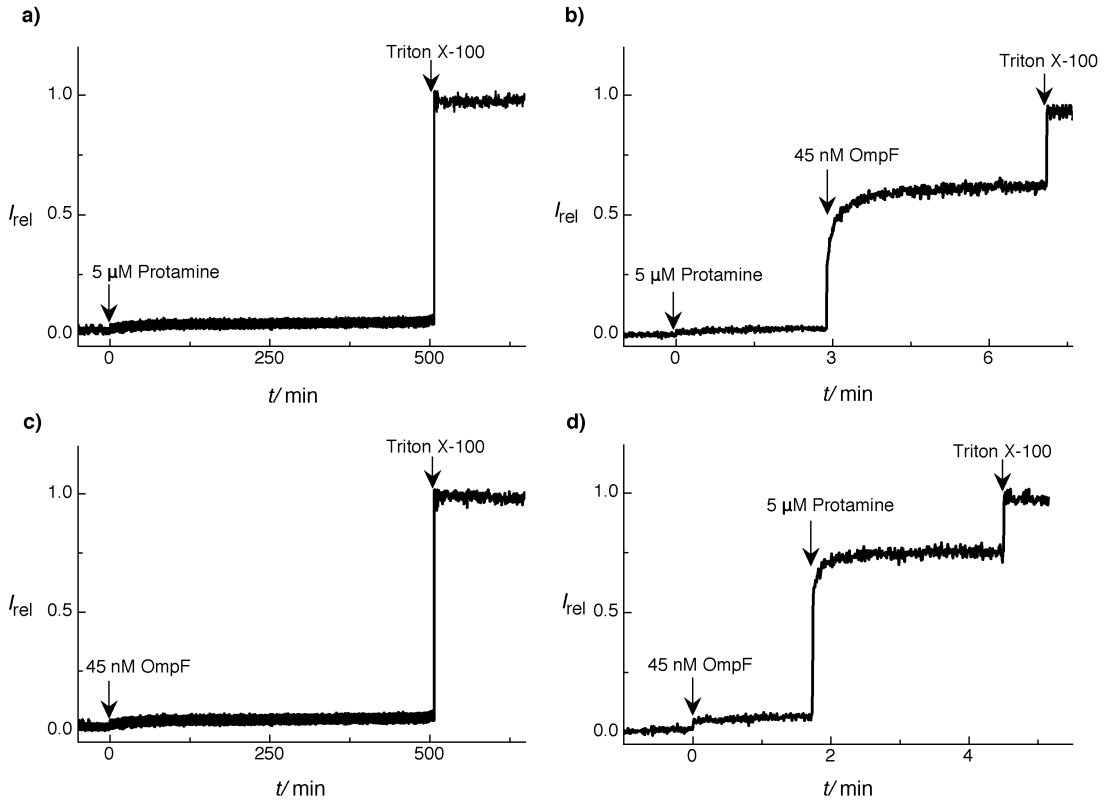

Figure 2.1.4: a–d) Fluorescence intensity of CX4•LCG-loaded liposomes (λ_{exc} = 367 nm and λ_{obs} = 500 nm) upon addition of a) 5 µM protamine; b) 5 µM protamine, and subsequently 45 nM OmpF; c) 45 nM OmpF; d) 45 nM OmpF followed by 5 µM protamine. Modified from ref.[79]

Our first control experiment was to verify that CX4 or LCG did not diffuse through OmpF. This was easily proven by the lack of fluorescence change when OmpF was injected into CX4•LCG-loaded liposomes in the absence of protamine. In this case, i.e. with liposomes already containing OmpF, a fluorescence change was only observed upon addition of protamine (Fig. 2.14c & d). This proved that neither the host nor the dye escaped through the channel, and the fluorescence change was only observed upon addition of protamine to the liposomes already containing OmpF. It should be noted that the detergent n-octylpolyoxyethylene (Octyl-POE) is implicitly added along with OmpF, therefore our second control experiment was to demonstrate that the detergent is not responsible for protamine translocation. This was concluded from a negative control experiment with the same amount of neat detergent (SI Figure 1.3). In the backdrop of the results presented so far, we were able to conclude that translocation of protamine into liposomes is mediated by channel protein OmpF.

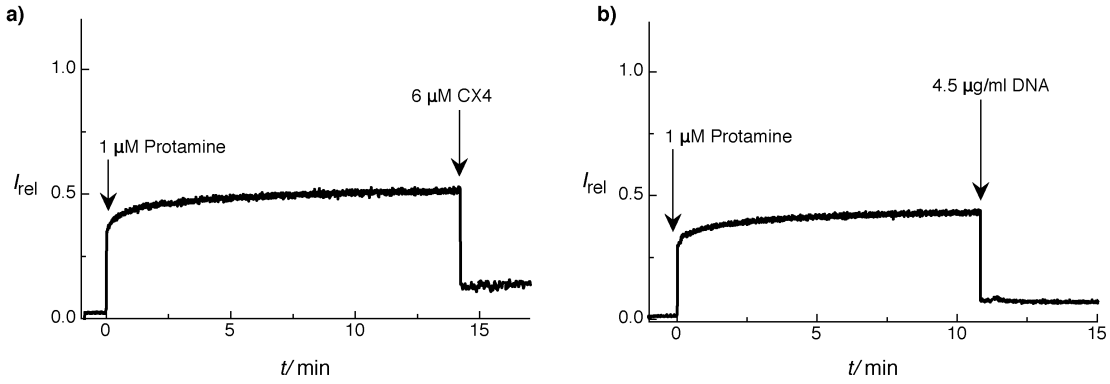

Figure 2.1.5: a & b) Change in fluorescence intensity of CX4•LCG-loaded liposomes containing 30 nM OmpF upon addition of 1 µM of protamine (t = 0 min), and, subsequently, a) 6 µM of CX4 at t = 14 min or b) 4.5 mg/ml DNA at t = 11 min.

2.1.3. Influx and Efflux Tandem Membrane Assays

We additionally used the tandem membrane assay to provide evidence that the translocation of protamine through OmpF is reversible. For this purpose, protamine was first added to the preformed proteoliposomes containing the reporter pair which resulted in the expected influx of protamine and the associated increase in fluorescence (Figure 2.1.5). When, in a second step, an excess of CX4 (Figure 2.1.5a) or a natural protamine binder

(DNA, Figure 2.1.5b) were added to the solution, a steep drop in fluorescence was observed, signalling an effective and fast efflux of protamine from the liposomes This is due to the fact that both CX4 and DNA bind strongly to protamine, and thereby lower the effective concentration of free protamine. In other words, it is possible to first observe the translocation of protamine into the liposomes and subsequently invert the concentration gradient by addition of competitive binder to the aqueous bulk. The influx-efflux experiment also demonstrated that the reporter pair inside the liposomes had remained intact. It also rules out the unlikely possibility that protamine first enters the liposome and subsequently facilitates the efflux of either host or dye, in which case no reversibility would have been expected.

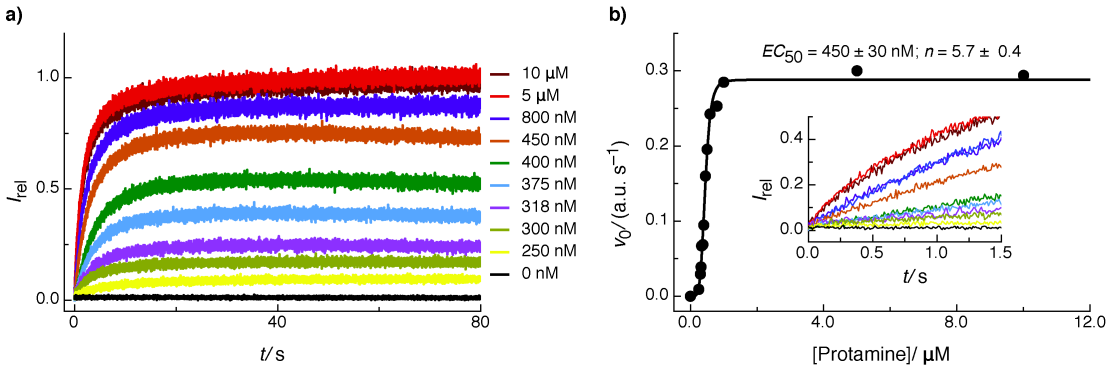

Figure 2.1.6: Stopped-flow tandem membrane assay experiments in 10 mM sodium phosphate buffer at pH 7.0 and 25 °C. a) Fluorescence kinetic traces upon mixing of protamine (0–10 µM) with a solution of OmpF reconstituted CX4•LCG-loaded liposomes. b) Fitting of initial rates of translocation at different protamine concentrations, by Hill equation.[104] Inset: The initial rate increases with protamine concentration. Modified from ref.[79]

2.1.4. Kinetic Analysis of the OmpF-mediated Translocation of Protamine

In order to accurately measure the translocation kinetics of protamine through OmpF (Figure 2.1.4b), fluorescence stopped-flow measurements were carried out. Different concentrations of protamine were rapidly mixed with liposomes containing CX4•LCG reporter pair and OmpF channels (Figure 2.1.6a). Increasing the protamine concentrations resulted in a faster kinetics and a higher final fluorescence intensity, which reached a plateau at high protamine concentration. This demonstrated that the translocation rate reached a

limiting value and that the displacement became quantitative at higher protamine concentration in the liposomes reconstituted with OmpF channels.[79] Indeed, channel protein-mediated translocation resembles enzyme kinetics in that the rates of both processes reach a limiting value at high substrate/analyte concentrations.[104] Hill analysis of the initial translocation rates at varying protamine concentrations yielded a half-saturation constant (EC_{50}) of 450 nM with a Hill slope of ca. 6 (Figure 2.1.6b).[79]

The lipid-peptide interaction between negatively charged liposomes and positively charged peptide is well recognized.[105] We speculated if similar interactions existed with neutral liposomes (liposomes made entirely of POPC) and if such lipid-peptide interactions had any impact on the translocation of protamine through OmpF. Indeed, the adsorption of protamine to POPC liposomes was corroborated by zeta potential measurement, which afforded a negative surface charge for POPC liposome that was effectively neutralized upon addition of ca. 500 nM protamine (SI Figure 1.5). In addition, we were able to demonstrate that the effective concentration of free protamine available for translocation was reduced by the adsorption to the external liposomal surface.

2.1.5. Tuning the Rate of Protamine Translocation

Expectedly, the rate of protamine translocation into liposomes increases with the number of channels per liposome, and – although it cannot be ensured that the channels are evenly distributed over all liposomes – this number is expected to increase proportionally with concentration of added channel (Figure 2.1.7a). Accordingly, a concentration range between 30–50 nM was preferred in our experiments, because it presented a compromise between high fluorescence response, fast translocation rates, and economical use of the purified OmpF samples (including mutants).

Translocation processes through channel proteins resemble enzymatic reactions also in the sense that both can be competitively inhibited and modulated by mutations that alter the protein functionality. Various transmembrane channels are co-regulated by polyamines[99,106] and, among them, spermine is the most potent inhibitor of the OmpF channel.[106] Indeed, when we conducted the tandem assay at different concentrations of spermine, the translocation rate, as depicted by the fluorescence response, decreased (Figure

2.1.7b) with increasing spermine concentration, and the dose response curve afforded an IC_{50} of 820±20 nM. Using the equation, $K_i = IC_{50}/(1 + ([\text{Protamine}]/ EC_{50})$ and EC_{50} = 445 nM we obatined a K_i value of ca. 70 nM which corresponded well to a literature estimate (low nanomolar range).[106,107] Incidentally, since spermine is known to anchor at the constriction region of the OmpF channel,[107] the efficient inhibition of protamine translocation also demonstrates that this analyte indeed passes *through* the OmpF channel and not, to rule out a less likely detour, along the outer walls of the protein, i.e., along the lipid-protein interface.[79]

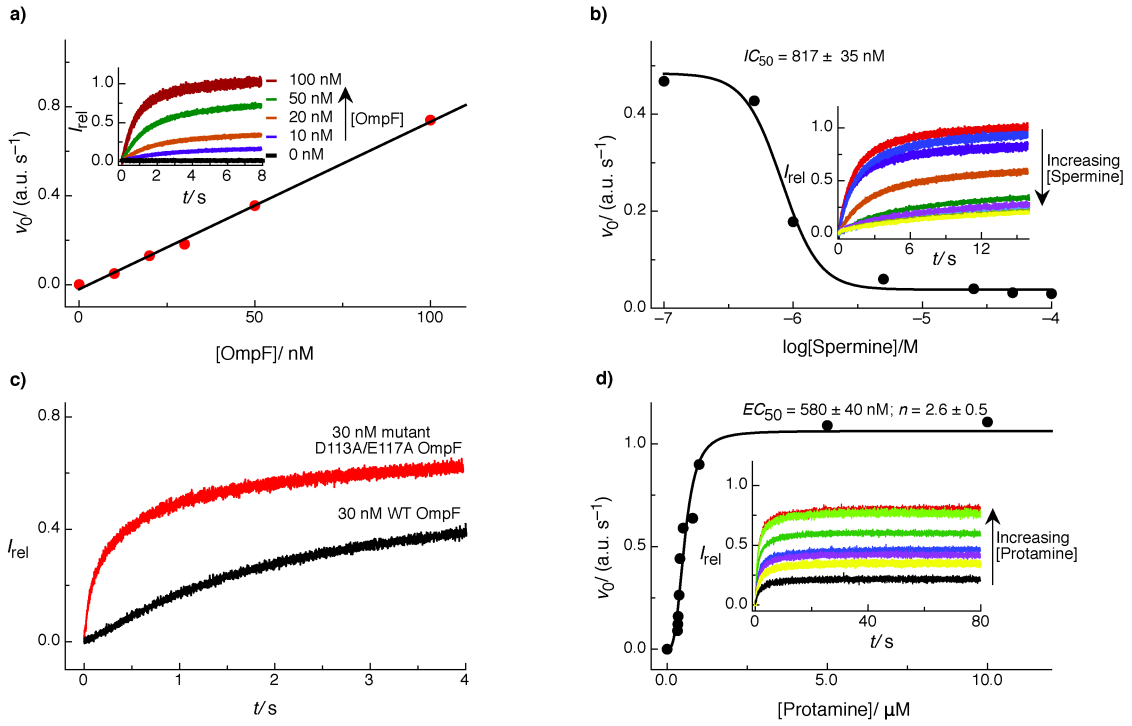

Figure 2.1.7: a) Initial translocation rates for varying concentrations of OmpF channels. Inset: Stopped-flow fluorescence measurements using CX4•LCG-loaded liposomes with varying concentration of OmpF (0–100 nM) and 20 µM protamine. b) Dose-response curve for the inhibition of protamine translocation by spermine. Inset: The fluorescence kinetics at various spermine concentrations (0–100 µM). c) Fluorescence kinetics of protamine translocation through wild-type OmpF and through the double mutant D113A/E117A OmpF. The reaction was initiated by adding 5 µM protamine to the CX4•LCG-loaded proteoliposomes. d) Initial rates of protamine translocation through the mutant D113A/E117A OmpF (10 nM) plotted against protamine concentration. Inset: fluorescence kinetics at various protamine concentrations. Due to the faster translocation kinetics of the mutant (see panel c) a lower channel concentration was employed. Modified from ref.[79]

The constriction region of OmpF presents the bottleneck for the translocation of molecules, including hydrophilic antibiotics such as ampicillin and penicillin.[108] Inspired by previous electrophysiological studies where an enhanced uptake of such beta-lactam antibiotics through singly substituted OmpF mutants D113A and R132A were reported,[100] we wanted to investigate if the flux of protamine was also affected by the charge and size of the OmpF channel. With that in mind, we selected a doubly substituted OmpF mutant, whereby, the two negatively charged residues aspartate 113 and glutamate 117 were replaced by alanine through site-directed mutagenesis, and indeed, the rate of protamine influx via D113A/E117A OmpF increased threefold (Figure 2.1.7c & d). While the arguments that account for the faster translocation kinetics are transferrable from those used in the electrophysiological studies,[100] particularly a decrease in residue-substrate interactions, supramolecular tandem membrane assays allow the direct monitoring of the translocation kinetics of an antimicrobial peptide by fluorescence.

2.1.6. Translocation of Heptaarginine and Acetylcholine Through OmpF

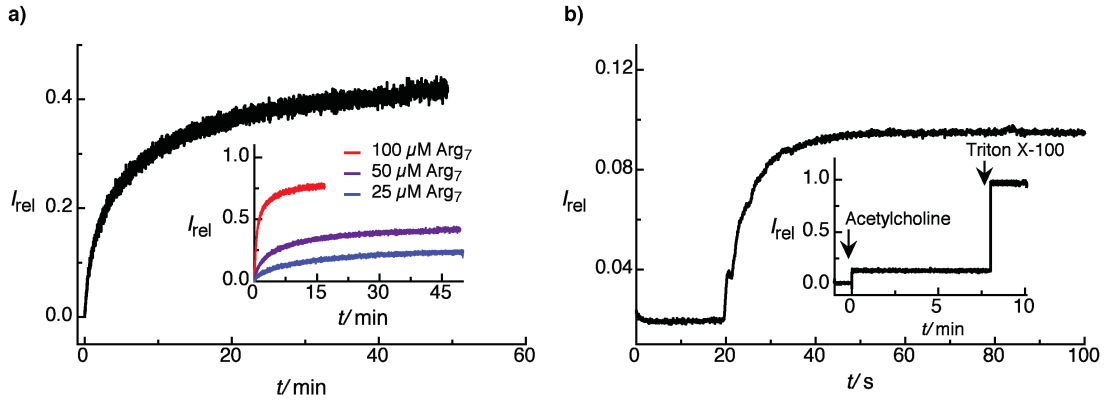

Figure 2.1.8: Translocation kinetics upon mixing a) 50 μM Arg_7 (stopped-flow experiment, inset: at different concentrations) and, b) 500 μM acetylcholine with a solution of CX4•LCG-containing OmpF proteoliposomes. Inset: Steady-state fluorescence measurement of acetylcholine translocation. Adapted from ref.[79]

While, we have focused on a singular substrate/channel pair the general approach is transferable to other classes of biological analytes. For example, the tandem assay principle was used to demonstrate the successful translocation of heptaarginine (Arg_7), a shorter

oligopeptide, and also of acetylcholine, a low molecular weight neurotransmitter through OmpF (Figure 2.1.8).

2.2. A SUPRAMOLECULAR FLUORESCENCE-BASED METHOD TO QUANTIFY LIPID-BILAYER MEMBRANE PERMEABILITY OF ORGANIC COMPOUNDS BY REAL-TIME KINETICS

In earlier section of this chapter, we introduced a label-free technique based on selective encapsulation of sensing ensemble composed of macrocycle•fluorescent dye complexes to monitor translocation of peptides through channel proteins. In this section we will demonstrate the applicability of tandem membrane assays as an economic, facile and versatile method to investigate the diffusion of molecules through phospholipid bilayer. Four significant advances in tandem membrane assays are described in this chapter.

- First, in addition to dye displacement approach (Chapter 1) a new mode of signal transduction is introduced in this study – associative binding assay
- Second, passive diffusion of more than 90 compounds are investigated.
- Third, kinetics of membrane diffusion for 28 different analytes is provided.
- Fourth, the utility of supramolecular tandem membrane assays is transferred to giant unilamellar vesicles, allowing the use of confocal microscopy technique, and microplate readers.

2.2. A SUPRAMOLECULAR FLUORESCENCE-BASED METHOD TO QUANTIFY LIPID-BILAYER MEMBRANE PERMEABILITY OF ORGANIC COMPOUNDS BY REAL-TIME KINETICS

The permeability of molecules through biological membranes is a fundamental physicochemical property which to a large degree narrows down their potential modes of biological actions, because cell membranes prevent unregulated influx/efflux of nutrients, neurotransmitters, pharmaceutical drugs, or building blocks. Equally important, membranes also act as the first defense layer to restrict the entry of undesirable chemical "intruders". Facile and robust screening methods allowing the quantification of the membrane-permeability of molecules, in particular organic compounds, are therefore in high demand, for instance to evaluate their pharmacokinetic properties (drugs) or potential risk (toxins).

The passive diffusion of molecules through lipid membranes is a prominent route of entry for most xenobiotics.[109] Over the years, various methods have been described in the literature,[110-112] of which two methods have become particularly prominent for permeability screening, the Caco-2 cell permeability assay and the parallel artificial membrane assay (PAMPA).[113] The Caco-2 assays mimic the passage of molecules through intestinal mucosa by exploiting the tight film formation of human epithelial colorectal adenocarcinoma cells. Unfortunately, in addition to a slow turnaround time and high cost per assay, the method does not always reflect the passive diffusion of a particular compound through lipid membrane due to the presence of cellular transporters or efflux systems, whose involvement needs to be excluded through additional, tedious control experiments. The alternative PAMPA set-up allows for the rapid screening of the membrane permeability of a drug-candidate through several types of flat membranes, mostly phospholipids in inert organic solvent or hexadecane-based, at a lower, but still substantial cost per compound.[114-117] A persistent and only partially resolved issue with PAMPA assays is the chemical and physical difference between natural phospholipid and artificial membranes, which leads to both, false negatives and positives. Moreover, both Caco-2 and PAMPA require a sensitive analytical method to detect the molecules that have passed through the membrane(s). This is frequently HPLC-MS/MS,[118] in special cases UV, which leads to additional challenges in regard to the adaptability in high-throughput screening and high instrumental base costs. As another

severe limitation, neither the Caco-2 nor PAMPA assays allow real-time measurement of analyte permeation.

a)

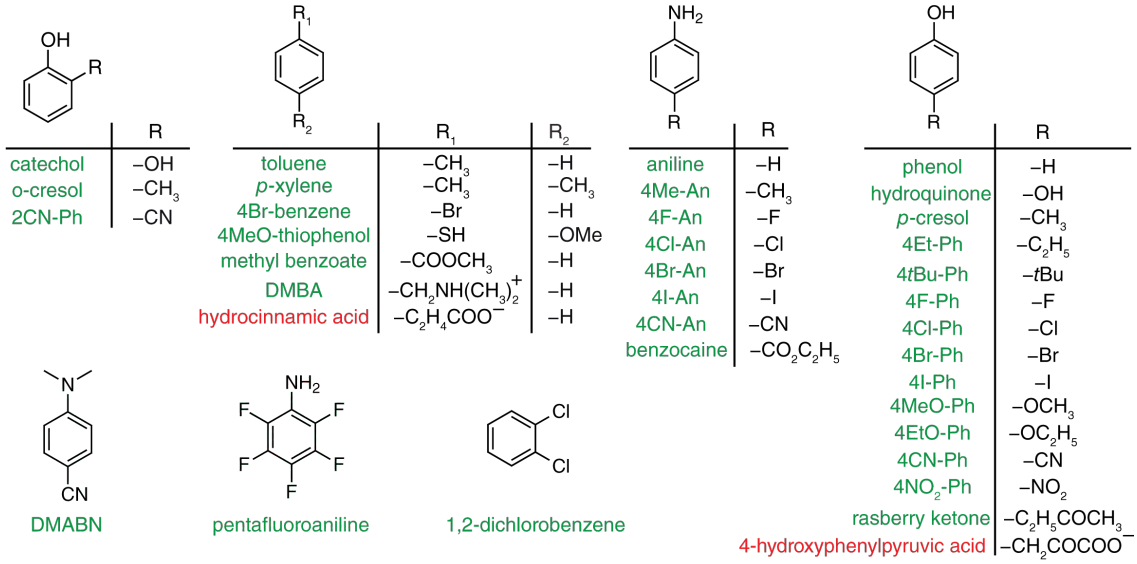

b)

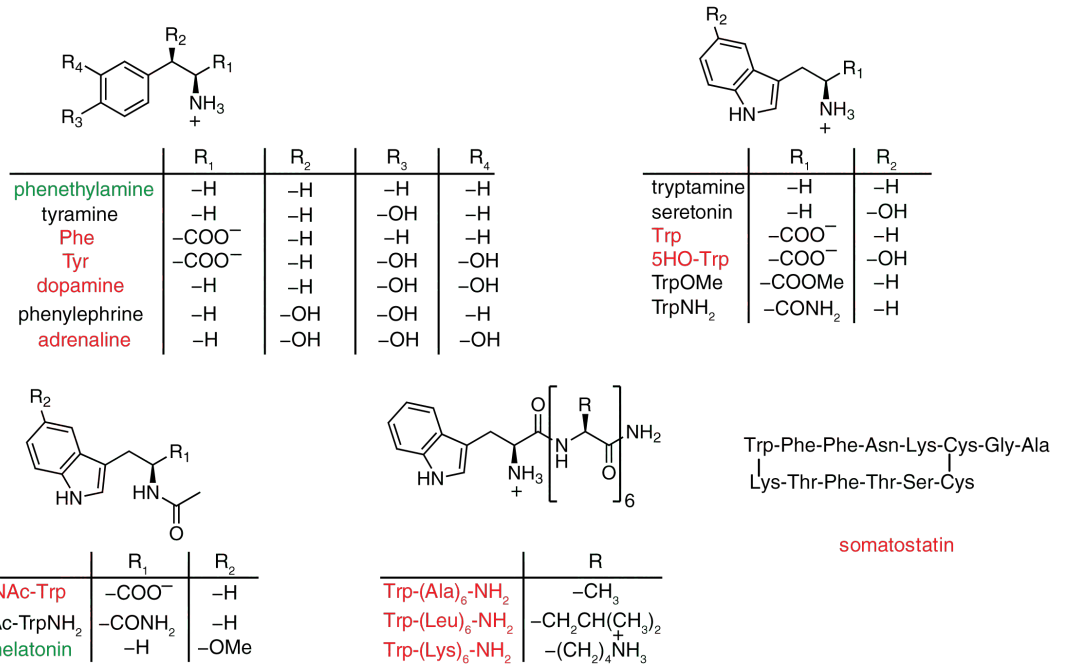

c)

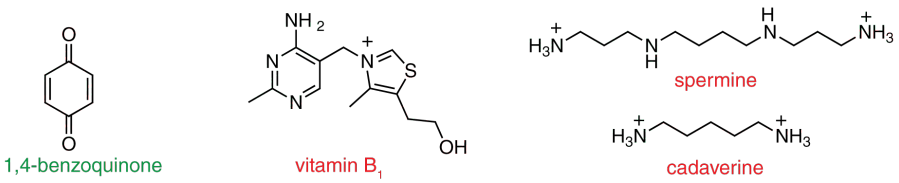

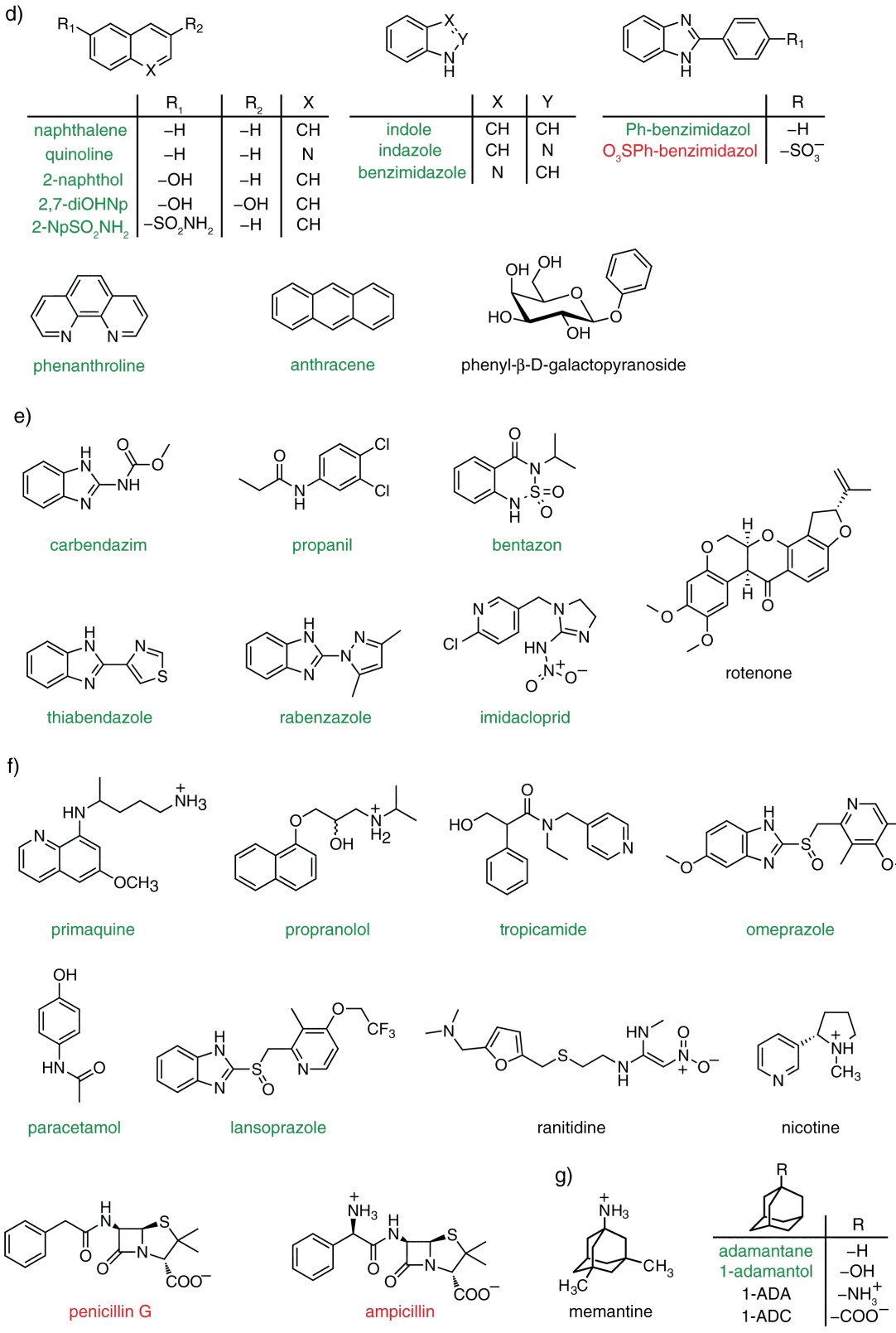

Figure 2.2.1: Chemical structures of compounds investigated in this study (color code: green: rapidly permeable, black: permeable, and red: impermeable), a) benzene derivatives, b) amino acid derivatives and peptides, c) miscellaneous compounds, d) polycyclic aromatic and heterocyclic compounds, e) drug molecules, f) adamantane derivatives, and g) pesticides.

The permeability of aromatic molecules, such as phenyl, indoyl, and napthyl species is of pivotal importance in pharmaceutical research, because approximately 80% of oral drugs contain at least one aromatic unit.[119] In addition, aryl moieties are ubiquitously occurring in toxins, biocides, and colorants. Finally, the natural aromatic amino acids tryptophan, phenylalanine and tyrosine are aromatic and derivatives thereof have important functions as hormones and neurotransmitters. While aromatic compounds are chromophoric, and thus in principle detectable by spectrophotometry, past experience has shown that generally 50-100 μM analyte loadings are required, which is often well above the solubility limit.[116] Consequently, an estimated fraction of 40% of all samples failed UV/Vis detection because of low solubility, low absorptivity or because their absorbance is restricted to the far UV spectral region.[118,120] This rationalizes why commercialized membrane permeation assays still need to resort to alternative detection techniques such as HPLC-MS/MS (see above), even for aromatic compounds. Owing to the sensitivity and ease of operation, fluorescence-based methods are arguably the most popular and sought after detection method. Thus, the development of fluorescence-based detection of membrane permeable substances has been a long-standing goal.[121,122] Most importantly, *label-free* assays are highly desirable since most analytes of interest are not emissive and structural modification with fluorescent dyes can largely influence their permeability properties.[85,87]

In a preliminary communication,[79] we have introduced a label-free emission-based supramolecular method to monitor membrane transport processes, for the special case of channel-protein assisted translocation of protamine, an antimicrobial peptide, through a phospholipid bilayer.[123] In such a supramolecular tandem membrane assay,[79] a host•dye complex is positioned in the inside of liposomes, which subsequently allows spatiotemporal monitoring of analyte influx (Figure 2.2.2). Until now, dye displacement has been employed for signal transduction which leads to either a fluorescence switch-off response (Figure 2.2.2a) or a switch-on response (not shown in Figure 2.2.2, see ref.[79]) as the analyte permeates through the membrane.[79] Now, we extend our methodological repertoire by using for the first time the fluorescence response of binary or ternary macrocyclic complexes of cucurbit[8]uril (CB8) for sensing (Figure 2.2.2b & c). This allowed us to not only realize an assay variant in which the analyte displaces a dye from a ternary complex (Figure 2.2.2b) but also an *associative* rather than dissociative variant, in which the analyte binds to a preassembled binary CB8•dye complex under formation of ternary complex with an altered

fluorescence (Figure 2.2.2c). In the last case, the analyte generally quenches the dye in the ternary complex (switch-off response, Figure 2.2.2c), while in rare cases (SI Figure 1.15a) new switch-on excimer fluorescence can emerge.

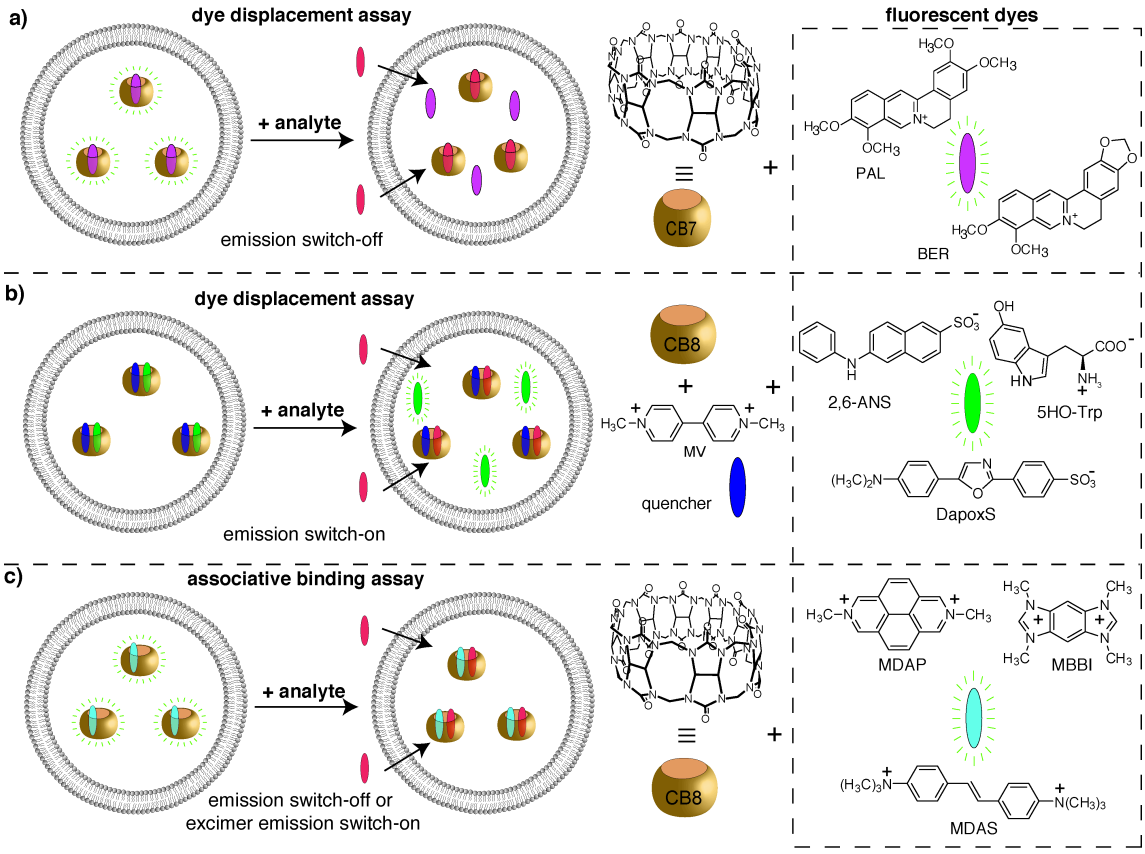

Figure 2.2.2: Supramolecular tandem membrane assays to monitor the diffusion of analytes through a lipid membrane: Displacement of the dye from a (a) host•dye or (b) host•dye•quencher complex by the analyte leads to reduction or enhancement in the emission intensity, respectively. c) Associative binding of the analyte with a host•dye complex results in emission quenching. Chemical structures of supramolecular sensing ensembles comprised of macrocycles, fluorescent dyes and a quencher are shown on the right.

Herein, we demonstrate that the tandem assay toolbox (Figure 2.2.2) establishes a novel, a powerful tool to screen the permeating propensities of organic aromatic molecules through biomembranes. A complimentary method to Caco-2 and PAMPA assays is now in hand, which remedies several shortcomings addressed above. We establish the method by characterizing the passive diffusion of more than 90 structurally diverse analytes (Figure 2.2.1) in real time, ranging from μs (stopped-flow fluorescence measurements) to hours

timescale (steady-state fluorescence). We demonstrate that nM to low μM analyte concentration are sufficient to continuously record the permeation profile in real time, and to unambiguously classify analytes as membrane permeable or impermeable. Furthermore, we illustrate the application potential for high-throughput screening by parallelized measurements in fluorescence multiplate reader format, and for imaging by microscopy of giant unilamellar vesicles (GUVs) as compartmentalized "cell" models to study analyte permeation into individual entities rather than performing ensemble measurements.

Results

2.2.1. CBn Macrocycles as Analyte-binding Units of the Chemosensing Ensembles

The glycoluril-based macrocycles cucurbit[7]uril (CB7) and cucurbit[8]uril (CB8) were chosen as molecular hosts because of their high affinity for a wide range of charged and non-charged organic guests in aqueous solution.[44,46,124-126] Furthermore, CB*n* macrocycles and their host-guest complexes were found to be membrane impermeable (see Supporting Information), which was an important prerequisite for their use in this study. Equally important, analyte binding can be coupled to a quantifiable spectroscopic response by precomplexing the host and a suitable dye under formation of a binary or ternary complex as chemosensing ensemble.[52,74,127-129]

*Detection of Analytes by Using Dye Displacement from the Chemosensing Ensembles***.** Complexation of dyes such as berberine (BE)[130] or palmatine (PAL)[131] by CB7 leads to an increase in their fluorescence quantum yield. Subsequent competitive *displacement* of the dye from such CB7•dye complexes upon analyte addition restores the fluorescence features of the dye in solution, *i.e.*, analyte detection is accomplished through a decrease in emission intensity (*switch-off* assay, Figure 2.2.2a).[79] Alternatively, the ability of CB8 to form 1:1:1 ternary complexes can be exploited to reversibly juxtapose a fluorescent dye such as 2-(phenylamino)-naphthalene-6-sulfonate (2,6-ANS) or dapoxyl sulfonate (DapoxS) right next to an efficient quencher such as methyl viologen (MV).[132-134] Upon addition of an analyte, the fluorescent dye, the quencher, or both are displaced from the CB8 cavity, which is invariably reflected in an increase in the emission intensity of the dye (*switch-on* assay, Figure 2.2.2b).[97,135]

Detection of Analytes by Using Associative Binding to a Fluorescent Receptor. Self-assembled binary complexes can also be selected as receptors; these consist of the large macrocycle CB8 and a fluorescent, dicationic dye, such as the fully N,N'-methylated variants of benzo-bis-imidazolium (MBBI),[127] 2,7-diazapyrene (MDAP),[136] and 4,4'-diaminostilbene (MDAS).[137] These fluorescent 1:1 CB8•dye complexes associatively bind aromatic moieties (*e.g.*, phenyl, naphthyl, and indoyl species) under formation of 1:1:1 CB8•dye•analyte complexes. This causes emission quenching of the dye (*switch-off* assay, 2.2.2c),[127,132,136,138] and, in special cases, the appearance of excimer-emission bands (SI Figure 1.15a).[44,124,132] An example for the latter is the combination of MDAS as dye and tryptophan-derivatives as analytes (Supporting Information). Noteworthy, the rational design of the auxiliary dye for CB8 does not only allow for tuning of the photophysical properties related to sensing, but also provides an additional handle for modifying the selectivity of the receptor for certain classes of analytes.[128]

Analyte Binding and Permeability. The response of the self-assembled CB*n*•dye complexes and CB8•quencher•dye complexes towards the addition of analytes was evaluated in homogenous solution by fluorescence titration experiments to verify and quantify binding to our chemosensors, Figure 2.2.3a. A detailed description of the experimental results can be found in the Supporting Information (SI Figure 1.6), see, in particular, Table S1 for binding constants. On account of the broad selectivity of cucurbit[*n*]uril-based receptors for many organic analytes, we were able to determine the permeability of almost 100 organic compounds, (Figure 2.2.1) through a rational choice of the chemosensing ensembles. The analyte library contained phenols, anilines, indoles, naphthalenes, polyaromatic hydrocarbons (PAC), benzimidazoles, pyridines, alkylated benzenes, halogenated aryl-species, quinolines, furans, adamantanes and alkyl amines. The analytes carried a wide range of electron-donating and electron-withdrawing functional groups (–COOR, –COOH, –CONHR, –COR, $–NH_2$, $–NR_2$, –OR, –OH, –SH, $–SO_2NH_2$, $–SO_3H$, –F, –Cl, –Br, –I, –CN, $–NO_2$, –ROOH). Subject to the adaptation of the chemosensing ensemble, all analytes were found to be compatible with the permeability assay method, demonstrating its broad applicability.[139-142] Representative analytes with immediate biological relevance are aromatic amino acids (*e.g.*, tryptophan), neurotransmitters (*e.g.*, serotonin), antibiotics (*e.g.*, penicillin

G), drugs (*e.g.*, memantine), herbicides (*e.g.*, propanil), fungicides (*e.g.*, thiabendazole), cancerogenics (*e.g.*, anthracene), toxins (*e.g.*, nicotine), food additives (*e.g.*, raspberry ketone), and bioactive peptides (*e.g.*, somatostatin).

2.2.2. Label-free Fluorescence-based Permeation Assays

Analytes that are capable of diffusing through the biomembrane caused either an increase or decrease in fluorescence intensity, depending on the encapsulated chemosensing ensemble inside the liposomes (Figure 2.2.2). For instance, using CB7•PAL–loaded liposomes, we were able to detect thpermeation of tyramine, a naturally occurring monoamine and phenylethylamine, a neuromodulator and transmitter, through a decrease in fluorescence response (displacement-assay, Figure 2.2.2a and Figure 2.2.3b). Non-permeating analytes, on the other hand, are not expected to cause significant change in the fluorescence response. Indeed, addition of the charged and hydrophilic, thus membrane-impermeable, vitamin B1 had an insignificant effect on the relative emission intensity (I_{rel}) of the CB7•PAL–loaded liposomes (Figure 2.2.3b). Reassuringly, similar observations for membrane-permeable and -impermeable analytes were made using CB7•BE as fluorescent chemosensing ensemble (SI Figure 1.7). Experiments carried out with liposomes loaded with CB8•dye and CB8•quencher•dye complexes led to the same pattern: Non-permeating analytes did not cause significant changes in fluorescence signal, whereas permeating analytes produced an increase in emission intensity (dye displacement from CB8•quencher•dye complexes, SI Figure 1.16) or a decrease (associative binding to CB8•dye complexes, SI Figure 1.9).

Figure 2.2.3c gives a representative example for the slow translocation of tryptamine, a neurotransmitter, through the phospholipid membrane, as monitored by four different chemosensing ensembles. Despite the contrasting fluorescence response (switch-on *vs.* switch-off) the rate constants were identical, within error. This provided compelling evidence that tandem membrane assays genuinely probe the diffusion rate of one and the same organic compound through the phospholipid membrane bilayer. Additional control experiments were carried out to ensure that the observable fluorescence changes were not due to the leakage of the reporter pairs; the emission remained unaffected for >100 min in the absence of analytes or in the presence non-permeating analytes, as for instance tested for somatostatin (>1000 min) with CB8•MBBI, see the Supporting Information (SI Figure 1.8). Moreover,

there was no change in the fluorescence signal upon analyte addition to dye-only-loaded liposomes, *i.e.*, in the *absence* of the CB*n* host. This demonstrated that the macrocycle was essential for molecular recognition and, thus, signal transduction (SI Figure 1.10b & 1.12).

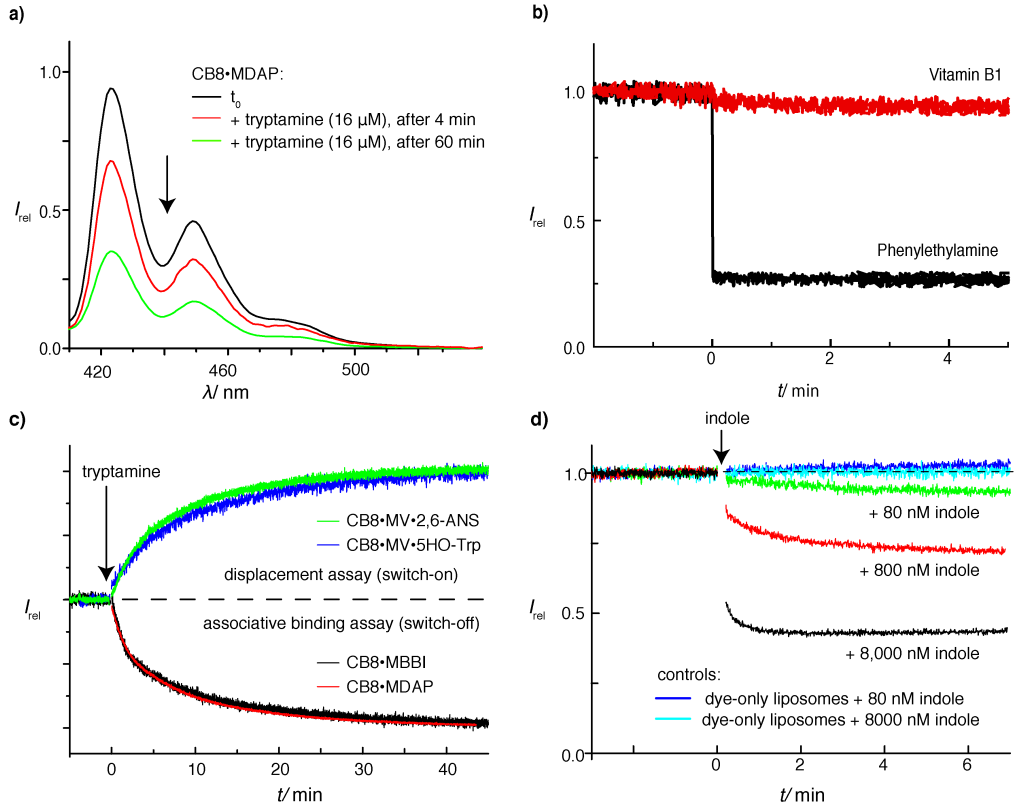

Figure 2.2.3: a) Fluorescence emission spectra of CB8•MDAP-loaded liposomes before and after addition of tryptamine. b) Evolution of fluorescence intensity upon addition of phenylethylamine and vitamin B1 to CB7•PAL-loaded liposomes (λ_{exc} = 347 nm, λ_{obs} = 500 nm). The experiments were carried out in 10 mM sodium phosphate buffer pH 7.0. c) Switch-on and switch-off fluorescence responses after addition of tryptamine to liposomes loaded with CB8•MV•2,6-ANS (λ_{exc} = 380 nm, λ_{obs} = 463 nm), CB8•MV•5OH–Trp (λ_{exc} = 310 nm, λ_{obs} = 337 nm), CB8•MBBI (λ_{exc} = 310 nm, λ_{obs} = 350 nm), and CB8•MDAP (λ_{exc} = 400 nm, λ_{obs} = 450 nm) liposomes. d) Normalized emission intensity (λ_{exc} = 310 nm, λ_{obs} = 350 nm) of CB8•MBBI-encapsulated liposomes upon addition of different amounts of indole. Control experiments with MBBI-loaded liposomes are also shown (blue traces). All experiments were carried out in 10 mM HEPES buffer, pH 7.

The series of experiments showed that typically an analyte loading of 10 μM is sufficient to differentiate permeating from non-permeating analytes, in particular when using the sensitive associative binding approach with CB8•dye receptors. In fact, for many high affinity analytes, such as indole and tryptamine, even sub-μM to nM concentration of the analyte resulted in a quantifiable response in the emission intensity (Figure 2.2.3d and SI Figure 1.12). For instance, 80 nM loading of indole was sufficient to confirm that it permeates through the membrane (Figure 2.2.3d). The successive addition of aliquots of analyte can be employed to unambiguously demonstrate that the analyte is responsible for the fluorescence response, see example for 2-methyl-phenol in SI Figure 1.10b. For displacement assays with CB7•dye and CB8•quencher•dye as chemosensing ensembles, low loadings (1-10 μM) were also sufficient to generate clear changes in emission intensity if the analyte binding was strong, *i.e.* on the order of the host•dye interaction (Figure 2.2.2b, Table S1, and SI Figure 1.7 & 1.16).

2.2.3. Kinetic Information on the Permeation of Analytes

Kinetic traces and parameters can now be readily obtained with our real-time optical detection method even for non-fluorescent analytes, whereas generally only the uptake of inherently spectroscopically active compounds such as labeled peptides and nanoparticles could be previously monitored in real time.[122,131,143,144]

Indeed, access to stopped-flow measurements, which are compatible with fluorescence detection, allowed us to resolve even "immediate" permeation processes ($t_{1/2}$ in the second range). A representative data set is shown in Figure 2.2.4a for the addition of phenol to CB8•MBBI-loaded liposomes. Fitting of the time-resolved emission intensities with monoexponential decay function (SI Figure 1.14) yielded the experimental rate constant (k_{obs}). A linear fit of k_{obs} *versus* the concentration of phenol yielded a slope of $(6.5 \pm 0.5) \times 10^4$ $M^{-1}s^{-1}$ (Figure 2.2.4b), which was assigned to the translocation rate (k_{trans}). However, since even the fastest permeation processes were much slower than the time scale of host-guest association processes, including the almost diffusion-limited rates for formation of CB7 and CB8 complexes,[129,130,145,146] it is invariably the membrane passage, and not the supramolecular recognition and signaling event, which is rate-determining. For 28 non-charged, rapidly

permeating aromatic analytes, apparent k_{obs} values, all obtained at a fixed analyte concentration of 40 μM to allow direct comparison, can be found in Table 2.2.1.

Table 2.2.1. Experimental rate constants (k_{obs}) for the permeation of non-charged aromatic analytes through liposomal POPS:POPC bilayer membranes and their corresponding octanol-water partition coefficients (log*P*) as well as van der Waals volumes (vdW).

Entry	Analytes	k_{obs} / (10^{-3} s^{-1}) [a]	log*P* [b]	vdW / (Å^3) [c]
1	4*t*Bu-Ph	0.062	3.4	160
2	Phenethylamine	0.22	1.4	134
3	4Et-Ph	0.24	2.6	127
4	2Me-Ph	0.33	2.1	110
5	4Me-Ph	0.40	2.1	110
6	pentafluoroaniline	0.51	2.0	111
7	DMABN	0.68	2.4	150
8	4I-Ph	0.69	3.0	122
9	4Br-Ph	1.6	2.5	115
10	4Cl-Ph	2.2	2.2	107
11	aniline-succinimide	2.2	0.87	175
12	benzimidazol	2.7	1.2	112
13	Ph	2.7	1.6	93
14	4F-Ph	2.8	1.8	96
15	4I-aniline	3.1	2.6	127
16	4Cl-aniline	4.0	1.8	112
17	4Br-aniline	4.0	2.1	119
18	4F-aniline	4.4	1.4	100
19	Indole	4.5	1.6	117
20	Indazole	5.0	1.4	112
21	4CN-aniline	6.5	1.3	116
22	Aniline	7.5	1.2	98
23	2CN-Ph	10	1.7	111
24	*p*-xylene	17	3.0	120
25	4NO_2-Ph	38	1.4	112
26	4CN-Ph	40	1.7	111
27	Propanil	120	2.7	179
28	Toluene	160	2.5	103

[a] Obtained from monoexponential fits for the fluorescence kinetic traces at 40 μM analyte concentration, *cf.* Figure 2.2.4a. [b] Calculated by using ChemDraw or [c] HyperChem.

We extended our kinetic investigation to the more complex case of charged analytes in order to illustrate how our real-time kinetic method can potentially be used to obtain novel biophysical information. For example, it is well accepted that the translocation of a

charged species requires the co-transport of a counter ion or the neutralization of the charge by a prior deprotonation step; both of which are expected to cause deviations from a simple mono-exponential kinetics and such multistep processes would also not be necessarily first-order in analyte concentration.[147,148] Indeed, clearly non-monoexponential kinetic traces were observed for charged, slowly permeating analytes, such as tryptamine (Figure 2.2.3c) or serotonin (SI Figure 1.9). Furthermore, the concentration dependence of the apparent translocation rate (k_{obs}), determined in an exploratory study through the initial rate method for the analyte NATA, showed clearly a non-linear behavior with saturation at high analyte concentration (SI Figure 1.14). Unlike the limited information available from state-of-the art end-point determination permeability assays, our membrane assays now allow ready access to the full kinetic traces (to pin-point multiexponential uptake) and rapid measurements of different analyte concentrations (to pin-point saturation behavior) which are likely to become indispensable tools in the mechanistic and kinetic analysis of membrane transport processes.

2.2.4. Transferring Tandem Membrane Assays on Other Instrumental Platforms: Giant Unilamellar Vesicles (GUVs) and Microplate Readers

Confocal Microscopy Experiments with Receptor-encapsulated GUVs. Giant unilamellar vesicles loaded with CB8•MDAP were prepared by using electroformation (see Materials and Methods).[149] In order to facilitate their use, we skipped a potential separation step to remove the non-encapsulated reporter pair from the buffer medium. Instead, the non-permeating analyte tryptophan was added to the media which saturates the binding sites of the non-encapsulated CB8•MDAP reporter pairs and, thus, quenches their emission. The inner compartment of the CB8•MDAP-encapsulated GUVs, however, remains available for analyte binding and, thus, emissive, Figure 2.2.4b. When the methyl ester of tryptophan (TrpOMe) as a representative slowly permeating analyte is added to this GUV solution in a second step, a gradual loss of the fluorescence emission from the interior of the GUVs over time is observed, indicating that TrpOMe reaches the GUV-encapsulated CB8•MDAP receptor complex (Figure 2.2.4c). As can be seen, the method is not limited to ensemble measurements in liposomal solutions, but can be extended to single objects such as GUVs (and possibly cells), allowing access to not only real temporal but also spatial resolution through confocal microscopy.

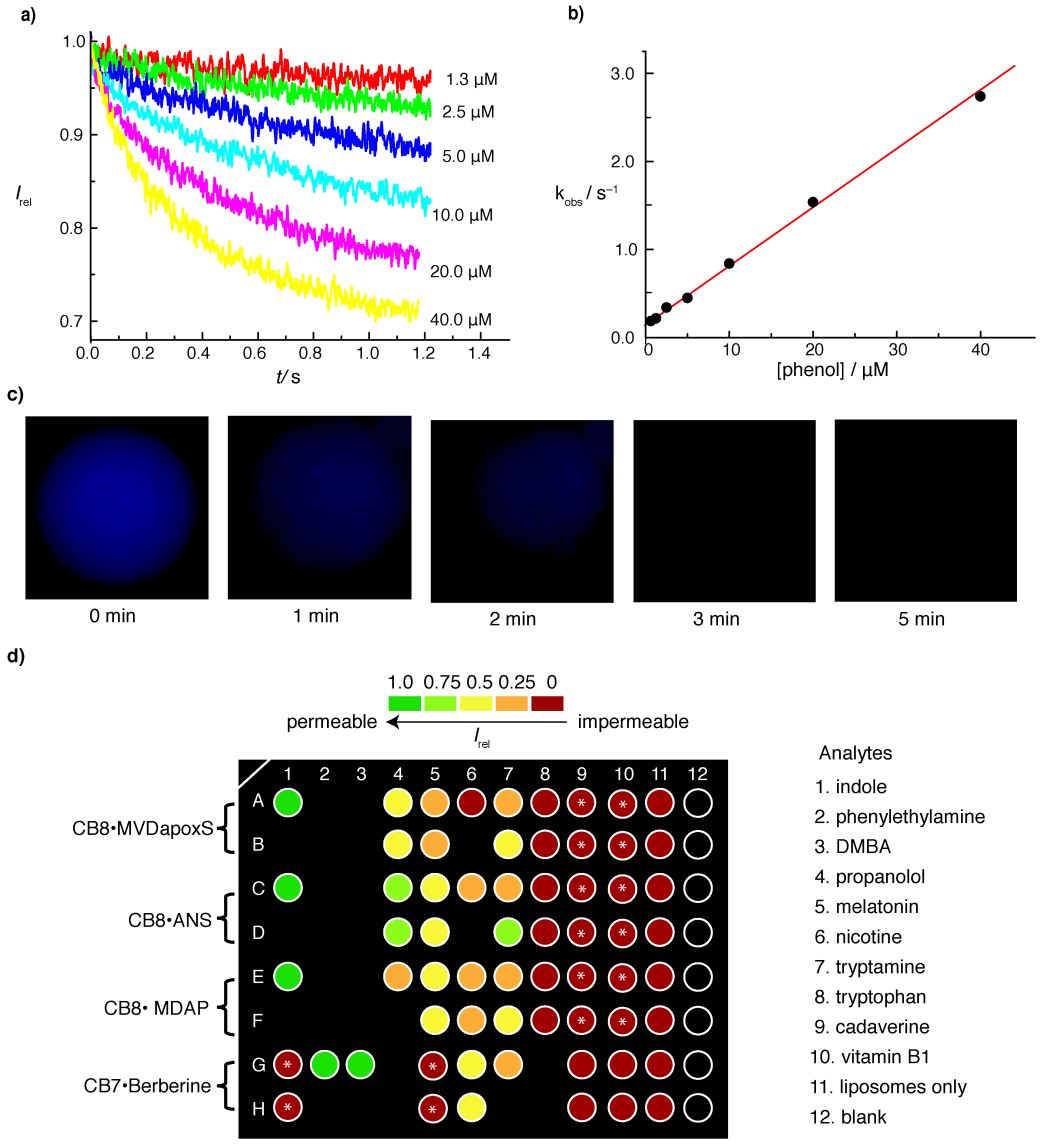

Figure 2.2.4: a) Kinetic traces from stopped-flow experiments of CB8•MBBI-loaded liposomes upon rapid mixing (1:1 v/v) with an aqueous solution of phenol. The labels refer to the analyte loading after mixing. b) Plot of k_{obs}, as obtained from monoexponential fits of the kinetic traces, *versus* the analyte loading. c) Time series of confocal microscopy images (G 365 nm, FT 395 nm and BP 420 nm) of a CB8•MDAP-loaded GUV after addition of 5 µL of TrpOMe (800 µM stock) to the medium. d) Microplate reader output obtained by adding 10 different biomolecules to reporter pair-loaded liposome solutions. The normalized changes in fluorescence intensities (I_{rel}) are color-coded (SI Figure 1.18-1.19). For each reporter pair, the first row and second row represent the change in I_{rel} 5 min and 60 min after analyte addition, respectively. Note that the lack of a fluorescence response of the wells

marked with (*) indicates insignificant or no binding of the particular analyte to the respective reporter pair.

Analyte Permeability Screening in Microplate Reader Format. Microplate readers are the instruments of choice when it comes to screening large libraries of compounds. One of the major concerns when transferring tandem membrane assays to microplate reader system was the non-specific adsorption of liposomes to the material surfaces of commonly available microplates, which could affect the stability of liposomes. Fortunately, by monitoring the change in fluorescence of chemosensor-loaded liposomes in the absence of analyte (Figure 2.2.4c, column 11), we were able to confirm the stability of the liposomes over several hours. Indeed, four different reporter pairs could be employed to screen the membrane permeability of 10 different compounds (Figure 2.2.4d). To illustrate, let us consider the diffusion of indole. A strong change in fluorescence was observed upon addition of indole to liposomes loaded with CB8•MVDapoxS (switch-on response), CB8•ANS (switch-on), and CB8•MDAP (switch-off), indicating a rapid passive diffusion of indole into liposomes contained in microwells (SI Figure 1.18-1.19). Note that for the particular case of indole as analyte, the fourth reporter pair (CB7•BE) did not produce a fluorescence response because indole has a low affinity to this receptor. In turn, this expected absence of a fluorescence response confirmed that the analyte does not cause any lysis of the liposomes (an unlikely possibility which needed to be ruled out); analyte-induced lysis, which is known, for example, for melittin, would invariably lead to a fluorescence response on account of a dilution effect (SI Figure 1.7).[79]

2.2.5 Discussion

With advances in the area of host-guest chemistry, there are now aqueous high-affinity receptors available that substantially enlarge the number of detectable analytes from simple metal cations to structurally diverse organic molecules.[11,150,151] Encapsulation of suitable, membrane impermeable receptors, such as *para*-sulfonated calixarenes, into compartmentalized entities such as liposomes, provides a novel, label-free, real-time method to detect analyte permeability through a lipid bilayer membrane, which we have shown recently for the channel assisted translocation of a peptide through a phospholipid bilayer.[79]

Apart from calixarenes and cyclodextrins, in particular, the glycoluril-based cucurbit[*n*]urils (CB*n*, n = 5-8, 10) macrocycles are receiving growing interest as molecular hosts for a wide range of organic analytes on account of their large affinities ranging from typically 10^3 - 10^{18} M^{-1} in aqueous solutions.[44,46,124-126] Most notably, the medium sized host CB7 (V_{cavity} = 242 $Å^3$) predominately binds aliphatic and aromatic compounds in a 1:1 stoichiometry,[44,48,59,124,152] whereas the larger host CB8 (V_{cavity} = 367 $Å^3$) has a preference for 2:1 or 1:1:1 ternary complex formation with a pair of two identical or different aromatic moieties.[44,88,124,125,132,133,153-155] Therefore, we have tested the utility of liposome encapsulated CB*n* macrocycles to address standing questions in membrane permeation research by extending our method to a wide range of biologically relevant analytes. CB*n* and their host guest complexes tested were membrane impermeable, as is required in our method. In addition, membrane impermeable dyes are also mandatory.

Detection with Dye Displacement versus Associative Binding. In order to obtain a truly functional receptor, the analyte binding event needs to provide an easily quantifiable and sensitive spectroscopic response.[15,150,151] For the systems presented herein, a sensitive fluorescence signal upon analyte binding was generated through either *i)* displacement of the fluorescent dye by the analsiyte from a CB7•dye or a CB8•quencher•dye complex, or *ii)* associative binding of the analyte to a fluorescent CB8•dye complex. The dye-displacement and the associative-binding approach possess each unique advantages and disadvantages, and are complementary.

Specifically, the dye displacement approach is applicable to *any* analyte that can be bound by a host, however, the affinity of the analyte for the host should be comparable or higher to that of the dye, *i.e.* K_a(analyte) ≥ K_a(dye).[74] Otherwise, a comparably high concentration of analyte is needed such that sensitive detection of analytes with a low affinity, for instance small molecules, can be problematic using dye displacement strategy. Conversely, associative binding of the analyte to the CB8•dye chemosensing ensemble does not "waste" binding energy to displace a dye, which enables high-sensitive detections even of small molecules. However, this sensing strategy is limited to *certain analyte classes.* For instance, the emission of the CB8•MBBI chemosensor is quenched by *aromatic* analytes whereas no exploitable changes in the emission properties of the reporter-dye would result if

"electronically inert" aliphatic analytes were bound in a 1:1:1 CB8•dye•analyte complexes. To further exemplify, only substantially electron-rich analyte classes (anilines, phenols and PACs but not simple benzenes) cause a significant change in the emissive properties of the CB8•MDAP chemosensor, because the excited state energy of MDAP is lower than of MBBI. The most analyte-restrictive chemosensor introduced herein is CB8•MDAS, which gives rise to an excimer emission in the presence of some tryptophan-species, but not with the parent chromophore indole and other aromatic analytes (benzenes, phenols, anilines).

In summary, dye displacement assays are a versatile "all-round" detection strategy that is in principle applicable to both aromatic and aliphatic analytes. The associative binding assays are limited to (some) aromatic analytes, but allows for a highly sensitive detection of analytes (*e.g.* 80 nM detection of indole and the ~10 μM detection of small-molecule benzenes). In fact, because of the predominant practical relevance of aromatic analytes as drugs, toxins, pollutants, etc., the majority of the herein demonstrated membrane-permeation assays were conducted using the associative binding detection-strategy.

Classification of Analytes with Respect to their Permeability. From the permeation experiments, we have classified analytes into non-permeating, permeating, and rapidly permeating – color-coded in Figure 2.2.1. It is generally accepted that most anionic species or those having a negatively charged functional group (*e.g.* aromatic amino acid derivatives,[156] ampicllin,[108]) are membrane impermeable, which can be rationalized by the Columbic repulsion by the analyte and the negatively charged phospholipid POPS:POPC bilayer membrane. Our experiments confirm this rational with the noteworthy exception of 2-adamantylcarboxylic acid, which is membrane permeable, albeit slower than its non-charged (2-adamantanol) and positively charged (2-aminoadamantane) analogues (SI Figure 1.15). In fact, lipidization of drugs through connection to adamantyl-moieties is a known approach to increase their membrane permeability and thus bioavailability.[157,158] Almost all neutral and positively charged species were found to be membrane permeable, unless they are large (such as peptides), very hydrophilic (such as dopamine[159]), or dicationic (such as the dyes MBBI, MDAP and MDAS). The positively charged neurotransmitters tryptamine, tyramine, and serotonin were shown to pass the membrane within several minutes to hours, where more hydrophilic species permeate slower, *e.g.* phenylethylamine > tyramine and tryptamine > serotonin. The slow membrane permeation of biologically occurring substances is not

surprising as many building blocks and signaling molecules need to be retained inside compartmentalized structures until their release is triggered. On the other hand, most non-charged small organic substances were found to penetrate through the phospholipid bilayer membrane within a few seconds, which is one reason for their toxic/irritant properties.

Rationalization of Permeability Trends. In order to obtain more detailed information about the membrane permeation process, time-resolved permeation data are required to test chemical intuition against biophysical models. We provide such data for a series of 28 non-charged guests in Table 1 representing permeation rates for some of the "most simple" organic aromatic molecules. It is not surprising that a combination of several factors affect the membrane permeability because the passive diffusion of chemical compounds through a lipid bilayer is a multi-step process that can be divided into *i*) analyte enrichment near/in the membrane, *ii*) diffusion through the membrane, and *iii*) exciting the membrane and diffusing away from it. It is therefore clear that hydrophilic analytes do not readily diffuse through a membrane, but less intuitively, also very hydrophobic analytes may be retained for some time in the membrane, slowing their overall translocation rate. Moreover, there is also a viscous force reducing the diffusion speed of large analytes through the membrane (viscosity of water = 1.0 cP, viscosity of a membrane = 57.2 cP).[160] To rationalize the apparent diffusion rates displayed in Table 1, macroscopic physiochemical parameters, such as lipophilicitiy (log*P*), molecular volume (vdW), polar surface area can be employed and yield correlations with the translocation rate that are in most cases in line with the chemical intuition. For example, more hydrophilic analytes permeate slower through the biomembrane, *e.g.* the k_{obs} of phenol (log*P* =1.64) is 20 times slower than that of toluene (log*P* = 2.52),[161] which is in analogy to the aforementioned low permeation-rate of charged species. Furthermore, an inverse correlation between the molecular vdW-volume and the permeation rate is nicely observed for the subset of alkyl, and halo – substituted phenols, whereby, k_{obs} for Ph > 4Me-Ph > 4Et-Ph > 4*t*Bu-Ph and 4F-Ph ≥ Ph > 4-Cl-Ph > 4-Br-Ph > 4I-Ph, *i.e.* larger species translocate slower. However, exceptions can be found even in our small exploratory set of experimentally determined rate-constants; 4-*tert*-butylphenol (4-*t*Bu–Ph) is more lipophilic (= less hydrophilic) and smaller than propranil but permeates much slower (factor 10^3) through the lipid bilayer. Such a counter-intuitive exception exemplifies the complexity of the passive diffusion through a membrane and provides interesting "test-

data" for the available membrane-transport models. It has been indeed discussed that highly lipophilic molecules (log*P* > 3) can be retained in the lipid membrane and therefore exit the membrane slowly, causing an overall decrease in the analyte translocation rate.[161,162]

The ease and real-time monitoring capability of our fluorescence-based method is major advantage over other high sensitivity detection with LC-MS/MS or radioactive labeling, recall for instance that charged analytes do not show a monoexponential permeation profile with time (see Results section), which is an important piece of experimental data to test and refine permeability models that is not available by simple end-point measurements. Our method will therefore likely find application to obtain reliable experimental data to test the predictions of physicochemical membrane transport models.

Application to Giant Unilamellar Vesicles as Cell-models. Among many lipid bilayer models, giant unilamellar vesicles, comes closest to mimicking cell membrane.[163] Therefore, we were curious if the tandem membrane assay could be used to monitor the passive diffusion of molecules into GUVs. It should be emphasized that most fluorescence-based GUV experiments reported to date to monitor passive diffusion through a lipid bilayer require a fluorescent analyte or a fluorescently labeled lipid.[164] A notable exception is the use of pH-sensitive dye loaded GUVs which were employed to monitor diffusion of low molecular weight carboxylic acids.[165] Herein we have demonstrated, a direct visualization of analyte diffusion through lipid bilayer using reporter pair CB8•MDAP encapsulated inside the GUVs (Figure 2.2.4c and SI Figure 1.17), which provides a direct verification that the chemosensor remains encapsulated inside the compartmentalized structure under the experimental conditions and that lysis of the membrane upon analyte addition does not occur.These findings open the door for future use of chemosensor encapsulated GUVs as cell models to detect the translocation of a variety of analytes across a membrane, both by passive diffusion or supported by transport proteins, with the help of confocal microscopy imaging.

Fluorescence-based label-free in vitro permeability assays are a valuable tool for researchers in both academic and industrial setting during design or optimization of novel compounds. In this work we have demonstrated that supramolecular tandem membrane assay can be employed to investigate diffusion though the lipid membrane for large variety of drugs, toxins and other organic compounds in real-time. In addition to qualitative

information about permeability of compounds, our assays were able to provide kinetic behavior of permeating compounds. This kinetic information are imperative to make predictions or "scientific common sense" for estimating and screening the phospholipid bilayer permeating properties of existing and novel compounds. The relative ease with which the method is transferred to various instrumental setups (microplate reader, confocal imaging) suggests that the method has the potential to outperform existing techniques.

– Chapter 3–
Supramolecular Tandem Protease Assays

3. Supramolecular Tandem Protease Assays

This chapter is derived from the contents of following two publications.

1. Ghale, G., Ramalingam, V., Urbach, A. R. & Nau, W. M. Determining protease substrate selectivity and inhibition by label-free supramolecular tandem enzyme assays. *J. Am. Chem. Soc.* **133**, 7528-7535 (2011).
2. Ghale, G., Kuhnert, N., Nau, W. M. Monitoring stepwise proteolytic degradation of peptides by supramolecular domino tandem assays and mass spectrometry for trypsin and leucine aminopeptidase, *Nat. Prod. Commun.* **7**, 343-348 (2012).

The first-generation of tandem enzyme assays targeted low molecular weight metabolites, whereby the entire analyte was immersed into the macrocyclic cavity (Figure 1.2.4). Here we introduce the applicability of macrocyclic host•fluorophore sensing ensembles to investigate enzymatic transformations of large biomolecules such as peptides. In this second-generation tandem enzyme assays, it is not a substrate (peptide) as a whole that is recognized by a macrocyclic receptor, rather it is a residue of the substrate (e.g., aromatic amino acid for CB7) that functions as a recognition motif. Following are the highlights of this chapter.

- Development of label-free fluorescence based assays for proteases – an exploratory study using thermolysin.
- Absolute kinetic parameters were extracted from the fluorescence signal generated by enzymatic transformation. This allowed us to profile the substrate specificity of protease. Additionally, the fluorescence signal also served as a signature of expected products of proteolysis.
- Peptide fingerprinting by recording fluorescence response during stepwise proteolytic degradation of a peptide.

3.3. Supramolecular Tandem Enzyme Assays to Monitor Protease-Catalyzed Reactions – An Exploratory Study Using Thermolysin

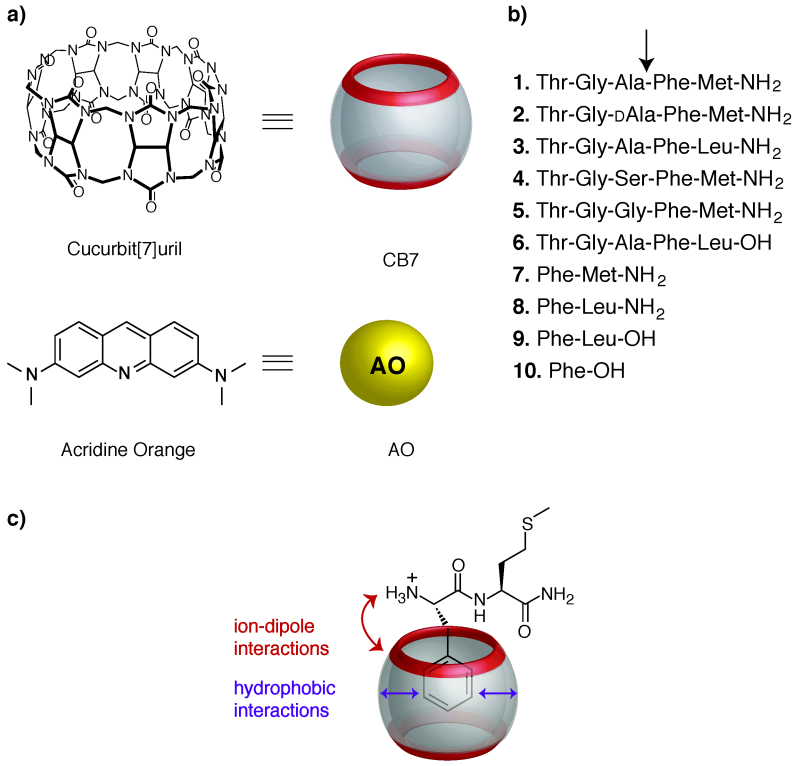

Figure 3.1.1: a) Chemical structures of supramolecular chemosensor composed of a macrocyclic host CB7 and a fluorescent dye AO. b) Sequences of peptide (substrates, **1 –6**) and their corresponding hydrolytic product (**7–10**). The arrow indicates the cleavage site for thermolysin. c) Hydrophobic interactions between the CB7 cavity and the aromatic ring of *N*-terminal phenylalanine (Phe) is augmented with ion-dipole interactions. From ref.[51]

In order to develop a label free protease assay and expand the tandem enzyme assays for structurally more complex, high molecular weight analytes, we selected thermolysin and enkephalin-based peptides as our protease/substrate pair. Thermolysin is a metalloendopeptidase that cleaves amide bond at the *N*-terminal of bulky hydrophobic amino acids like Phe and Leu.[51] Enkephalin based peptides are similar to neurological pentapeptides of sequence Tyr-Gly-Gly-Phe-Met-OH or Tyr-Gly-Gly-Phe-Leu-OH which

are hydrolyzed at the Gly–Phe bond by thermolysin. The list of enkephalin-based peptides investigated in our study is given in Figure 3.1.1b.

Table 3.1: Binding constants (K) of peptides **1-9** and an amino acid **10** with CB7 and proteolytic constants (k_{cat}/K_M) for their reaction with thermolysin.

Entry	Peptide sequence	K/(10^4 M^{-1})[a]	k_{cat}/K_M /(10^4 s^{-1} M^{-1})[b]
1	Thr-Gly-Ala-Phe-Met-NH_2	1.3	14
2	Thr-Gly-DAla-Phe-Met-NH_2	2.6	≤0.005[c]
3	Thr-Gly-Ala-Phe-Leu-NH_2	0.35	3.2[d]
4	Thr-Gly-Ser-Phe-Met-NH_2	1.9	6.9
5	Thr-Gly-Gly-Phe-Met-NH_2	1.4	2.3
6	Thr-Gly-Ala-Phe-Leu-OH	0.18	1.2
7	Phe-Met-NH_2	1500±500	[e]
8	Phe-Leu-NH_2	2700±1500	[e]
9	Phe-Leu-OH	210	[e]
10	Phe-OH	2.0 [2.5][f]	[e]
11	Phosphoramidon	0.12	[g]

[a] Determined by competitive dye displacement (SI Figure 2.1). [b]Determined by supramolecular tandem enzyme assay at varying peptide concentrations (5-55 μM, n = 5-6), *cf.* Figure 3.1.3; the kinetic parameters were determined by nonlinear regression. [c] Insignificant hydrolysis due to the presence of DAla. [d] The kinetic parameter represents the rate of hydrolysis of Ala-Phe bond by thermolysin. [e] No conversion detected due to Phe *N* terminus. [f] In 0.1 M aqueous NaCl solution.[166] Phosphoramidon was employed as an inhibitor for thermolysin. Adapted from ref.[51]

Recall that the choice of a macrocyclic receptor and fluorescent dye is critical to the design of tandem enzyme assay (Chapter 1.1.4). First we needed to identify a suitable macrocyclic receptor that is able to recognize and differentiate the substrate and the corresponding products. Since our substrate was a peptide, we looked into macrocycles that are able to bind amino acids. Given our previous experiences with aromatic amino acids with macrocycles from CBn family, CB7 was the most viable option.[48,49] CB7 and CB8 are able to recognize and bind aromatic amino acids. Owing to the hydrophobic cavity and the negatively charged portals of CBs, the binding affinity of CBs towards a guest molecule is

driven by both hydrophobic and ion–dipole interactions (Figure 3.1.1c).[133,167,168] As a result, the binding of CBs to *N*-terminal aromatic amino acid is substantially higher than that to internal or *C*-terminal aromatic amino acids. Therefore, by exploiting these differences in the binding affinity of CBs with the aromatic amino acids in a peptide, supramolecular tandem enzyme assays for proteases using unlabelled substrate was designed.

Next, we chose acridine orange (AO) as a fluorescent dye. AO is a weakly fluorescent dye, however upon encapsulation by CB7 (K = 2.9 × 10^5 M^{-1}), the fluorescence intensity of AO is significantly enhanced. After the selection of CB7•AO as our reporter pair we carried out competitive fluorescence titration experiments with the substrates and the corresponding product of interest, i.e. dipeptides, Table 3.1. This is important to ensure that the binding of CB7 with AO is in between the substrates and the corresponding product. Indeed, the binding affinity of CB7 varied from 3.5 × 10^3 M^{-1} for a substrate (peptide with an internal phenylalanine, no adjacent charges) up to 2.7 × 10^7 M^{-1} for the corresponding dipeptide product (*N*-terminal phenylalanine, adjacent ammonium site).

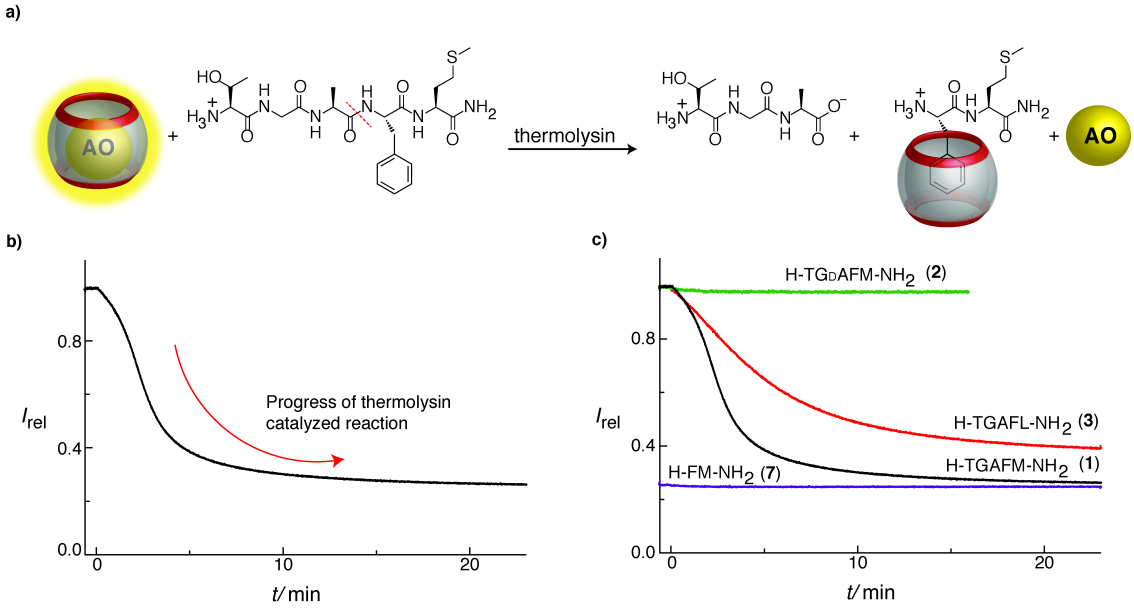

Figure 3.1.2: a) Supramolecular tandem enzyme assays for monitoring the activity of a protease thermolysin. b) The proteolytic activity of thermolysin on peptide **1** is reflected by a time-dependent decrease in fluorescence signal. c) Substrate selectivity of thermolysin monitored using CB7•AO reporter pair. Continuous fluorescent traces (λ_{exc} = 485 nm, λ_{obs} = 510 nm) were measured using (8 μM/0.5 μM), reaction upon addition of thermolysin (t = 0 min, 15 nM) to peptides **1-3** and **7** (30 μM), at 37 °C. Derived from ref.[51]

The working principle for protease assay is given by Figure 3.1.2. Behaving as a weak competitor, the peptide substrate allows the complexation of AO with CB7, indicated by an increase in fluorescence intensity. Upon addition of thermolysin, it selectively cleaves Gly-Phe bond, releasing a strong competitor, i.e. a dipeptide with *N*-terminal Phe residue, which then displaces the dye from CB7 cavity. As a result, the progress of thermolysin-catalyzed reaction can be seen as a decrease in fluorescence intensity.

3.1.1. Determination of Absolute Kinetic Parameters

While it was gratifying to develop a label free protease assay using supramolecular tandem enzyme assays, we wanted to take a step further and determine the absolute kinetic parameters. In order to do so, first, we chose the concentration of host such that it fell under the linear region of the host•dye titration curve (Figure 3.1.3a). Second, we calibrated the fluorescence response by independent titration of enzymatic products responsible for the signal generation (Figure 3.1.3b).

In detail, for each fluorescence trace, the intensity before the addition of the enzyme (I_0) was recorded (Figure 3.1.3c). As the enzymatic reaction progressed, the products (Phe-Met-NH_2, Phe-Leu-NH_2, Phe-Leu-OH) displaced the dye which is indicated by the decrease in fluorescence intensity. This change in fluorescence signal was correlated with the fluorescence intensity decrease observed in the direct titration by the products (Figure 3.1.3b). Consider the enzymatic trace of 5 μM of Thr-Gly-Ala-Phe-Met-NH_2 (Figure 3.1.3c, I_0 = 503 a.u.), as an example. The enzymatic reaction was initiated at t_0 = 1.3 min by adding thermolysin. From the direct titration, we knew that 1 μM of PheMet-NH_2 (the product derived from this substrate), reduces the fluorescence intensity by a factor of 1.2 (Figure 3.1.3b). In the enzymatic trace, the same drop (from I_0 = 503 to I_1 = 419 a.u.) was observed at t_1 = 3.0 min. Therefore, the rate was derived as v = 1 μM /1.7 min = 0.59 μM min^{-1}. For each substrate concentration, the amounts of products formed (read from the intensities I_1, I_2, etc.) were determined for at least 3 different times (t_1, t_2, etc.) after the addition of enzyme. These conversion rates were determined at 5-6 varying substrate concentrations, assuring [S] >> [E] to work within the Michaelis-Menten (MM) regime, and analyzed by nonlinear fitting according to the MM model.[169] The catalytic coefficients for each

investigated peptides are given in Table 3.1. This paragraph was derived from the supporting information of ref.[51]

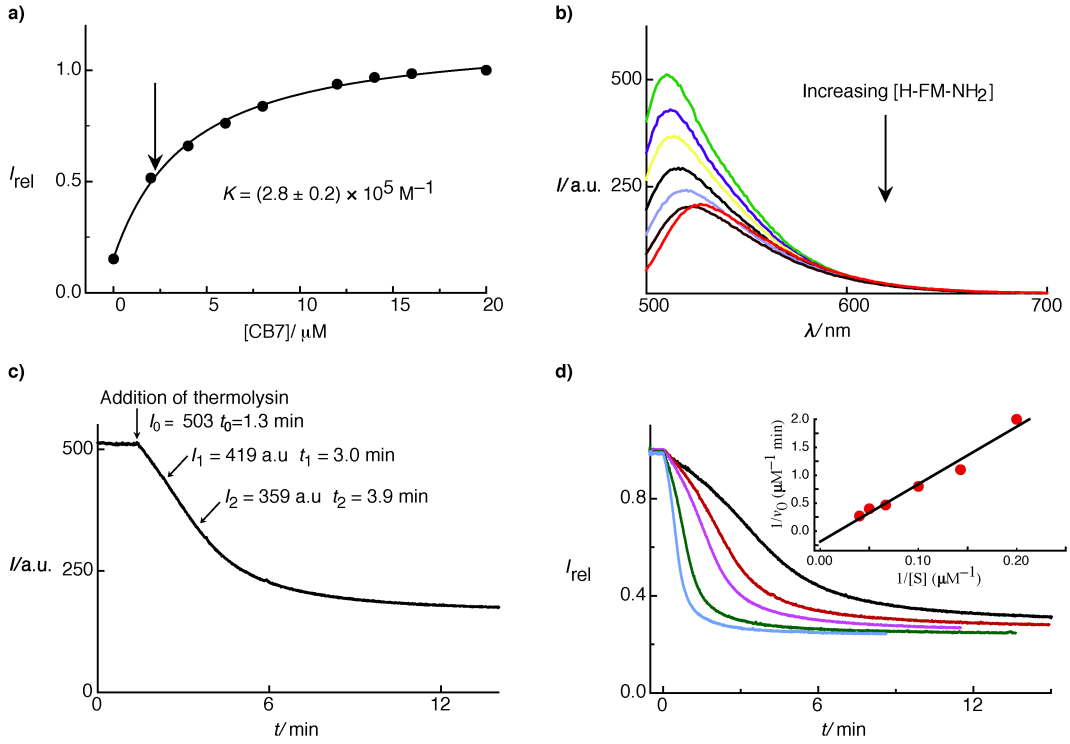

Figure 3.1.3: a) Fluorescence titration plot of CB7 with acridine orange. The arrow indicates the concentration of CB7 (2.5 μM) that we have selected for kinetic studies. b) Fluorescence titration for the competitive displacement of AO (0.5 μM) from CB7 (2.5 μM) (CB7•AO green trace) by Phe-Met-NH_2 (up to 4 μM). c) Evolution of fluorescent trace (2.5 μM CB7 and 0.5 μM AO) for 5 μM of Thr-Gly-Ala-Phe-Met-NH_2. d) Determination of kinetic parameters by monitoring of thermolysin (15 nM) activity with varying concentration of **1** (5–25 μM). Inset: Lineweaver-Burk plot for peptide **1**. Adapted from ref.[51]

3.1.2. Substrate Selectivity of Thermolysin

Our initial screening of peptide substrates reflected the previously established substrate specificity of thermolysin including the remarkable stereospecificity of enzyme for the substrate at P_1 position (Figure 3.1.2c). The amino acid residues at P_1 position significantly affected the proteolytic coefficients (k_{cat}/K_M) of thermolysin (see Table 3.1). The proteolytic coefficients are markedly reduced for the peptide where Gly and Ser were substituted at the P_1 position. The binding of the substrate at the P_1 position is mainly governed by

hydrophobic interactions, which explains the Gly < Ser < Ala preference at P_1 position.[170,171] The similar k_{cat}/K_M for peptides Thr-Gly-Ala-Phe-Leu-NH_2 and Thr-Gly-Ala-Phe-Leu-OH further corroborated that the binding of a peptide substrate with the catalytic site of thermolysin is strongly dependent on hydrophobic interaction and only weakly on electrostatic interactions. Additionally, the bond between Phe-Met is immune to the cleavage by thermolysin demonstrated by the lack of fluorescence change because; the hydrolysis of Phe-Met bond in peptide **7** would have resulted in a free phenylalanine (weak competitor) thereby allowing the complexation of CB7•AO.

3.1.3 Exo– and Endopeptidase Behaviour of Thermolysin

Using supramolecular tandem protease assay we were able to pinpoint the cleavage site for the peptides with more than one susceptible amide bonds. For example with peptide **3**, we discovered that apart from the obvious Ala-Phe bond, thermolysin also cleaved Phe-Leu bond. How did we stumble upon such behaviour of thermolysin?

For two substrates Thr-Gly-Ala-Phe-Leu-NH_2 and Thr-Gly-Ala-Phe-Met-NH_2, their corresponding products *i*) H-Phe-Leu-NH_2 and *ii*) H-Phe-Met- NH_2 are responsible for the change in fluorescnce intensity during enzymatic reaction. Since these products bind tightly and with similar affinity to CB7 (Figure 3.1.4 a & b, Table 3.1), we expected for the equal amount of substrates, the final steady state fluorescence response after the enzymatic digestion to be similar. For example, the steady state final fluorescnce response for 5 μM of peptide **1** after complete enzymatic digestion, resulted in a complete displacement of AO from CB7 (Figure 3.1.4c). This fluorescence response corresponded to the competitive fluorescence titration plot for H-Phe-Met-NH_2, whereby 5 μM of H-FM-NH_2 completely displaces the AO from the CB7 (Figure 3.1.4a & c). However, the fluorescence response upon the enzymatic hydrolysis of 5 μM of the substrate **3** is less than the fluorescence response caused by the competitive fluorescence titration of 5 μM of its corresponding product, H-FL-NH_2 (*cf.* Figure 3.1.4b & d). In fact, even 10 μM of the substrate **3** was insufficient to produce similar final fluorescence intensity as that produced by 5 μM of **1** (*cf* Figure 3.1.4c & d). This led to our speculation that the expected product H-Phe-Leu-NH_2, was not quantitatively formed and we suspected a possible *exo*peptidase activity, i.e., cleavage

at Phe-Leu amide bond, possibly leading to the formation of a product with *C*-terminal Phe, which would in fact bind weakly to the host because of *C*- terminal carboxyl group.

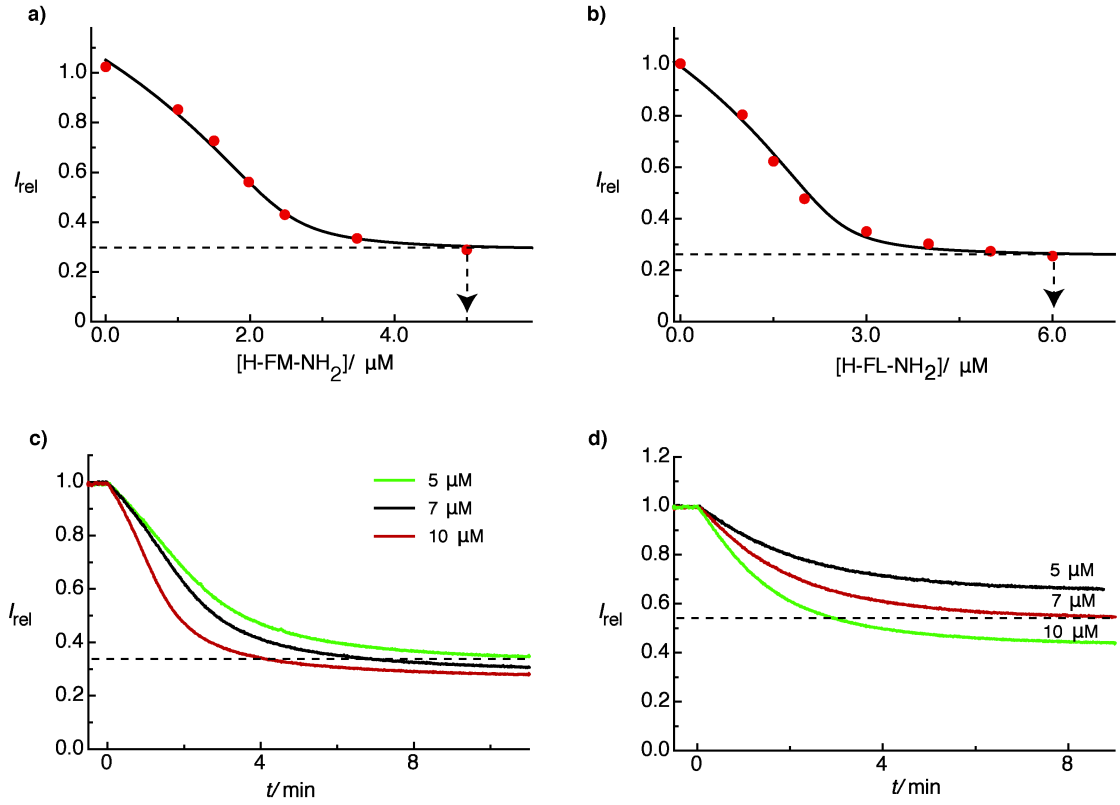

Figure 3.1.4: a, b) Competitive fluorescence titration plots of Phe-Met-NH_2 (**7**) and Phe-Leu-NH_2 (**8**). c, d) Continuous fluorescence enzyme assays for thermolysin (15 nM) with substrates c) Thr-Gly-Ala-Phe-Met-NH_2 (**1**)and d) Thr-Gly-Ala-Phe-Leu-NH_2 (**3**). Fluorescence measurements were performed using CB7•AO (2.5 µM CB7 and 0.5 µM AO, λ_{exc} = 485 nm, λ_{obs} = 510 nm) as a reporter pair in 10 mM ammonium phosphate buffer, pH 7.2, at 37 °C. Modified from ref.[51]

In order to confirm our suspicion about the possible exopeptidase activity of thermolysin on peptide **3**, mass spectrometry was used to monitor the hydrolysis of amidated (Thr-Gly-Ala-Phe-Leu-NH_2) and non-amidated peptide (Thr-Gly-Ala-Phe-Leu-OH) by thermolysin (SI Figure 2.3). A peak at m/z = 393.2 indicated the cleavage of peptide **3** at the Phe-Leu amide bond. However, the peak at m/z = 393.2 was absent for the non-amidated peptide **6**, ruling out a cleavage of the Phe-Leu amide bond (SI Figure 2.3). The absence of exopeptidase activity of thermolysin on peptide **6** was further verified by supramolecular tandem enzyme assays (Figure 3.1.5a). More specifically, the enzymatic hydrolysis of 15 µM

of Thr-Gly-Ala-Phe-Leu-OH brought about the complete displacement of the dye AO from the CB7 which corresponded with the competitive fluorescence titration plot of Phe-Leu-OH. Additionally, no thermolysin activity was observed for the dipeptide H-Phe-Leu-NH_2. Our results are in agreement with previous studies, which conclude that the presence of an α–amino or an α –carboxyl group decreases the susceptibility of hydrolysis by thermolysin.[172-174]

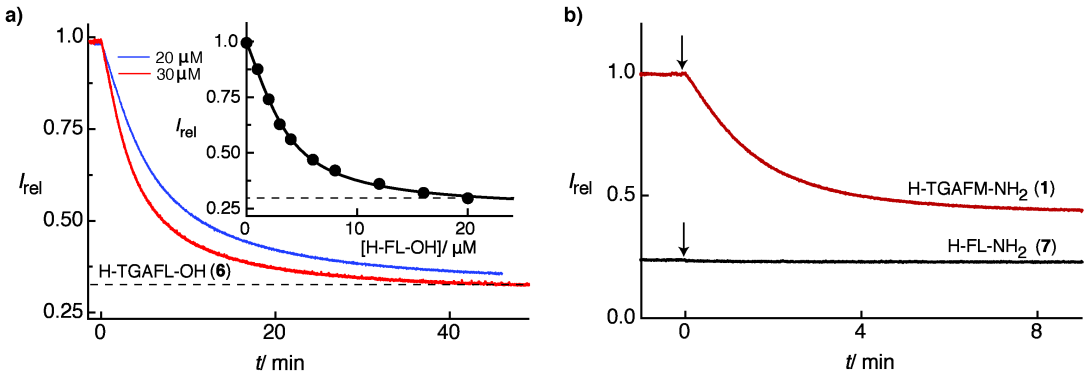

Figure 3.1.5: a) Continuous fluoresence enzyme assay for thermolysin (15 nM) with substrate Thr-Gly-Ala-Phe-Leu-OH (**6**). Inset: Competitive fluorescence titration plots for Phe-Leu-OH. c) Continuous fluorescence assays with the CB7•AO reporter pair (2.5 µM• 0.5 µM, λ_{exc} = 485 nm, λ_{obs} = 510 nm) during the enzymatic treatment of peptides **3** and **7** (30 µM) by thermolysin (15 nM). Adapted from ref.[51]

3.1.4. Inhibition Experiments

One immediate application of our protease assay was the screening for the inhibitors. Using peptide **1** as a substrate, inhibition studies for thermolysin was were carried out using a competitive inhibitor phosphoramidon.[175-178] Figure 3.1.6a clearly depicts the decreasing thermolysin activity upon increasing the concentration of phosphoramidon. Important to note here is typical behaviour of competitive inhibitors, i.e., it allows the irreversible peptidase reaction to completion, as observed by similar steady state fluorescence intensities at all concentrations of inhibitor (same fluorescence plateau region reached after enzymatic conversion, Figure 3.1.6a). Additionally, we were able to derive the inhibition constant by extracting the relative enzyme activities from the progress curves at varying inhibitor

concentrations (Figure 3.1.6a). Hill plots of the relative initial rates readily afforded inhibitor constant (K_i) of 2.2 nM, which were in nice agreement with those reported in the literature by alternative methods.[179]

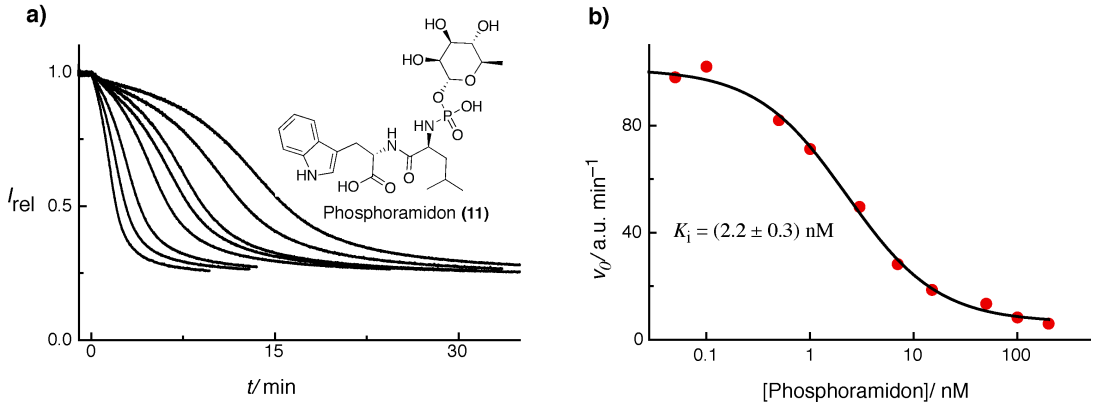

Figure 3.1.6. Determination of thermolysin inhibition by phosphoramidon, obtained by tandem enzyme assays. a) Continuous fluorescence traces (λ_{exc} = 485 nm, λ_{obs} = 510 nm) upon addition of 10 µM Thr-Gly-Ala-Phe-Met-NH_2 (**1**) to a solution containing 2.5 µM CB7, 0.5 µM AO and 0–100 nM of phosphoramidon in 10 mM ammonium phosphate buffer at 37 °C. b) Corresponding dose–response curve of the initial rates. Adapted from ref.[51]

3.2 Fluorescence-based Method to Monitor Stepwise Proteolytic Degradation of Peptides by Domino Tandem Assays

Complying with domino tandem assay (Figure 1.5 in Chapter 1), we wanted to follow stepwise degradation of an entire peptide by fluorescence. Our aim was to present a very simplistic version of Edman degradation in which the fluorescence response signals that the degradation has reached an aromatic amino acid residue. For this purpose, we selected Leucine amino peptidase (LAP), an exopeptidase that cleaves amide bonds from *N*-terminal of a peptide, unless preceded by an amino acid proline.

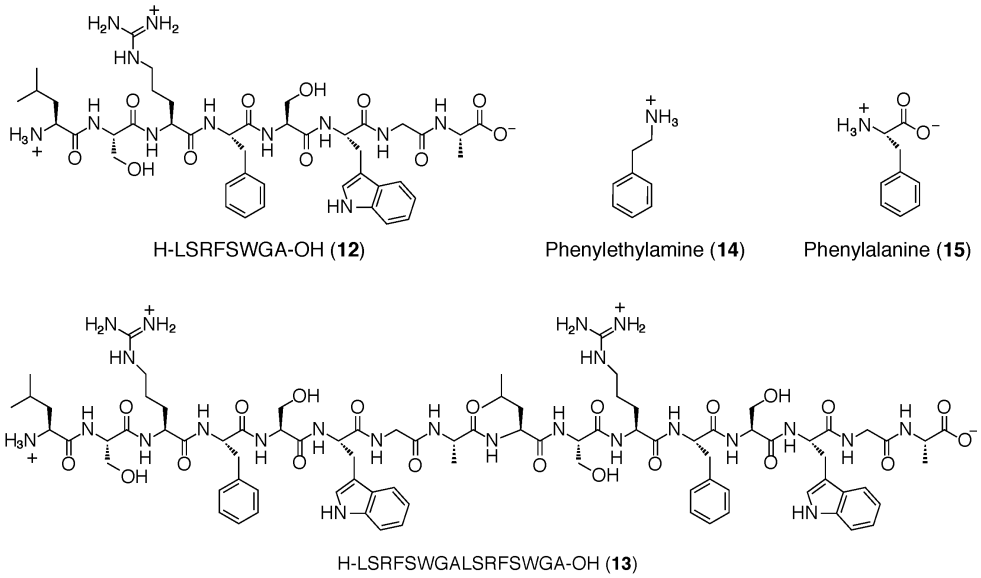

Figure 3.2.1: Chemical structures of substrates (**12** and **13**), intermediary (**14**) and final products (**15**) that bind to the macrocyclic host CB7. Adapted from ref.[52]

Recall that the requirement for the domino tandem assay is the alternating binding affinity of the sequentially formed metabolites. In this scenario, the macrocyclic host CB7 would need to differentiate between a peptide substrate (internal Phe, **12** & **13**), an intermediary product (peptide fragment with *N*-terminal Phe, **14**) and the final product (**15**), i.e., free amino acid Phe. During the experiment, at the beginning AO is favourably complexed with macrocyclic host CB7 (Figure 3.2.2). As the degradation of a peptide is kicked off by addition of LAP, amino acids from the *N*-terminal of a peptide are removed,

during which no change in fluorescence is observed. However, once the amino acid arginine (Arg) is cleaved off, the *N*-terminal Phe gets exposed, which shows strong binding towards the host CB7 and displaces the fluorophore AO. The formation of a *N*-terminal Phe, or the fact that peptide degradation has reached an aromatic amino acid residue (in this case Phe) is indicated by a decrease in fluorescence intensity (switch off, Figure 3.2.2). Next, the *N*-terminal Phe is enzymatically digested to free amino acid, which now has a weaker binding affinity, allowing the recomplexation of AO with CB7 depicted by an increase in fluorescence intensity and hence fluorescence switch on. Therefore, a "valley" made of fluorescence switch-off and switch-on indicated the presence of a single Phe in a peptide.

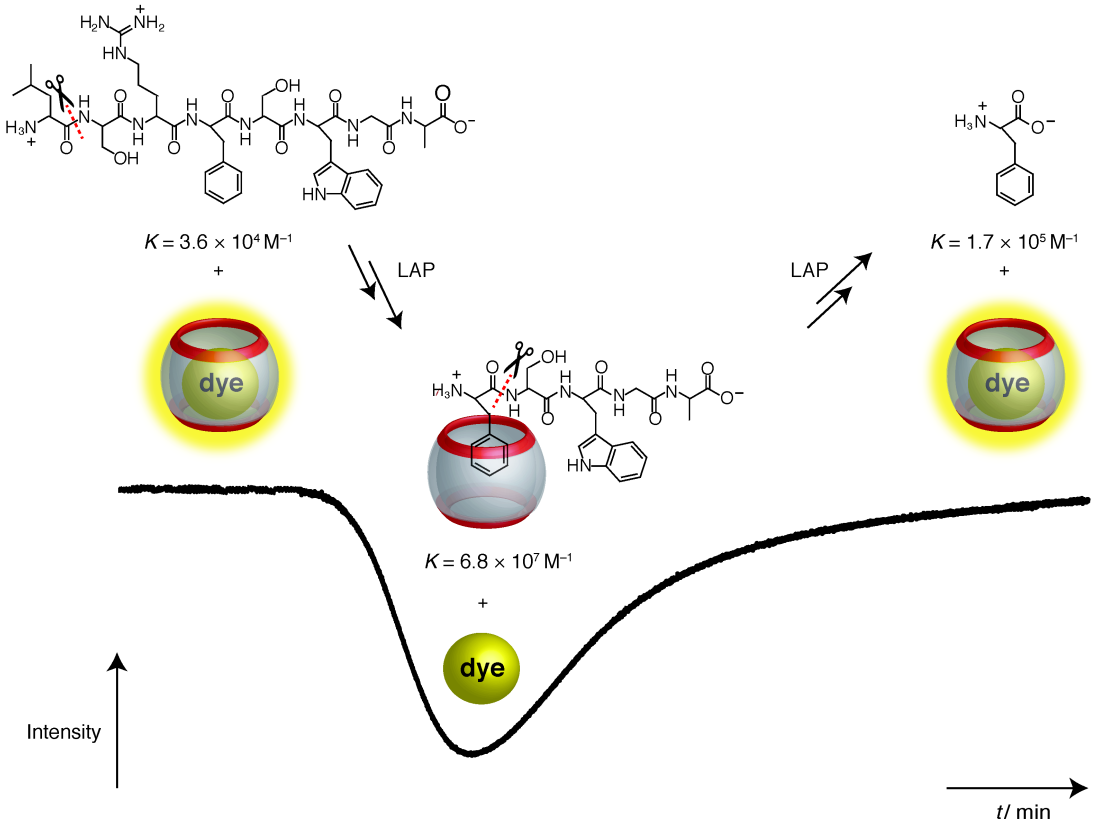

Figure 3.2.2: Domino tandem assay for monitoring the stepwise degradation of peptide **12** by LAP. The binding affinity of CB7 towards peptide **12** and corresponding intermediary product was calculated by competitive displacement of the dye.

3.2.1. Mass Spectrometry

In order to verify that the observed marked fluorescence change indeed corresponded to the presumed pathway – degradation of peptide to amino acid residues –real-time mass

spectrometry was used to monitor the degradation of peptide by LAP. As LAP cleave amide bonds, the molecular mass of peptide fragments are expected to decrease in predictable sequence specific manner.[52] In absence of LAP, the pseudomolecular ion peak of a singly charged peptide substrate is observed as its sodium ion adduct at 945, and doubly charged substrate at 484.2 (Figure 3.2.3 top-left). After addition of LAP, MS were taken at different time intervals. Figure 3.2.3 (top-right) shows MS spectra taken after 30 minutes. Apart from a dominant molecular ion peak, additional peaks at m/z 810, m/z 723 and at m/z 589 are observed. These peaks correspond to the peptide fragments formed after the cleavage of *N*-terminal amino acids, Leu and Ser respectively. As the degradation of peptide by LAP proceeded, amino acid residues from the *N*-terminus of the peptide were sequentially cleaved off, forming shorter peptide fragments (Figure 3.2.3 bottom-right). The completion of peptide substrate degradation is signalled by the absence of molecular ion peak (Figure 3.2.3 bottom-left).

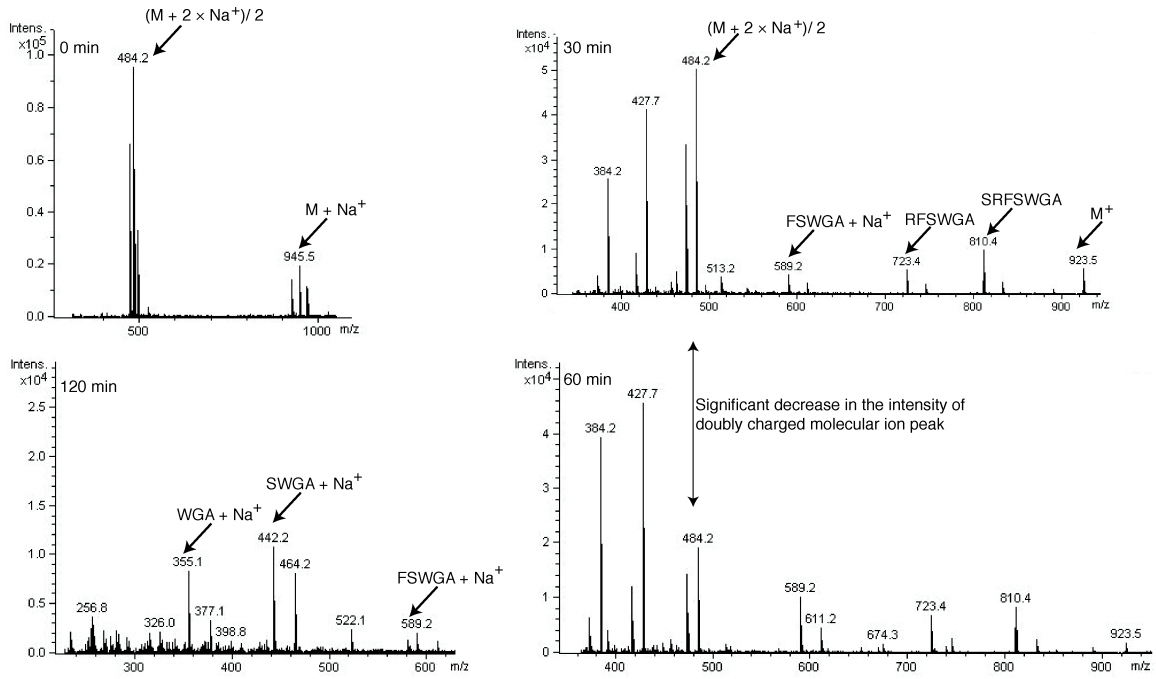

Figure 3.2.3: Mass spectra recorded after 0, 30, 60 and 120 minutes of reaction time respectively. Adapted from ref.[52]

These observations with MS confirmed that the fluorescence change observed earlier (Figure 3.2.2) indeed reported on the biochemical degradation of a peptide by LAP. We then

continued with our quest to develop a simplistic version of Edman degradation using supramolecular sensing ensembles.

3.2.3. Peptide Fingerprinting

Inspired by our earlier observation (Figure 3.2.2), a fluorescence decrease and an increase for peptide **12** (one internal Phe), we continued with our quest to employ fluorescence signal as landscapes of fingerprints to identify number of aromatic amino acid residues in a peptide. Next step towards our goal was to use a peptide with two Phe (**13**), with an expectation to see two switch-off and switch-on fluorescence responses. The first fluorescence switch-off and switch-on would indicate the release of the first Phe residue, while the second fluorescence switch off and switch on response would imply the release of the second Phe residue.

For peptide **13**, in contrast to what we had expected – two "valleys" corresponding to two fluorescence switch-off and switch-on fluorescence response – only single fluorescence switch-off and switch-on was observed (Figure 3.2.4 a). In an effort to understand this unanticipated fluorescence response, we compared the changes in fluorescence signal for peptide **12** and peptide **13**. First, the degradation of peptide 12 was faster compared to peptide **13** under the same conditions (Figure 3.2.4 b. Second, although the concentrations had been adjusted to equal amounts of Phe residues, the drop in fluorescence intensity for peptide **13** (factor of 1.6 difference) was less than the change in fluorescence intensity for peptide **12** (by a factor of 2). From these two observations we were able to conclude that that the fluorescence switch off and switch on for the peptide **13** is actually a statistical average response for the release of both free Phe residues.

We attempted to overcome this problem by optimizing the ratio of the reporter pair (Figure 3.2.3). By decreasing the concentration of host, we were able to manipulate our host•dye system to such an extent that it responds to even the slightest changes in concentration of analytes during enzymatic transformations (Figure 3.2.3c & d). The two fluorescence switch-off and switch-on responses indicated the presence of two Phe residues in the peptide.

As can be seen that the idea that different peptides give rise to different recognition patterns in the form of fluorescence "landscapes" or fingerprints can be obtained by simply

recording the fluorescence works in principle. However, in detail it is quiet challenging to realize for longer peptides, due to sequence and length dependent activity of enzyme, in addition to multiple equilibrium involved with host•guest, substrate, intermediary and final products.

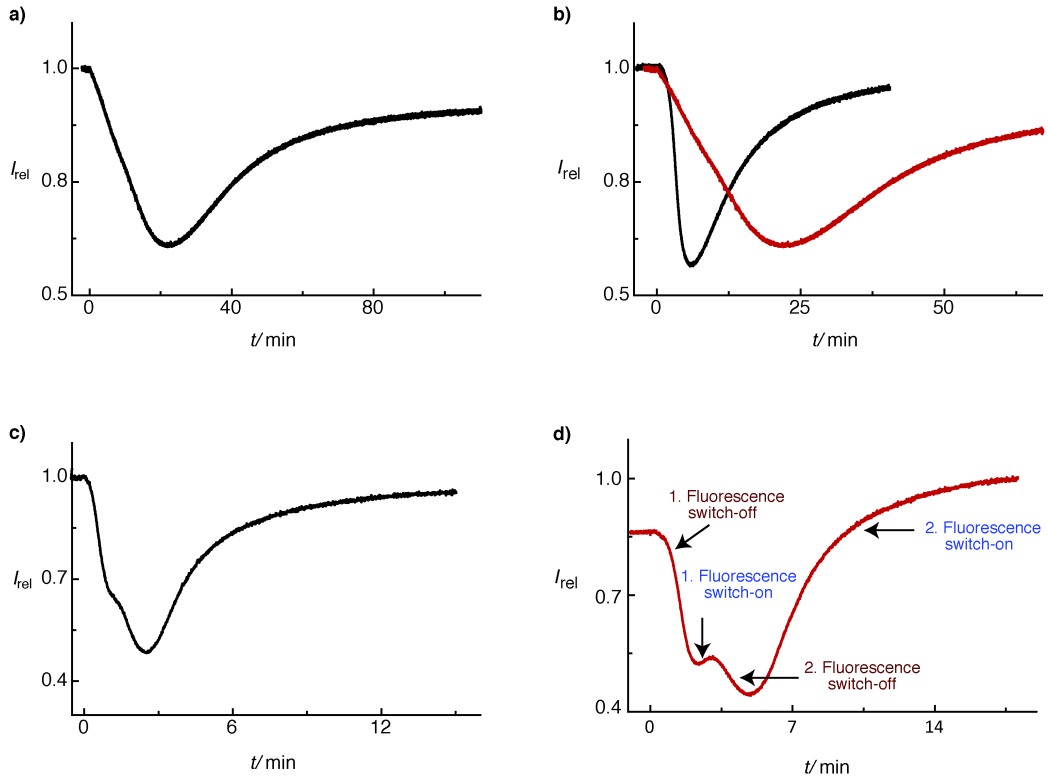

Figure 3.2.3: a) Continuous fluorescence trace of 0.5 µM AO and 4 µM CB7 upon proteolytic degradation of peptide **13** (10 µM) by 10 nM LAP, b) Comparison between 20 µM peptide **12** (black trace) and 10 µM peptide **13** (red trace). c & d) Kinetic traces obtained during the hydrolysis of 10 µM peptide **13** by 50 nM LAP using 0.5 µM AO at different CB7 concentrations: c) 2 µM CB7, and d) 1 µM CB7. The reactions were carried out in 0.05 mM tris buffer, pH 7.6 at 37 °C (λ_{exc} = 485 nm, λ_{obs} = 510 nm). Adapted from ref.[52]

– Chapter 4 –
Materials and Methods

4. Materials and Methods

4.1 SUPRAMOLECULAR TANDEM MEMBRANE ASSAYS

A stepwise procedure is described in this section for carrying out tandem membrane assays. Even though the method is detailed for liposomes loaded with CX4•LCG for protamine translocation through OmpF, it is transferrable to any other systems. The experiences that I have gathered while developing tandem membrane assays that might be useful in cases other than CX4•LCG-loaded liposomes are listed as bullet point throughout this experimental Section.

4.1.2 Materials

Lipids: 1-palmitoyl-2-oleoyl-*sn*-glycero-3-phosphocholine (POPC) and 1-palmitoyl-2-oleoyl-*sn*-glycero-3-phospho-L-serine (POPS) were purchased from Avanti Polar Lipids as 100 and 10 mg solutions in chloroform, respectively.

Macrocyclic hosts: p-sulfonatocalix[4]arene (CX4) was purchased from Sigma–Aldrich and used as received. Cucurbit[7]uil (CB7) was synthesized according to the literature,[45-47] and CB8[46] was synthesized by Dr. Frank Bidermann.

Fluorescent dyes: Lucigenin, Berberine chloride and Palmatine were all purchased from Sigma–Aldrich and used as received, while the MBBI[127] and MDAP[180,181] dyes were prepared by Dr. Frank Bidermann according to the literature procedures.

Analytes and guest molecules: Protamine sulphate (from Herring, grade III), spermine, succinylcholine, acetylcholine, choline and all the other small weight compounds were purchased and used as received.

NAP–25 columns were purchased from GE healthcare

4.1.2. Preparation and Separation of CX4•LCG Loaded-liposomes

A solution of 2.5 mg/ml of POPC in chloroform is purged with nitrogen and dried overnight under high-pressure vacuum. The lipid film is then re-dissolved in 1 ml of 10 mM sodium phosphate buffer containing the reporter pair composed of 700 μM CX4 and 500 μM LCG.

The liposome suspension is subjected to 12 freeze-thaw cycles (freezing in liquid nitrogen and thawing at 40 °C for 1 and 5 minutes, respectively). Adapted from ref.[79]

- Anionic liposomes can be prepared by combining POPC (2.5 mg/ml) with POPS (0.33 mg/ml). Similar procedure was applied to the preparation of liposomes POPC/POPS liposome for CB8•fluorescent dye combinations, specifically, CB8•MBBI (500 / 550 μM), CB8•MDAS (500/550 μM), CB8•MV•2,6-ANS (500 / 550 / 500 μM), CB8•MV•DapoxS (500 / 550 / 500 μM) in HEPES buffer. While, CB7•BE (300 / 300 μM) and CB7•PAL (300 / 300 μM) were prepared in sodium phosphate buffer (pH 7), but can also be prepared in HEPES buffer.

- The reporter pair is always added at this point, along with the buffer.

- Liposomes do not form or are unstable if prepared in pure water.

After the preparation of liposomes loaded with CX4•LCG, the unencapsulated material is removed by size-exclusion chromatography (NAP-25 column) while maintaining the same buffer. In order to verify the complete removal of reporter pairs, in this case CX4•LCG, from the extravesicular phase, a fluorescence spectrum of liposome (20 μl from collected fractions in 1 ml buffer) is taken, followed by the addition of a membrane impermeable and a strong competitor for macrocyclic host (in this case protamine). Constant fluorescence intensity upon addition of protamine confirms the complete removal of unencapsulated material (SI Figure 1.1)

- For reporter pairs that employ CB7 or CB8 as macrocyclic host, succinylcholine or tryptophan can be used to validate the removal of unencapsulated material.

The final lipid content in the liposomes after preparation and separation was determined by using Stewart assay[182] and the effective concentration were found to be 1.3 mM lipid, 500 μM LCG and 450 μM CX4. Note that the concentration of CX4 (450 μM) is lower than what we initially started with (700 μM). In order to calculate the concentration of reporter pair inside liposomes, a detailed method is provided in ref.[79]

4.1.3. Liposome Characterization

Size: The size of liposomes is measured using a Zetasizer Nano from Maelvern Instruments.

The Freeze-thaw (10-15 cycles) method is used to obtain 150–200 nm diameter liposomes.

4.1.4. Reconstitution of Membrane Proteins Into Liposomes

In a direct injection method, membrane proteins such as OmpF are injected directly into the reporter pair-loaded liposomes. In order to confirm OmpF reconstitution into liposomes, I did a control experiment using dye release assay (SI Figure 1.4), which validated the successful formation of proteoliposomes (channel protein inserted liposomes). However, not all membrane proteins are inserted into bilayer by direct injection method. For example, if membrane proteins are provided as vesicle membrane fragments, a different reconstitution method is required. One method that I have successfully used is described as follows and is slightly modified from the original method ref.[183]

- A mixture of phosphatidylethanolamine (POPE, 2.5 mg/ml), phosphtadiylserine (POPS, 1.25 mg/ml) and phosphatidylcholine (POPC, 1.125 mg/ml) is dried under nitrogen flow. POPE is used to promote vesicle fusion, while POPS and POPC are used to form stable liposomes. After drying the lipids, 10 mM sodium phosphate buffer containing 500 μM LCG and 700 μM LCG were added and the mixture was vortexed for two minutes and sonicated in a water bath at ambient temperature for a total of 90 s. After the first 60 s of sonication the mixture was vortexed and then sonicated again for the remaining 30 s.

- For protein reconstitution, 200 μl solution of vesicle membrane fragment is added to the liposome solution and vortexed. Vesicular fragments are fused into liposomes by quick freezing in liquid nitrogen. Freezing is then followed by thawing at 40 °C for 5 minutes followed by a 15 s long sonication. This freeze/thaw/sonicate cycle is repeated three times. Note that after the final thaw, the mixture is vortexed and sonicated only for 5 s.

Following sections 4.1.5, 4.1.6, and 4.1.7 are adapted from ref.[79]

4.1.5. Fluorescence Titrations to Determine Binding Constants of LCG and Protamine with the Macrocyclic Host CX4.

The binding constant of CX4 with LCG was determined by titrating CX4 into a solution of 500 nM LCG and recording the fluorescence spectrum after each addition of CX4 until no fluorescence change was observed anymore (Figure 2.1.2a, Chapter 2.1). The concentration of the dye remained constant throughout the entire titration. The fluorescence intensity at the emission maxima wavelength was then correlated with the molar fraction of the dye to afford the binding constant.[65]

To determine the binding affinity of CX4 towards protamine, a competitive displacement titration was carried out. To a solution containing 500 nM LCG and 1 μM CX4, protamine was gradually added, in small amounts (Figure 2.1.2b). The same concentrations of host and dye were present in the protamine solution, such that they remained constant throughout the displacement titration. The fluorescence intensities were then correlated with the molar fraction of the dye to allow the determination of the binding constant (Appendix 3).

4.1.6. Tandem Membrane Assays

20 μl of liposome solution loaded with CX4•LCG (450/500 μM), in 10 mM sodium phosphate solution, pH 7.0 at 25 °C, was prepared and its fluorescence intensity was recorded in a 1 mlcuvette, followed by the addition of 2.8 μl of 2 mg/ml of stock of OmpF (45 nM) solution to form proteoliposomes. Subsequently, 5 μM protamine was added and the time–resolved fluorescence response was recorded. Triton-X (20 μl of 100 % triton-X) was added as a control to get the maximum fluorescence intensity.

The fluorescence of the liposome–entrapped dye was always monitored by exciting at 367 nm and following the 500 nm emission, with a Varian Eclipse spectrofluorimeter. The fluorescence intensities were normalized as $I = (I_t - I_0)/(I_\infty - I_0)$, where I_0 is the initial intensity at $t = 0$, I_t is the intensity at time t, and I_∞ is the maximum intensity, i.e., after the lysis of liposomes by Triton-X.

4.1.7. Stopped-flow Fluorescence Measurements

Stopped-flow measurements were performed with a Bio-Logic stopped-flow SFM-20 module coupled to a JASCO FP-8500 spectrofluorometer. In a standard experimental setup, 200 µl of a CX4•LCG–loaded–liposome solution was diluted in 4800 µl of 10 mM buffer. To this solution of liposomes, 60 nM of OmpF was added to insert the OmpF channel into the liposomes and the solution was placed in Syringe 1, while Syringe 2 contained 0–20 µM protamine. The two syringe mixing ratio was set-up to be of equal volumes (total volume = 200 µl, flow speed of 4.5 ml/s), such that the final concentrations for measurements were 26.5 µM lipids with 30 nM of OmpF and 0–10 µM protamine, in the stopped-flow chamber. All experiments were carried out in 10 mM sodium phosphate buffer, pH 7.0, at 25 °C.

Fluorescence intensities were recorded at 500 nm emission with an excitation wavelength of 367 nm. Each measurement data was an average of 7 to 13 injections and each experiment was repeated (including independent liposomes preparation) at least three times to ensure reproducibility. The fluorescence intensities were normalized as $I = (I_t - I_0)/(I_\infty - I_0)$, where I_0 is the initial intensity at $t = 0$, I_t is the intensity at time t, and I_∞ is the intensity obtained the addition of a high (≥ 1 mM) concentration of protamine.

4.1.8. Giant Unilamellar Vesicles (GUVs) Preparation and Observation

GUVs were prepared using the Vesicle Prep Pro from Nanion Technologies. Specifically, a mixture of a 30 µL POPC solution (25 mg/mL in $CHCl_3$) and 10 µL POPS solution (5 mg/mL in $CHCl_3$) was spread as a thin film on an ITO–coated glass slide. After solvent evaporation and film drying, it was hydrated with 300 mM of sucrose solution containing CB8•MDAP and it was then covered up with another ITO–coated glass slide. After 2 h of preparation in vesicle prep pro, the GUVs have formed and the suspension was collected. All subsequent measurements were carried out within 24h as follows: A drop of the GUVs suspension was pipetted on a glass slide and the formation of GUVs was confirmed by bright-field microscopy (SI Figure 1.9 GUVs phase contrast pictures). To this suspension, 5 µL of tryptophan (1 mM stock) was added to quench the fluorescence of the unencapsulated

CB8•MDAP chemosensing ensemble. Fluorescence images of GUVs treated as such were taken with a fluorescence microscope (Axiovert 200, Carl Zeiss, filter set 02, *i.e.,* G365 nm, FT 395 nm and BP 420 nm), equipped with a digital camera (Evolution QEi monochrome). The first image was taken immediately after the addition of 5 μL of TrpOMe (800 μM stock) to the suspension. Subsequent images were taken at regular intervals (1 min) thereafter. Constant illumination was avoided to reduce potential photobleaching, *i.e.,* the sample was illuminated only when the images were taken. Exposure time and camera settings were constant for all images. The data was analysed using the Image J software. In order to ensure that the apparent decrease in fluorescence over time was not due to the photobleaching of the dye, experiments were carried out exactly as described above, except for the addition of TrpOMe. Indeed, in the absence of TrpOMe no noticeable change in fluorescence intensity was observed.

4.2. PROTEASE ASSAYS

4.2.1. Materials

Peptides **1**-**8** were kindly supplied by Prof. Adam R. Urbach, while the Phe-Leu-OH peptide (**9**) and the Phe-OH amino acid (**10**) were used as received from Bachem and Applichem respectively. Peptides **12** and **13** were purchased from Biosyntan GmbH (Berlin, Germany), in >95% purity. Acridine orange (AO), thermolysin (lyophilized powder, 36.5 U/mg), Leucine aminopeptidase (type IV-S, from porcine kidney microsomes, 28 U/mg), phenylethylamine and phosphoramidon were used as received from Sigma-Aldrich.

The concentration of peptides **1**-**9** were determined from the extinction coefficient of free phenylalanine at 257 nm, ε_{257} = 195 M^{-1} cm^{-1},[184] while the concentration of peptides **12** and **13** were determined form the extinction coefficient of amino acid tryptophan, ε_{280} = 3400 $M^{-1}cm^{-1}$).[185] For thermolysin and phosphoramidon, ε_{280} = 61100 M^{-1} cm^{-1} and ε_{280} = 5500 M^{-1} cm^{-1}, respectively, were used.[176,186] All the stock solutions were prepared in water except for the leucine amino peptidase (LAP), which was prepared in an activation buffer composed of 2 mM $MnCl_2$ and 0.05 mM tris, pH 8.5 and activated for 2 h at 37°C. The extinction coefficient of ε_{280} = 320000 M^{-1} cm^{-1} was used to determine the concentration of LAP.[187] Absorption measurements were performed with a Varian Cary 4000 spectrophotometer.

4.2.2. Protease Assays Using a Reporter Pair

The total assay volume was 1 mL. Assays for thermolysin were performed in 10 mM ammonium buffer, pH 7.2, in a variable–temperature cell holder at 37.0 ± 0.1 °C, using 2.5 μM CB7, 0.5 μM AO and 0–55 μM of peptide substrate. The reaction was initiated by addition of 15 nM thermolysin. For inhibition studies, the mixture of 10 nM thermolysin and phosphoramidon (0-100 nM) was pre-incubated for 15 minutes at 37.0 ± 0.1 °C in the presence of the reporter pair and the reaction was initiated by the addition of 10 μM Thr-Gly-Ala-Phe-Met-NH_2 (1). Continuous fluorescence assays were performed with 0–80 μM peptide, 4 μM CB7 and 0.5 μM AO in 0.05 mM Tris buffer (pH 7.6 at 37 °C), and the reaction was initiated by the addition of 10 nM LAP. A Varian Eclipse spectrofluorometer

equipped with a thermostat-cell-holder was used for the collection of this kinetic data (λ_{exc} = 485 nm, λ_{obs} = 510 nm). Intensities were normalized as $I_{rel} = I_t/I_0$ where I_0 is fuorescnce intensity at t = 0 min.

4.2.3. Electrospray ionization mass spectrometry (ESI-MS)

ESI-MS measurements were carried out with a Micro–TOF Focus mass spectrometer (Burker Daltonics) equipped with an ESI source, and internal calibration was achieved using the enhanced quadratic calibration mode with 10 μL of 0.1 M sodium formate solution injected prior to each measurement.

52 μL of 1.9 mM peptide stock solution was added to 200 μL of 10 mM borate buffer in 6 individual Eppendorf tubes. The reaction was initiated by adding 20 μL of a 100 μM LAP solution to five of these tubes at precisely recorded addition–times. A 200 μL sample from each Eppendorf tube was loaded into a 1 mL Hamilton syringe. The sample was then infused into the Micro–TOF mass spectrometer via a syringe pump, at a constant flow rate of 180 mL/min. The mass spectra for all five samples were acquired over a mass range of 100-1500 Da in the positive ion mode with reaction times of 20, 30, 40, 60, and 120 minutes, after the enzyme addition.

– Chapter 5 –
Future Outlook

5. Future Outlook

As I mentioned in chapter 1, label-free fluorescence-based methods to study biomembrane transport are scarce if not non-existent. With the new introduced method that utilizes supramolecular chemosensing ensembles encapsulated inside vesicles (LUVs, GUVs), several biomembrane translocation/permeation processes can now easily be tapped into, both qualitatively and quantitatively. There are two such immediate applications that I anticipate which I have described below. However, before I begin, let me introduce two newly realized (and currently under investigation) reporter pairs.

5.1. Reporter Pairs Under Investigation

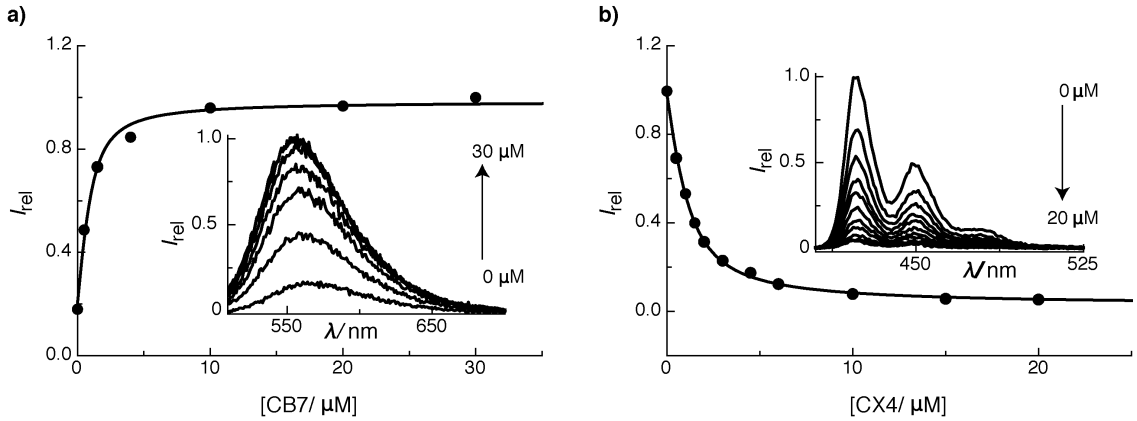

Figure 5.1: Fluorescence titrations of a) 5 μM S2166 with CB7, and, b) 1 μM MDAP with CX4 in 10 mM sodium phosphate buffer, pH 7.0.

One of these reporter pairs is comprised of CB7 with the hemicyanine dye S2166 and the other one is CX4 with MDAP, (Figure 1.2 in Chapter 1). The emission of a weakly the fluorescent S2166 was enhanced by a factor of 5 upon encapsulation by CB7 with a binding affinity of $K_{CB7 \cdot S2166}$ = 2.4 ×10^6 M^{-1} (Figure 5.1a). The strong fluorescence of MDAP,[136] on the other hand, was efficiently quenched by a factor of 20 upon addition of CX4 ($K_{CX4 \cdot MDAP}$ = 1.7 ×10^6 M^{-1}, Figure 5.1b). These reporter pairs were screened with the expectation that they could be exploited for tandem membrane assays. However, a further study revealed that the dye S2166 diffuses out through the lipid membrane and, therefore was unsuitable for membrane studies. Nevertheless, the reporter pair could be easily used for

other sensor systems where lipid permeability is not an issue. CX4•MDAP is currently being investigated in membrane permeation studies.

5.2. Tandem Membrane Assays to Study Drug-membrane Interactions

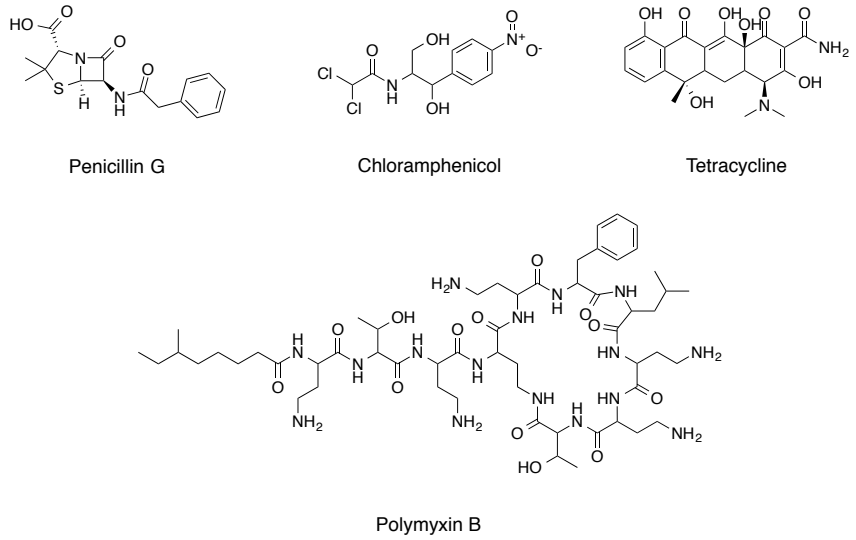

Figure 5.2: Analytes of interest.

As demonstrated in chapter 2, we screened drugs and pesticides for their membrane permeability using supramolecular tandem membrane assays (Figure 2.2.1). Our next step would be to perform a systematic study on drug-membrane interactions, in particular the kinetics of uptake of drugs as a function of temperature (activation energy, E_a) with different lipid compositions. If we look at the physical properties (pKa, lipophilicity) of currently available drug molecules (75 % of available drugs are cationic-amphiphilic),[188] it is not surprising that drug-membrane interactions play a significant role in accumulation and permeation of these molecules.[189] One pertinent example is the reduced uptake of an anticancer drug doxorubicin, upon increasing the amount of negatively charged phospholipids and cholesterol.[190] Out of various mechanisms for antibiotic resistance, the effect of bacterial lipid composition on the passive diffusion of antibiotics has been less explored. Hence, to continue along similar line would be to investigate the permeation of antibiotics through liposomes mimicking different bacterial lipid composition or multidrug resistant cells (Figure 5.2). A good starting point would be to study antibiotics for which the effect of lipid composition has already been demonstrated. These include penicillin,[191] tetracyclines,[192] chloramphenicol[193] and polymyxin.[192]

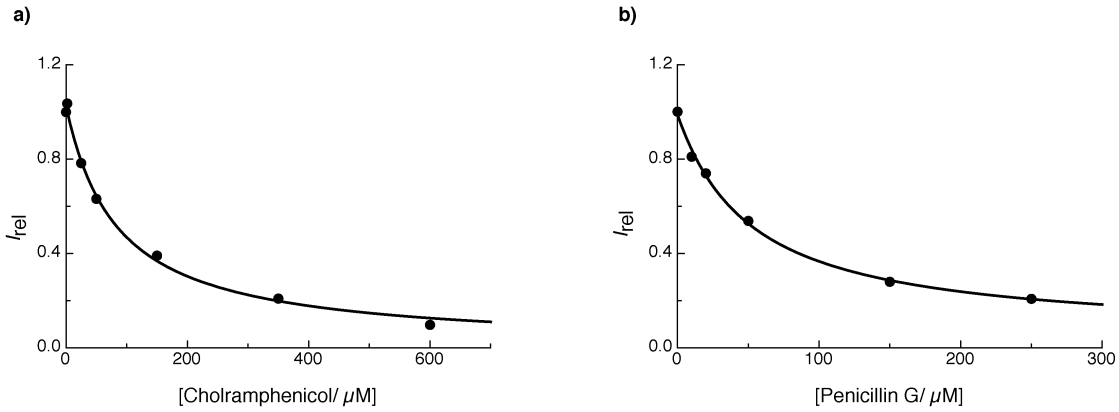

Figure 5.3: Competitive fluorescence titration plots for a) Chloramphenicol, and b) Penicllin G, using 5 μM BE and 5 μM CB7 in 10 mM sodium phosphate buffer, pH 7.0.

The first step in employing tandem membrane assays is the selection of a macrocyclic receptor and a fluorescent dye as sensing ensembles. Our preliminary experiments show that both chloramphenicol and penicillin G bind to CB7 with moderate affinity, $K = 2.37 \times 10^4$ M^{-1} and $K = 3.94 \times 10^4$ M^{-1} respectively (Figure 5.3).

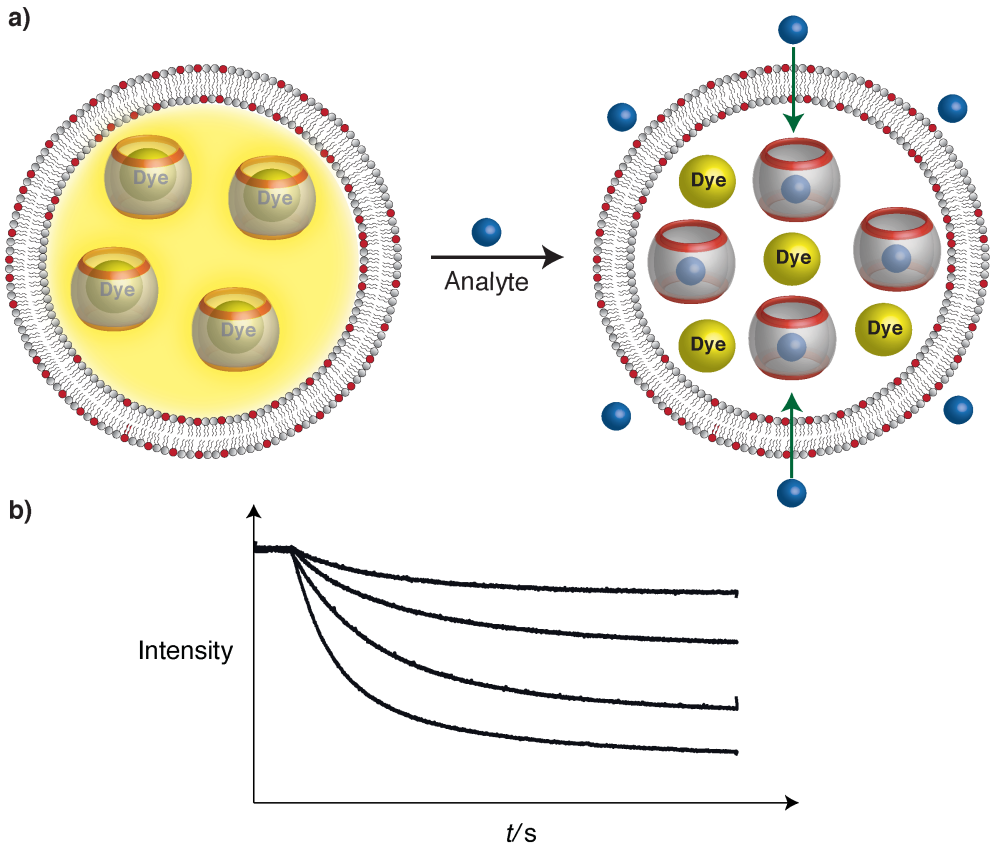

Figure 5.4: a) Supramolecular tandem membrane assays to study drug-membrane interactions. The red and gray coloured lipid represents liposomes prepared from different

combination of lipids, for example, POPC:POPS, and POPC:POPE. b) Anticipated fluorescence response upon permeation of analytes into liposomes with different membrane charge, or other physical characteristics such as membrane fluidity.

While the successful diffusion of drug molecules into liposomes are easily indicated by changes in fluorescence (Figure 5.4a), we are interested in how fast the process, depending lipid composition, LPS and cholesterol content (Figure 5.4b). Since tandem membrane assays does not require any labelling of lipids or analytes, these studies can be carried out effortlessly.

5.2. Supramolecular Sensors to Study Transmembrane Diffusion of Cell-penetrating Peptides.

Over the past 20 years, peptide transduction domains, or commonly known as cell-penetrating peptides (CPPs) has become a centre of attraction as a delivery vehicle for cargoes such as drugs, oligonucleotides, and peptides.[86,87] However, very few fluorescence-based methods have been developed to screen the internalization of CPPs *in vitro* and the limitations of several other available methods have previously been described.[84,91] Tandem membrane assays present as appealing alternative to available methods, as it does not require labelling of the peptide and can be used to investigate the vesicle size dependent translocation of CPPs (LUVs and GUVs).[194] Additionally, the method can also be extended to provide information on the behaviour of CPPs with and without cargoes.

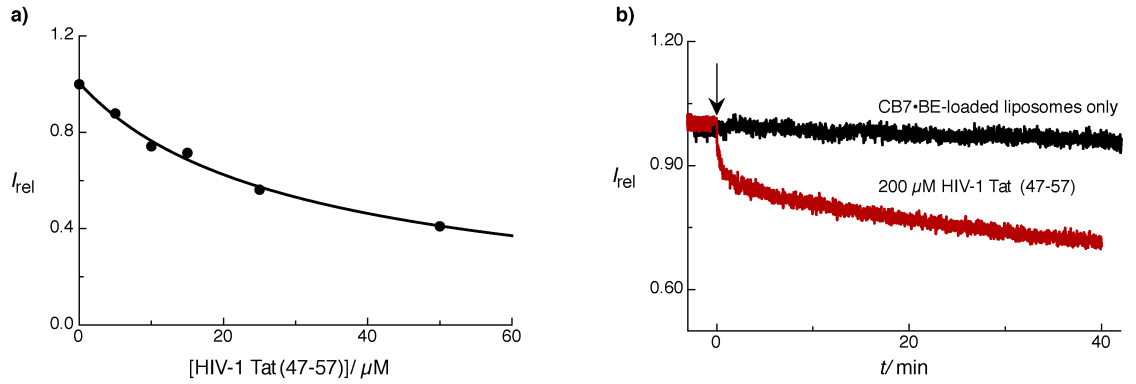

Figure 5.5: a) Competitive fluorescence titration plot of HIV-1 Tat (47-57) using 5 μM PAL and 5 μM CB7. b) Evolution of fluorescence trace upon addition of 200 μM HIV-1 Tat (47-57) to CB7•BE-loaded liposomes. Lack of fluorescence change in absence of analyte

indicated that CB7•BE-loaded liposomes were stable. The experiments were carried out in 10 mM sodium phosphate buffer, pH 7.0.

We started our preliminary experiments with protein transduction domain (Tat) of Human immunodeficiency virus type 1 (HIV-1) with eleven amino acid long basic residues (47-57).[195] The amino acid sequence of HIV-1 Tat (47-57) is H-YGRKKRRQRRR-OH. Since the *N*-terminal aromatic group (tyrosine) acts a recognition motif for CB7 ($K_{CB7•HIV\text{-}1\ Tat}$ = 2.0 ×10^5 M^{-1}, Figure 5.5a),[48,49] we proceeded with CB7 and BE as our sensing ensemble encapsulated inside liposomes. In absence of an analyte, no fluorescence change was observed (Figure 5.5b). However, upon addition of our analyte of interest, a time-resolved decrease in fluorescence signal was observed due to the displacement of the dye BE from the CB7 cavity upon successful permeation of HIV-1 Tat (47-57) into CB7•BE-loaded liposomes (Figure 5.5b).

The results presented so far are only the glimpses of different applications, and research problems supramolecular tandem membrane assays could address in near future. A systematic follow-up to these studies would unleash the potential of supramolecular chemosensors as a powerful analytical tool in biomembrane research.

– Chapter 6 –
References

References

(1) Cram, D. J.; Cram, J. M. *Science* **1974**, *183*, 803.
(2) Lehn, J. M. *Angew. Chem. Int. Ed.* **1988**, *27*, 89.
(3) Pedersen, C. J. *J. Am. Chem. Soc.* **1967**, *89*, 2495.
(4) Luo, Z. G.; Xu, X. M.; Zhang, X. M.; Hu, L. M. *Mini-Rev. Med. Chem.* **2013**, *13*, 1160.
(5) Challa, R.; Ahuja, A.; Ali, J.; Khar, R. K. *AAPS PharmSciTech* **2005**, *6*, E329.
(6) Ghosh, I.; Nau, W. M. *Adv. Drug Deliv. Rev.* **2012**, *64*, 764.
(7) Breslow, R.; Dong, S. D. *Chem. Rev.* **1998**, *98*, 1997.
(8) Klock, C.; Dsouza, R. N.; Nau, W. M. *Org. Lett.* **2009**, *11*, 2595.
(9) Pemberton, B. C.; Raghunathan, R.; Volla, S.; Sivaguru, J. *Chem. Eur. J.* **2012**, *18*, 12178.
(10) Quesada, R. In *Supramolecular Chemistry: From Molecules to Nanomaterials*; John Wiley & Sons, Ltd: 2012.
(11) Schneider, H. J. *Angew. Chem. Int. Ed.* **2009**, *48*, 3924.
(12) Beer, P. D.; Blackburn, C.; Mcaleer, J. F.; Sikanyika, H. *Inorg. Chem.* **1990**, *29*, 378.
(13) Suzuki, I.; Ohkubo, M.; Ueno, A.; Osa, T. *Chem. Lett.* **1992**, 269.
(14) Valeur, B.; Leray, I. *Inorg. Chim. Acta* **2007**, *360*, 765.
(15) Ghale, G.; Nau, W. M. *Acc. Chem. Res.* **2014**, DOI: 10.1021/ar500116d.
(16) Metzger, A.; Anslyn, E. V. *Angew. Chem. Int. Ed.* **1998**, *37*, 649.
(17) Nguyen, B. T.; Anslyn, E. V. *Coord. Chem. Rev.* **2006**, *250*, 3118.
(18) Wiskur, S. L.; Ait-Haddou, H.; Lavigne, J. J.; Anslyn, E. V. *Acc. Chem. Res.* **2001**, *34*, 963.
(19) Inouye, M.; Hashimoto, K.; Isagawa, K. *J. Am. Chem. Soc.* **1994**, *116*, 5517.
(20) Bissell, R. A.; De Silva, A. P.; Gunaratne, H. Q. N.; Lynch, P. L. M.; Maguire, G. E. M.; Sandanayake, K. R. A. S. *Chem. Soc. Rev.* **1992**, *21*, 187.
(21) Piątek, A. M.; Bomble, Y. J.; Wiskur, S. L.; Anslyn, E. V. *J. Am. Chem. Soc.* **2004**, *126*, 6072.
(22) Niikura, K.; Bisson, A. P.; Anslyn, E. V. *J. Chem. Soc., Perkin Trans. 2* **1999**, 1111.
(23) Nguyen, B. T.; Wiskur, S. L.; Anslyn, E. V. *Org. Lett.* **2004**, *6*, 2499.
(24) Wright, A. T.; Anslyn, E. V.; McDevitt, J. T. *J. Am. Chem. Soc.* **2005**, *127*, 17405.
(25) Zhang, T. Z.; Anslyn, E. V. *Org. Lett.* **2007**, *9*, 1627.
(26) Leung, D.; Folmer-Andersen, J. F.; Lynch, V. M.; Anslyn, E. V. *J. Am. Chem. Soc.* **2008**, *130*, 12318.
(27) Joyce, L. A.; Maynor, M. S.; Dragna, J. M.; da Cruz, G. M.; Lynch, V. M.; Canary, J. W.; Anslyn, E. V. *J. Am. Chem. Soc.* **2011**, *133*, 13746.
(28) Barrett, G.; Mckervey, M. A.; Malone, J. F.; Walker, A.; Arnaudneu, F.; Guerra, L.; Schwingweill, M. J.; Gutsche, C. D.; Stewart, D. R. *J. Chem. Soc., Perkin Trans. 2* **1993**, 1475.
(29) Gutsche, C. D.; Levine, J. A. *J. Am. Chem. Soc.* **1982**, *104*, 2652.
(30) No, K. H.; Gutsche, C. D. *J. Org. Chem.* **1982**, *47*, 2713.
(31) Assmus, R.; Bohmer, V.; Harrowfield, J. M.; Ogden, M. I.; Richmond, W. R.; Skelton, B. W.; White, A. H. *J. Chem. Soc., Dalton Trans.* **1993**, 2427.

(32) Mnuk, P.; Feltl, L. *Chem. Listy* **1993**, *87*, 613.
(33) Shinkai, S. *Tetrahedron* **1993**, *49*, 8933.
(34) McMahon, G.; O'Malley, S.; Nolan, K.; Diamond, D. *Arkivoc* **2003**, 23.
(35) Jose, P.; Menon, S. *Bioinorg. Chem. Appl.* **2007**, *2007*, 65815.
(36) Shinkai, S.; Araki, K.; Tsubaki, T.; Arimura, T.; Manabe, O. *J. Chem. Soc., Perkin Trans. 2* **1987**, 2297.
(37) Böhmer, V. *Angew. Chem. Int. Ed.* **1995**, *34*, 713.
(38) Mokhtari, B.; Pourabdollah, K.; Dalali, N. *J. Inclusion Phenom. Macrocyclic Chem.* **2011**, *69*, 1.
(39) Lucas, D.; Minami, T.; Iannuzzi, G.; Cao, L. P.; Wittenberg, J. B.; Anzenbacher, P.; Isaacs, L. *J. Am. Chem. Soc.* **2011**, *133*, 17966.
(40) Jon, S. Y.; Selvapalam, N.; Oh, D. H.; Kang, J. K.; Kim, S. Y.; Jeon, Y. J.; Lee, J. W.; Kim, K. *J. Am. Chem. Soc.* **2003**, *125*, 10186.
(41) Behrend, R.; Meyer, E.; Rusche, F. *Justus Liebigs Ann. Chem.* **1905**, *339*, 1.
(42) Freeman, W. A.; Mock, W. L.; Shih, N. Y. *J. Am. Chem. Soc.* **1981**, *103*, 7367.
(43) Mock, W. L. In *Supramolecular Chemistry II - Host Design and Molecular Recognition*; Weber, E., Ed.; Springer Berlin Heidelberg: 1995; Vol. 175, p 1.
(44) Lagona, J.; Mukhopadhyay, P.; Chakrabarti, S.; Isaacs, L. *Angew. Chem. Int. Ed.* **2005**, *44*, 4844.
(45) Day, A.; Arnold, A. P.; Blanch, R. J.; Snushall, B. *J. Org. Chem.* **2001**, *66*, 8094.
(46) Kim, J.; Jung, I. S.; Kim, S. Y.; Lee, E.; Kang, J. K.; Sakamoto, S.; Yamaguchi, K.; Kim, K. *J. Am. Chem. Soc.* **2000**, *122*, 540.
(47) Marquez, C.; Huang, F.; Nau, W. M. *IEEE Trans. Nanobiosci.* **2004**, *3*, 39.
(48) Hennig, A.; Bakirci, H.; Nau, W. M. *Nat. Methods* **2007**, *4*, 629.
(49) Bailey, D. M.; Hennig, A.; Uzunova, V. D.; Nau, W. M. *Chem. Eur. J.* **2008**, *14*, 6069.
(50) Nau, W. M.; Ghale, G.; Hennig, A.; Bakirci, H.; Bailey, D. M. *J. Am. Chem. Soc.* **2009**, *131*, 11558.
(51) Ghale, G.; Ramalingam, V.; Urbach, A. R.; Nau, W. M. *J. Am. Chem. Soc.* **2011**, *133*, 7528.
(52) Ghale, G.; Kuhnert, N.; Nau, W. M. *Nat. Prod. Commun.* **2012**, *7*, 343.
(53) Florea, M.; Nau, W. M. *Angew. Chem. Int. Ed.* **2011**, *50*, 9338.
(54) Miyahara, Y.; Abe, K.; Inazu, T. *Angew. Chem. Int. Ed.* **2002**, *41*, 3020.
(55) Lim, Y. B.; Kim, T.; Lee, J. W.; Kim, S. M.; Kim, H. J.; Kim, K.; Park, J. S. *Bioconjugate Chem.* **2002**, *13*, 1181.
(56) Dsouza, R. N.; Pischel, U.; Nau, W. M. *Chem. Rev.* **2011**, *111*, 7941.
(57) Wagner, B.; Fitzpatrick, S. *J. Inclusion Phenom. Macrocyclic Chem.* **2000**, *38*, 467.
(58) Megyesi, M.; Biczok, L. *Chem. Phys. Lett.* **2006**, *424*, 71.
(59) Mohanty, J.; Nau, W. M. *Angew. Chem. Int. Ed.* **2005**, *44*, 3750.
(60) Koner, A. L.; Nau, W. M. *Supramol. Chem.* **2007**, *19*, 55.
(61) Nau, W. M.; Mohanty, J. *Int. J. Photoenergy* **2005**, *7*, 133.
(62) Shaikh, M.; Mohanty, J.; Singh, P. K.; Nau, W. M.; Pal, H. *Photochem. Photobiol. Sci.* **2008**, *7*, 408.
(63) Bakirci, H.; Koner, A. L.; Dickman, M. H.; Kortz, U.; Nau, W. M. *Angew. Chem. Int. Ed.* **2006**, *45*, 7400.
(64) Bakirci, H.; Koner, A. L.; Nau, W. M. *Chem. Commun.* **2005**, 5411.
(65) Bakirci, H.; Nau, W. M. *Adv. Funct. Mater.* **2006**, *16*, 237.
(66) Gribbon, P.; Sewing, A. *Drug Discovery Today* **2003**, *8*, 1035.

(67) Goddard, J. P.; Reymond, J. L. *Trends Biotechnol.* **2004**, *22*, 363.
(68) Reymond, J. L.; Fluxa, V. S.; Maillard, N. *Chem. Commun.* **2009**, 34.
(69) Su, J.; Rajapaksha, T. W.; Peter, M. E.; Mrksich, M. *Anal. Chem.* **2006**, *78*, 4945.
(70) Geymayer, P.; Bahr, N.; Reymond, J. L. *Chem. Eur. J.* **1999**, *5*, 1006.
(71) Tawfik, D. S.; Green, B. S.; Chap, R.; Sela, M.; Eshhar, Z. *Proc. Natl. Acad. Sci. U. S. A.* **1993**, *90*, 373.
(72) Florea, M.; Nau, W. M. *Org. Biomol. Chem.* **2010**, *8*, 1033.
(73) Guo, D.-S.; Uzunova, V. D.; Su, X.; Liu, Y.; Nau, W. M. *Chem. Sci.* **2011**, *2*, 1722.
(74) Dsouza, R. N.; Hennig, A.; Nau, W. M. *Chem. Eur. J.* **2012**, *18*, 3444.
(75) Florea, M.; Kudithipudi, S.; Rei, A.; Gonzalez-Alvarez, M. J.; Jeltsch, A.; Nau, W. M. *Chem. Eur. J.* **2012**, *18*, 3521.
(76) Logsdon, L. A.; Urbach, A. R. *J. Am. Chem. Soc.* **2013**, *135*, 11414.
(77) Hennig, A.; Ghale, G.; Nau, W. M. *Chem. Commun.* **2007**, 1614.
(78) Guo, D. S.; Yang, J.; Liu, Y. *Chem. Eur. J.* **2013**, *19*, 8755.
(79) Ghale, G.; Lanctot, A. G.; Kreissl, H. T.; Jacob, M. H.; Weingart, H.; Winterhalter, M.; Nau, W. M. *Angew. Chem. Int. Ed.* **2014**, *53*, 2762.
(80) Terstappen, G. C.; Roncarati, R.; Dunlop, J.; Peri, R. *Future Med. Chem.* **2010**, *2*, 715.
(81) Mahendran, K. R.; Hajjar, E.; Mach, T.; Lovelle, M.; Kumar, A.; Sousa, I.; Spiga, E.; Weingart, H.; Gameiro, P.; Winterhalter, M.; Ceccarelli, M. *J. Phys. Chem. B* **2010**, *114*, 5170.
(82) Matile, S.; Sakai, N.; Hennig, A. In *Supramolecular Chemistry: From Molecules to Nanomaterials.*; Gale, P. A., Steed, J. W., Eds.; John Wiley & Sons: Chichester, 2012; Vol. 8, p 473.
(83) McNally, B. A.; Koulov, A. V.; Smith, B. D.; Joos, J. B.; Davis, A. P. *Chem. Commun.* **2005**, 1087.
(84) Henriques, S. T.; Melo, M. N.; Castanho, M. A. R. B. *Mol. Membr. Biol.* **2007**, *24*, 173.
(85) Szeto, H. H.; Schiller, P. W.; Zhao, K.; Luo, G. *FASEB J.* **2005**, *19*, 118.
(86) Jones, A. T.; Sayers, E. J. *J. Controlled Release* **2012**, *161*, 582.
(87) Heitz, F.; Morris, M. C.; Divita, G. *Br. J. Pharmacol.* **2009**, *157*, 195.
(88) Boll, A.; Jatho, A.; Czudnochowski, N.; Geyer, M.; Steinem, C. *Biochim. Biophys. Acta, Biomembr.* **2011**, *1808*, 2685.
(89) Conner, S. D.; Schmid, S. L. *Nature* **2003**, *422*, 37.
(90) Hurtley, S. M. *Science* **2005**, *310*, 1451.
(91) Madani, F.; Lindberg, S.; Langel, Ü.; Futaki, S.; Gräslund, A. *J. Biophys.* **2011**, *2011*, 414729
(92) Schmidt, N.; Mishra, A.; Lai, G. H.; Wong, G. C. L. *FEBS Lett.* **2010**, *584*, 1806.
(93) Joliot, A.; Prochiantz, A. *Nat. Cell Biol.* **2004**, *6*, 189.
(94) Lochmann, D.; Jauk, E.; Zimmer, A. *Eur. J. Pharm. Biopharm.* **2004**, *58*, 237.
(95) Sorgi, F. L.; Bhattacharya, S.; Huang, L. *Gene Ther.* **1997**, *4*, 961.
(96) Brogden, K. A. *Nat. Rev. Microbiol.* **2005**, *3*, 238.
(97) Apetrei, A.; Asandei, A.; Park, Y.; Hahm, K. S.; Winterhalter, M.; Luchian, T. *J. Bioenerg. Biomembr.* **2010**, *42*, 173.
(98) Aspedon, A.; Groisman, E. A. *Microbiology* **1996**, *142*, 3389.
(99) Pagès, J. M.; James, C. E.; Winterhalter, M. *Nat. Rev. Microbiol.* **2008**, *6*, 893.
(100) Vidal, S.; Bredin, J.; Pagès, J. M.; Barbe, J. *J. Med. Chem.* **2005**, *48*, 1395.

(101) Housden, N. G.; Hopper, J. T. S.; Lukoyanova, N.; Rodriguez-Larrea, D.; Wojdyla, J. A.; Klein, A.; Kaminska, R.; Bayley, H.; Saibil, H. R.; Robinson, C. V.; Kleanthous, C. *Science* **2013**, *340*, 1570.
(102) Lamichhane, U.; Islam, T.; Prasad, S.; Weingart, H.; Mahendran, K.; Winterhalter, M. *Eur. Biophys. J.* **2013**, *42*, 363.
(103) Minaker, S. A.; Daze, K. D.; Ma, M. C. F.; Hof, F. *J. Am. Chem. Soc.* **2012**, *134*, 11674.
(104) Van Winkle, L. J.; Bussolati, O.; Gazzola, G.; McGiven, J.; Mackenzie, B.; Saier Jr, M. H.; Taylor, P. M.; Rennie, M. J.; Low, S. Y. In *Biomembrane Transport*; Academic Press: San Diego, 1999, p 65.
(105) Seelig, J. *Biochim. Biophys. Acta* **2004**, *1666*, 40.
(106) Baslé, A.; Delcour, A. H. In *Bacterial and Eukaryotic Porins*; 1 ed.; Benz, R., Ed.; Wiley-VCH Verlag GmbH & Co. KGaA: Weinheim, 2005, p 79.
(107) Bredin, J.; Simonet, V.; Iyer, R.; Delcour, A. H.; Pagès, J. M. *Biochem. J.* **2003**, *376*, 245.
(108) Nestorovich, E. M.; Danelon, C.; Winterhalter, M.; Bezrukov, S. M. *Proc. Natl. Acad. Sci. U. S. A.* **2002**, *99*, 9789.
(109) Dobson, P. D.; Kell, D. B. *Nat. Rev. Drug. Discov.* **2008**, *7*, 205.
(110) Vargas, C.; Klingler, J.; Keller, S. In *Membrane Biogenesis*; Rapaport, D., Herrmann, J. M., Eds.; Humana Press: 2013; Vol. 1033, p 253.
(111) Eyer, K.; Paech, F.; Schuler, F.; Kuhn, P.; Kissner, R.; Belli, S.; Dittrich, P. S.; Kramer, S. D. *J. Controlled Release* **2014**, *173*, 102.
(112) Flaten, G. E.; Bunjes, H.; Luthman, K.; Brandl, M. *Eur. J. Pharm. Sci.* **2006**, *28*, 336.
(113) Fujikawa, M.; Ano, R.; Nakao, K.; Shimizu, R.; Akamatsu, M. *Bioorg. Med. Chem.* **2005**, *13*, 4721.
(114) Di, L.; Kerns, E. H.; Fan, K.; McConnell, O. J.; Carter, G. T. *Eur. J. Med. Chem.* **2003**, *38*, 223.
(115) Kansy, M.; Senner, F.; Gubernator, K. *J. Med. Chem.* **1998**, *41*, 1007.
(116) Wohnsland, F.; Faller, B. *J. Med. Chem.* **2001**, *44*, 923.
(117) Zhu, C.; Jiang, L.; Chen, T. M.; Hwang, K. K. *Eur. J. Med. Chem.* **2002**, *37*, 399.
(118) Liu, H. L.; Sabus, C.; Carter, G. T.; Du, C.; Avdeef, A.; Tischler, M. *Pharm. Res.* **2003**, *20*, 1820.
(119) Bickerton, G. R.; Paolini, G. V.; Besnard, J.; Muresan, S.; Hopkins, A. L. *Nat. Chem.* **2012**, *4*, 90.
(120) Mensch, J.; Noppe, M.; Adriaensen, J.; Melis, A.; Mackie, C.; Augustijns, P.; Brewster, M. E. *J. Chromatogr. B Analyt. Technol. Biomed. Life Sci.* **2007**, *847*, 182.
(121) Payne, D. J.; Gwynn, M. N.; Holmes, D. J.; Pompliano, D. L. *Nat. Rev. Drug Discov.* **2007**, *6*, 29.
(122) Marks, J. R.; Placone, J.; Hristova, K.; Wimley, W. C. *J. Am. Chem. Soc.* **2011**, *133*, 8995.
(123) We have coined the name supramolecular tandem assays for sensing methods that combine the supramolecular recognition features of synthetic receptors for analyte recognition with biological selectivity features, either enzymatic conversions (tandem enzyme assays, see refs. 15 & 74) or membrane passage (tandem membrane assays, see ref. 79).
(124) Masson, E.; Ling, X. X.; Joseph, R.; Kyeremeh-Mensah, L.; Lu, X. Y. *Rsc Advances* **2012**, *2*, 1213.

(125) Biedermann, F.; Uzunova, V. D.; Scherman, O. A.; Nau, W. M.; De Simone, A. *J. Am. Chem. Soc.* **2012**, *134*, 15318.
(126) Cao, L.; Sekutor, M.; Zavalij, P. Y.; Mlinaric-Majerski, K.; Glaser, R.; Isaacs, L. *Angew. Chem. Int. Ed.* **2014**, *53*, 988.
(127) Biedermann, F.; Rauwald, U.; Cziferszky, M.; Williams, K. A.; Gann, L. D.; Guo, B. Y.; Urbach, A. R.; Bielawski, C. W.; Scherman, O. A. *Chem. Eur. J.* **2010**, *16*, 13716.
(128) Biedermann, F.; Vendruscolo, M.; Scherman, O. A.; De Simone, A.; Nau, W. M. *J. Am. Chem. Soc.* **2013**, *135*, 14879.
(129) Biedermann, F.; Nau, W. M. *Angew. Chem. Int. Ed.* **2014**, doi: 10.1002/anie.201400718.
(130) Miskolczy, Z.; Biczok, L.; Megyesi, M.; Jablonkai, I. *J. Phys. Chem. B* **2009**, *113*, 1645.
(131) Li, C.; Li, J.; Jia, X. *Org. Biomol. Chem.* **2009**, *7*, 2699.
(132) Kim, H. J.; Heo, J.; Jeon, W. S.; Lee, E.; Kim, J.; Sakamoto, S.; Yamaguchi, K.; Kim, K. *Angew. Chem. Int. Ed.* **2001**, *40*, 1526.
(133) Bush, M. E.; Bouley, N. D.; Urbach, A. R. *J. Am. Chem. Soc.* **2005**, *127*, 14511.
(134) Biedermann, F.; Rauwald, U.; Zayed, J. M.; Scherman, O. A. *Chem. Sci.* **2011**, *2*, 279.
(135) Note that 2,6-ANS likely partitions into the membrane after displacement from the CB8•MVcomplex, while other dyes such as 5-hydroxytryptophan (5HO-Trp) stay in the aqueous phase.
(136) Sindelar, V.; Cejas, M. A.; Raymo, F. M.; Chen, W.; Parker, S. E.; Kaifer, A. E. *Chem. Eur. J.* **2005**, *11*, 7054.
(137) Taylor, R. W.; Coulston, R. J.; Biedermann, F.; Mahajan, S.; Baumberg, J. J.; Scherman, O. A. *Nano Lett.* **2013**, *13*, 5985.
(138) Biedermann, F.; Scherman, O. A. *J. Phys. Chem. B* **2012**, *116*, 2842.
(139) Korbakov, N.; Timmerman, P.; Lidich, N.; Urbach, B.; Sa'ar, A.; Yitzchaik, S. *Langmuir* **2008**, *24*, 2580.
(140) Pavia, K. E.; Spinella, S. A.; Elmore, D. E. *Biochim. Biophys. Acta, Biomembr.* **2012**, *1818*, 869.
(141) None of the functional groups are essential for the detection/binding of the analyte, because molecular recognition with CB7 occurs mainly by an unspecific hydrophobic effect (including the release of high-energy water) while CB8•dye complexes require an aromatic moiety as common recognition motif.
(142) Water-insoluble analytes such as anthracene could be added as ethanolic solutions because small volumes of ethanol did neither affect the liposome integrity nor the operation of the chemosensing ensembles (SI Figure 1.11).
(143) Welsher, K.; Yang, H. *Nat. Nanotechnol.* **2014**, *9*, 198.
(144) Kolesinska, B.; Podwysocka, D. J.; Rueping, M. A.; Seebach, D.; Kamena, F.; Walde, P.; Sauer, M.; Windschiegl, B.; Meyer-Acs, M.; Bruggen, M. V. D.; Giehring, S. *Chem. Biodiversity* **2013**, *10*, 1.
(145) Tang, H.; Fuentealba, D.; Ko, Y. H.; Selvapalam, N.; Kim, K.; Bohne, C. *J. Am. Chem. Soc.* **2011**, *133*, 20623.
(146) Complex formation was tested in stopped flow experiments and to fast to yield time resolved traces that could be analysed in terms of complexation rates.
(147) Gutknecht, J.; Tosteson, D. C. *Science* **1973**, *182*, 1258.
(148) Saparov, S. M.; Antonenko, Y. N.; Pohl, P. *Biophys. J.* **2006**, *90*, L86.
(149) Angelova, M. I.; Dimitrov, D. S. *Faraday Discuss.* **1986**, *81*, 303.

(150) Mirsky, V. M.; Yatsimirsky., A. *Artificial Receptors for Chemical Sensors*; Wiley-VCH: Weinheim, 2011.
(151) In *Chemosensors: Principles, Strategies, and Applications*; Wang, B., Anslyn, E. V., Eds.; John Wiley & Sons, Inc.: 2011.
(152) Nau, W. M.; Florea, M.; Assaf, K. I. *Isr. J. Chem.* **2011**, *51*, 559.
(153) Isobe, H.; Tomita, N.; Lee, J. W.; Kim, H. J.; Kim, K.; Nakamura, E. *Angew. Chem. Int. Ed.* **2000**, *39*, 4257.
(154) Heitmann, L. M.; Taylor, A. B.; Hart, P. J.; Urbach, A. R. *J. Am. Chem. Soc.* **2006**, *128*, 12574.
(155) Large aliphatic molecules such as adamantanes are also effectively complexed by CB8 in a 1:1 stoichiometry.
(156) Chakrabarti, A. C. *Amino Acids* **1994**, *6*, 213.
(157) Ranganathan, D.; Haridas, V.; Madhusudanan, K. P.; Roy, R.; Nagaraj, R.; John, G. B. *J. Am. Chem. Soc.* **1997**, *119*, 11578.
(158) Witt, K. A.; Gillespie, T. J.; Huber, J. D.; Egleton, R. D.; Davis, T. P. *Peptides* **2001**, *22*, 2329.
(159) Rickhag, M.; Owens, W. A.; Winkler, M. T.; Strandfelt, K. N.; Rathje, M.; Sorensen, G.; Andresen, B.; Madsen, K. L.; Jorgensen, T. N.; Wortwein, G.; Woldbye, D. P.; Sitte, H.; Daws, L. C.; Gether, U. *J. Biol. Chem.* **2013**, *288*, 27534.
(160) Simon, S. A. *J. Gen. Physiol.* **1977**, *70*, 123.
(161) Potts, R. O.; Guy, R. H. *Pharm. Res.* **1995**, *12*, 1628.
(162) Alvarez-Figueroa, M. J.; Pessoa-Mahana, C. D.; Palavecino-Gonzalez, M. E.; Mella-Raipan, J.; Espinosa-Bustos, C.; Lagos-Munoz, M. E. *AAPS PharmSciTech* **2011**, *12*, 573.
(163) Walde, P.; Cosentino, K.; Engel, H.; Stano, P. *ChemBioChem* **2010**, *11*, 848.
(164) Henriques, S. T.; Melo, M. N.; Castanho, M. A. *Mol. Membr. Biol.* **2007**, *24*, 173.
(165) Li, S.; Hu, P. C.; Malmstadt, N. *Biophys. J.* **2011**, *101*, 700.
(166) Rekharsky, M. V.; Yamamura, H.; Inoue, C.; Kawai, M.; Osaka, I.; Arakawa, R.; Shiba, K.; Sato, A.; Ko, Y. H.; Selvapalam, N.; Kim, K.; Inoue, Y. *J. Am. Chem. Soc.* **2006**, *128*, 14871.
(167) Rajgariah, P.; Urbach, A. R. *J. Inclusion Phenom. Macrocyclic Chem.* **2008**, *62*, 251.
(168) Urbach, A. R.; Ramalingam, V. *Isr. J. Chem.* **2011**, *51*, 664.
(169) Pingoud, A.; Urbanke, C.; Hogget, J.; Jeltsch, A. *Biochemical Methods*; 1 ed.; Wiley-VCH, Weinheim, 2001; Vol. XIV.
(170) Oda, K.; Takahashi, T.; Takada, K.; Tsunemi, M.; Ng, K. K. S.; Hiraga, K.; Harada, S. *FEBS Lett.* **2005**, *579*, 5013.
(171) Hersh, L. B.; Morihara, K. *J. Biol. Chem.* **1986**, *261*, 6433.
(172) Matsubara, H. *Biochem. Biophys. Res. Commun.* **1966**, *24*, 427.
(173) Pauthe, E.; Dauchez, M.; Berry, H.; Berjot, M.; Monti, J.-P.; Alix, A. J. P.; Larreta-Garde, V. R. *Ann. N. Y. Acad. Sci.* **1998**, *864*, 458.
(174) Ligne, T.; Pauthe, E.; Monti, J. P.; Gacel, G.; Larreta-Garde, V. *Biochim. Biophys. Acta, Protein Struct. Mol. Enzymol.* **1997**, *1337*, 143.
(175) Inouye, K.; Kuzuya, K.; Tonomura, B. *J. Biochem.* **1994**, *116*, 530.
(176) Kitagishi, K.; Hiromi, K. *J. Biochem.* **1984**, *95*, 529.
(177) Komiyama, T.; Suda, H.; Aoyagi, T.; Takeuchi, T.; Umezawa, H. *Arch. Biochem. Biophys.* **1975**, *171*, 727.
(178) Tronrud, D. E.; Monzingo, A. F.; Matthews, B. W. *Eur. J. Biochem.* **1986**, *157*, 261.
(179) Hudgin, R. L.; Charleson, S. E.; Zimmerman, M.; Mumford, R.; Wood, P. L. *Life Sci.* **1981**, *29*, 2593.

(180) Blacker, A. J.; Jazwinski, J.; Lehn, J. M. *Helv. Chim. Acta* **1987**, *70*, 1.
(181) Basuray, A. N.; de Rouville, H. P. J.; Hartlieb, K. J.; Kikuchi, T.; Strutt, N. L.; Bruns, C. J.; Ambrogio, M. W.; Avestro, A. J.; Schneebeli, S. T.; Fahrenbach, A. C.; Stoddart, J. F. *Angew. Chem. Int. Ed.* **2012**, *51*, 11872.
(182) Stewart, J. C. *Anal. Biochem.* **1980**, *104*, 10.
(183) Kelly, M. L.; Woodbury, D. J. *Biophys. J.* **1996**, *70*, 2593.
(184) Fasman, G. D. In *Handbook of Biochemistry and Molecular Biology, Proteins*; 3rd ed.; Fasman, G. D., Ed.; CRC Press: 1976, p 183.
(185) Berg, J. M.; Tymoczko, J. L.; Stryer, L. *Biochemistry*; 5 ed.; W. H. Freeman and Company.: New York, 2002.
(186) Yang, J. J.; Vanwart, H. E. *Biochemistry* **1994**, *33*, 6508.
(187) Hennig, A.; Florea, M.; Roth, D.; Enderle, T.; Nau, W. M. *Anal. Biochem.* **2007**, *360*, 255.
(188) Seydel, J. K. In *Drug-Membrane Interactions*; Wiley-VCH Verlag GmbH & Co. KGaA: 2003, p 217.
(189) Seddon, A. M.; Casey, D.; Law, R. V.; Gee, A.; Templer, R. H.; Ces, O. *Chem. Soc. Rev.* **2009**, *38*, 2509.
(190) Frezard, F.; Garnier-Suillerot, A. *Biochim. Biophys. Acta, Lipids Lipid Metab.* **1998**, *1389*, 13.
(191) Hugo, W. B.; Stretton, R. J. *J. Gen. Microbiol.* **1966**, *42*, 133.
(192) Dunnick, J. K.; O'Leary, W. M. *J. Bacteriol.* **1970**, *101*, 892.
(193) Vaczi, L.; Szita, J.; Cieleszky, V. *Acta Microbiol. Acad. Sci. Hung.* **1957**, *4*, 437.
(194) Persson, D.; Thoren, P. E.; Esbjorner, E. K.; Goksor, M.; Lincoln, P.; Norden, B. *Biochim. Biophys. Acta* **2004**, *1665*, 142.
(195) Herce, H. D.; Garcia, A. E. *Proc. Natl. Acad. Sci. U. S. A.* **2007**, *104*, 20805.
(196) Strömstedt, A. A.; Wessman, P.; Ringstad, L.; Edwards, K.; Malmsten, M. *J. Colloid Interface Sci.* **2007**, *311*, 59.
(197) Moncelli, M. R.; Becucci, L.; Guidelli, R. *Biophys. J.* **1994**, *66*, 1969.
(198) Rauwald, U.; Biedermann, F.; Deroo, S.; Robinson, C. V.; Scherman, O. A. *J. Phys. Chem. B* **2010**, *114*, 8606.
(199) Lagona, J.; Mukhopadhyay, P.; Chakrabarti, S.; Isaacs, L. *Angew. Chem. Int. Ed.* **2005**, *44*, 4844.
(200) Masson, E.; Ling, X. X.; Joseph, R.; Kyeremeh-Mensah, L.; Lu, X. Y. *Rsc Adv.* **2012**, *2*, 1213.
(201) Holde, K. E. v.; Johnson, C.; Ho, P. S. In *Principles of Physical Biochemistry*; 2nd ed.; Prentice Hall: New Jersey, 2006, p 605.

– Appendices –

Appendix 1. Supporting Information for Chapter 2

1.1. Complete Removal of Unencapsulated CX4•LCG Complex

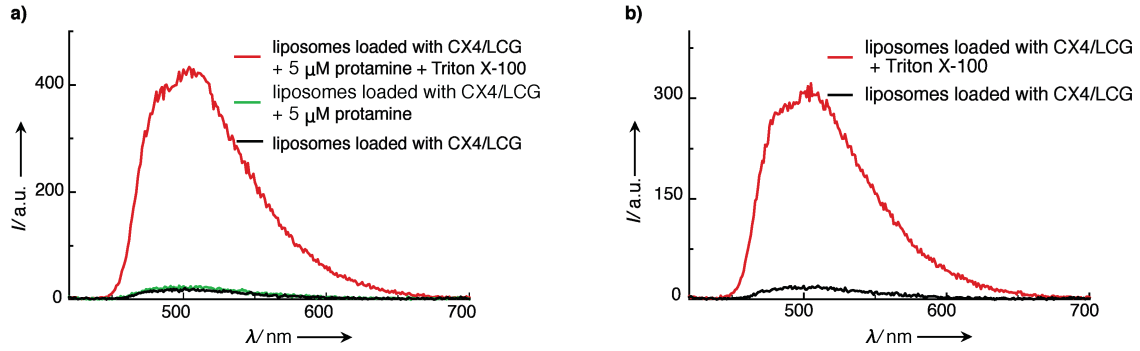

SI Figure 1.1: a) Fluorescence emission spectra of CX4•LCG-loaded liposomes before and after addition of 5 μM protamine, and after addition of both, protamine and triton X. b) Fluorescence emission spectra of CX4•LCG-loaded liposomes before and after addition of triton X. Measurements were carried out using 25 μl of CX4•LCG-loaded liposome solutions in a 1-ml cuvette in 10 mM sodium phosphate buffer at pH 7.0 and 25 °C. [79]

1.2. Absence of Protamine-induced Fusion of Liposomes

No significant changes upon addition of protamine were observed, ruling out that the additive induces liposome fusion (SI Figure 1.2).

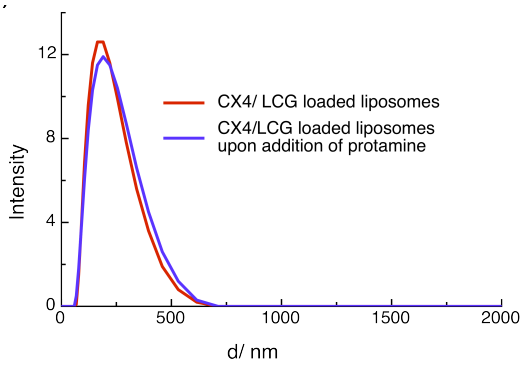

SI Figure 1.2: Size distribution of CX4•LCG-loaded liposomes before and after addition of protamine (20 μM).[79]

1.3. Absence of Protamine or Detergent-induced Membrane Leakage

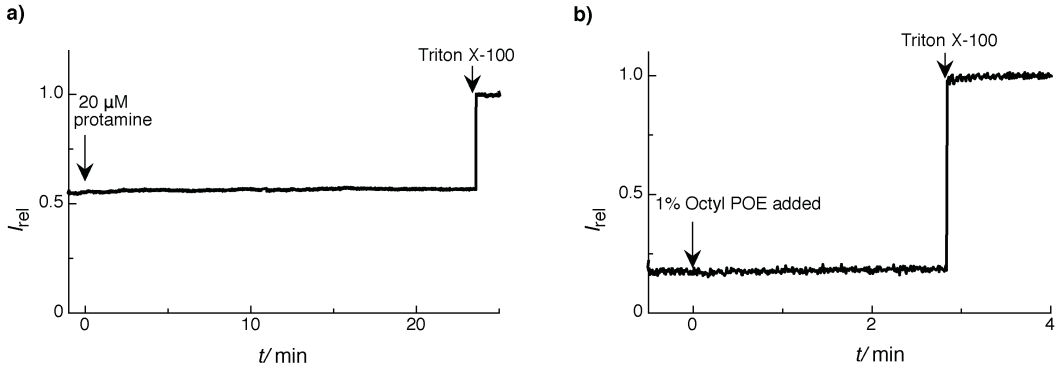

SI Figure 1.3. a) Fluorescence trace (λ_{exc} = 490 nm, λ_{obs} = 520 nm) for a solution containing carboxyfluorescein (CF, 2.5 mM)-loaded liposomes upon addition of 20 µM protamine. b) Fluorescence signal (λ_{exc} = 367 nm, λ_{obs} = 500 nm) of CX4•LCG-loaded liposomes upon addition of 2 µl of 1 % Octyl POE. Lack of change in fluorescence signal in both cases ensured that the observed change in fluorescence intensity (see Figure 2.2.3 in Chapter 2) was indeed due to translocation of protamine into liposomes through OmpF and not a mere membrane instability.[79]

1.4. Confirming Insertion of OmpF into Liposomes

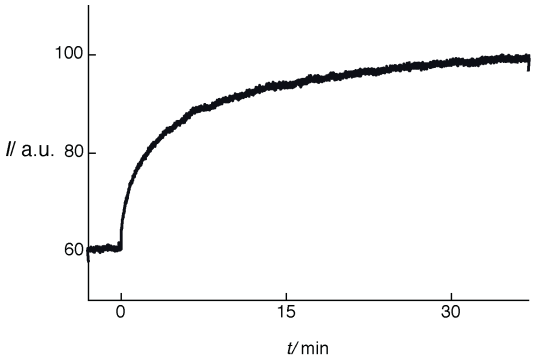

SI Figure 1.4: Confirming the insertion of OmpF into POPC bilayer-using carboxyfluorescein (λ_{exc} = 490 nm, λ_{obs} = 520 nm) loaded liposomes. Fluorescence kinetics after OmpF (45 nM) was added to liposomes containing carboxyfluorescein (CF). The inserted channels allow CF permeation into the bulk solution. The liposomal CF concentration decreases and the CF fluorescence increases due to reduced CF self-quenching. The measurement was carried out using 25 ml of liposomes in 1 ml of 10 mM sodium phosphate buffer at pH 7.0 at 25 °C.

Following section 1.5 is derived from.[79]

1.5. Adsorption of Protamine to the Liposome Surface

Two different sets of measurements were carried out to test possible adsorption of protamine (SI Figure 1.5): a) Tandem membrane assays with two different liposome concentrations, and c) Zeta-potential measurements of liposomes in the absence and presence of protamine.

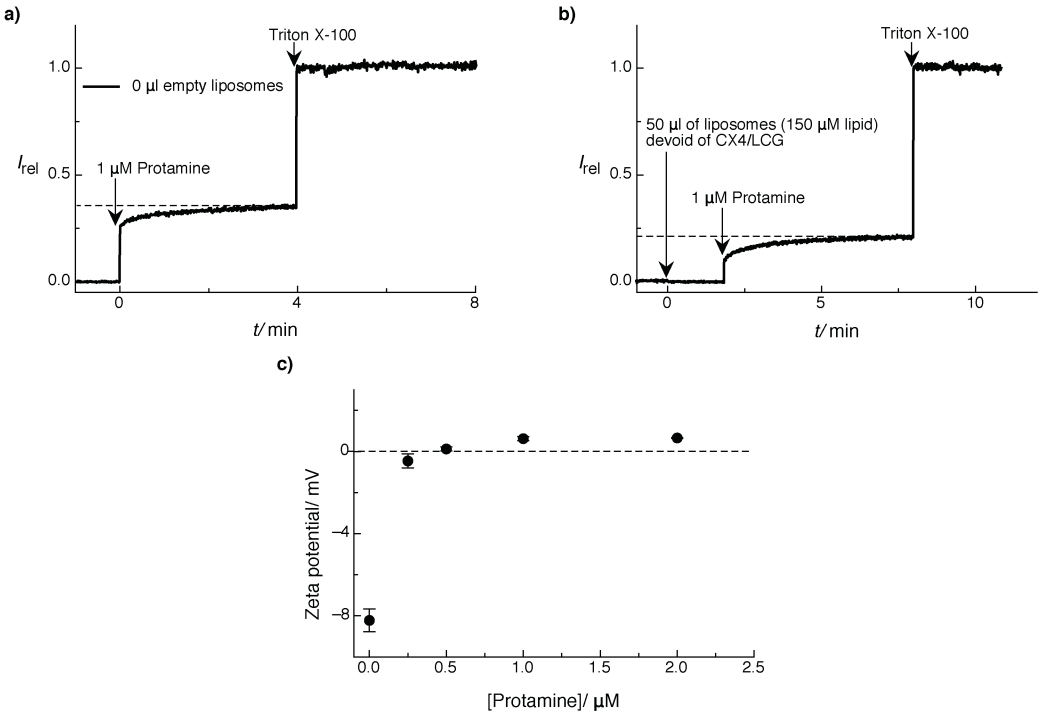

SI Figure 1.5: Fluorescence response in tandem membrane assays upon addition of 1 µM of protamine to CX4•LCG-loaded proteoliposomes a) in the absence and b) in the presence of 50 µl of a solution of "empty" liposomes (150 µM lipids). The measurements were terminated by adding triton X. Panel c) illustrates the change in zeta-potential of liposomes (25 µM lipid) with protamine concentration (0–2 µM). Measurements were carried out in 10 mM sodium phosphate buffer at pH 7.0 and 25 °C, $\lambda_{exc} = 367$ nm and $\lambda_{obs} = 500$ nm. Modified from ref.[79]

As can be readily seen from SI Figure 1.5a & b, the addition of liposomes containing neither dye nor channels strongly reduced the fluorescence response, suggesting that the effective protamine concentration was decreased by the presence of the putatively inactive liposomes. In the second control, we observed a steep increase in the zeta potential of POPC liposomes, from – 8.2 mV in the absence of protamine, consistent with previous investigations,[196,197] to +0.7 mV upon addition of 2 µM protamine (SI Figure 1.5c).

1.6. Determination of Binding Constants

SI Figure 1.6 shows representative traces for determining binding constants of several analytes with CB8, while Table S-1 list quenching efficiencies and binding affinities of 99 different organic compounds with macrocyclic receptors CB7 and CB8 in homogenous solution.

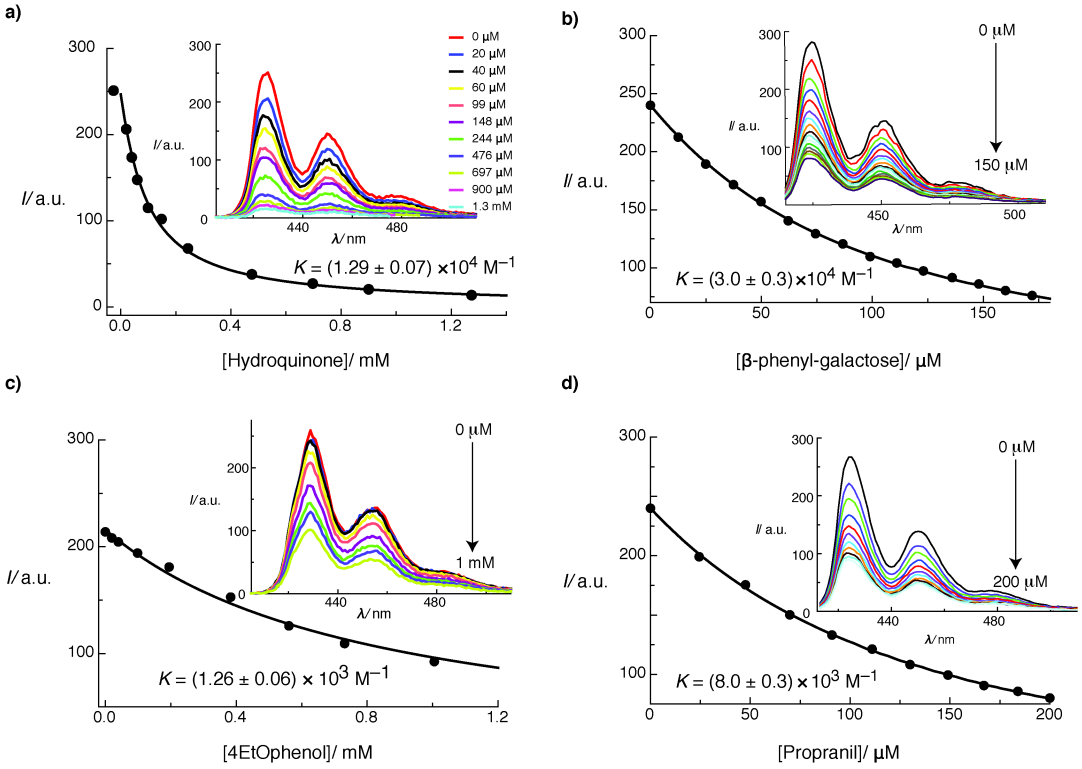

SI Figure 1.6: Fluorescence titration plots for different analytes using CB8•MDAP reporter pair in 10 mM HEPES buffer.

Table S-1. Quenching efficiencies and binding constants for the formation of macrocycle•analyte complexes in 10 mM HEPES buffer, as determined by fluorescence titrations.

Receptor	analyte	QE[a]	K_a / $(10^3\ M^{-1})^b$
CB8•MDAP	benzene	< 0.3	4
CB8•MDAP	Phe	0.5	5
CB8•MDAP	phenylethylamine	0.4	8
CB8•MDAP	aniline	0.9	33
CB8•MDAP	phenol	>0.9	56

Receptor	analyte	QE[a]	K_a / (10^3 M^{-1})[b]
CB8•MDAP	4-ethylphenol	0.6	1.2
CB8•MDAP	4-ethoxyphenol	>0.9	1
CB8•MDAP	1,2-dihydroxybenzene	>0.9	20
CB8•MDAP	1,4-dihydroxybenzene	>0.9	13
CB8•MDAP	*p*-benzoquinone	>0.9	0.5
CB8•MDAP	β-phenyl-galactose	>0.9	30
CB8•MDAP	Trp	>0.9	150
CB8•MDAP	5HO-Trp	>0.9	7.7
CB8•MDAP	tryptamine	>0.9	50
CB8•MDAP	seretonin	>0.9	5
CB8•MDAP	dopamine	>0.9	0.10
CB8•MDAP	4-hydroxyphenylpyruvic acid (HPP)	>0.9	17
CB8•MDAP	homogentisic acid (HGA)	>0.9	0.14
CB8•MDAP	naphthalene	>0.9	>50
CB8•MDAP	propanil	>0.9	8
CB8•MDAP	ranitidine	0.2	2
CB8•MDAP	naproxen	0.5	2
CB8•MDAP	chloramphenicol	-	< 1
CB8•MDAP	ceftazidime	-	< 1
CB8•MDAP	adrenaline	-	< 1
CB8•MDAP	anilinesuccinimide	>0.9	30
CB8•MDAP	benzimidazole	0.8	7.5
CB8•MDAP	hydroquinone	>0.9	13
CB8•MDAP	phenoazoaniline	0.8	39
CB8•MDAP	prochloraz	0.7	2.8
CB8•MDAP	propanolol	0.7	2.1
CB8•MDAP	quinoline	0.6	2.2
CB8•MDAP	rotenone	0.7	4.8
CB8•MBBI	hydroquinone	>0.9	2.9
CB8•MBBI	4-methoxyphenol	>0.9	2.4
CB8•MBBI	4-ethoxyphenol	>0.9	1.0

Receptor	analyte	QE[a]	K_a / (10^3 M^{-1})[b]
CB8•MBBI	4-methoxyphenylboronic acid	>0.9	4.8
CB8•MBBI	2-cyanophenol	>0.9	5.8
CB8•MBBI	4-cyanophenol	>0.9	5.2
CB8•MBBI	aniline	>0.9	25
CB8•MBBI	sodium benzoate	n.a.	<<1
CB8•MBBI	2-naphthol	>0.9	140[c]
CB8•MBBI	2,6-dihydroxynapthalene	>0.9	72[c]
CB8•MBBI	2,7-dihydroxynapthalene	>0.9	66[c]
CB8•MBBI	phenol	>0.9	15[c]
CB8•MBBI	4-iodophenol	>0.9	4.1[c]
CB8•MBBI	indole	>0.9	180[c]
CB8•MBBI	Trp	>0.9	34[c]
CB8•MBBI	TrpGlyGly	>0.9	120[c]
CB8•MBBI	GlyTrpGly	>0.9	17[c]
CB8•MBBI	GlyGlyTrp	>0.9	4.1[c]
CB8•MBBI	sesamol	>0.9	4.2[c]
CB8•MV	Phe	n.a	5.3[d]
CB8•MV	Tyr	n.a.	2.2[d]
CB8•MV	Trp	n.a.	43[d]
CB8•MV	TrpOMe	n.a.	63[d]
CB8•MV	*N*AcTrpNH$_2$	n.a.	3.1[d]
CB8•MV	tryptamine	n.a.	54[d]
CB8•MV	TrpGlyGly	n.a.	130[d]
CB8•MV	GlyTrpGly	n.a.	21[d]
CB8•MV	GlyGlyTrp	n.a.	3.1[d]
CB8•MV	2-naphthol	n.a.	610[e]
CB8•MV	2,6-dihydroxynapthalene	n.a.	590[e]
CB8•MV	2,7-dihydroxynapthalene	n.a.	160[e]
CB8•MV	phenol	n.a.	22[e]
CB8•MV	4-iodophenol	n.a.	13[e]
CB7•Pal	vitamin B1	>0.9[f]	6920[g]

Receptor	analyte	QE[a]	K_a / (10^3 M^{-1})[b]
CB7•Pal	dimethylbenzylamine (DMBA)	>0.9[f]	3040[g]
CB7•DAP	tryptamine	0.8[f]	130[h]
CB7•DAP	tyramine	>0.9[f]	3800[h]
CB7•AO	cadaverine	>0.9[f]	4500[i]
CB7•AO	pheylethylamine	>0.9[f]	6800[j]
CB7•AO	phenylalanine	0.8[f]	170[j]

[a] quenching efficiency [b] fitted by least-square fit to a 1:1 binding model in 10 mM phosphate buffer, taken from ref [127]. [c] from ref [127], in 10 mM sodium phosphate buffer (pH 7). [d] from ref [133,198] in 10 mM sodium phosphate buffer (pH 7). Note that MV is not emissive. [e] from ref [198] in 10 mM sodium phosphate buffer (pH 7). For other representative binding constants of CB8•MV with aromatic compounds, see also there. Note that MV is not emissive. [f] In a dye-displacement titration, the quenching efficiency is represented by the total change in fluorescence intensity upon complete displacement of the dye from the host cavity. [g] in 10mM phosphate buffer. n.a.: not available. [h] ref [49]. [i] ref [50]. [j] ref [52].

1.7. Supramolecular Tandem Membrane Assays

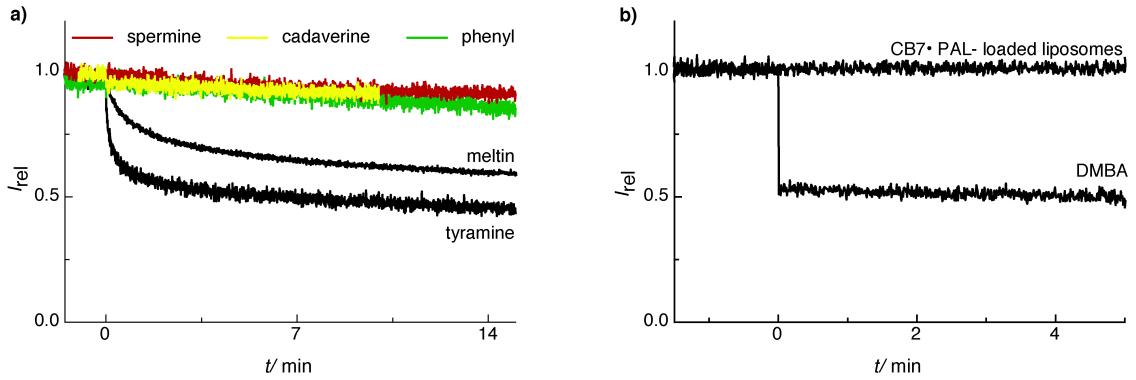

SI Figure 1.7: a) Time dependent change in fluorescence intensity of CB7•BE-loaded liposomes (λ_{exc} = 347, λ_{obs} = 500 nm) upon addition of membrane permeable analyte, tyramine, and membrane destabilizing peptide melittin. No fluorescence change is observed upon addition of spermine, cadaverine and phenylalanine. b) Evolution of fluorescence intensity after addition of dimethylbenzylamine (DMBA) to CB7•PAL-loaded liposomes (λ_{exc} = 347, λ_{obs} = 500 nm).

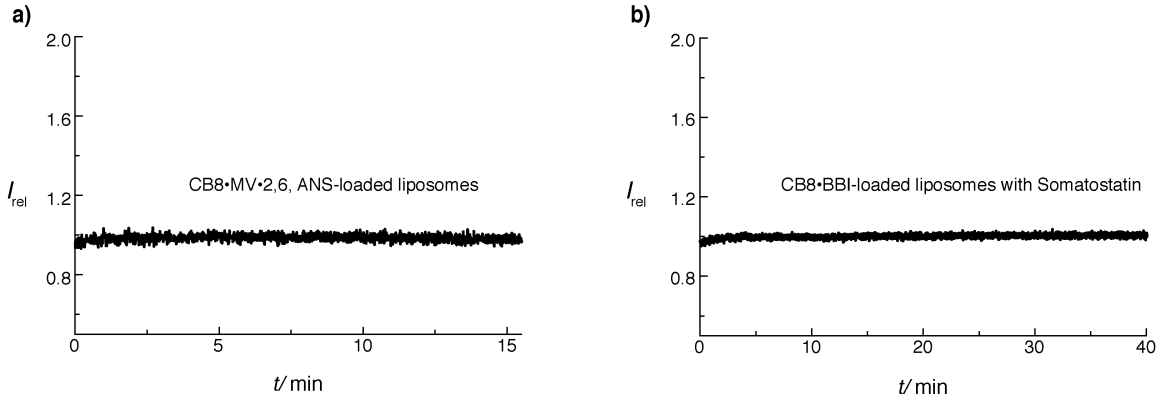

SI Figure 1.8: Control experiments in 10 mM HEPES buffer were carried out to ensure that the chemosensing ensembles did not permeate through the membrane. Evolution of fluorescence intensity of a) CB8•MV•2,6, ANS-loaded liposomes, and b) CB8•BBI-loaded liposomes with somatostanin, a membrane impermeable analyte. Permeation of either component of chemosensors, *i.e.,* CB8, MV, 2,6 ANS or BBI would have resulted in an increase in emission intensities.

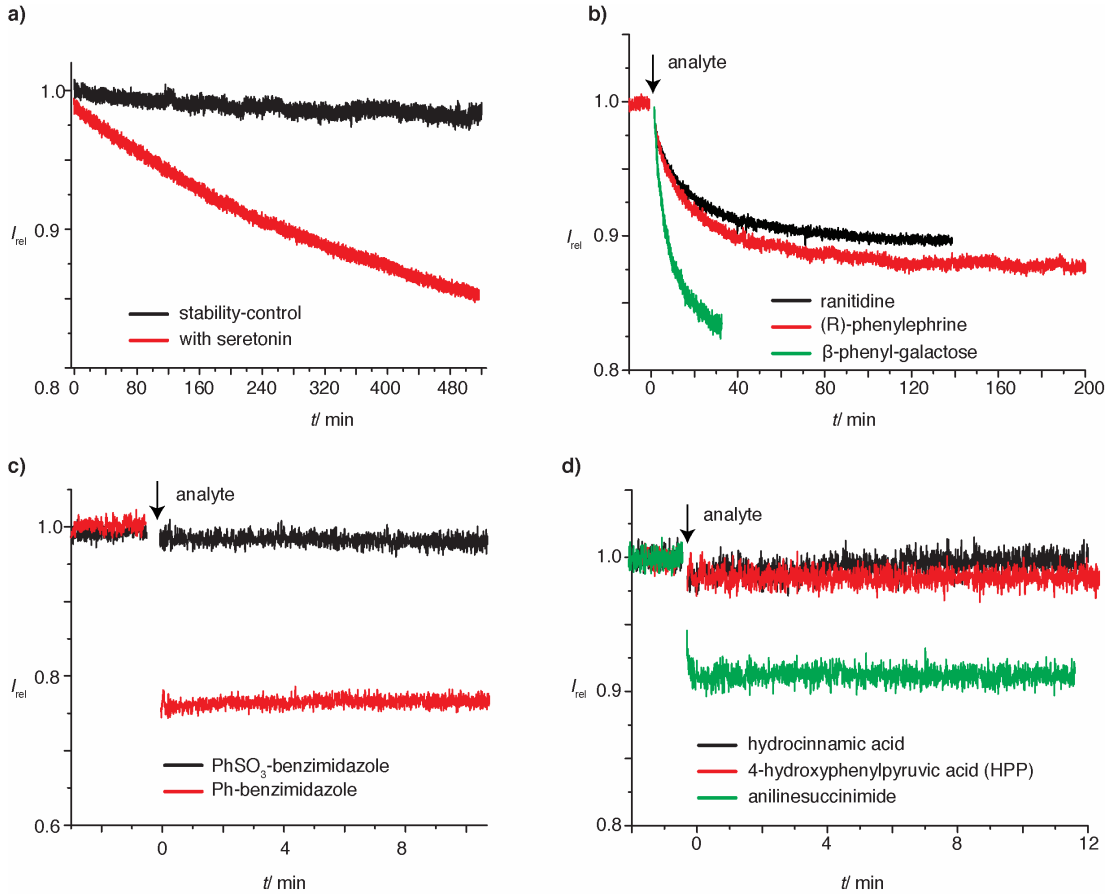

SI Figure 1.9: Fluorescence intensity upon addition of analytes to CB8•MDAP-loaded liposomes. a) & b) represents typical membrane impermeable and slowly permeating

compounds, while c) & d) represents membrane impermeable and rapidly permeating compounds. The only small change in fluorescence intensity for CB8•MDAP-loaded liposomes (a) in absence of analyte further confirms that CB8 nor MDAP is diffusing through the membrane – the small decrease in I_{rel} may be explained by the photobleaching of the dye at the timescale of >100 min.

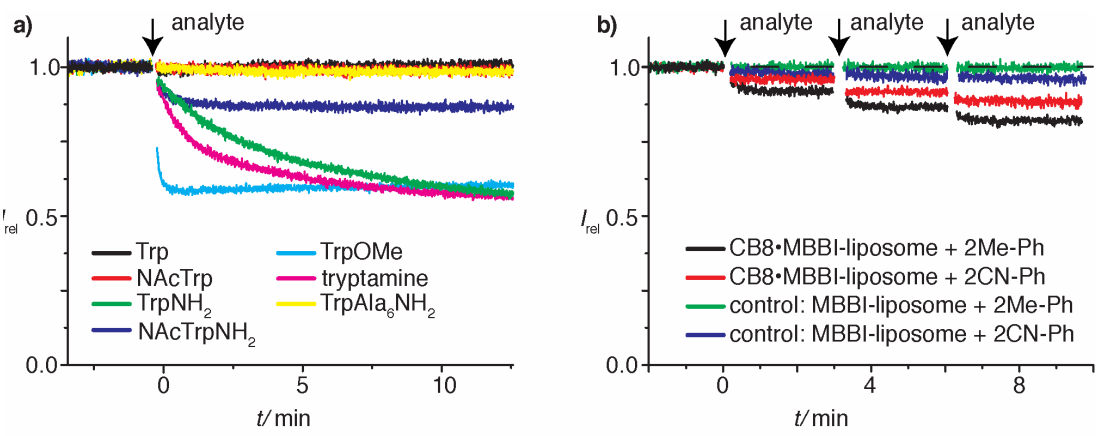

SI Figure 1.10: Evolution of fluorescent trace upon addition of a) amino acid derivatives and peptides, and b) phenol derivatives to CB8•MBBI-loaded liposomes (8 μM analyte). Additional control experiment with only MBBI-loaded liposomes (b) revealed the absence of any direct molecular recognition between the dye and the analyte in most cases.

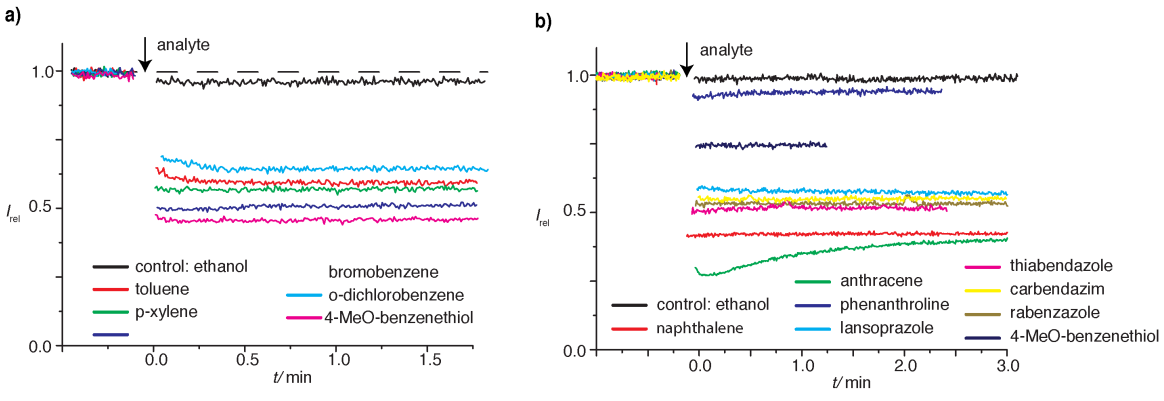

SI Figure 1.11: a) CB8•MBBI-loaded liposomes with 80 μM analyte and b) CB8•MDAP-loaded liposomes with 8 uM analyte. In both experiments 1 mM stock solution in ethanol were prepared.

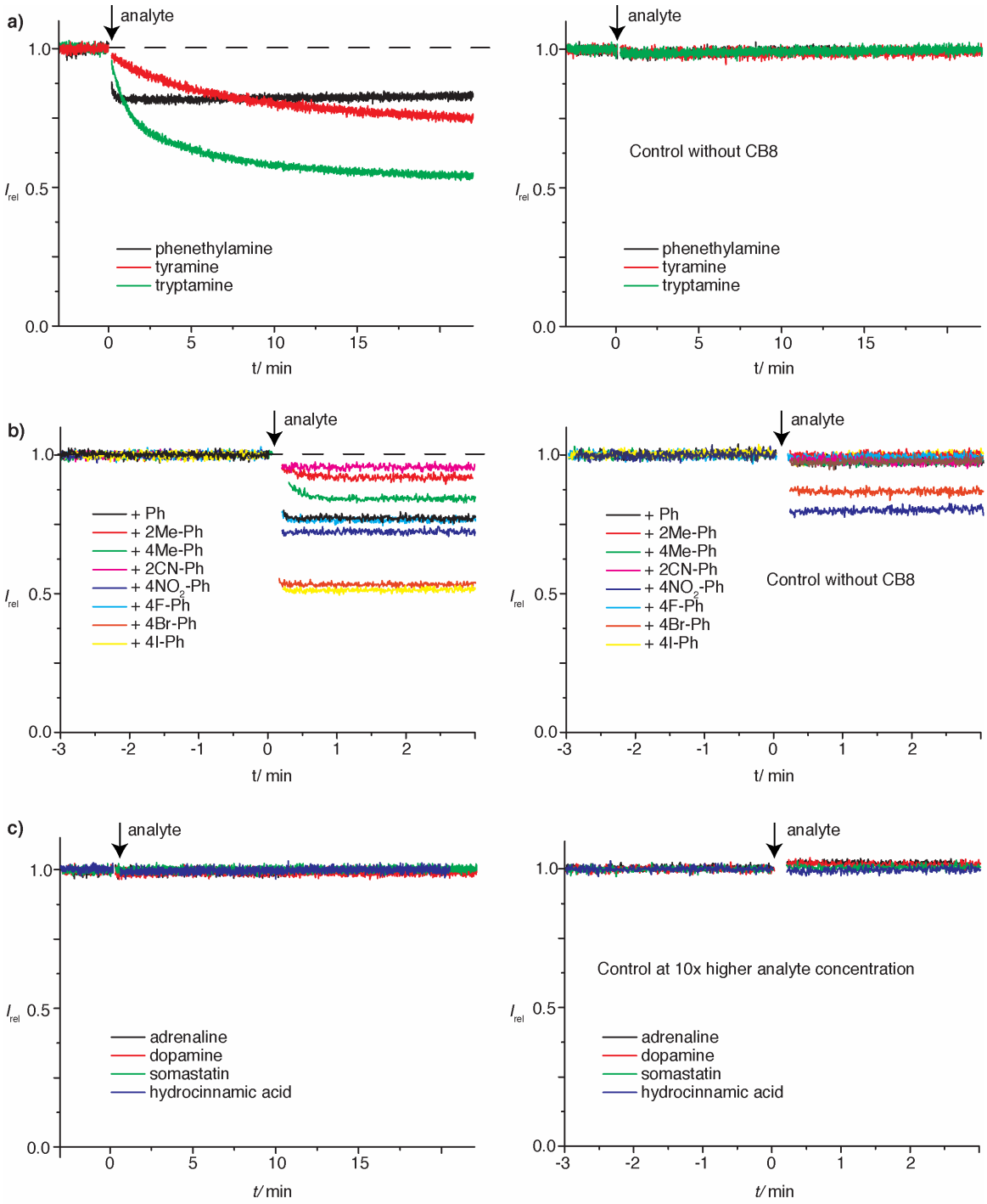

SI Figure 1.12: Fluorescent traces of a, b) CB8•MBBI-loaded liposomes (on the left) with 8 μM analyte loadings. On the right, control experiments with MBBI-loaded liposomes (no CB8) upon addition of 8 μM analyte. c) Liposomes loaded with CB8•MBBI with impermeable analytes at 8 μM (left) and 80 μM (right) analyte loading.

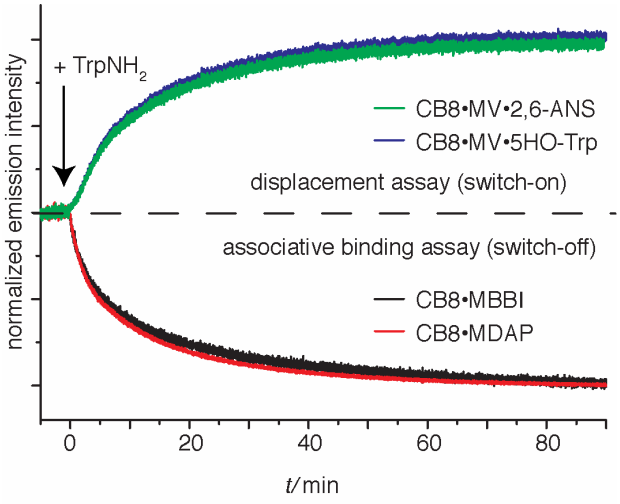

SI Figure 1.13: Permeation of $TrpNH_2$ (16 μM) through phospholipid bilayer monitored with different chemosensor-loaded liposomes.

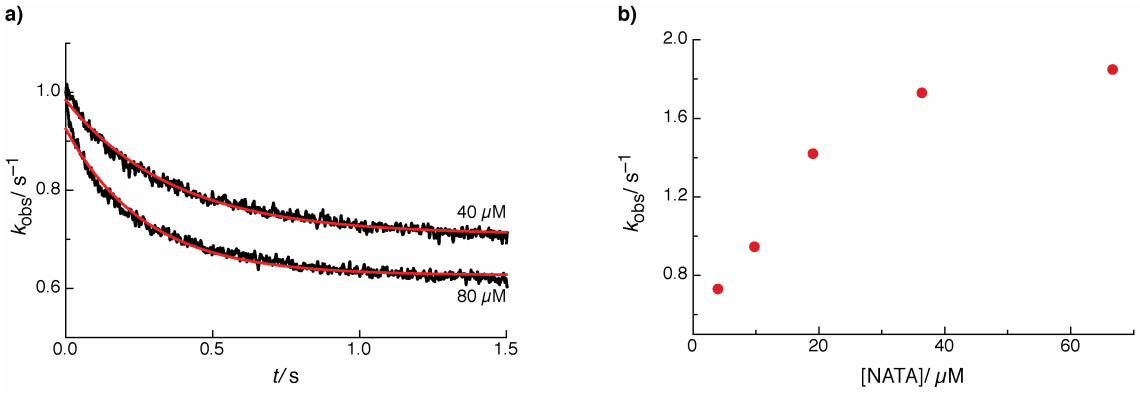

SI Figure 1.14: a) Representative time-resolved traces for the rapidly permeating analyte phenol obtained by stopped-flow fluorescence measurement. The fluorescent traces were fitted with a monoexponential function by a least-square algorithm. The resulting k_{obs} versus phenol-concentration plot is shown in Figure 4b in the main text. b) Plot of k_{obs} versus NATA-concentration.

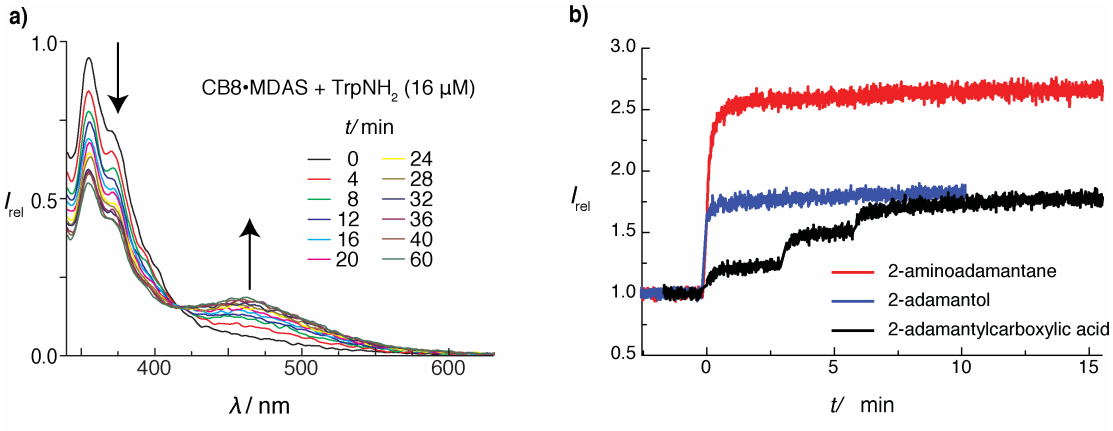

SI Figure 1.15: a) Emergence of excimer fluorescence upon permeation of $TrpNH_2$ into CB8•MDAS-loaded liposomes. b) Addition of 50 µM adamantine derivatives to CB8•MV•5OHTrp-loaded liposomes. On account of the comparably small changes in I_{rel} for the negatively charged analyte 2-adamantylcarboxylate, multiple additions were performed to undoubtedly verify its membrane-permeation. Note that the affinity differences of analogous guests for CB*n* macrocycles generally follows the trend K_a(cation) > K_a(neutral) >> K_a(anion),[152,199,200] as is also seen in this example.

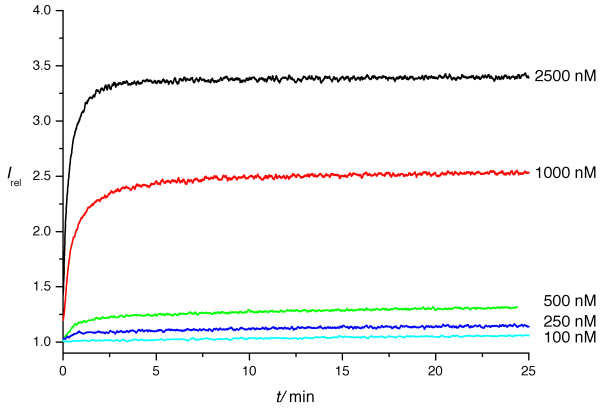

SI Figure 1.16: Change in fluorescence intensity upon addition of memantine to CB8•MV•5OH-loaded liposomes.

1.8. Membrane permeability of more than 90 different organic compounds along with reporter pairs employed for the tandem membrane assays.

SI Table 2. Membrane permeability of 97 different organic compounds investigated using *i*) membrane displacement assay (CB8•MV•2,6-ANS, CB8•MV•5OH-Trp, CB7•BE, and CB7•PAL), and *ii*) associative binding assay (CB8•MDAP, CB8•MBBI, and CB8•MDAS).

Analyte	CB8•MDAP[b]	CB8•MBBI[c]	CB8•MDAS[d]	CB8•MV•2,6-ANS[e]	CB8•MV•5HO-Trp[f]	CB7•BE[g]	CB7•PAL[h]
1,2-dihydroxybenzene (catechol)	+	+[i]					
(*R*)-phenylephrine	+	+					
1-adamantane methylamine				+	+		
1-adamantanecarboxylic acid				+	+		
1-adamantanol				+	+		
1,2-dichlorobenzene		+[k]					
1,4-benzoquinone	+[k]						
1,4-dihydroxybenzene (hydroquinone)	+						
1,4-dimethylbenzene (*p*-xylene)		+[k]					
2-cyanophenol	+	+					
2-methylphenol (*o*-cresol)	+	+					
2-naphthol	+			+[o]			
2-naphthylsulfonamide	+			+[o]			
2-phenylbenzimidazole	+			+			
2-phenylbenzimidazole-5-sulfonic acid	–			–			
2,7-dihydroxynaphthalene (2,7-diOHNp)	+			+[o]			
3-phenylpropanoic acid (hydrocinnamic acid)	–	–					
3,5-dimethyladamantan-1-amine (memantine)		+		+	+		
4-(*N*,*N*-dimethylamino)benzonitrile (DMABN)		+					

Analyte	CB8• MDAP[b]	CB8• MBBI[c]	CB8• MDAS[d]	CB8•MV• 2,6-ANS[e]	CB8•MV• 5HO-Trp[f]	CB7• BE[g]	CB7• PAL[h]
4-bromoaniline	+	+					
4-bromobenzene		+ [k]					
4-bromophenol	+	+ [n]					
4-chloroaniline	+	+					
4-chlorophenol	+	+ [n]					
4-cyanoaniline	+	+					
4-cyanophenol	+	+ [n]					
4-ethoxyphenol	+						
4-ethylphenol	+	+ [n]					
4-fluoroaniline	+	+					
4-fluorophenol	+	+ [n]					
4-hydroxybenzyl acetone (raspberry *k*etone)	+						
4-hydroxyphenylpyruvic acid (HPPA)	–						
4-iodoaniline	+	+					
4-iodophenol	+	+ [n]					
4-methoxyaniline	+						
4-methoxyphenol	+						
4-methoxythiophenol	+ [k]	+ [k]					
4-methylphenol (*p*-cresol)	+	+ [n]					
4-nitrophenol	+	+ [n]					
4-*tert*-butylphenol		+ [n]					
5-hydroxytryptophan (5HO-Trp)	–				–		
adamantane				+			
adrenaline		–					
ampicillin		–					
aniline	+	+ [n]					
aniline-succinimide	+						
anthracene	+ [k]						
bentazon		+ [k]					
benzene		+ [k]					

Analyte	CB8• MDAP[b]	CB8• MBBI[c]	CB8• MDAS[d]	CB8•MV• 2,6-ANS[e]	CB8•MV• 5HO-Trp[f]	CB7• BE[g]	CB7• PAL[h]
benzimidazole	+	+	+				
bisphenol A	+ [i,k]	+ [k]					
cadaverine						–	–
carbendazim	+ [k]			+ [k]			
dimethylbenzylamine						+	+
dopamine	–	–					
ethyl 4-aminobenzoate (benzocaine)	+						
imidachlorpid		+ [k]					
indazole	+	+					
indole	+	+	+	+	+		
lansoprazole	+ [k]						
melatonin	+ [n]			+ [n]			
melittin	+ [p]	+ [p]	+ [p]	+ [p]		+ [p]	+ [p]
methyl benzoate		+ [k]					
N-acetyl tryptophan (*N*Ac-Trp)	–	–					
N-acetyl tryptophan amide (*N*Ac-TrpNH$_2$)	+	+	+ [m]				
naphthalene	+ [k]			+ [o]			
nicotine		+		+		+	
omeprazole	+ [k]						
paracetamol	+	+ [i]					
penicillin G		–					
pentafluoroaniline	+	+					
phenanthroline	+ [k]						
phenol	+	+					
phenyl-β-D-galactopyranoside	+	+					
phenylalanine (Phe)		–					
phenylethylamine	+	+				+	+
primaquine	+			+	+		
propranil	+	+					

Analyte	CB8• MDAP[b]	CB8• MBBI[c]	CB8• MDAS[d]	CB8•MV• 2,6-ANS[e]	CB8•MV• 5HO-Trp[f]	CB7• BE[g]	CB7• PAL[h]
propranolol	+			+			
quinoline	+	+	+ [m]	+ [o]			
rabenzazole	+ [k]						
ranitidine	+						
rotenone	+						
seretonin	+	+		+			
somatostatin	–	–					
spermine						–	–
thiabendazole	+ [k]			+ [k]			
toluene		+ [k]					
tropicamide		+ [k]					
Trp-$(Ala)_6$-NH_2	–	–					
Trp-$(Leu)_6$-NH_2	–	–					
Trp-$(Lys)_6$-NH_2	–	–					
tryptamine	+	+	+ [m]	+	+	+	
tryptophan (Trp)	–	–		–	–		
tryptophan amide ($TrpNH_2$)	+	+	+ [m]	+	+		
tryptophan methyl ester (TrpOMe)	+	+	+ [m]	+			
tyramine	+	+				+	
tyrosine (Tyr)		–					
vitamin B1						–	–

[a] see also Figure 2.2.1 in Chapter 2 for chemical structures; [b] λ_{exc} = 400 nm, λ_{obs} = 450 nm; [c] λ_{exc} = 310 nm, λ_{obs} = 350 nm; [d] λ_{exc} = 330 nm, λ_{obs} = 370 nm; [e] λ_{exc} = 380 nm, λ_{obs} = 463 nm; [f] λ_{exc} = 310 nm, λ_{obs} = 337 nm; [g] λ_{exc} = 347, λ_{obs} = 500 nm; [h] λ_{exc} = 347, λ_{obs} = 500 nm; [i] small changes (higher conc); [k] analyte (10 mM) was dissolved in ethanol; [m] appearing excimer band at λ_{obs} = 500 nm was monitored; [n] control experiment in the absence of host (CB8) was also carried out; [o] λ_{obs} = 500 nm was chosen to avoid emission band from analyte; [p] Melittin is a membrane disrupting peptide. The fluorescence response is due to the release of reporter pairs from liposomes, shifting complexation equilibria towards left, i.e. uncomplexed fluorescent dye.

1.9. Transferability of Tandem Membrane Assays to GUVs and Microplate Reader

Reporter pair encapsulated GUVs to monitor diffusion of tryptophan methyl ester through phospholipid bilayer. Representative fluorescence emission spectra of two complimentary (fluorescence switch-on and switch-off) reporter pair loaded liposomes upon addition of analytes. Presence of analyte by CB8•MDAP is indicated by decrease in fluorescence owing to the formation of CB8•MDAP•analyte ternary complex. On contrary, the presence of an analyte by CB8•MV•DapoxS causes an increase in the emission intensity, since the dye is displaced from the CB8•MV complex by the analyte.

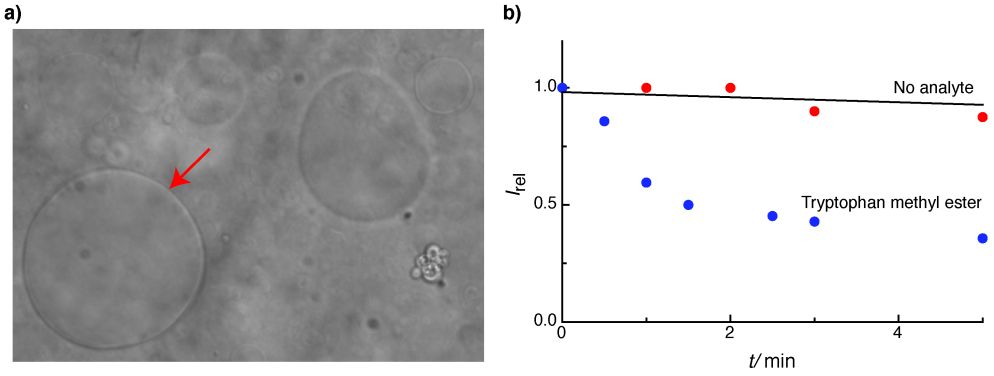

SI Figure 1.17: a) Phase contrast image of CB8•MBBI encapsulated GUVs. Red arrow indicates the GUV that we selected to follow after adding the analyte, tryptophan methyl ester (TrpOMe). b) Normalized fluorescence intensity of GUV in absence and presence of TrpOMe. Intensities were normalized using $I_{rel} = I_t/I_0$ whereby I_0 and I_t are the grey intensities inside GUV before and after addition of analyte respectively.

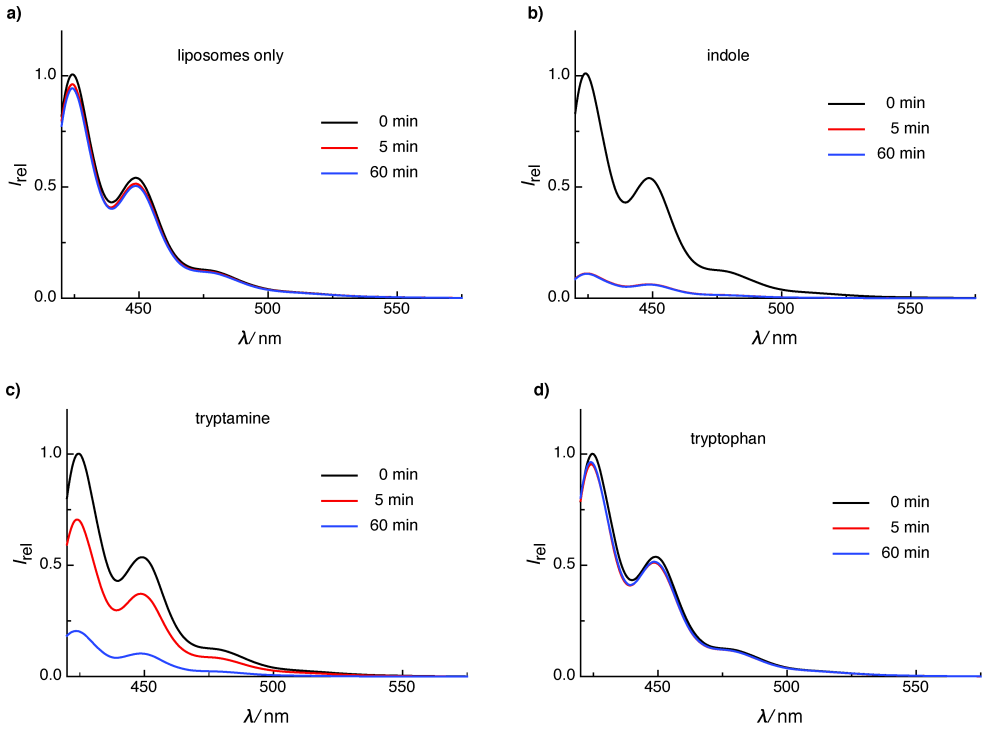

SI Figure 1.18: Emission spectra of CB8•MDAP-loaded liposomes (Associative binding, fluorescence switch-off assay) recorded using microplate reader. a) Lack of fluorescence response over 1 hr time indicated that "reporter pair" loaded liposomes composed of phospholipids were stable with standard microplate surfaces. Fluorescence reading were taken at 0, 5 and 60 minutes after addition of analytes b) indole, b) tryptamine and c) tryptophan. Intensities were normalized using $I_{rel} = I_t/I_0$ whereby I_0 and I_t were the fluorescence response before and after addition of analytes.

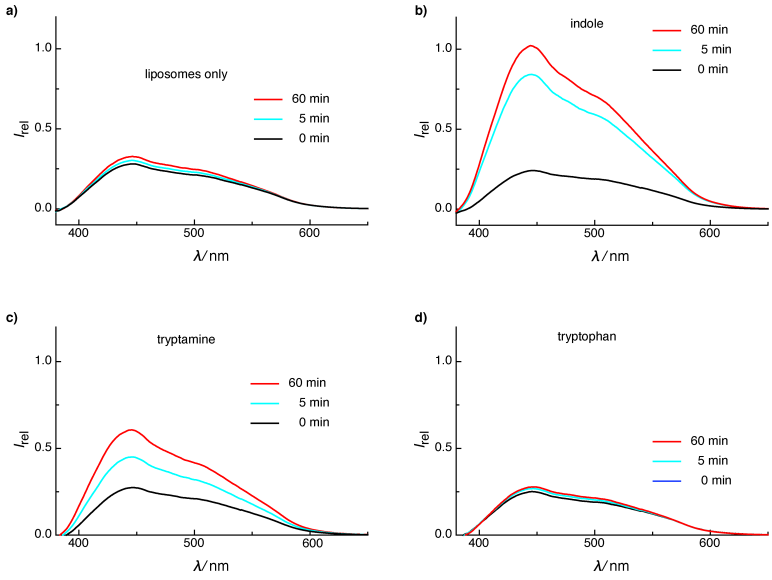

SI Figure 1.19: Emission spectra of CB8•MVDapoxS-loaded (displacement assay, fluorescence switch-on assay) liposomes recorded using microplate reader. a) Lack of fluorescence response over 1 hr time indicated that "reporter pair" loaded liposomes composed of phospholipids were stable with standard microplate surfaces. Fluorescence reading were taken at 0, 5 and 60 minutes after addition of analytes b) indole, b) tryptamine and c) tryptophan. Intensities were normalized using $I_{rel} = I/I_{\infty}$ whereby I_{∞}, in this case is the fluorescence signal upon complete displacement of the dye by indole and I is fluorescence response before and after addition of test compounds.

Appendix 2. Supporting Information for Chapter 3

Following sections 2.1, and 2.2 are derived from ref, [51,52] (the supporting information from two publications – Appendix 4.2, and 4.3)

2.1. Fluorescence Titrations for Peptides and Their Corresponding Proteolytic Products

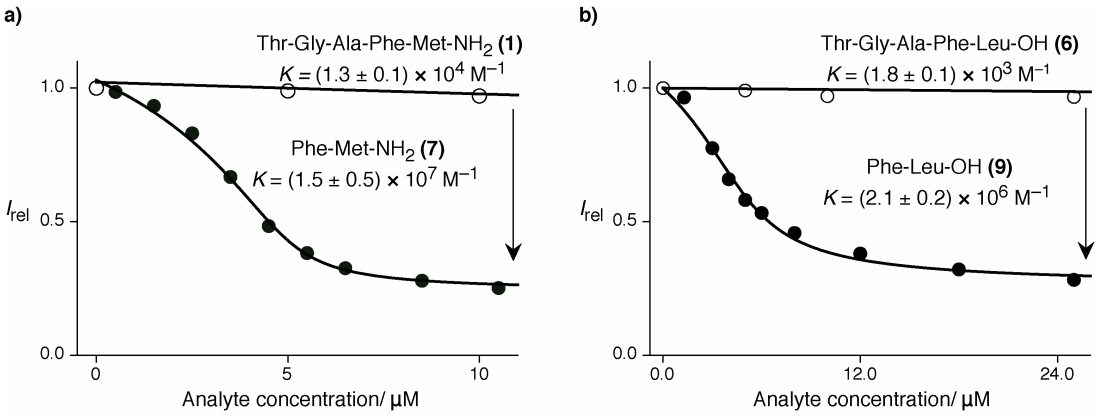

SI Figure 2.1: Fluorescence titrations of peptide–substrates and their proteolysis products (dipeptides) by using competitive displacement of AO (0.5 µM) from CB7 (5 µM) in 10 mM ammonium phosphate buffer at pH 7.2, 37 °C.

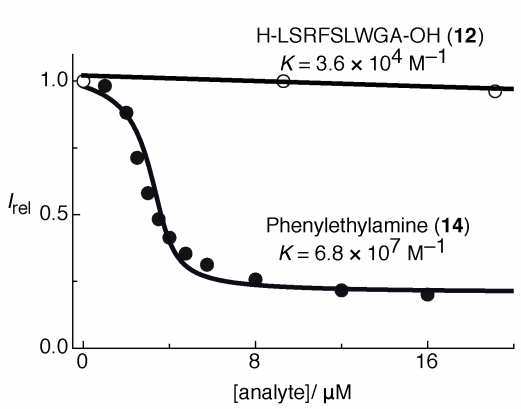

SI Figure 2.2: Titration plots for the substrate H-LSRFSWGA-OH (**12**) and phenylethylamine (as a model for the peptide hydrolysis product with Phe at the *N*-terminus, **14**) with 0.5 µM AO and 4 µM CB7 in 0.05 mM tris buffer, pH 7.6, at 37 °C.

2.2. Mass Spectrometry

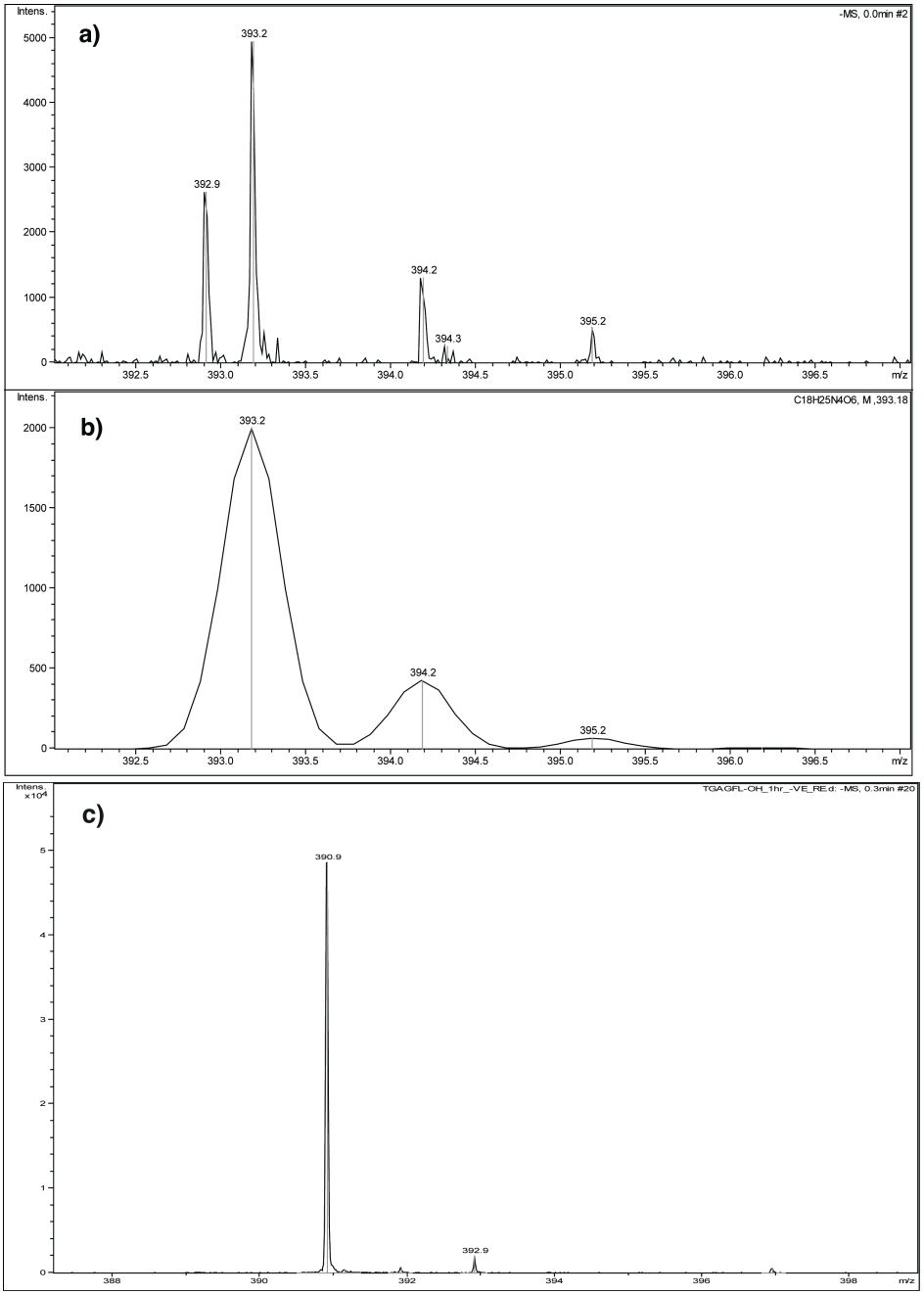

SI Figure 2.3: MS of the thermolysin digestion products of Thr-Gly-Ala-Phe-Leu-NH_2 (**3**); note the peak at m/z = 393.3, which corresponds to the product derived from exopeptidase cleavage of the Phe-Leu amide bond (Thr-Gly-Ala-Phe-OH). b) Simulated MS spectra for Thr-Gly-Ala-Phe–OH. c) MS of the thermolysin digestion products of Thr-Gly-Ala-Phe-Leu-OH (**6**); note the absence of the peak at m/z = 393.3, which signals the lack of exopeptidase activity for this substrate. All the measurements were carried out in negative ion mode.

Appendix 3. Fitting Function for 1 Competitor with "n" Number of Host

The following derivation is taken from ref.[79]

Binding equation for competitive displacement titration

Let us consider a fluorescent guest (G) that can bind to the cavity of a host (H) in a 1:1 stoichiometry with an equilibrium constant K_G. The concentration of host-guest complex is then given by equation 3.

$$H + G \rightleftharpoons HG \quad (1)$$

$$K_G = \frac{[HG]}{[H][G]} \quad (2)$$

$$[HG] = K_G[H][G] \quad (3)$$

For a competitive fluorescence titration, let us add a competitor (C) with *n* binding sites for the host (equation 4) to a mixture containing host and guest. The equilibrium constant (K_C) between host and competitor is given by equation 5.

$$C + nH \rightleftharpoons H_nC \quad (4)$$

$$K_C = \frac{[H_nC]}{[C][H]^n} \quad (5)$$

Assuming that the binding sites of the competitor molecule are identical and independent, i.e., the affinity of any site does not depend on whether or not the other sites are occupied, equation 5 can be simplified and rewritten as equation 6. A detailed derivation is given in ref.[201]

$$[H_nC] = \frac{nK_C[H][C]}{1+K_C[H]} \quad (6)$$

In a competitive fluorescence displacement titration, added competitor displaces the dye from the host cavity. The accompanying change in fluorescence intensity, *I*, follows equation 7, where I_{GH} is the intensity when all guest molecules are complexed and I_G when they are uncomplexed (or fully displaced).

$$I = \frac{[G]}{[G]_0} I_G + \frac{[HG]}{[G]_0} I_{GH} \tag{7}$$

The initial concentration of dye, $[G]_0$, and the two intensities I_G and I_{GH} are known experimental parameters. However, to solve the equation we need to determine the amount of free guest, [G], and host/guest complex, [HG], during the titration. The law of mass conservation leads to equations 8–10.

$$[HG] = [G]_0 - [G] \tag{8}$$

$$[H]_C = [C]_0 - [C] \tag{9}$$

$$[H] = [H]_0 - [HG] - [H]_C \tag{10}$$

Combining equations 3 and 8 leads to equation 11 for the concentration of the complex [HG].

$$\begin{gathered} [HG] = K_G [H][G] = K_G [H]\{[G]_0 - [HG]\} = K_G [H][G]_0 - K_G [H][HG] \\ \Leftrightarrow \\ [HG] = \frac{K_G [H][G]_0}{1 + K_G [H]} \end{gathered} \tag{11}$$

The concentration of host/guest complex during the titration (eq. 11) has now been obtained as a function of free host [H]. By substituting equations 6 and 11 into equation 10, we can express the amount of free host as a function of known parameters and the equilibrium constants (eq. 12).

$$\begin{gathered} [H] = [H]_0 - \frac{K_G [H][G]_0}{1 + K_G [H]} - \frac{nK_C [H][C]_0}{1 + K_C [H]} \\ [H] = [H]_0 - \frac{K_G [H][G]_0 - K_G K_C [H]^2 [G]_0 - nK_C [H][C]_0 - nK_C K_G [H]^2 [C]_0}{1 + K_C [H] + K_G [H] + K_C K_G [H]^2} \Leftrightarrow \\ [H] + K_C [H]^2 + K_G [H]^2 + K_G K_C [H]^3 = [H]^2 \{K_G K_C [H]_0 - K_G K_C [G]_0 - nK_C K_G [C]_0\} \\ + [H]\{K_C [H]_0 + K_G [H]_0 - K_G [G]_0 - nK_C [C]_0\} + [H]_0 \Leftrightarrow \\ K_G K_C [H]^3 + [H]^2 \{K_C + K_G - K_G K_C [H]_0 + K_G K_C [G]_0 + nK_C K_G [C]_0\} + \\ [H]\{1 - K_C [H]_0 - K_G [H]_0 + K_G [G]_0 + nK_C [C]_0\} - [H]_0 = 0 \end{gathered} \tag{12}$$

Simplifying and rearranging equation 12 leads to a cubic equation (eq. 13),

$$a[\mathrm{H}]^3 + b[\mathrm{H}]^2 + c[\mathrm{H}] - d = 0$$
$$\text{with } a = K_G K_C,\ b = K_C + K_G - K_G K_C [\mathrm{H}]_0 + K_G K_C [\mathrm{G}]_0 + n K_C K_G [\mathrm{C}]_0, \quad (13)$$
$$c = 1 - K_C [\mathrm{H}]_0 - K_G [\mathrm{H}]_0 + K_G [\mathrm{G}]_0 + n K_C [\mathrm{C}]_0, \text{ and } d = [\mathrm{H}]_0$$

The cubic equation is solved by using the Netwon-Raphson method. Therefore, by substituting the amount of free guest (eq. 13) and host/guest complex (eq. 11) into equation 10, we finally arrive at the equation for competitive binding titration for a competitor with *n* binding sites (eq.14).

$$I = I_G + \frac{[\mathrm{HG}]}{[\mathrm{G}]_0}\{I_{GH} - I_G\} = I_G + \frac{1}{[\mathrm{G}]_0}\frac{K_G[\mathrm{H}][\mathrm{G}]_0}{1+K_G[\mathrm{H}]}\{I_{GH} - I_G\} = I_G + \frac{K_G[\mathrm{H}]}{1+K_G[\mathrm{H}]}\{I_{GH} - I_G\} \quad (14)$$

The experimental data from the titration were fitted to equation 17 with the software pro Fit 6.1.16 (Quantumsoft, Uetikon am See, Switzerland) by using a subroutine to solve equation 16 by the Newton-Raphson method. The fitting of the experimental data yielded a binding constant of protamine with CX4, K_C = (1.24±0.31) × 10^9 M^{-1} with n = 4.0±0.1 (compare Figure S3b).

The fitting modules for pro Fit as well as for the alternative software MS Origin are available from the web page of the authors (http://www.jacobs-university.de/ses/wnau) under "Fitting Functions".

Appendix 4.1 Publications

ACCOUNTS of chemical research

Article

pubs.acs.org/accounts

Dynamically Analyte-Responsive Macrocyclic Host–Fluorophore Systems

Garima Ghale and Werner M. Nau*

School of Engineering and Science, Jacobs University Bremen, Campus Ring 1, 28759 Bremen, Germany

CONSPECTUS: Host–guest chemistry commenced to a large degree with the work of Pedersen, who in 1967 first reported the synthesis of crown ethers. The past 45 years have witnessed a substantial progress in the field, from the design of highly selective host molecules as receptors to their application in drug delivery and, particularly, analyte sensing. Much effort has been expended on designing receptors and signaling mechanism for detecting compounds of biological and environmental relevance. Traditionally, the design of a chemosensor comprises one component for molecular recognition, frequently macrocycles of the cyclodextrin, cucurbituril, cyclophane, or calixarene type. The second component, used for signaling, is typically an indicator dye which changes its photophysical properties, preferably its fluorescence, upon analyte binding. A variety of signal transduction mechanisms are available, of which displacement of the dye from the macrocyclic binding site is one of the simplest and most popular ones. This constitutes the working principle of indicator displacement assays.

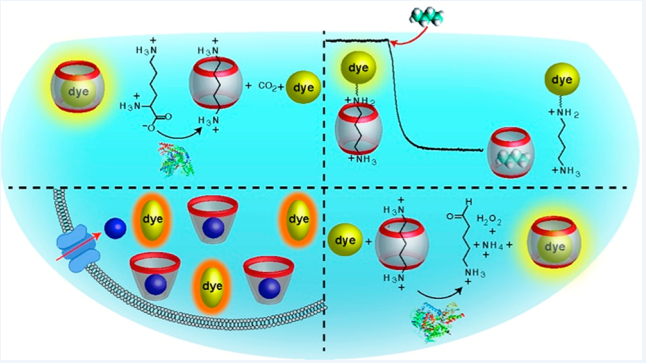

However, indicator displacement assays have been predominantly exploited in a static fashion, namely, to determine absolute analyte concentrations, or, by using combinations of several reporter pairs, to achieve a differential sensing and, thus, identification of specific food products or brands. In contrast, their use in biological systems, for example, with membranes, cells, or with enzymes has been comparably less explored, which led us to the design of the so-called tandem assays, that is, dynamically analyte-responsive host–dye systems, in which the change in analyte concentrations is induced by a biological reaction or process. This methodological variation has practical application potential, because the ability to monitor these biochemical pathways or to follow specific molecules in real time is of paramount interest for both biochemical laboratories and the pharmaceutical industry.

We will begin by describing the underlying principles that govern the use of macrocycle-fluorescent dye complexes to monitor time-dependent changes in analyte concentrations. Suitable chemosensing ensembles are introduced, along with their fluorescence responses (switch-on or switch-off). This includes supramolecular tandem assays in their product- and substrate-selective variants, and in their domino and enzyme-coupled modifications, with assays for amino acid decarboxylases, diamine, and choline oxidase, proteases, methyl transferases, acetylcholineesterase (including an unpublished direct tandem assay), choline oxidase, and potato apyrase as examples. It also includes the very recently introduced tandem membrane assays in their published influx and unpublished efflux variants, with the outer membrane protein F as channel protein and protamine as bidirectionally translocated analyte. As proof-of-principle for environmental monitoring applications, we describe sensing ensembles for volatile hydrocarbons.

■ INTRODUCTION

The first competitive binding assay was described by Berson and Yalow in 1960, for measuring plasma insulin.[1,2] Since then, competitive assays have found widespread applications in biomedicine. In addition, nonradioactive techniques using *enzymes* have evolved, specifically enzyme-linked immunosorbent assays (ELISA)[3,4] and enzyme-multiplied assays (EMIT),[5] which frequently exploit chemoluminescence[6] and fluorescence for detection.[7,8] Immunoassays were perhaps the first demonstration of a "biotic" receptor–ligand system responsive to external stimuli such as the addition of an unlabeled analyte.

With the advancement of supramolecular chemistry, conceptually related indicator displacement assays (IDAs)[9−12] have been introduced which exploit the potential of synthetic receptors, particularly macrocyclic hosts, for analyte sensing. IDAs bypass the demanding design of chemosensors containing the (macrocyclic) recognition unit with a covalently linked signaling unit, typically a tethered chromophore.[13,14] The sensing principle of IDAs relies on the competition between a test substance and an indicator for the same binding site on the host. When an analyte is added to a solution containing host·indicator complex, the analyte displaces the indicator from the binding site. Upon displacement of the indicator, a change in

Special Issue: Responsive Host–Guest Systems

Received: March 11, 2014

signal is observed, for example, of its fluorescence (Figure 1). These assays have been popularized in supramolecular chemistry by Anslyn and co-workers;[10,15,16] many other groups have also contributed to this area.[17−22]

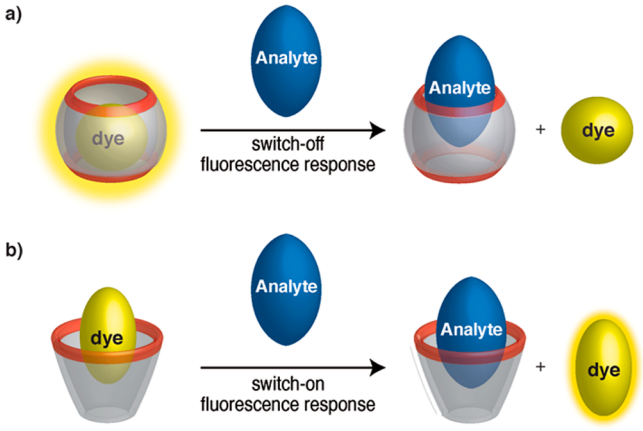

Figure 1. Indicator displacement assays for analyte sensing using a macrocyclic host and a fluorescent dye. The addition of an analyte is signaled by either (a) a fluorescence decrease or (b) a fluorescence increase due to displacement of the dye from the host.

Macrocycles (Figure 2a) are capable of binding and recognizing guest molecules such as fluorescent dyes (Figure 2b). The photophysical properties of a dye are changed upon formation of a macrocycle·dye complex.[23] Specifically, for cyclodextrins and cucurbiturils (Figure 2a), the fluorescence of the encapsulated dye is frequently enhanced due to relocation into a more hydrophobic, solvent-protected environment. In contrast, for the electron-rich cyclophanes and calixarenes (Figure 2a), a charge-transfer induced quenching of the complexed fluorescent dyes generally applies. Conversely, when the dye is displaced from the cavity due to a competitive binding of an analyte, its original fluorescence is restored (Figure 2c). This spectroscopic response of the host·dye complex allows its use as a "reporter pair" or "chemosensing ensemble". Herein, we demonstrate how host·dye systems can be exploited to track, in real time, changes in concentrations of diverse analytes (Figure 3) as they occur in enzymatic reactions, during membrane transport, or upon dissolution of volatile gases.

SUPRAMOLECULAR TANDEM ENZYME ASSAYS

The fundamental principles of supramolecular chemistry dictate that the selectivity of macrocyclic receptors is determined, among others, by the complementary charge and size of their guest molecules.[35,36] Consequently, we projected that any chemical process that alters the overall charge or size of an analyte, such as that resulting from an enzymatic transformation, could be monitored by using a host·dye complex as a dynamically analyte-responsive "reporter pair". This conceptual approach afforded a new label-free and versatile method to monitor enzymatic activity, which we introduced as supramolecular tandem enzyme assays The enzymes, enzyme classes, and the substrate/product combinations for the successfully investigated biotransformations are shown in Table 1, along with the photophysical response. Different variants of tandem assays are discussed next, followed by specific examples as highlights.[24−32]

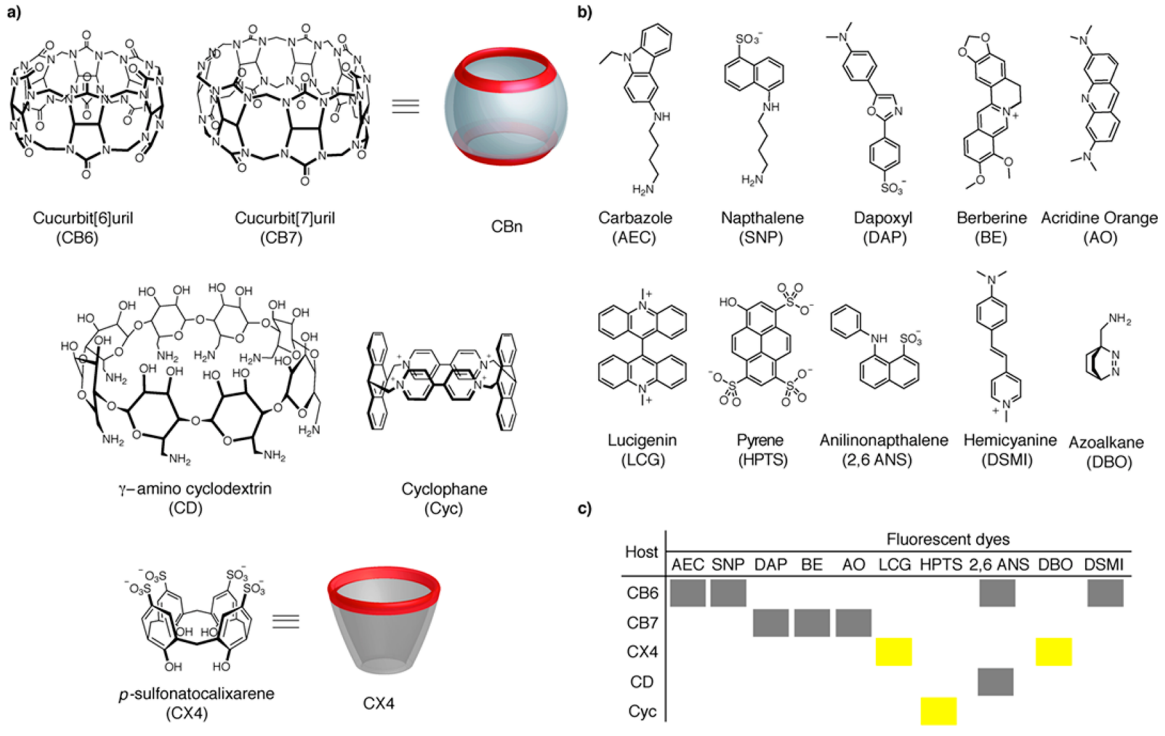

Figure 2. Chemical structures of (a) macrocyclic hosts as synthetic receptors and (b) fluorescent dyes investigated by our group as indicators. (c) Matrix representation for combinations of host and dye complexes suitable as chemosensing ensembles in tandem assays are indicated by a bar, where the photophysical response upon analyte binding is color-coded in yellow and gray, indicating an enhancement and quenching of the fluorescence intensity, respectively.[23]

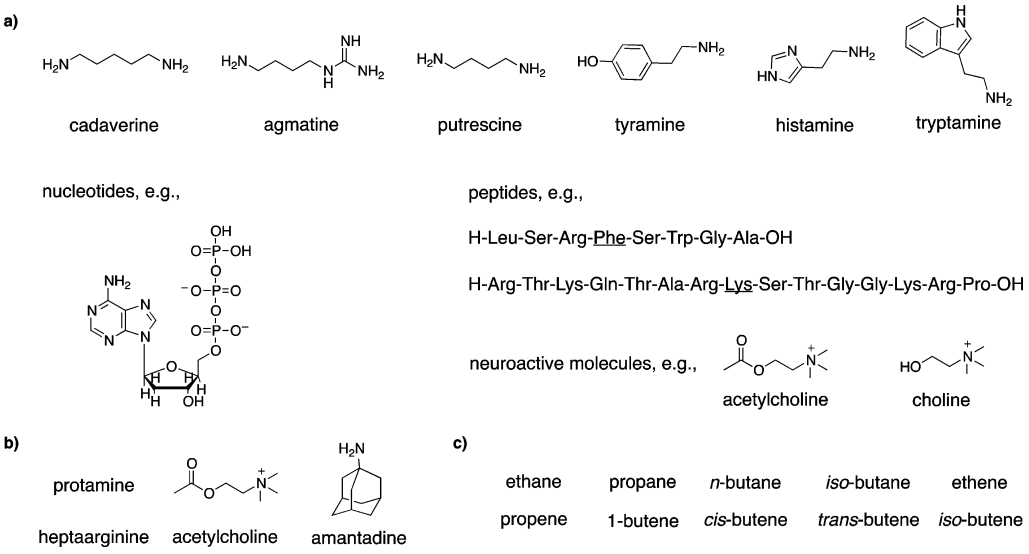

Figure 3. Chemical structures of analytes detected during (a) enzymatic transformations,[24−32] (b) membrane translocation,[33] and (c) gas dissolution.[34] For enzymatic reactions, only the strong competitor from the substrate/product pair is shown. The underlined amino acids indicate the residue where enzymatic cleavage or conversion takes place.

Table 1. Dynamically Analyte-Responsive Host·Dye Systems for the Detection of Analytes Generated or Depleted during Enzymatic Transformations

host·dye[a]	enzyme (enzyme class)[b]	substrate/product[c]	ref
	assays with switch-on fluorescence response		
CX4·DBO	amino acid decarboxylase (EC4)	amino acid/biogenic amine	31
	arginase (EC3)	arginine/ornithine	32
CX4·LCG	choline oxidase (EC1)	choline/betaine	30
	histone methyl transferase (EC2)	unmethylated/methylated peptide	26
Cyc·HPTS	potato apyrase (EC3)	nucleotide tri-/monophosphates	27
OH-β-CD·2,6-ANS	isomerase (EC5)	aromatic/arranged aromatic	37
	assays with switch-off fluorescence response		
CB7·DAP	amino acid decarboxylase (EC4)	amino acid/biogenic amines	31
CB7·AO	lysine decarboxylase (EC4)	lysine/cadaverine	32
	diamine oxidase (EC1)	cadaverine/aminoaldehyde	32
	thermolysin (EC3)	polypeptides/dipeptides	29
	leucine aminopeptides (EC3)	polypeptides/amino acids	28
	trypsin (EC3)	polypeptides/peptide fragments	28
CX4·LCG	butylcholinesterase (EC3)	succinylcholine/choline	38
CB6·DSMI	acetylcholinesterase (EC3)	acetylcholine/choline	*d*
CB6·AEC	lysine decarboxylase (EC4)	lysine/cadaverine	39
CD·2,6-ANS	potato apyrase (EC3)	nucleotide tri-/monophosphates	27

[a]See Figure 2 for chemical structures. [b]EC1, oxidoreductases; EC2, transferases; EC3, hydrolases; EC4, lyases; EC5, isomerases; and EC6, ligases. [c]Analyte that binds more strongly to the host is underlined. [d]This work.

■ ASSAY VARIANTS

Product-Selective Supramolecular Tandem Assays

At the heart of supramolecular tandem assays lies the reversible and competitive binding of a macrocyclic host with a fluorescent dye and an analyte, and its differential binding with the enzymatic substrate or product. The assay setup is particularly straightforward when the product binds more strongly to the macrocycle which leads to a *product*-selective assay. This is the case for amino acid decarboxylases, where a macrocyclic host (for example, CB7) is chosen such that it binds weakly with a substrate (lysine), but strongly with the corresponding enzymatic product (cadaverine). Upon addition of lysine decarboxylase, lysine, the weak competitor, undergoes enzymatic decarboxylation to form the biogenic amine, the strong competitor. This results in a continuous displacement of the fluorescent dye (AO) from the host molecule (Figure 4, left), such that the enzymatic conversion is reported as a decrease in fluorescence (switch-off response, Figure 4, bottom). Ideally, the fluorescent dye is selected such that its affinity to the host (defined as its binding constant times its concentration)[25,32] lies in between that of the substrate and the corresponding product.

Product-selective tandem assays closely resemble fluorescence-based antibody−antigen assays, where a fluorescently tagged antigen is displaced from the antibody by the enzymatic product (the unlabeled antigen) during the course of enzyme reaction. With tandem enzyme assays, however, macrocyclic receptors serve as an economic and less selective substitute for antibodies. For example, using one macrocyclic host, CB7, the

dx.doi.org/10.1021/ar500116d | Acc. Chem. Res. XXXX, XXX, XXX−XXX

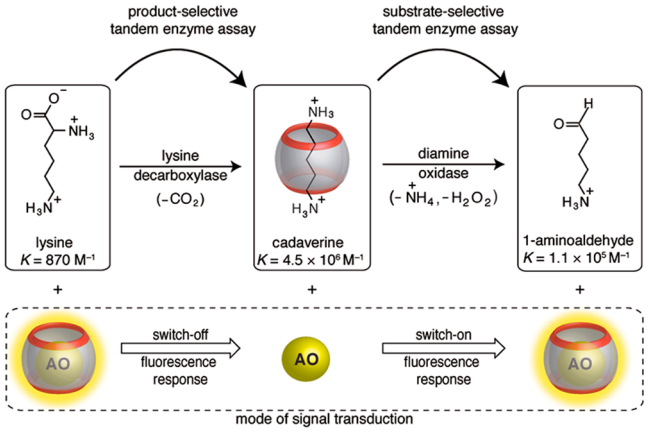

Figure 4. Schematic representation of supramolecular tandem enzyme assays showing the product-selective variant (left), the substrate-selective one (right), and their combination to set up a domino tandem assay. The chemosensing ensemble comprises the macrocyclic host CB7 and the fluorescent dye AO ($K_{CB7\cdot AO}$ = 2.9 × 10^5 M^{-1}).[32]

enzymatic activity of several amino acid decarboxylases can be monitored,[24,31] while an antibody would be specific for a single biogenic amine, if it could be raised for such simple, omnipresent metabolites at all.

Substrate-Selective Supramolecular Tandem Assays

When the host binds more strongly to the substrate rather than to the enzymatic product, a substrate-selective assay can be set up in which the depletion of substrate in the course of the enzymatic transformation is being directly followed through an uptake of fluorescent dye.[32] A substrate-selective enzyme assay can be set up, for example, with cadaverine (strong competitor) as substrate undergoing oxidation (Figure 4, right). In the presence of the preassembled host·dye complex (CB7·AO), cadaverine displaces the dye from the host. Addition of the enzyme diamine oxidase leads to the formation of an amino aldehyde as a weaker competitor. This results in a continuous increase in fluorescence because the strong competitor is diminished, allowing the fluorescent dye to be immersed in the macrocycle. Given that the macrocyclic receptor binds to the substrate, thereby lowering its effective concentration, we needed to consider an apparent inhibitory effect of the receptor on the enzymatic activity.[40,41] However, since the absolute amount of receptor can be tuned down (low μM concentration) compared to the concentration of substrate (mM), the rate of enzymatic conversion was not significantly inhibited by the presence of the reporter pair. As a limitation, while enzyme kinetic parameters (K_M, k_{cat}) can be obtained from product-selective tandem assays, this can be more difficult for the substrate-selective variants due to a lag phase observed at higher substrate concentrations.[25,32] Only in special cases, for example, the tandem enzyme assay for butyrylcholinesterase (BuChE) recently reported by Liu et al. kinetic parameters have been determined.[38] In any case, both methods, substrate- and product-selective tandem assays, are well suited for screening of inhibitors or activators where the concentration of substrates and enzymes can be preoptimized.[25,32]

Domino Tandem Assays

By consecutively combining the product- and substrate-selective tandem enzyme assays to follow a cascade of enzymatic transformations, in the same reaction mixture with a single chemosensing ensemble, a new line of tandem assays was developed, the domino ones (Figure 4).[25,28,32] The only requirement for the operation of a domino tandem assay is an alternating binding affinity of the macrocyclic host with the sequentially formed metabolites. The simplest example is the production and degradation of biogenic amines by using the CB7·AO reporter pair.[32] First, the conversion of lysine (weak competitor) to cadaverine (strong competitor) by lysine decarboxylase was monitored as a fluorescence decrease due to the displacement of AO. If an oxidation of cadaverine is subsequently affected by addition of diamine oxidase to form aminoaldehyde (weak competitor), an increase in fluorescence signal is observed, owing to the recomplexation of CB7 and AO (Figure 4, bottom).

CASE STUDIES

Macrocyclic Host·Fluorescent Dye Sensing Ensembles for Anions

The tandem assays described above are limited to cationic analytes as strong competitors. In order to detect changes in the concentration of anions, macrocycles with anion-receptor properties (Cyc or CD, Figure 2a) need to be employed.[27] A class of analytes that appealed to us was that of nucleotides, particularly adenosine triphosphate (ATP), one of the most common cofactors of enzymatic reactions. Two complementary reporter pairs (in terms of photophysical response), Cyc·HPTS (switch-on)[42] and CD·2,6-ANS (switch-off), were selected for monitoring the activity of potato apyrase, an enzyme which hydrolyzes nucleotide triphosphates to monophosphates. Our selected receptors show preferential binding to ATP over AMP. As a result, the enzymatic dephosphorylation was monitored as a decrease (CD·2,6-ANS) or as an increase in fluorescence (Cyc·HPTS).[27] Screening for activators and assaying dephosphorylation of other nucleotide triphosphates (GTP, CTP, and TTP) further extended the utility and transferability of these substrate-coupled, anion receptor-based tandem assays.

The Quest for Acetylcholine and Choline Sensing Systems

When neither the charge nor the size of an analyte undergoes a sufficiently large change to result in a differential binding of substrate and product to the synthetic receptors, tandem assays reach their limit. The conversion of acetylcholine (ACh) to choline (Ch) is such an example, and, in fact, the quest for supramolecular receptors that can differentiate ACh from Ch has presented a seminal challenge in supramolecular chemistry, owing to its importance for neuroscience.[12,30,43−45] For example, *p*-sulfonatocalixarenes are excellent receptors for ACh and Ch, but unfortunately with virtually identical affinities.[43] In order to make up for this low selectivity of CX4, in particular, we combined, in collaboration with the group of Liu, the enzymatic activity of two enzymes, acetylcholinesterase and choline oxidase, in order to detect and quantify both. This resulted in the setup of an enzyme-coupled tandem assay (Figure 5).[30]

The transformation of acetylcholine to choline by acetylcholinesterase could not be monitored because the receptor CX4 was unable to differentiate between the substrate and the product (Figure 5, left). The underlying idea was that—although ACh and Ch could not be differentiated on account of their identical positive charge and the same NMe_3^+ recognition motif, the oxidation product of Ch, betaine, could be detected, because it is zwitterionic, and therefore much more weakly bound (Figure 5, right). LCG (Figure 2b) was found to be an excellent indicator dye for CX4 (fluorescence enhancement

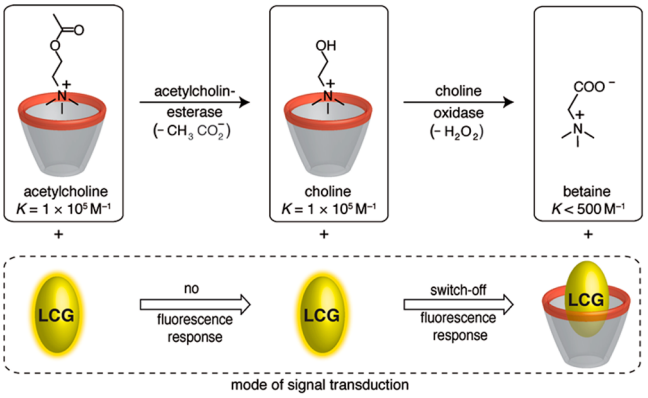

Figure 5. Substrate-selective enzyme-coupled assay for the detection and quantification of acetylcholine and choline by using the supramolecular chemosensing ensemble CX4·LCG ($K_{CX4\cdot LCG}$ = 1.6 × 10^7 M^{-1}). Adapted from ref 30 with permission from The Royal Society of Chemistry.

factor up to 140; this reporter pair has also been successfully used by Hof et al.).[22] Thus, when the reaction was conducted in the presence of an excess of choline oxidase and a rate-determining concentration of acetylcholinesterase, the CX4·LCG reporter pair afforded a decrease in fluorescence signal. This resulted from the formation of betaine as weak competitor, which allowed the dye to be taken up by the macrocycle in the course of the reaction. Through adaptations in the assay setup, it became possible to determine in sequence the absolute concentrations of both, ACh and Ch, in the same reaction mixture with micromolar sensitivity.[30]

From Low Molecular-Weight Metabolites to Biomacromolecules as Substrates

The first-generation of tandem enzyme assays targeted low molecular-weight analytes, whereby the entire analyte was encapsulated in the macrocyclic host. We wanted to expand the applicability of supramolecular sensing ensembles to detect changes in concentration of large biomolecules such as peptides. For this to be achieved, the assay would need to become compatible with the recognition of specific groups or residues rather than the recognition of an entire analyte. Based on earlier reports on the differential binding affinity of CB7 toward the aromatic amino acid Phe residues carrying different neighboring charges,[24,46−48] we hypothesized that CB7·dye systems could be employed to rapidly and conveniently measure many transformations that produce or destroy *N*-terminal aromatic residues. In these second-generation tandem enzyme assays, the aromatic residues of peptides function as recognition motifs. This led to the development of economic and versatile label-free fluorescence-based assays for proteases, which remain prime targets in drug discovery. Indeed, we were able to follow—in collaboration with the group of Urbach and CB7·AO as a fluorescent reporter pair—the enzymatic activity of thermolysin.[29] This metallo-endopeptidase hydrolyzes the *N*-terminal amide bond of hydrophobic amino acids and we tested the tandem enzyme assay principle for enkephalin-based peptides as substrates.

Assays for exopeptidases are particularly scarce,[28] because they evade detection by established assays involving fluorescently labeled peptides.[49] Leucine amino peptidase (LAP) is one of them; it cleaves amino acids in peptides from the *N*-terminus.[28] As a variation of the domino tandem assay concept,[32] we used the Phe-selective CB7·AO complex to monitor the stepwise proteolytic degradation of an extended peptide by LAP. The assay principle is illustrated in Figure 6.

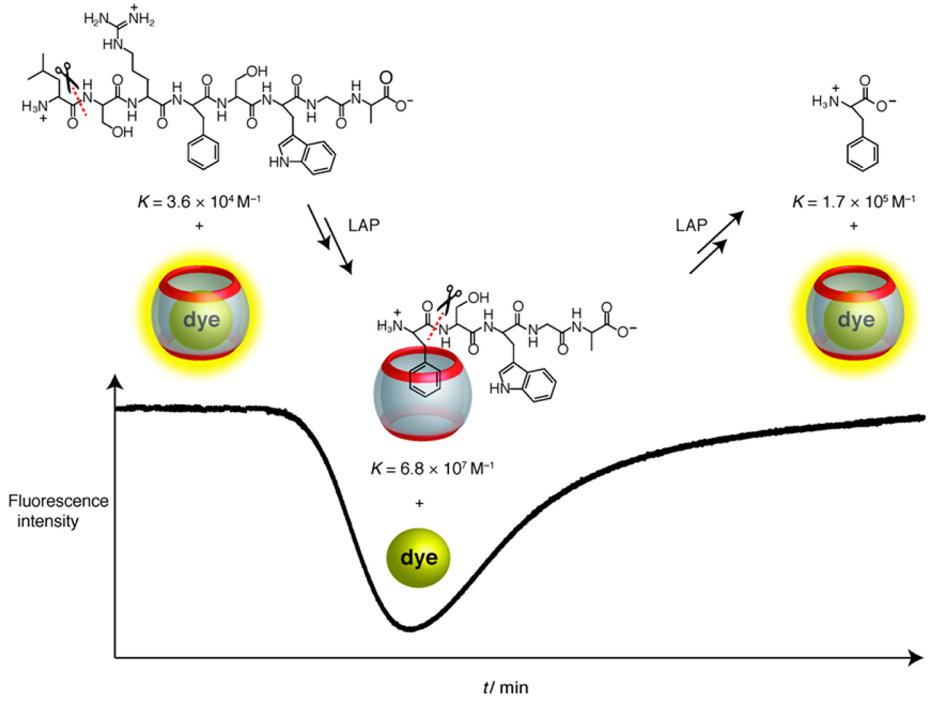

Figure 6. Stepwise proteolytic degradation of an entire peptide monitored via a domino tandem assay.[28] The initial degradation of the substrate to the intermediary peptide with an *N*-terminal Phe residue is indicated by a fluorescence switch-off response. Further hydrolysis leads to the formation of Phe, which is reflected by a fluorescence increase.

dx.doi.org/10.1021/ar500116d | *Acc. Chem. Res.* XXXX, XXX, XXX−XXX

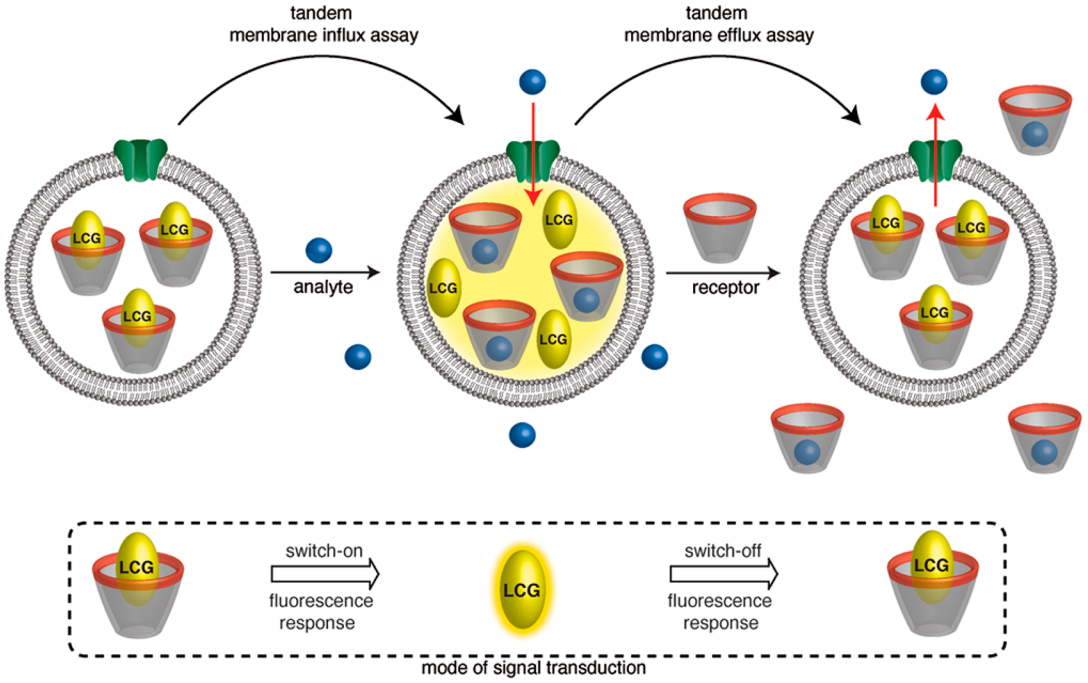

Figure 7. Supramolecular tandem membrane assays to follow the influx (left)[33] and efflux (right) of an analyte (blue) through a channel protein (green). Analytes that enter into the proteoliposomes displace the dye LCG from CX4 which is signaled by an increase in fluorescence.[33] In contrast, the efflux of analytes from proteoliposomes results in a fluorescent dye uptake and associated fluorescence intensity quenching.

Initially, the dye is included inside the CB7 cavity (left). As LAP hydrolyzes the peptide, it cleaves off step-by-step *N*-terminal amino acids. When the enzyme reaches Phe, it exposes the *N*-terminal Phe residue that acts as a strong competitor due to the synergy of hydrophobic and ion-dipole interactions with CB7 (middle). Eventually, LAP continues to hydrolyze the peptide chain, thereby releasing free Phe, which is a weak competitor due to the presence of the negatively charged carboxyl group (right).[24] As a result, the degradation of an entire peptide can be monitored as a down-and-up change in fluorescence.[30] This domino variant includes again a combination of a product- and substrate-selective assay and is subject to the same advantages and limitations (see above).[40]

While CB7 can be used to recognize aromatic amino acids in peptides, CX4 can be used to recognize trimethylated lysine residues in peptides and to differentiate them from unmethylated lysine residues. There are other marcocycles which have similarly selective amino acid recognition features, for example, for arginines.[50] The CX4·LCG system, already used for enzymatic reactions of neurotransmistters (see above), allowed indeed the monitoring of the enzymatic activity of DIM5 from *Neurospora crassa*.[26] This histone lysine methyltransferase specifically trimethylates one lysine residue (Lys9) of the histone H3 tail peptide. The product peptide acts as a strong competitor because the trimethylated lysine residue, in contrast to the unmethylated one in the substrate peptide, has a better size fit with CX4 and is additionally stabilized by CH–π interactions in the host–guest complex.[43] Accordingly, the methylation reaction was followed by the corresponding product-selective tandem assay. A continuous fluorescence increase was observed (switch-on),[26] because in this case the fluorescence of the dye is quenched by the electron-rich macrocycle.

Supramolecular Tandem Membrane Assays

If host·dye reporter pairs can be used to continuously follow the changes in concentration of either a substrate or a product (a chemical reaction), it should also be feasible to monitor the time-resolved change of the concentration of an analyte in general, that is, without a chemical reaction happening. An example is the buildup of an analyte inside compartmentalized structures such as vesicles. This conceptually novel approach resulted in the development of a versatile supramolecular method to monitor biomembrane transport processes: tandem *membrane* assays.[33] Our motivation for exploiting supramolecular chemosensing ensembles for investigating membrane transport stemmed from the fact that fluorescence-based methods to study transport of bioorganic analytes through the lipid bilayer or channel proteins in a label-free fashion in real-time were nonexistent.[51]

The working principle of tandem membrane assays relies on the selective coencapsulation of a membrane impermeable reporter pair (such as CX4·LCG or CB7·BE) inside vesicles and the reversible interaction of the receptor with the translocated analyte (Figure 7). When an analyte that translocates into the liposomes through a channel protein is added to a solution of host·dye-loaded proteoliposomes (channel-protein reconstituted liposomes), a time-resolved change in fluorescence is expected due to the displacement of the dye from the host cavity, whereas addition of a nontranslocating analyte is not expected to affect the signal.

Influx and Efflux Tandem Membrane Assays

To prove the principle of tandem membrane assays, we performed an exploratory investigation on the diffusion of an arginine-rich antimicrobial peptide, protamine, through the bacterial channel outer membrane protein F (OmpF). In the actual experiment, liposomes loaded with CX4·LCG were first prepared, followed by the addition of OmpF to form proteoliposomes (Figure 7, left).[33] When protamine was

dx.doi.org/10.1021/ar500116d | *Acc. Chem. Res.* XXXX, XXX, XXX–XXX

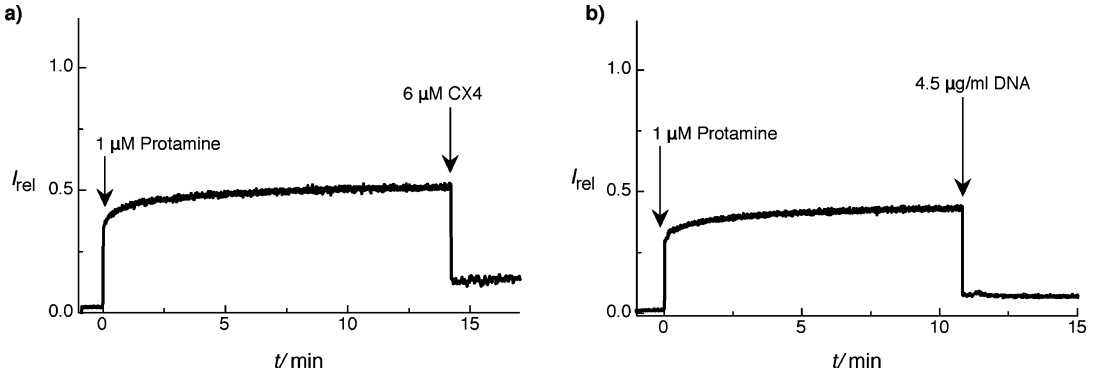

Figure 8. Change in fluorescence of CX4·LCG-loaded liposomes containing 30 nM OmpF upon addition of 1 μM protamine (t = 0 min) and, subsequently, (a) 6 μM CX4, at t = 14 min or (b) 4.5 μg/mL DNA, at t = 11 min. Experiments were performed in 10 mM sodium phosphate buffer, at pH 7.0 and 25 °C in this work.

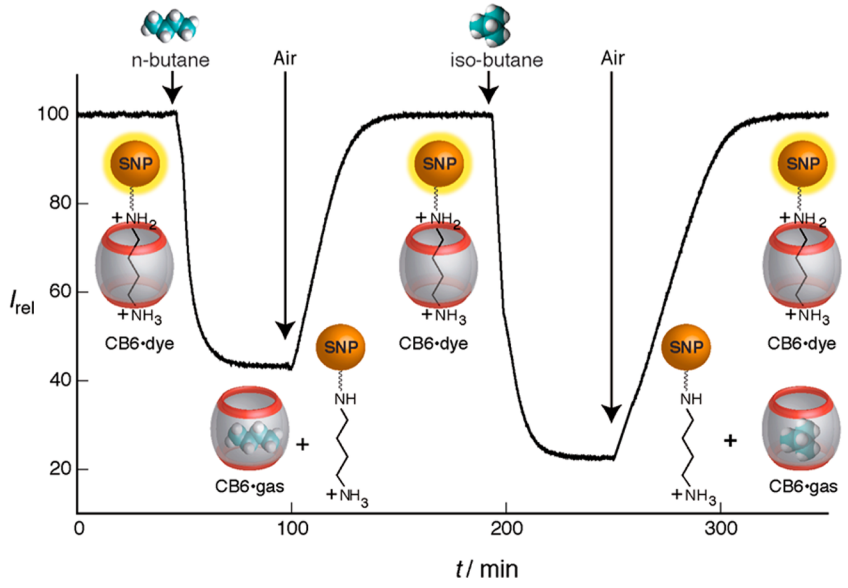

Figure 9. Encapsulation of volatile hydrocarbons (butane and isobutane) by CB6 continuously monitored via fluorescence of the dye SNP. Modified from ref 34 with permission from John Wiley and Sons.

added to the CX4·LCG-loaded proteoliposome solution (Figure 8, t = 0 min), a steep increase in fluorescence was observed. This indicated the displacement of LCG from the CX4 cavity by protamine; this peptide binds strongly to CX4 due to electrostatic and cation–π interactions with the multiple arginine residues.

The translocation of protamine into the liposomes through the channel protein is driven by a concentration gradient. In principle, the process should be reversible; that is, upon inversion of the concentration gradient protamine should translocate out from the vesicles. In order to test this unpublished hypothesis, we added, after protamine had been allowed to diffuse into the liposomes through OmpF, either an excess of CX4 (Figure 8a) or DNA (Figure 8b), as synthetic and natural protamine binders, respectively. In both cases, a steep drop in fluorescence was observed, signaling an effective and fast efflux of protamine from the liposomes. This is due to the fact that both CX4 and DNA bind strongly to protamine, thereby lowering the effective concentration of free protamine in the extravesicular space. In other words, it is possible to first observe the translocation of analytes into the liposomes, and, subsequently, to invert the concentration gradient through addition of a competitive binder to the aqueous bulk. This influx–efflux experiment also unambiguously demonstrated that the reporter pair inside the liposomes had remained intact; that is, it rules out the unlikely possibility that protamine first enters the liposome and subsequently facilitates the efflux of either host or dye, in which case no reversibility can be expected.

Tandem membrane assays constitute not only a label-free method to investigate a bidirectional transport of biomolecules through the lipid bilayer or through membrane proteins, but they have manifold additional functionalities in membrane research. For example, they can also be utilized to screen the activity of channel proteins or channel modulators.[33]

Hydrocarbon Sensing

Other areas, in which the time-resolved detection of analytes with macrocyclic host–dye reporter pairs is of interest, are the monitoring of analytes outside of any biological context, for example, for environmental monitoring. A simple example is the use of macrocyclic host·dye complexes for the monitoring of hydrocarbon gases. Toward this end, we used the anchor dye SNP (Figure 2b) in combination with the macrocyclic host CB6.[34]

dx.doi.org/10.1021/ar500116d | Acc. Chem. Res. XXXX, XXX, XXX–XXX

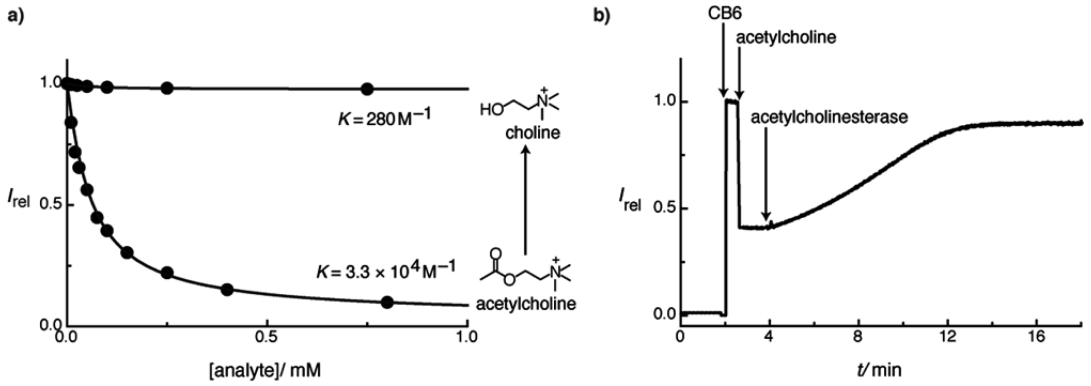

Figure 10. (a) Competitive displacement fluorescence titrations of acetylcholine and choline using 5 μM DSMI and 15 μM CB6. (b) Time-resolved change in fluorescence upon sequential addition of CB6 (10 μM) and then acetylcholine (100 μM) to a solution of 5 μM DSMI. For the substrate-selective tandem assay, 10 μL of 1 mg/mL of acetylcholinesterase was added and the progress of the enzymatic transformation was monitored as an increase in fluorescence. The experiments were carried out in 10 mM sodium phosphate buffer, at pH 7.0 and 25 °C in this work.

When gaseous analytes such as butane or isobutane are bubbled through a solution containing the preassembled, highly fluorescent CB6·SNP reporter pair, a continuous displacement of the dye with an associated decrease in fluorescence is observed (Figure 9). While the decrease in fluorescence reported on the absolute concentration of the dissolved gas, the observation of the plateau region indicated that the water solubility of the hydrophobic gas had been reached. By comparing the plateau regions for butane and isobutane, one could easily infer the difference in binding affinities of CB6 toward these isomeric guests; the latter is more spherical and shows a better size-shape fitting with the host cavity, resulting in a 3 times higher affinity (ca. 10^6 M^{-1}). The most interesting observation, perhaps, was the rapid reversibility of gas encapsulation, which is an essential requirement for potential gas monitoring applications. Thus, by simply purging the solution with air, the volatile analyte was displaced from the CB6 cavity, reflected by the restoration of the initial fluorescence.[34] The method can also be used to determine the affinity of the gases under different conditions, for example, in the presence of salts, where the competitive binding of cations to the CB6 portals lowers the affinity of the encapsulated gases.

Reporter Pairs under Investigation

Inspired by earlier reports on the selective binding of acetylcholine over choline by water-soluble *derivatives* of CB6,[52] we reckoned that the high sensitivity of tandem assays could be exploited to even employ *parent* CB6, a notoriously poorly soluble host in neat water, for time-resolved acetylcholine sensing by using DSMI as an indicator ($K_{CB6\cdot DSMI}$ = 4.2 × 10^4 M^{-1}).[53] DSMI is weakly fluorescent in its uncomplexed, but strongly fluorescent in its CB6-complexed form.

As demonstrated by simple fluorescence titration experiments (Figure 10a), the binding constant of CB6 with acetylcholine is 100 times higher than that with choline. Although the affinity of acetylcholine to CB6 is smaller than that to CX4, the ability of CB6 to differentiate between Ch and ACh can easily be exploited to now directly tandem-assay the enzymatic activity of acetylcholinesterase (Figure 10b), instead of taking the enzyme-coupled route (Figure 5). The direct, CB6-based assay is, however, slightly less sensitive (100 versus 10 μM).[30]

CONCLUSIONS

Supramolecular tandem assays exploit dynamically analyte-responsive macrocyclic host–fluorophore systems to achieve a time-resolved monitoring of enzymatic reactions and membrane transport processes. Originally introduced to monitor the formation of biogenic amines by enzymatic decarboxylation of amino acids,[31] they have subsequently been implemented into many more enzymatic transformations and have proven useful for all enzyme types, except ligases (EC6). For those isomerases (EC5) that affect an interconversion of enantiomers or their racemization, we were also not yet able to apply the tandem assay approach, mainly due to the lack of suitable stereo-discriminating macrocycles.[54] The application of tandem assays in membrane transport, translocation, and permeation processes is now beginning to unfold.

The exploitation of the specificity of enzymatic reactions in combination with signaling events resulting from supramolecular analyte recognition is presently also receiving attention in other fields, for multiparameter sensing,[24] for enantiomeric excess determination,[24] in two-component array systems to report simultaneously on the concentrations and identities of enzyme modifications,[22] in chirality sensing and chirogenesis,[55] for dye release from mesoporous hybrid systems,[56] and in allosteric dye release assays.[57,58] The expansion of the library of suitable host·dye combinations to address diverse analytes, to increase the sensitivity, to achieve either a switch-on or switch-off fluorescence response, or to ensure compatibility with lipids presents an ongoing challenge to supramolecular design as well as to combinatorial testing.

AUTHOR INFORMATION

Corresponding Author

*E-mail: w.nau@jacobs-university.de.

Notes

The authors declare no competing financial interest.

Biographies

Garima Ghale was born in Kathmandu, Nepal. She received her BSc in Chemistry (2008) and MSc in Nanomolecular Science (2010) from Jacobs University Bremen, where she is currently pursuing her PhD. Her research interests include supramolecular chemistry and its applications in biochemistry.

Werner M. Nau was born in Fulda, Germany. He received his MSc in 1991 from St. Francis Xavier University, Canada, in spectroscopy and his PhD from the University of Würzburg, Germany, in 1994 with Waldemar Adam in organic chemistry. After a postdoctoral stay at the University of Ottawa, Canada, with J .C. "Tito" Scaiano in photochemistry, he completed his habilitation in physical chemistry with J. Wirz at the University of Basel, Switzerland and moved to Jacobs University Bremen in 2002. His research combines physical organic chemistry with supramolecular chemistry and photochemistry, and ranges from fundamental studies on intermolecular interactions to fluorescent probes and the development of new (bio)analytical methods based on macrocyclic recognition.

■ ACKNOWLEDGMENTS

We thank the Deutsche Forschungsgemeinschaft (DFG Grant NA-686/5) for financial support.

■ REFERENCES

(1) Yalow, R. S.; Berson, S. A. Assay of plasma insulin in human subjects by immunological methods. *Nature* **1959**, *184*, 1648−1649.
(2) Yalow, R. S.; Berson, S. A. Immunoassay of endogenous plasma insulin in man. *J. Clin. Invest.* **1960**, *39*, 1157−1175.
(3) Engvall, E.; Perlmann, P. Enzyme-linked immunosorbent assay (ELISA). Quantitative assay of immunoglobulin G. *Immunochemistry* **1971**, *8*, 871−874.
(4) Van Weemen, B. K.; Schuurs, A. H. W. Immunoassay using antigen-enzyme conjugates. *FEBS Lett.* **1971**, *15*, 232−236.
(5) Okennedy, R.; Byrne, M.; Ofagain, C.; Berns, G. A review of enzyme-immunoassay and a description of a competitive enzyme-linked-immunosorbent-assay for the detection of immunoglobulin concentrations. *Biochem. Educ.* **1990**, *18*, 136−140.
(6) Deaver, D. R. A new non-isotopic detection system for immunoassays. *Nature* **1995**, *377*, 758−760.
(7) Soini, E.; Hemmila, I. Fluoroimmunoassay: present status and key problems. *Clin. Chem.* **1979**, *25*, 353−361.
(8) Visor, G. C.; Schulman, S. G. Fluorescence immunoassay. *J. Pharm. Sci.* **1981**, *70*, 469−475.
(9) Metzger, A.; Anslyn, E. V. A chemosensor for citrate in beverages. *Angew. Chem., Int. Ed.* **1998**, *37*, 649−652.
(10) Nguyen, B. T.; Anslyn, E. V. Indicator-displacement assays. *Coord. Chem. Rev.* **2006**, *250*, 3118−3127.
(11) Wiskur, S. L.; Ait-Haddou, H.; Lavigne, J. J.; Anslyn, E. V. Teaching old indicators new tricks. *Acc. Chem. Res.* **2001**, *34*, 963−972.
(12) Inouye, M.; Hashimoto, K.; Isagawa, K. Nondestructive detection of acetylcholine in protic media artificial-signaling acetylcholine receptors. *J. Am. Chem. Soc.* **1994**, *116*, 5517−5518.
(13) Bissell, R. A.; De Silva, A. P.; Gunaratne, H. Q. N.; Lynch, P. L. M.; Maguire, G. E. M.; Sandanayake, K. R. A. S. Molecular fluorescent signalling with 'fluor−spacer−receptor' systems: approaches to sensing and switching devices via supramolecular photophysics. *Chem. Soc. Rev.* **1992**, *21*, 187−195.
(14) Liu, Y. L.; Minami, T.; Nishiyabu, R.; Wang, Z.; Anzenbacher, P. Sensing of carboxylate drugs in urine by a supramolecular sensor array. *J. Am. Chem. Soc.* **2013**, *135*, 7705−7712.
(15) Umali, A. P.; LeBoeuf, S. E.; Newberry, R. W.; Kim, S.; Tran, L.; Rome, W. A.; Tian, T. A.; Taing, D.; Hong, J.; Kwan, M.; Heymann, H.; Anslyn, E. V. Discrimination of flavonoids and red wine varietals by arrays of differential peptidic sensors. *Chem. Sci.* **2011**, *2*, 439−445.
(16) You, L.; Anslyn, E. V. Competition experiments. In *Supramolecular Chemistry*; Gale, P., Steed, J., Eds.; John Wiley & Sons, Ltd: Chichester, 2012.
(17) Buryak, A.; Zaubitzer, F.; Pozdnoukhov, A.; Severin, K. Indicator displacement assays as molecular timers. *J. Am. Chem. Soc.* **2008**, *130*, 11260−11261.
(18) Zhang, J. H.; Umemoto, S.; Nakatani, K. Fluorescent indicator displacement assay for ligand-RNA interactions. *J. Am. Chem. Soc.* **2010**, *132*, 3660−3661.
(19) Neelakandan, P. P.; Nandajan, P. C.; Subymol, B.; Ramaiah, D. Study of cavity size and nature of bridging units on recognition of nucleotides by cyclophanes. *Org. Biomol. Chem.* **2011**, *9*, 1021−1029.
(20) Buryak, A.; Severin, K. A chemosensor array for the colorimetric identification of 20 natural amino acids. *J. Am. Chem. Soc.* **2005**, *127*, 3700−3701.
(21) Guo, D.-S.; Liu, Y. Supramolecular chemistry of *p*-sulfonatocalix[*n*]arenes and its biological applications. *Acc. Chem. Res.* **2014**, DOI: 10.1021/ar500009g.
(22) Minaker, S. A.; Daze, K. D.; Ma, M. C. F.; Hof, F. Antibody-free reading of the histone code using a simple chemical sensor array. *J. Am. Chem. Soc.* **2012**, *134*, 11674−11680.
(23) Dsouza, R. N.; Pischel, U.; Nau, W. M. Fluorescent dyes and their supramolecular host/guest complexes with macrocycles in aqueous solution. *Chem. Rev.* **2011**, *111*, 7941−7980.
(24) Bailey, D. M.; Hennig, A.; Uzunova, V. D.; Nau, W. M. Supramolecular tandem enzyme assays for multiparameter sensor arrays and enantiomeric excess determination of amino acids. *Chem.—Eur. J.* **2008**, *14*, 6069−6077.
(25) Dsouza, R. N.; Hennig, A.; Nau, W. M. Supramolecular Tandem Enzyme Assays. *Chem.—Eur. J.* **2012**, *18*, 3444−3459.
(26) Florea, M.; Kudithipudi, S.; Rei, A.; Gonzalez-Alvarez, M. J.; Jeltsch, A.; Nau, W. M. A fluorescence-based supramolecular tandem assay for monitoring lysine methyltransferase activity in homogeneous solution. *Chem.—Eur. J.* **2012**, *18*, 3521−3528.
(27) Florea, M.; Nau, W. M. Implementation of anion-receptor macrocycles in supramolecular tandem assays for enzymes involving nucleotides as substrates, products, and cofactors. *Org. Biomol. Chem.* **2010**, *8*, 1033−1039.
(28) Ghale, G.; Kuhnert, N.; Nau, W. M. Monitoring stepwise proteolytic degradation of peptides by supramolecular domino tandem assays and mass spectrometry for trypsin and leucine aminopeptidase. *Nat. Prod. Commun.* **2012**, *7*, 343−348.
(29) Ghale, G.; Ramalingam, V.; Urbach, A. R.; Nau, W. M. Determining protease substrate selectivity and inhibition by label-free supramolecular tandem enzyme assays. *J. Am. Chem. Soc.* **2011**, *133*, 7528−7535.
(30) Guo, D. S.; Uzunova, V. D.; Su, X.; Liu, Y.; Nau, W. M. Operational calixarene-based fluorescent sensing systems for choline and acetylcholine and their application to enzymatic reactions. *Chem. Sci.* **2011**, *2*, 1722−1734.
(31) Hennig, A.; Bakirci, H.; Nau, W. M. Label-free continuous enzyme assays with macrocycle-fluorescent dye complexes. *Nat. Methods* **2007**, *4*, 629−632.
(32) Nau, W. M.; Ghale, G.; Hennig, A.; Bakirci, H.; Bailey, D. M. Substrate-selective supramolecular tandem assays: monitoring enzyme inhibition of arginase and diamine oxidase by fluorescent dye displacement from calixarene and cucurbituril macrocycles. *J. Am. Chem. Soc.* **2009**, *131*, 11558−11570.
(33) Ghale, G.; Lanctot, A. G.; Kreissl, H. T.; Jacob, M. H.; Weingart, H.; Winterhalter, M.; Nau, W. M. Chemosensing ensembles for monitoring biomembrane transport in real time. *Angew. Chem., Int. Ed.* **2014**, *53*, 2762−2765.
(34) Florea, M.; Nau, W. M. Strong binding of hydrocarbons to cucurbituril probed by fluorescent dye displacement: A supramolecular gas-sensing ensemble. *Angew. Chem., Int. Ed.* **2011**, *50*, 9338−9342.
(35) Lehn, J. M. Supramolecular chemistry - scope and perspectives molecules, supermolecules, and molecular devices. *Angew. Chem., Int. Ed.* **1988**, *27*, 89−112.
(36) Albrecht, M. Supramolecular chemistry-general principles and selected examples from anion recognition and metallosupramolecular chemistry. *Naturwissenschaften* **2007**, *94*, 951−966.
(37) Nau, W.; Bakirci, H.; Hennig, A. Determination of changes in concentration. Patent PCT/EP2007/004139.
(38) Guo, D. S.; Yang, J.; Liu, Y. Specifically monitoring butyrylcholinesterase by supramolecular tandem assay. *Chem.—Eur. J.* **2013**, *19*, 8755−8759.
(39) Praetorius, A.; Bailey, D. M.; Schwarzlose, T.; Nau, W. M. Design of a fluorescent dye for indicator displacement from

cucurbiturils: A macrocycle-responsive fluorescent switch operating through a pK_a shift. *Org. Lett.* **2008**, *10*, 4089−4092.
(40) Logsdon, L. A.; Urbach, A. R. Sequence-specific inhibition of a nonspecific protease. *J. Am. Chem. Soc.* **2013**, *135*, 11414−11416.
(41) Hennig, A.; Ghale, G.; Nau, W. M. Effects of cucurbit[7]uril on enzymatic activity. *Chem. Commun.* **2007**, 1614−1616.
(42) Neelakandan, P. P.; Hariharan, M.; Ramaiah, D. A supramolecular ON-OFF-ON fluorescence assay for selective recognition of GTP. *J. Am. Chem. Soc.* **2006**, *128*, 11334−11335.
(43) Bakirci, H.; Nau, W. M. Fluorescence regeneration as a signaling principle for choline and carnitine binding: A refined supramolecular sensor system based on a fluorescent azoalkane. *Adv. Funct. Mater.* **2006**, *16*, 237−242.
(44) Korbakov, N.; Timmerman, P.; Lidich, N.; Urbach, B.; Sa'ar, A.; Yitzchaik, S. Acetylcholine detection at micromolar concentrations with the use of an artificial receptor-based fluorescence switch. *Langmuir* **2008**, *24*, 2580−2587.
(45) Lehn, J. M.; Meric, R.; Vigneron, J. P.; Cesario, M.; Guilhem, J.; Pascard, C.; Asfari, Z.; Vicens, J. Binding of acetylcholine and other quaternary ammonium cations by sulfonated calixarenes - Crystal-structure of a [choline-tetrasulfonated calix[4]arene] complex. *Supramol. Chem.* **1995**, *5*, 97−103.
(46) Bush, M. E.; Bouley, N. D.; Urbach, A. R. Charge-mediated recognition of N-terminal tryptophan in aqueous solution by a synthetic host. *J. Am. Chem. Soc.* **2005**, *127*, 14511−14517.
(47) Rekharsky, M. V.; Yamamura, H.; Ko, Y. H.; Selvapalam, N.; Kim, K.; Inoue, Y. Sequence recognition and self-sorting of a dipeptide by cucurbit[6]uril and cucurbit[7]uril. *Chem. Commun.* **2008**, 2236−2238.
(48) Urbach, A. R.; Ramalingam, V. Molecular recognition of amino acids, peptides, and proteins by cucurbit[n]uril receptors. *Isr. J. Chem.* **2011**, *51*, 664−678.
(49) Wysocka, M.; Lesner, A. Future of protease activity assays. *Curr. Pharm. Des.* **2013**, *19*, 1062−1067.
(50) Bier, D.; Rose, R.; Bravo-Rodriguez, K.; Bartel, M.; Ramirez-Anguita, J. M.; Dutt, S.; Wilch, C.; Klarner, F. G.; Sanchez-Garcia, E.; Schrader, T.; Ottmann, C. Molecular tweezers modulate 14−3-3 protein-protein interactions. *Nat. Chem.* **2013**, *5*, 234−239.
(51) Terstappen, G. C.; Roncarati, R.; Dunlop, J.; Peri, R. Screening technologies for ion channel drug discovery. *Future Med. Chem.* **2010**, *2*, 715−730.
(52) Lee, J. W.; Samal, S.; Selvapalam, N.; Kim, H. J.; Kim, K. Cucurbituril homologues and derivatives: New opportunities in supramolecular chemistry. *Acc. Chem. Res.* **2003**, *36*, 621−630.
(53) Note that the binding constant that we report here for DSMI dye with CB6 is in 10 mM sodium phosphate buffer. The reported binding constant in neat water is 1.02×10^5 M^{-1}; see Li, Z. Y.; Sun, S. G.; Liu, F. Y.; Pang, Y.; Fan, J. L.; Song, F. L.; Peng, X. J. Large fluorescence enhancement of a hemicyanine by supramolecular interaction with cucurbit[6]uril and its application as resettable logic gates. *Dyes Pigm.* **2012**, *93*, 1401−1407.
(54) Hembury, G. A.; Borovkov, V. V.; Inoue, Y. Chirality-sensing supramolecular systems. *Chem. Rev.* **2008**, *108*, 1−73.
(55) Biedermann, F.; Nau, W. M. Noncovalent chirality sensing ensembles for the detection and reaction monitoring of amino acids, peptides, proteins, and aromatic Drugs. *Angew. Chem., Int. Ed.* **2014**, DOI: 10.1002/anie.201400718.
(56) Liu, J.; Du, X.; Zhang, X. Enzyme-inspired controlled release of cucurbit[7]uril nanovalves by using magnetic mesoporous silica. *Chem.—Eur. J.* **2011**, *17*, 810−815.
(57) Jose, D. A.; Elstner, M.; Schiller, A. Allosteric indicator displacement enzyme assay for a cyanogenic glycoside. *Chem.—Eur. J.* **2013**, *19*, 14451−14457.
(58) Vilozny, B.; Schiller, A.; Wessling, R. A.; Singaram, B. Enzyme assays with boronic acid appended bipyridinium salts. *Anal. Chim. Acta* **2009**, *649*, 246−251.

Appendix 4.2 Publications

Reprinted with permission from Wiley-VCH. Ghale, G.; Lanctot, A. G.; Kreissl, H. T.; Jacob, M. H.; Weingart, H.; Winterhalter, M.; Nau, W. M. "Chemosensing ensembles for monitoring biomembrane transport in real time." *Angew. Chem. Int. Ed.* **2014**, *53*, 2762-2765. Publisher's version can be found at: http://onlinelibrary.wiley.com/doi/10.1002/anie.201309583/full

Supramolecular Chemistry Hot Paper

DOI: 10.1002/anie.201309583

Chemosensing Ensembles for Monitoring Biomembrane Transport in Real Time**

*Garima Ghale, Adrienne G. Lanctôt, Hannah T. Kreissl, Maik H. Jacob, Helge Weingart, Mathias Winterhalter, and Werner M. Nau**

Abstract: *The efficacy of drugs and biomolecules relies on their ability to pass through the bilayer. The development of methods to directly and sensitively monitor these membrane transport processes has remained an experimental challenge. A macrocyclic host (p-sulfonatocalix[4]arene or cucurbit[7]uril) and a fluorescent dye (lucigenin or berberine) are encapsulated as a chemosensing ensemble inside liposomes, which allows for a direct, real-time fluorescence monitoring of the passage of unlabeled bioorganic analytes. This in vitro assay is transferable to different channel proteins and analytes, has potential for fluorescence-based screening, e.g., of channel modulators, and yields the absolute kinetics of translocation. Using this new biophysical method, we observed for the first time direct rapid translocation of protamine, an antimicrobial peptide, through the bacterial transmembrane protein OmpF.*

Ion channels and transporter proteins are the third most common drug targets after membrane receptors and enzymes.[1] Robust and sensitive methods to investigate permeation or translocation through channel proteins are consequently of paramount interest. In fact, the lack of biomembrane assays suitable for rapid screening presents a bottleneck in antibiotics and drug discovery.[2] Similarly, many mechanistic questions about the translocation of hydrophilic molecules such as arginine-rich peptides through an intrinsically hydrophobic barrier remain unresolved owing to lack of sensitive in vitro methods for monitoring their translocation.[2d] Whether these polycationic peptides permeate on their own or translocate through channel proteins remains an open but crucial question in regard to their antimicrobial activity and other putative functions.[3]

Only a handful of label-free methods to monitor membrane translocation are at hand. The most prominent biophysical method to monitor analyte translocation through membranes is electrophysiology, which, however, cannot readily differentiate between translocation and binding.[4] Alternative methods involve radioactive uptake, NMR spectroscopy, or isothermal calorimetry.[5] For high-throughput screening in a pharmaceutical-industrial setting, fluorescence-based membrane assays are preferred. The repertoire of these is presently limited to the detection of changes in pH value, detection of chloride influx,[6] or membrane rupture (Supporting Information).

A fluorescence-based method that allows monitoring of the translocation of organic analytes with micromolar sensitivity is still called for. The in vitro method we introduce here—supramolecular tandem membrane assays—affords real-time kinetics, employs unlabeled analytes, and is applicable to a series of structurally related biomolecules. It is based on the co-encapsulation of a fluorescent dye with a macrocyclic host to form a "reporter pair" inside liposomes. The macrocycles in our assay are utilized as receptors for the translocated analyte, which introduces a genuine molecular recognition feature that increases the sensitivity to the micromolar range. It should be noted that macrocycles have already been exploited in membrane research, but for different reasons, that is, to either insert in membranes or to interact directly with membrane proteins.[7]

The working principle of our supramolecular chemical method is illustrated in Figure 1. Liposomes containing the host/dye reporter pair are prepared and purified, such that a subsequently added analyte affects the dye fluorescence only if it is able to enter the vesicle and to displace the dye from the macrocycle (Figure 1b,c). The reporter pair is selected to fulfil the following requirements: a) Neither host nor dye must dissolve in or permeate through the membrane; this is a limiting factor which distinctly raises the physicochemical complexity compared to our previously introduced enzyme assays,[8] a time-resolved variant of indicator displacement assay;[9] b) the macrocyclic host needs to display a high affinity to the target analyte(s), for example, polycationic peptides or cationic neurotransmitters; and c) the dye must show a strong fluorescence response upon release from the host. Consequently, tandem membrane assays can be set up with several reporter pairs for many biological analytes. In fact, a large library of reporter pairs with varying receptor properties is available, many of which commercially.[10] Herein, we first used *p*-sulfonatocalix[4]arene (CX4) and lucigenin (LCG),[8b,11] which are jointly suited to signal the binding of several cationic analytes (Figure 1a).

To document the key steps in the development of a tandem membrane assay for the translocation of a biologically important analyte and to demonstrate the functionality of the assay for measuring the kinetics and identifying ion channel modulators, we have chosen protamine as the analytical target and the outer membrane protein F (OmpF)

[*] G. Ghale, A. G. Lanctôt, H. T. Kreissl, Dr. M. H. Jacob, Dr. H. Weingart, Prof. Dr. M. Winterhalter, Prof. Dr. W. M. Nau
School of Engineering and Science, Jacobs University Bremen
Campus Ring 1, 28759 Bremen (Germany)
E-mail: w.nau@jacobs-university.de

[**] G.G. and W.M.N. acknowledges the financial support from the Deutsche Forschungsgemeinschaft (DFG Grant NA-686/5) and the COST Action CM1005 "Supramolecular Chemistry in Water". We thank R. Benz and K. R. Mahendran for helpful discussions.

Supporting information for this article is available on the WWW under http://dx.doi.org/10.1002/anie.201309583.

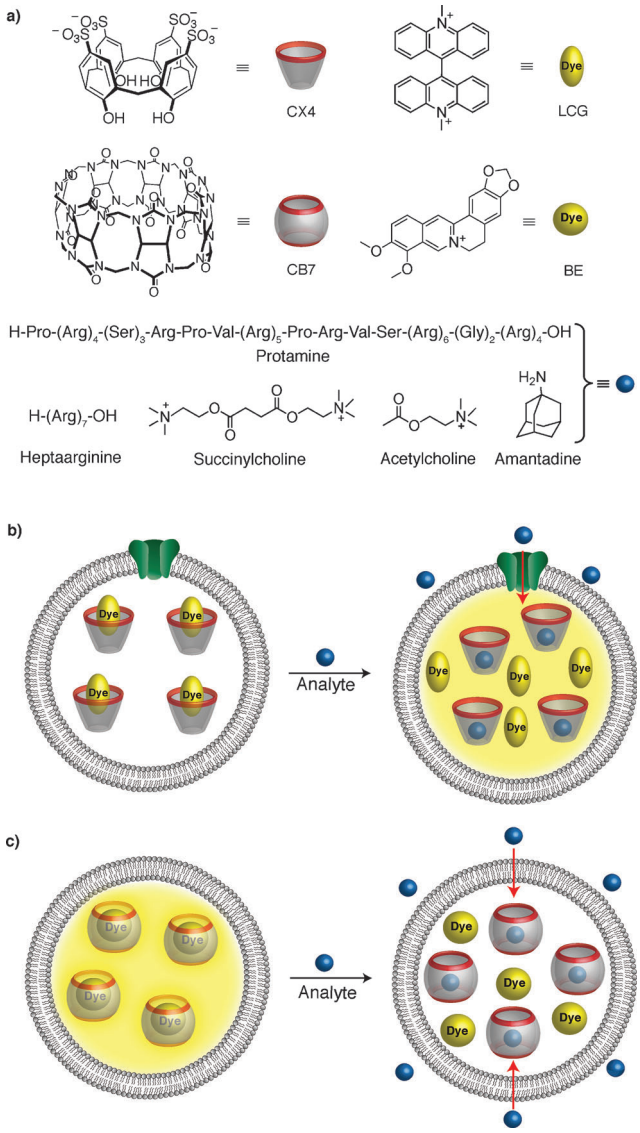

Figure 1. a) Macrocycles and dyes used as reporter pairs as well as the analytes investigated. b,c) Working principle of a supramolecular tandem membrane assay. Illustration of macrocyclic host–dye complexes encapsulated inside a liposome before (left) and after (right) translocation of an analyte (blue) through b) a channel protein (green) or c) directly through the biomembrane; the analyte binds to the macrocycle, thereby displaces the dye, which in turn becomes either b) strongly fluorescent in its uncomplexed form (switch-on fluorescence response) or c) weakly fluorescent (switch-off response).

as a representative channel protein. Cationic antimicrobial peptides, such as protamine (MW ca. 5000 Da), are bactericidal;[3b,12] however, they do not cause any lysis of the outer membrane in gram-negative bacteria. An open, and mechanistically utmost important question is therefore whether the internalization observed for cationic antimicrobial peptides occurs through channel proteins. OmpF, as an example of a cation-selective channel, allows the direct passage of small molecules (MW < 600 Da), including many antibiotics.[1b] Based on this empirical cut-off, passage of protamine is not expected. Nevertheless, the passage of a bacteriocin, colicin E9, has recently been observed, assisted by a membrane surface receptor.[13]

Fluorescence titrations with the pre-formed CX4–LCG reporter pair in homogeneous solution (see the Supporting Information) showed that the addition of micromolar concentrations of protamine led to an efficient fluorescence recovery. This effect is due to a competitive binding, because protamine has a higher affinity ($K_{CX4\text{–protamine}} = (1.24 \pm 0.31) \times 10^9\,M^{-1}$, Figure S3b) to CX4 than the dye ($K_{CX4\text{–LCG}} = (1.03 \pm 0.04) \times 10^7\,M^{-1}$, Figure S3a). Consequently, the reporter pair can be used as a chemosensing ensemble for protamine, while the spatial isolation in the inner liposomal space gives us a handle to directly monitor changes in local protamine concentration.

For the actual assays, CX4–LCG was first encapsulated into the liposomes. An inner-phase concentration of 500 μM LCG allowed for sufficient sensitivity while a slight shortfall of CX4 (450 μM) was needed to produce a linear response to analyte (see the Supporting Information). OmpF was then added to form proteoliposomes (Figure 2a). When protamine was administered, a steep increase in fluorescence was observed (Figure 2b). This was an interesting observation because it immediately demonstrated that this porin (with a putative MW cut-off near 600 Da) facilitated the uptake of this large polycationic peptide (MW 5000 Da) into the interior of the liposome, even in the absence of an auxiliary membrane surface receptor.[13]

Numerous control experiments were performed. In particular, we demonstrated that direct addition of protamine to a solution of liposomes containing the reporter pair did not trigger a fluorescence response (Figure 2c), which provided direct and unequivocal evidence that protamine did not permeate on its own through the biomembrane under our experimental conditions, up to 10 h. Of course, since there was no fluorescence response, it could also be ruled out that protamine caused any pore formation or fusion of the liposomes (Figures S5 and S6). Similarly, we verified that neither host nor dye can escape through the channel (Figure 2d) and that the fluorescence increase is affected only by the presence of both OmpF and protamine, also when added in the reverse order (Figure 2e). Therefore, the fluorescence increase observed in the presence of OmpF provides compulsory evidence for direct channel-mediated translocation of an arginine-rich peptide. This is a critical finding when discussing the potential of antimicrobial peptides as next-generation antibiotics against gram-negative bacteria.[3b,14]

As a unique asset, our method allows real-time measurement of the translocation kinetics. The passage of protamine through OmpF was found to be surprisingly fast, requiring stopped-flow experiments with rapid mixing of the analyte with the proteoliposomes containing the CX4–LCG reporter pair (Figure 3a). Increasing the analyte concentrations resulted in both a faster kinetics and a higher final fluorescence intensity, which reached a plateau at high protamine concentration (Figure 3b). This demonstrated that the translocation rate reached a limiting value and that the displacement became quantitative at high analyte concentration (see the Supporting Information and Figure S11). Hill analysis of the initial rates yielded a half-saturation constant (EC_{50}) of

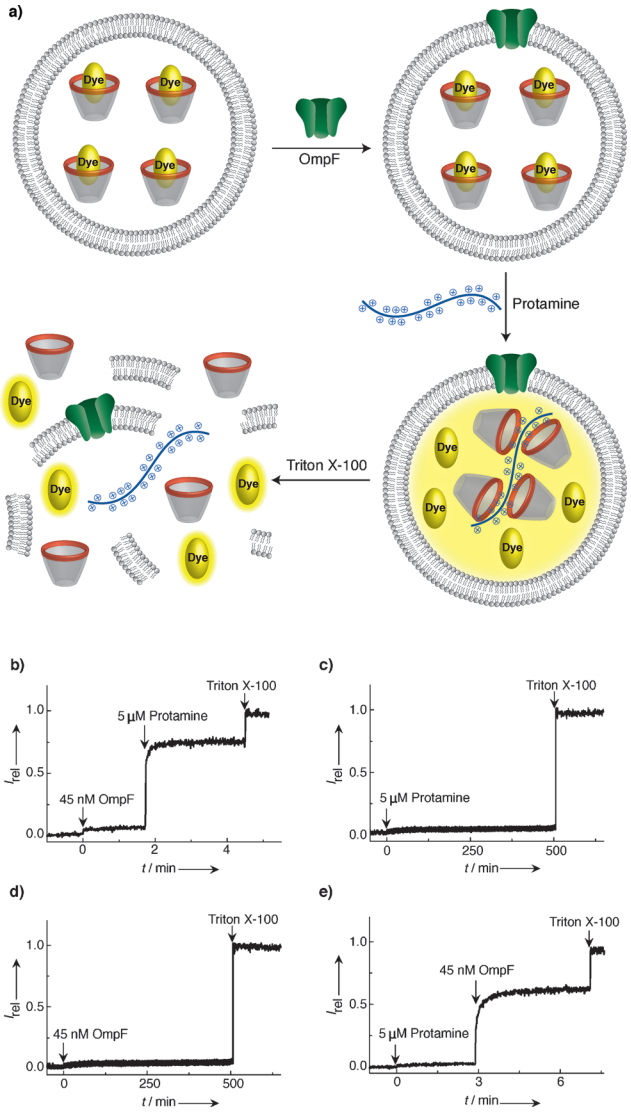

Figure 2. Supramolecular tandem membrane assays to monitor translocation of protamine by fluorescence. a) Schematic representation of spontaneous insertion of OmpF (green) into the membrane of CX4–LCG-loaded liposomes (450 μM/500 μM). Protamine (blue) enters into the liposome through OmpF and displaces LCG from CX4 to result in a switch-on fluorescence response. The addition of Triton X-100 lyses the membrane releasing reporter pairs and analytes into the bulk solution causing supramolecular disassembly and a large dilution (factor of ca. 5000, Figure S9). The supramolecular tandem membrane assay allows monitoring of the translocation of protamine through the LCG fluorescence response. b–e) Fluorescence intensity of CX4–LCG-loaded liposomes upon addition of b) 45 nM OmpF then 5 μM protamine, c) 5 μM protamine, d) 45 nM OmpF, e) 5 μM protamine, then 45 nM OmpF.

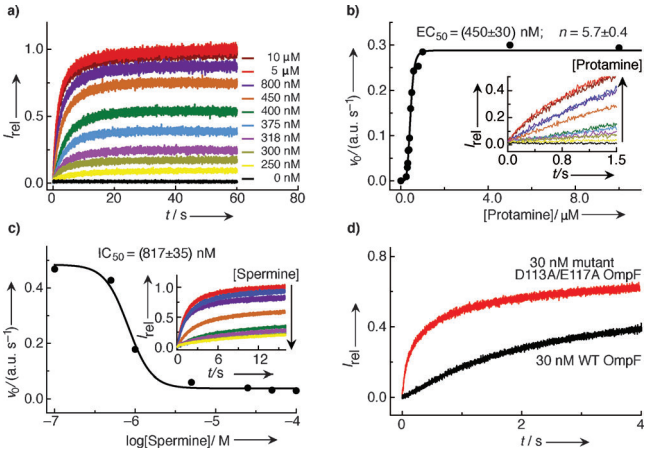

Figure 3. Kinetics of OmpF-mediated translocation of protamine into liposomes, monitored by stopped-flow experiments. a) Fluorescence kinetic traces upon mixing of protamine (0–10 μM) with a solution of CX4–LCG-loaded proteoliposomes (450 μM/500 μM and 30 nM OmpF). b) Fitting of initial rates of translocation at different protamine concentrations according to the Hill equation.[15] Inset: The initial rate increases with protamine concentration. c) Dose-response curve for the inhibition of protamine translocation by spermine. The measurement was initiated by adding 5 μM protamine to a solution of CX4–LCG-loaded liposomes, 45 nM OmpF, and 0–100 μM spermine. Inset: The fluorescence kinetics at various spermine concentrations (red trace: 0 μM, yellow trace: 100 μM). d) Fluorescence kinetics of protamine translocation through wild-type OmpF (30 nM, black trace) and through the double mutant D113A/E117A OmpF (30 nM, red trace). The reaction was initiated by adding 5 μM protamine to the CX4–LCG-loaded proteoliposomes.

450 nM with a Hill slope of approximately 6.[15] The tandem membrane assays therefore complement the electrophysiological measurements, in which the differentiation between analyte binding to the channel or translocation through it, as well as the determination of actual kinetics becomes difficult, in particular for high-molecular-weight analytes and slow translocation rates (see the Supporting Information).[3c,4,16]

Various transmembrane channels are co-regulated by polyamines and, among them, spermine is the most potent modulator of OmpF.[1b,17] When the tandem assays were conducted at different concentrations of spermine, the translocation rate, as monitored by the fluorescence response, decreased (Figure 3c), and the dose-response curve afforded an IC_{50} value of (820 ± 40) nM. With $K_i = IC_{50}/(1+[\text{Protamine}]/EC_{50})$ a K_i value of approximately 70 nM is obtained, which corresponds well to a literature estimate (low nanomolar range).[17] As can be seen, a label-free supramolecular method is now available to pin-point the functions of channels and to screen for modulators, all by fluorescence. Furthermore, since spermine anchors at the constriction region of the OmpF channel, the efficient inhibition of protamine translocation also demonstrates that this analyte indeed passes through the OmpF channel interior and not, to rule out a less-likely detour, along the outer walls of the protein, that is, along the lipid–protein interface.[18]

The constriction region of OmpF is rate-limiting for the translocation of molecules, including hydrophilic antibiotics, such as ampicillin and penicillin.[1b] Electrophysiological studies have pointed to an accelerated uptake of such β-lactam antibiotics through singly substituted OmpF mutants D113A and R132A.[19] Consequently, we studied the effect of mutations that affect the charge and size of the OmpF channel in relation to the flux of protamine. The two negatively charged residues aspartate 113 and glutamate 117 were replaced by alanine through site-directed mutagenesis, and,

indeed, the rate of protamine influx through D113A/E117A OmpF increased threefold (Figure 3d). Again, and in contrast to other experiments, our method allows direct continuous monitoring of the translocation kinetics, a first-time observation for an antimicrobial peptide.[3c] It transpires that the screening of a large library of channel mutants could be readily conducted. The method is transferable to other channel proteins.

Because the method is based on an unselective molecular recognition, it is not limited to protamine, but transferable to other organic analytes (Figure 1a). For instance, we have unambiguously demonstrated the successful translocation of heptaarginine, a membrane transduction peptide, and of acetylcholine, a low-molecular-weight neurotransmitter, both through OmpF (Figure S12). Direct permeation (without channel) of analytes can also be conveniently monitored, for example, of amantadine, an anti-Alzheimer's drug (Figure S13); this assay was additionally performed in liposomes of different lipid composition and by utilizing an alternative chemosensing ensemble composed of cucurbit[7]uril (CB7) as macrocyclic receptor and berberine (BE) as fluorescent dye (Figure 1a).

In summary, the supramolecular chemical method introduced herein (after the necessary adaptations of the reporter pairs) will allow for the screening of diverse classes of analytes, different channel proteins, and channel modulators. It can monitor transport driven either by a concentration gradient, or, potentially, by an electrochemical gradient established by reconstituting highly selective ionophores, such as valinomycin, into liposomes. The micromolar sensitivity and versatility should find ample applications in fundamental and applied membrane research ranging from the simple detection of permeation to the measurement of the real-time transport kinetics of natural metabolites, toxins, and drugs. The applicability of the method to cellular studies is presently being explored.

Received: November 4, 2013
Published online: January 27, 2014

Keywords: antimicrobial peptides · calixarenes · fluorescence · macrocycles · membrane proteins

[1] a) M. Rask-Andersen, M. S. Almen, H. B. Schioth, *Nat. Rev. Drug Discovery* **2011**, *10*, 579 – 590; b) J. M. Pagès, C. E. James, M. Winterhalter, *Nat. Rev. Microbiol.* **2008**, *6*, 893 – 903.

[2] a) K. M. O'Connell, J. T. Hodgkinson, H. F. Sore, M. Welch, G. P. Salmond, D. R. Spring, *Angew. Chem.* **2013**, *125*, 10904 – 10932; *Angew. Chem. Int. Ed.* **2013**, *52*, 10706 – 10733; b) D. J. Payne, M. N. Gwynn, D. J. Holmes, D. L. Pompliano, *Nat. Rev. Drug Discovery* **2007**, *6*, 29 – 40; c) K. L. Brouwer, D. Keppler, K. A. Hoffmaster, D. A. Bow, Y. Cheng, Y. Lai, J. E. Palm, B. Stieger, R. Evers, *Clin. Pharmacol. Ther.* **2013**, *94*, 95 – 112; d) S. T. Henriques, M. N. Melo, M. A. R. B. Castanho, *Mol. Membr. Biol.* **2007**, *24*, 173 – 184.

[3] a) A. T. Jones, E. J. Sayers, *J. Controlled Release* **2012**, *161*, 582 – 591; b) K. A. Brogden, *Nat. Rev. Microbiol.* **2005**, *3*, 238 – 250; c) A. Apetrei, A. Asandei, Y. Park, K. S. Hahm, M. Winterhalter, T. Luchian, *J. Bioenerg. Biomembr.* **2010**, *42*, 173 – 180.

[4] K. R. Mahendran, E. Hajjar, T. Mach, M. Lovelle, A. Kumar, I. Sousa, E. Spiga, H. Weingart, P. Gameiro, M. Winterhalter, M. Ceccarelli, *J. Phys. Chem. B* **2010**, *114*, 5170 – 5179.

[5] a) C. M. Nimigean, *Nat. Protoc.* **2006**, *1*, 1207 – 1212; b) A. Watts, *Nat. Rev. Drug Discovery* **2005**, *4*, 555 – 568; c) A. D. Tsamaloukas, S. Keller, H. Heerklotz, *Nat. Protoc.* **2007**, *2*, 695 – 704; d) A. N. Tkachenko, P. K. Mykhailiuk, S. Afonin, D. S. Radchenko, V. S. Kubyshkin, A. S. Ulrich, I. V. Komarov, *Angew. Chem.* **2013**, *125*, 1526 – 1529; *Angew. Chem. Int. Ed.* **2013**, *52*, 1486 – 1489.

[6] a) S. M. Butterfield, A. Hennig, S. Matile, *Org. Biomol. Chem.* **2009**, *7*, 1784 – 1792; b) S. Matile, N. Sakai, A. Hennig in *Supramolecular Chemistry: From Molecules to Nanomaterials*, *Vol. 8* (Eds.: P. A. Gale, J. W. Steed), Wiley, Chichester, **2012**, pp. 473 – 500.

[7] a) J. T. Davis, O. Okunola, R. Quesada, *Chem. Soc. Rev.* **2010**, *39*, 3843 – 3862; b) Y. J. Jeon, H. Kim, S. Jon, N. Selvapalam, D. H. Oh, I. Seo, C. S. Park, S. R. Jung, D. S. Koh, K. Kim, *J. Am. Chem. Soc.* **2004**, *126*, 15944 – 15945; c) R. Zadmard, T. Schrader, *J. Am. Chem. Soc.* **2005**, *127*, 904 – 915; d) L. Q. Gu, S. Cheley, H. Bayley, *Science* **2001**, *291*, 636 – 640; e) Y. L. Ying, J. J. Zhang, F. N. Meng, C. Cao, X. Y. Yao, I. Willner, H. Tian, Y. T. Long, *Sci. Rep.* **2013**, *50*,1 – 8.

[8] a) A. Hennig, H. Bakirci, W. M. Nau, *Nat. Methods* **2007**, *4*, 629 – 632; b) D.-S. Guo, V. D. Uzunova, X. Su, Y. Liu, W. M. Nau, *Chem. Sci.* **2011**, *2*, 1722 – 1734; c) R. N. Dsouza, A. Hennig, W. M. Nau, *Chem. Eur. J.* **2012**, *18*, 3444 – 3459.

[9] a) L. You, E. V. Anslyn in *Supramolecular Chemistry: From Molecules to Nanomaterials*, *Vol. 1* (Eds.: P. A. Gale, J. W. Steed), Wiley, Chichester, **2012**, pp. 135 – 160; b) B. T. Nguyen, E. V. Anslyn, *Coord. Chem. Rev.* **2006**, *250*, 3118 – 3127.

[10] R. N. Dsouza, U. Pischel, W. M. Nau, *Chem. Rev.* **2011**, *111*, 7941 – 7980.

[11] S. A. Minaker, K. D. Daze, M. C. F. Ma, F. Hof, *J. Am. Chem. Soc.* **2012**, *134*, 11674 – 11680.

[12] A. Aspedon, E. A. Groisman, *Microbiology* **1996**, *142*, 3389 – 3397.

[13] N. G. Housden, J. T. S. Hopper, N. Lukoyanova, D. Rodriguez-Larrea, J. A. Wojdyla, A. Klein, R. Kaminska, H. Bayley, H. R. Saibil, C. V. Robinson, C. Kleanthous, *Science* **2013**, *340*, 1570 – 1574.

[14] C. D. Fjell, J. A. Hiss, R. E. Hancock, G. Schneider, *Nat. Rev. Drug Discovery* **2012**, *11*, 37 – 51.

[15] L. J. Van Winkle, O. Bussolati, G. Gazzola, J. McGiven, B. Mackenzie, M. H. Saier, Jr., P. M. Taylor, M. J. Rennie, S. Y. Low in *Biomembrane Transport*, Academic Press, San Diego, **1999**, pp. 65 – 131.

[16] U. Lamichhane, T. Islam, S. Prasad, H. Weingart, K. Mahendran, M. Winterhalter, *Eur. Biophys. J.* **2013**, *42*, 363 – 369.

[17] A. Baslé, A. H. Delcour in *Bacterial and Eukaryotic Porins*, 1st ed. (Ed.: R. Benz), Wiley-VCH, Weinheim, **2005**, pp. 79 – 98.

[18] T. G. Baboolal, M. J. Conroy, K. Gill, H. Ridley, V. Visudtiphole, P. A. Bullough, J. H. Lakey, *Structure* **2008**, *16*, 371 – 379.

[19] S. Vidal, J. Bredin, J. M. Pagès, J. Barbe, *J. Med. Chem.* **2005**, *48*, 1395 – 1400.

Appendix 4.3 Publications

Reprinted with permission from Natural Product Communications. Ghale, G.; Kuhnert, N; Nau, W. M. "Monitoring stepwise proteolytic degradation of peptides by supramolecular domino tandem assays and mass spectrometry for trypsin and leucine aminopeptidase." *Nat. Prod. Commun.* **2012**, *7*, 343-348. Publisher's version can be found at:
http://members.naturalproduct.us/Secure/Issue.aspx?volumeissueid=76

NPC Natural Product Communications

2012
Vol. 7
No. 3
343 - 348

Monitoring Stepwise Proteolytic Degradation of Peptides by Supramolecular Domino Tandem Assays and Mass Spectrometry for Trypsin and Leucine Aminopeptidase

Garima Ghale, Nikolai Kuhnert and Werner M. Nau*

School of Engineering and Science, Jacobs University Bremen, Campus Ring 1, 28759 Bremen, Germany

w.nau@jacobs-university.de

Received: October 20th, 2011; Accepted: November 18th, 2011

A label-free optical detection method has been designed that allows direct monitoring of enzymatic peptide digestion *in vitro*. The method is based on the addition of a reporter pair, composed of the macrocyclic host cucurbit[7]uril (CB7) and the fluorescent dye acridine orange (AO), to detect the proteolytic degradation of peptides. The enzymatic activity of trypsin and leucine aminopeptidase (LAP) was investigated using H-LSRFSWGA-OH as a substrate. The substrate as well as the intermediary and final products (i.e., H-FSWGA-OH and phenylalanine) formed during its enzymatic hydrolysis differ in their binding affinity to the receptor CB7, which results in varying degrees of dye displacement and, therefore, different fluorescence intensities. CB7 showed a relatively weak binding constant of $K \approx 10^4$ M^{-1} with the substrate, a relatively strong binding constant of $K \geq 10^6$ M^{-1} with H-FSWGA-OH (which is a final product formed by trypsin digestion and the intermediary product formed during the enzymatic activity of LAP), and a moderate binding constant of $K \leq 10^5$ M^{-1} with phenylalanine. Owing to this differential binding affinity of CB7 with the substrate and the corresponding products, the digestion of a peptide by trypsin was followed as a decrease in fluorescence signal, while the complete degradation of the peptide by LAP was monitored as a decrease and a subsequent increase in fluorescence signal. The k_{cat}/ K_M value for trypsin (2.0×10^7 $min^{-1}M^{-1}$) was derived from the change in fluorescence signal with time. Additionally, the complete degradation of the peptide by LAP was also followed by mass spectrometry. The use of a supramolecular sensing ensemble (macrocyclic host and dye) as a fluorescent reporter pair gives this method the flexibility to adapt for monitoring the stepwise degradation of different biologically relevant peptides by other proteases.

Keywords: Enzymes, Enzyme assays, Fluorescence, Supramolecular chemistry, Macrocycles, Cucurbituril, Proteases, Mass spectrometry.

Proteases are biological catalysts mediating numerous cellular and metabolic processes [1]. Several enzyme assays have been developed to understand and visualize their activity [2]. Customarily, these are fluorescence-based methods that rely on fluorescently labeled peptides as substrates. While endopeptidases (proteases that hydrolyze internal amide bonds) [3] can be conventionally detected using either fluorescently or radioactively labeled substrates, designing fluorescent assays for exopeptidases (proteases that cleave amide bonds at the N- or C-terminal positions of the peptide) [3], has remained substantially more demanding, because end-labeled substrates are frequently not accepted as substrates by the exopeptidases. Accordingly, only a handful of fluorescent methods have been reported for monitoring exopeptidases activity [4]. Another challenge in the investigation of exopeptidase activity is the monitoring of the sequential cleavage of a peptide from one end to the other (a process which is in the most trivial case that involved in gastrointestinal digestion). None of the existing fluorescence-based enzyme assays allows observation of multiple exo-cleavage events, i.e., the step-by-step degradation of a peptide, to be followed, which calls for structural analytical methods, such as mass spectrometry (MS) [5].

We have recently adapted an approach from supramolecular chemistry to design a novel line of enzyme assays [6]. The resulting supramolecular tandem assays [6a] employ reporter pairs composed of a synthetic macrocyclic receptor and a fluorescent dye. The two components form a supramolecular host-guest complex, which changes the photophysical properties of the dye. Leaning on the indicator displacement principle [7], an enzymatic substrate and the corresponding product are capable of displacing the fluorescent dye to different extents from the macrocycle, such that the change in fluorescence of the dye in the course of an enzymatic reaction can be correlated with the conversion, i.e., the enzymatic activity. If the macrocycle binds more strongly to the product of an enzymatic reaction (product-selective assay) [6a,6d], the progress of the enzymatic reaction is signaled by the displacement of the fluorescent dye from the macrocycle, leading to a concomitant change in fluorescence intensity. Conversely, if the substrate binds with higher affinity to the macrocycle (substrate-selective assay) [6b,6c,6e], the enzymatic transformation can be monitored as a change in fluorescence intensity due to the uptake of fluorescent dye into the macrocycle as the enzyme converts the substrate.

To by-pass the need for substrates with covalently attached fluorescent or radioactive labels, we have recently developed a label-free tandem assay for proteases and exemplified its use for a metalloendoprotease, thermolysin [6d]. Herein, we introduce supramolecular tandem assays for a selective endopeptidase, namely trypsin, and a relatively unselective exopeptidase, leucine aminopeptidase (LAP). The results obtained from the label-free assays, including the monitoring of stepwise exopeptidase activity, are structurally supported by MS data.

Selection of a reporter pair. We selected acridine orange (AO) and cucurbit[7]uril (CB7, Figure 1) as our reporter pair, which has already been successfully employed to follow the activities of the enzymes diamine oxidase and thermolysin [6b,6d]. The fluorescence of the weakly fluorescent dye AO is significantly enhanced upon encapsulation by CB7 due to a complexation-induced pK_a shift [8]. The formation of strongly binding analytes, as it may occur in the course of an enzymatic reaction, causes a dye displacement and fluorescence decrease, while the depletion of a strongly binding analyte causes the opposite response. The synthetic macrocyclic receptor, CB7, is a cyclic oligomer composed of

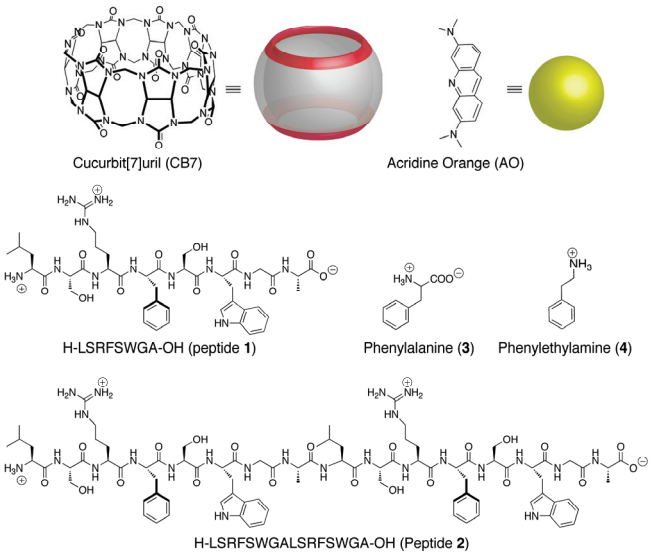

Figure 1: Chemical structures and graphical representations of the macrocyclic host CB7 and the fluorescent dye AO and structures of compounds **1**–**4**.

7 glycouril units synthesized by acid-catalyzed condensation of glycoluril with formaldehyde [9]. The hydrophobic interior of the barrel-shaped CB7, along with its two identical carbonyl-laced portals, make CB7 a suitable host for both non-polar hydrophobic and/or cationic guest molecules. The interplay of supramolecular interactions (hydrophobic *versus* ion-dipole) accounts also for its relatively high selectivity towards guest molecules [10]. Most pertinent in the context of protease assay development, the complexation of CB7 with the aromatic residue of internal phenylalanine (no adjacent charges) is driven solely by hydrophobic interactions and the binding is moderately strong ($K \approx 10^4$ M^{-1}) [6d]. In contrast, a very tight binding is observed between CB7 and the aromatic residue of *N*-terminal phenylalanine ($K \geq 10^6$ M^{-1}) [11], due to the presence of additional ion-dipole interactions between the ammonium group and the carbonyl portals. This precise stabilization of terminal ionic groups (in case of CB7 the stabilization at the N-terminus) is an important criterion in the design of artificial receptors for sequence-selective recognition of peptides [12].

Table 1: Binding constants of representative analytes with CB7.

Analyte	K (10^4 M^{-1}) [a]	
	borate buffer [b]	tris buffer [c]
Acridine orange (AO)	5.7 ± 0.3	250 ± 40
H-LSRFSWGA-OH (**1**)	0.73 ± 0.32	3.6 ± 0.2
H-LSRFSWGA-LSRFSWGA-OH (**2**)	0.77 ± 0.17	22 ± 5
Phenylalanine (**3**)	1.8 ± 0.3	17 ± 1
Phenylethylamine (**4**) [d]	540 ± 370	6800 ± 3200

[a] Binding constants were determined by using 0.5 μM AO and 4-8 μM CB7 (*cf.* Figures S1 and S2 in Supplementary Data). [b] 110 mM, pH 8, at 25°C. [c] 0.05 mM, pH 7.6, at 37°C. [d] Phenylethylamine serves as a model for the peptide fragment with Phe at the *N*-terminus of the peptide formed after the enzymatic hydrolysis of the substrate (**1**).

Selection of peptide substrates. Based on our previous experience in the development of protease assays with singly labeled peptides [4b], we selected peptide **1** (Figure 1) as a common substrate for both investigated enzymes. Given the reported inhibitory effect of CB7 on the activity of proteases by forming a host-substrate complex [13], CB7 may not seem to be an obvious choice. However, the concentrations of the host CB7 and of the substrate peptide employed in tandem assays (μM) are much lower than the amount required for inhibition (mM). This conjecture was confirmed by competitive titration experiments, which confirmed that peptide **1** displayed a relatively low affinity for CB7 and did not interfere with the formation of the strongly fluorescent CB7/AO complex (Table 1). Furthermore, its binding constants in the different buffers were at least 2 orders of magnitude lower than the expected (final or intermediary) peptide products of the proteolytic degradation. The latter contain a strongly binding *N*-terminal phenylalanine residue, which was modeled with respect to its binding affinity by determining the binding constant of phenylethylamine (**4**, Table 1). Note that the absolute binding constant to CB7 depends on the selected buffer, because alkali ions (present as Na^+ in the borate buffer) are known to show competitive binding [14]. Nevertheless, regardless of the variations in absolute binding constants (Table 1), tandem assays could be constructed for both buffers, because the method is based on the differential binding between substrate and product, which applies regardless of buffer. Peptide **2** (Figure 1) presents a longer repeat peptide sequence that was employed in the development of the exopeptidase tandem assays for LAP.

Supramolecular tandem assay for trypsin. Trypsin is widely used in peptide sequencing, tissue culture protocols, and as a diagnostic marker for pancreatic diseases [15]. Trypsin, from the family of serine proteases, is enzymologically well characterized such that the application of tandem assays in this case served mainly as a proof of principle. Upon addition of trypsin to a reaction mixture containing peptide **1** and the strongly fluorescent reporter pair (CB7/AO), a time-resolved decrease in fluorescence intensity was observed. This is because trypsin selectively cleaves peptide **1** at the carboxyl end of arginine [16], forming a peptide fragment with phenylalanine at the *N*-terminus that binds sufficiently strong (Table 1) to gradually displace AO from the CB7 cavity (product-selective tandem assay, *cf.* Scheme S1 in Supplementary Data). Therefore, trypsin activity can be continuously followed as a decrease in fluorescence intensity (switch-off fluorescence response, Figure 2). The time-dependent change in fluorescence intensity at various substrate concentrations (inset of Figure 2) was used to determine the proteolytic constant (k_{cat}/K_M). The resulting value, 2.0×10^7 $min^{-1}M^{-1}$, is in good agreement with the reported literature value (3.8×10^7 $min^{-1}M^{-1}$) determined by a single-label protease assay for a very similar peptide sequence (H-XLSLSRFSWGA-OH, X is a fluorescent label) [4b]. As can be seen, and as has already been shown for another protease (thermolysin) [6d], tandem assays for endopeptidases are straightforward to design when the enzymatic cleavage affords a product peptide with an *N*-terminal aromatic amino acid.

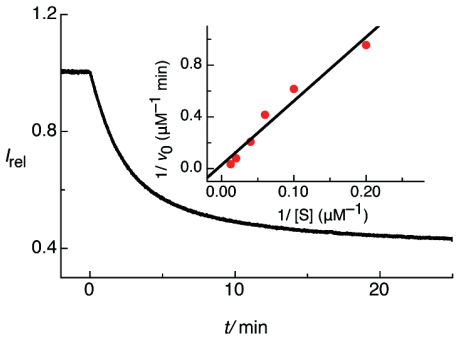

Figure 2: Continuous decrease in fluorescence intensity as a result of enzymatic hydrolysis of peptide **1** (50 μM) by trypsin (10 nM). The reaction was performed in 110 mM borate buffer, pH 8, at 25°C using 8 μM CB7 and 0.5 μM AO as a reporter pair (λ_{exc} = 485 nm and λ_{obs} = 510 nm). The figure in the inset represents the Lineweaver–Burk plot for the initial rates of peptide hydrolysis *versus* substrate concentration. The initial rates were obtained by linear fits of the normalized intensities (see Figure S3 in Supplementary Data), assuming a conversion linear with the fluorescence intensity and full conversion in the plateau region.

Supramolecular tandem assay for leucine amino peptidase. Since the assay principle should be similarly applicable to exopeptidases, we turned our attention to the enzyme LAP. LAP, a cytosolic metalloprotease, plays diverse biological and physiological roles by degrading bioactive peptides involved in peptide-dependent signaling [17]. For instance, LAP is implicated in the *N*-terminal trimming or degradation of oligopeptides generated from proteasomes to antigenic peptides or free amino acids [18]. As mentioned in the outset, fluorescent assays for exopeptidases suffer generally from the complication that the extrinsic label must be positioned directly where cleavage is supposed to occur, modulating the rate of cleavage or even inhibiting cleavage [4a,4e]. Accordingly, assays for exopeptidases such as LAP are scarce such that label-free assays, and in particular the tandem assays developed herein, are practically highly relevant.

LAP cleaves amide bonds from the *N*-terminal side of a peptide. It is know to remove leucine most effectively, but acts rather unselectively on all amino acid residues with L-configuration [19]. In contrast to trypsin, a straightforward product-selective tandem assay could not be implemented for LAP, because the enzyme was expected to cleave, at varying rates, the amino acid residues one after the other, including the phenylalanine residue. A combination of product-selective and substrate-selective recognition by CB7 with the associated off-and-on fluorescence response was, therefore, expected to take place in the course of the enzymatic reaction, a scenario which we have previously referred to as a "domino" tandem assay [6b]. Domino tandem assays are based on the same operational principle of tandem assays, but different ones in sequence. This allows, for example, in a first step, the formation of an initial enzymatic product to be probed (product-selective assay) and, in a second step, the depletion of the initial product, which now serves as substrate for a second enzymatic reaction (substrate-selective assay). In detail, LAP was first expected to form a strongly binding peptide fragment with the *N*-terminal phenylalanine residue (initial product, switch-off response), which could be subsequently converted, through a rapid host-guest exchange equilibrium, to the amino acid phenylalanine and another peptide fragment, which should both act as weak binders to CB7 (final products, switch-on response).

The general principle for assaying an exopeptidase is shown in Scheme 1. Initially (left side), the dye AO favorably competes with the internal phenylalanine residue for the complexation by CB7 (dye in, fluorescence on). As LAP starts cleaving the first amide bond from the *N*-terminus of the peptide, no change in fluorescence is observed. However, once LAP cleaves the Arg residue that is next to Phe, the *N*-terminal ammonium group of Phe is exposed.

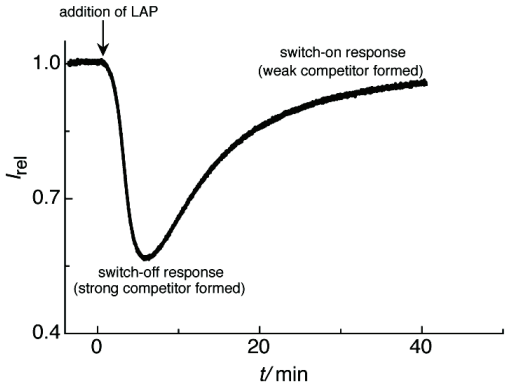

Figure 3: Evolution of fluorescence intensity upon addition of 10 nM LAP to 20 μM of peptide **1** in 0.05 mM tris buffer containing the CB7/AO reporter pair (4 μM CB7 and 0.5 μM AO, λ_{exc} = 485 nm, λ_{obs} = 510 nm).

The *N*-terminal Phe peptide fragment now competes for CB7, displacing the dye AO (product-selective), which is then reflected by the decrease in fluorescence intensity (dye out, fluorescence off, Figure 3). As LAP continues to hydrolyze *N*-terminal amide bonds, the *N*-terminal Phe is enzymatically digested to the free amino acid (substrate-selective), which again shows a weaker binding, facilitating the complexation of CB7 and AO (dye in, fluorescence on, Figure 3). Therefore, by alternating the binding affinities of the metabolites to the macrocyclic host from weak (substrate) to strong (*N*-terminal Phe peptide as intermediate) and again back to weak (Phe as product), the proteolytic activity of LAP could be continuously monitored through a down-and-up fluorescence response.

Additional tandem assays with LAP were carried out at different peptide concentrations (Figure S4 in Supplementary Data). By increasing the concentration of peptide, the enzymatic digestion time should increase. This showed up as a shift of the fluorescence minimum towards longer reaction times. Note that when the fluorescence reaches its minimum, the concentration of intermediary product (*N*-terminal Phe peptide) is expected to be at its maximum. The absolute steady-state concentrations of the *N*-terminal Phe peptide product were also larger, signaled by lower fluorescence intensities in the minimum due to a more efficient displacement of AO.

Proteolytic cleavage changes the molecular weight of the peptide, which can be exploited to monitor the enzymatic action of a protease by real-time MS. Real-time off-line FAB-MS has been used to monitor peptidase activity [20], while real-time ESI-MS has allowed monitoring of the activity of nuclease and glucosidase enzymes [21]. To our knowledge, we now report its first application

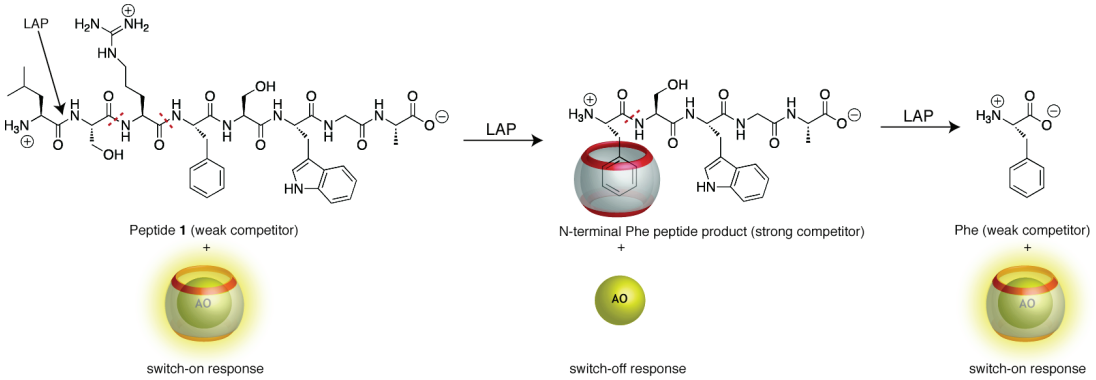

Scheme 1: Domino tandem assay combining fluorescence switch off and switch on response for monitoring the activity of LAP. The arrow indicates the initial site of cleavage and the dashed lines indicate the successive removal of amino acids from the *N*-terminus of peptide **1** by LAP.

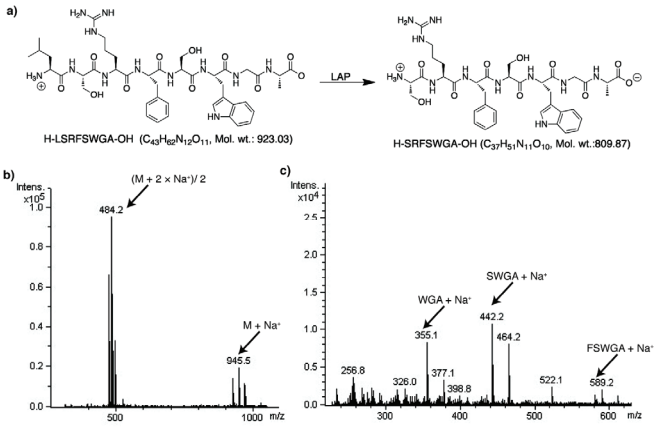

Figure 4: a) General scheme for monitoring the activity of LAP using MS. b) Singly and doubly charged molecular ion (M) peaks of peptide **1** in the absence of LAP. c) MS of the enzymatic reaction mixture taken after 120 minutes; the reaction was carried out in 10 mM borate buffer (pH 8) using 500 μM of peptide **1** and 10 nM of LAP.

for an exopeptidase. The enzymatic degradation of peptide **1** by LAP was, therefore, independently monitored by MS in order to verify that the marked fluorescence changes corresponded indeed to the presumed reaction pathway. As LAP cleaves off amino acids from the *N*-terminus, the molecular masses of the peptide fragments were expected to decrease in a predictable sequence-specific manner (Figure 4a), which allowed the progress of the enzymatic conversion to be followed with time, even if in a discontinuous fashion.

In the absence of LAP, the pseudomolecular ion peak of the singly charged substrate **1** was observed as its sodium adduct at *m/z* 945.5 and the doubly charged substrate as its disodiated ion at *m/z* 484.2 (Figure 4b) in a direct infusion experiment in the positive ion mode using an ESI-TOF mass spectrometer. After addition of LAP, MS were taken at different time intervals (see Figure S5 and Table S1 in Supplementary Data). After 30 minutes, additional ions were observed at *m/z* 810, 723, and 589 accounting for the presence of peptide fragments formed after the removal of Lys, Ser, and Arg from the *N*-terminus of the peptide. The identity of the ions resulting from LAP-induced amino acid cleavage was established by high-resolution mass measurements using ESI-TOF-MS measurements. As the reaction proceeded, amino-acid residues were sequentially cleaved off from the *N*-terminus and shorter peptide fragments were formed. After 120 minutes, the pseudomolecular ion signal corresponding to substrate **1** completely disappeared, which indicated complete substrate hydrolysis (Figure 4c). The time scale observed in this experiment corresponded well with the changes in fluorescence observed at similar substrate concentrations (Figure S4 in Supplementary Data), which confirmed that the domino tandem assay does indeed report on the biochemical reaction steps, namely when cleavage reaches the Phe residue (switch-off response) and when the Phe residue is cleaved off (switch-on response).

Peptide "fingerprinting". Interestingly, this particular fluorescence response (down-and-up) produced as a result of complete peptide cleavage by LAP opened a new perspective towards following the stepwise degradation of longer peptides by fluorescence through a domino tandem assay. This would present a very simplistic version of an Edman degradation, in which the fluorescence response signals that the degradation process has reached an aromatic amino acid. With that far-fetched goal of a peptide "fingerprinting" in mind, we selected a longer peptide composed of 16 amino acids (peptide **2**, which is essentially a peptide **1** repeat sequence). For peptide **1**, with one internal Phe, we

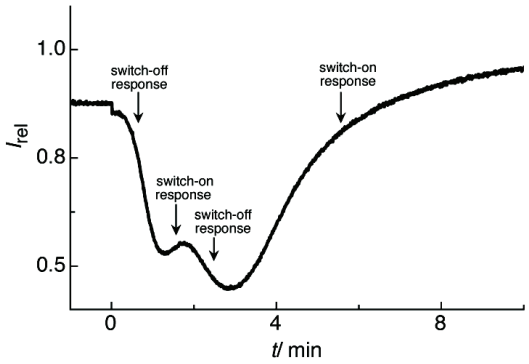

Figure 5: Fluorescence response (λ_{exc} = 485 nm, λ_{obs} = 510 nm) upon degradation of 10 μM peptide **2** by 50 nM LAP. The reaction was carried out by using 0.5 μM AO and 1 μM CB7 in 0.05 mM tris buffer (pH 7.6) at 37°C.

observed a single down-and-up fluorescence response. For peptide **2**, with two internal Phe, we expected two successive down-and-up fluorescence responses. The first switch-off and switch-on response would report that the first Phe had been reached, while the second one would indicate that the second Phe was being cleaved off.

Contrary to what we expected, only a single fluorescence switch-off and switch-on response was observed in initial experiments. Upon comparing the change in fluorescence signal for peptides **1** and **2**, we observed that the degradation of peptide **1** was much faster compared with that of peptide **2**. Furthermore, the drop in fluorescence intensity for peptide **2** (factor of 1.6 differentiation, Figure S6 in Supplementary Data) was more than half the change in fluorescence intensity for peptide **1** (factor of 2), although the concentrations had been adjusted to equal total amounts of Phe residues. The variations in the rate of enzymatic degradation and fluorescence intensities suggested that the fluorescence switch-off and switch-on response for peptide **2** was actually a statistical average response for the release of both free Phe residues, presumably arising from an overall slower hydrolysis of the longer peptide. We attempted to overcome this problem by optimizing the ratio of reporter pair i.e., CB7/AO, such that even the slightest changes in the concentration of analytes formed during enzymatic reaction could be detected (Figure S7 in Supplementary Data). Indeed, after optimizing the experimental conditions, the fluorescence response upon degradation of peptide **2** by LAP (Figure 5) revealed two overlapping but distinct fluorescence "valleys" attributable to the presence of two Phe residues in the same peptide.

As can be seen, the idea that different peptides give rise to different recognition patterns in the form of fluorescence "landscapes" and that "fingerprints" of peptide structures can be obtained by simply recording a fluorescence trace works in principle, but is in detail difficult to realize for longer peptides, due to sequence- and length-dependent variations in their K_M and k_{cat} values. Additionally, the multiple host-guest equilibria involved in the supramolecular tandem assay itself (with binding constants between host-dye, host-substrate, and between the host and all intermediary products) and also the statistics of the reaction, which prevents the individual cleavage steps to occur all at the same time and, therefore, affords mixtures of differently long peptide fragments as the reaction proceeds, prevent jointly that the number of phenylalanine residues in a peptide manifests itself always in well-separated dips in the fluorescence traces.

In conclusion, fluorescence-based assays are highly preferable to probe proteolytic activity due to their high sensitivity, ease of measurement, and possibility of continuous monitoring.

Supramolecular tandem enzyme assays stand out among fluorescence-based methods in that they can be utilized in real time on unlabeled substrates and in homogenous solution. We have successfully demonstrated that tandem assays can be easily transferable to other classes of proteases and especially exopeptidases as anticipated in our previous study [6d]. To our knowledge, tandem assay is the only fluorescence-based method that allows a continuous detection of exopeptidase activity by using an unlabeled peptide substrate [4f,22]. Additionally, the use of supramolecular tandem assays as a technique for simple pattern recognition of peptides, as attempted herein in the form of "domino" tandem assays, is still in its infancy and may require the choice of alternative exopeptidases and other recognition motifs but phenylalanine, some of which have recently been reported [23]. Furthermore, real-time ESI mass spectrometry was shown to be a valuable tool in studying complex step-wise enzymatic reactions, such as exopeptidase digestion of a shorter peptide.

Experimental

Materials and methods: Peptides **1** and **2** were purchased from Bio-syntan GmbH (Berlin, Germany) and obtained in >95% purity. Trypsin (from bovine pancreas, 2500 U/mg) and borate buffer, pH 8, were purchased from Applichem. Leucine aminopeptidase (type IV-S, from porcine kidney microsomes, 28 U/mg), acridine orange (AO), and phenylethylamine (**4**) were purchased from Sigma. Cucurbit[7]uril (CB7) was synthesized according to the literature [9b-d].

Peptide stock solutions were prepared in water and the concentration of the peptides was determined by assuming the extinction coefficient of the Trp residue to be the same as that of the free amino acid (ε_{280} = 3,400 $M^{-1}cm^{-1}$) [24]. Trypsin stock solutions were prepared in water. Leucine aminopeptidase (LAP) was prepared in activation buffer (2 mM $MnCl_2$ and 0.05 mM tris, pH 8.5) and activated for 2 h at 37°C. Reported extinction coefficients (ε_{280} = 33,600 $M^{-1}cm^{-1}$ for trypsin [25] and ε_{280} = 320,000 M^{-1} cm^{-1} for LAP [26]) were used to determine the enzyme concentrations. Absorption measurements were performed with a Varian Cary 4000 spectrophotometer.

Tandem enzyme assays: Assays for trypsin were performed in a mixture of 0.5 μM AO, 8 μM CB7, and 50 μM peptide **1** in 110 mM borate buffer, pH 8, at 25°C. Assays for LAP were performed in 0.05 mM tris buffer (pH 7.6 at 37°C) using 0.5 μM AO, 4 μM CB7, and the respective amount of peptide substrate. The reaction was initiated by addition of 10 nM LAP in a total assay volume of 1 mL. A Varian Eclipse spectrofluorometer equipped with a thermo-statted cell holder was used for the collection of the kinetic traces (λ_{exc} = 485 nm, λ_{obs} = 510 nm).

Electrospray ionization mass spectrometry (ESI-MS): ESI-MS measurements were carried out with a Micro-TOF Focus mass spectrometer (Burker Daltonics) fitted with an ESI source, and internal calibration was achieved with 10 mL of 0.1 M sodium formate solution injected prior to each measurement. Calibration was carried out using the enhanced quadratic calibration mode.

Peptide stock solution (1.9 mM, 52 μL) was added to 200 μL (reaction volume) of 10 mM borate buffer in 6 individual Eppendorf tubes. The reaction was initiated by adding 20 μL of a 100 μM LAP solution to each tube except for the first. The time of LAP addition to each vial was noted. A 200 μL sample from the first Eppendorf tube was loaded into a 1 mL Hamilton syringe. This sample was then infused into a time-of-flight mass spectrometer *via* a syringe pump, at a constant flow rate of 180 μL/min. Mass spectra were acquired over a mass range of 100-1500 Da in the positive ion mode. Additional MS data were obtained for the remaining 5 mixtures at fixed times (20, 30, 40, 60, and 120 minutes) after addition of enzyme.

Supplementary data: Host-guest and competitive titrations, additional tandem assays for trypsin and LAP, and more detailed MS data are available.

Acknowledgments - WMN and GG acknowledge financial support from the Deutsche Forschungsgemeinschaft (DFG grant NA-686/5), the COST Action CM1005 "Supramolecular Chemistry in Water", and the Fonds der Chemischen Industrie. The authors would like to thank Anja Müller for technical assistance.

References

[1] Puente XS, Sanchez LM, Overall CM, Lopez-Otin C. (**2003**) Human and mouse proteases: A comparative genomic approach. *Nature Reviews Genetics*, ***4***, 544-558.

[2] (a) Aoki T, Tsuchida S, Yahara T, Hamaue N. (**2008**) Novel assays for proteases using green fluorescent protein-tagged substrate immobilized on a membrane disk. *Analytical Biochemistry*, ***378***, 132-137; (b) Tamburini PP, Dreyer RN, Hansen J, Letsinger J, Elting J, Gorewillse A, Dally R, Hanko R, Osterman D, Kamarck ME, Yoowarren H. (**1990**) A fluorometric assay for HIV-protease activity using high-performance liquid-chromatography. *Analytical Biochemistry*, ***186***, 363-368; (c) Pazhanisamy S, Stuver CM, Livingston DJ. (**1995**) Automation of a high-performance liquid chromatography-based enzyme assay: evaluation of inhibition constants for human immunodeficiency virus-1 protease inhibitors. *Analytcial Biochemistry*, ***229***, 48-53; (d) Villanueva J, Nazarian A, Lawlor K, Tempst P. (**2009**) Monitoring peptidase activities in complex proteomes by MALDI-TOF mass spectrometry. *Nature Protocols*, ***4***, 1167-1183; (e) Zhao Z, Raftery MJ, Niu XM, Daja MM, Russell PJ. (**2004**) Application of in-gel protease assay in a biological sample: characterization and identification of urokinase-type plasminogen activator (uPA) in secreted proteins from a prostate cancer cell line PC-3. *Electrophoresis*, ***25***, 1142-1148.

[3] McDonald JK. (**1985**) An overview of protease specificity and catalytic mechanisms: aspects related to nomenclature and classification. *The Histochemical Journal*, ***17***, 773-785.

[4] (a) Marmé N, Weston KD, Staudt T, Spatz J, Knemeyer JP. (**2005**) A fluorescence-based assay for exopeptidases using self-quenching peptide probes with single-molecule sensitivity. *International Journal of Environmental Analytical Chemistry*, ***85***, 741-751; (b) Hennig A, Florea M, Roth D, Enderle T, Nau WM. (**2007**) Design of peptide substrates for nanosecond time-resolved fluorescence assays of proteases: 2,3-diazabicyclo[2.2.2]oct-2-ene as a noninvasive fluorophore. *Analytcial Biochemistry*, ***360***, 255-265; (c) Huang H, Tanaka H, Hammock BD, Morisseau C. (**2009**) Novel and highly sensitive fluorescent assay for leucine aminopeptidases. *Analytical Biochemistry*, ***391***, 11-16; (d) Marmé N, Knemeyer JP, Wolfrum J, Sauer M. (**2004**) Highly sensitive protease assay using fluorescence quenching of peptide probes based on photoinduced electron transfer. *Angewandte Chemie International Edition*, ***43***, 3798-3801; (e) Hennig A, Roth D, Enderle T, Nau WM. (**2006**) Nanosecond time-resolved fluorescence protease assays. *Chembiochem*, ***7***, 733-737; (f) Dean KE, Klein G, Renaudet O, Reymond JL. (**2003**) A green fluorescent chemosensor for amino acids provides a versatile high-throughput screening (HTS) assay for proteases. *Bioorganic & Medicinal Chemistry Letters*, ***13***, 1653-1656.

[5] Liesener A, Karst U. (**2005**) Monitoring enzymatic conversions by mass spectrometry: a critical review. *Analytical and Bioanalytcial Chemistry*, ***382***, 1451-1464.

[6] (a) Hennig A, Bakirci H, Nau WM. (**2007**) Label-free continuous enzyme assays with macrocycle-fluorescent dye complexes. *Nature Methods*, ***4***, 629-632; (b) Nau WM, Ghale G, Hennig A, Bakirci H, Bailey DM. (**2009**) Substrate-selective supramolecular tandem assays: monitoring enzyme inhibition of arginase and diamine oxidase by fluorescent dye displacement from calixarene and cucurbituril macrocycles. *Journal of the American Chemical Society*, ***131***, 11558-11570; (c) Florea M, Nau WM. (**2010**) Implementation of anion-receptor macrocycles in supramolecular tandem assays for enzymes involving nucleotides as substrates, products, and cofactors. *Organic & Biomolecular Chemistry*, ***8***, 1033-1039; (d) Ghale G, Ramalingam V, Urbach AR, Nau WM. (**2011**) Determining protease substrate selectivity and inhibition by label-free supramolecular tandem enzyme assays. *Journal of the American Chemical Society*, ***133***, 7528-7535; (e) Guo DS, Uzunova VD, Su X, Liu Y, Nau WM. (**2011**) Operational calixarene-based fluorescent sensing systems for choline and acetylcholine and their application to enzymatic reactions. *Chemical Science*, ***2***, 1722-1734.

[7] (a) Nguyen BT, Wiskur SL, Anslyn EV. (**2004**) Using indicator-displacement assays in test strips and to follow reaction kinetics. *Organic Letters*, ***6***, 2499-2501; (b) Zhang T, Anslyn EV. (**2007**) Using an indicator displacement assay to monitor glucose oxidase activity in blood serum. *Organic Letters*, ***9***, 1627-1629; (c) Dsouza RN, Pischel U, Nau WM. (**2011**) Fluorescent dyes and their supramolecular host-guest complexes with macrocycles in aqueous solution, *Chemical Reviews*, ***111***, 7941-7980.

[8] (a) Shaikh M, Mohanty J, Singh PK, Nau WM, Pal H. (**2008**) Complexation of acridine orange by cucurbit[7]uril and beta-cyclodextrin: photophysical effects and pKa shifts. *Photochemical and Photobiological Sciences*, ***7***, 408-414; (b) Zhou YY, Yu HP, Zhang L, Sun JY, Wu L, Lu Q, Wang L. (**2008**) Host properties of cucurbit [7] uril: fluorescence enhancement of acridine orange. *Journal of Inclusion Phenomena and Macrocyclic Chemistry*, ***61***, 259-264.

[9] (a) Lagona J, Mukhopadhyay P, Chakrabarti S, Isaacs L. (**2005**) The cucurbit[n]uril family. *Angewandte Chemie International Edition*, ***44***, 4844-4870; (b) Kim J, Jung I-S, Kim S-Y, Lee E, Kang J-K, Sakamoto S, Yamaguchi K, Kim K. (**2000**) New Cucurbituril Homologues: Syntheses, Isolation, Characterization, and X-ray Crystal Structures of Cucurbit[n]uril (n = 5, 7, and 8). *Journal of the American Chemical Society*, ***122***, 540-541; (c) Day A, Arnold AP, Blanch RJ, Snushall B. (**2001**) Controlling factors in the synthesis of cucurbituril and its homologues. *Journal of Organic Chemistry*, ***66***, 8094-8100; (d) Márquez C, Huang F, Nau WM. (**2004**) Cucurbiturils: Molecular nanocapsules for time-resolved fluorescence-based assays. *Ieee Transactions on Nanobioscience*, ***3***, 39-45.

[10] (a) Jeon WS, Moon K, Park SH, Chun H, Ko YH, Lee JY, Lee ES, Samal S, Selvapalam N, Rekharsky MV, Sindelar V, Sobransingh D, Inoue Y, Kaifer AE, Kim K. (**2005**) Complexation of ferrocene derivatives by the cucurbit[7]uril host: A comparative study of the cucurbituril and cyclodextrin host families. *Journal of the American Chemical Society*, ***127***, 12984-12989; (b) Liu SM, Ruspic C, Mukhopadhyay P, Chakrabarti S, Zavalij PY, Isaacs L. (**2005**) The cucurbit[n]uril family: Prime components for self-sorting systems. *Journal of the American Chemical Society*, ***127***, 15959-15967; (c) Nau WM, Florea M, Assaf KI. (**2011**) Deep inside cucurbiturils: Physical properties and volumes of their inner cavity determine the hydrophobic driving force for host-guest complexation. *Israel Journal of Chemistry*, ***51***, 559-577.

[11] Rekharsky MV, Yamamura H, Inoue C, Kawai M, Osaka I, Arakawa R, Shiba K, Sato A, Ko YH, Selvapalam N, Kim K, Inoue Y. (**2006**) Chiral recognition in cucurbituril cavities. *Journal of the American Chemical Society*, ***128***, 14871-14880.

[12] (a) Hossain MA, Schneider HJ. (**1998**) Sequence-selective evaluation of peptide side-chain interaction. New artificial receptors for selective recognition in water. *Journal of the American Chemical Society*, ***120***, 11208-11209; (b) Sirish M, Schneider HJ. (**1999**) Porphyrin derivatives as water-soluble receptors for peptides. *Chemical Communications*, 907-908.

[13] Hennig A, Ghale G, Nau WM. (**2007**) Effects of cucurbit[7]uril on enzymatic activity. *Chemical Communications*, 1614-1616.

[14] (a) Márquez C, Hudgins RR, Nau WM. (**2004**) Mechanism of host-guest complexation by cucurbituril. *Journal of the American Chemical Society*, ***126***, 5806-5816; (b) Nau WM. (**2010**) Supramolecular capsules: under control. *Nature Chemistry*, ***2***, 248-250; (c) Shaikh M, Mohanty J, Bhasikuttan AC, Uzunova VD, Nau WM, Pal H. (**2008**) Salt-induced guest relocation from a macrocyclic cavity into a biomolecular pocket: interplay between cucurbit[7]uril and albumin. *Chemical Communications*, 3681-3683; (d) Florea M, Nau WM. (**2011**) Strong binding of hydrocarbons to cucurbituril probed by fluorescent dye displacement: a supramolecular gas-sensing ensemble. *Angewandte Chemie International Edition*, ***50***, 9338-9342.

[15] (a) Yang M, Chen CZ, Wang XN, Zhu YB, Gu YJ. (**2009**) Favorable Effects of the Detergent and Enzyme Extraction Method for Preparing Decellularized Bovine Pericardium Scaffold for Tissue Engineered Heart Valves. *Journal of Biomedical Materials Research Part B-Applied Biomaterials*, ***91B***, 354-361; (b) Soleimani M, Nadri S. (**2009**) A protocol for isolation and culture of mesenchymal stem cells from mouse bone marrow. *Nature Protocols*, ***4***, 102-106; (c) Chen N, Zou J, Wang S, Ye Y, Huang Y, Gadda G, Yang JJ. (**2009**) Designing protease sensors for real-time imaging of trypsin activation in pancreatic cancer cells. *Biochemistry*, ***48***, 3519-3526; (d) Hedstrom J, Sainio V, Kemppainen E, Haapiainen R, Kivilaakso E, Schroder T, Leinonen J, Stenman UH. (**1996**) Serum complex of trypsin 2 and α_1 antitrypsin as diagnostic and prognostic marker of acute pancreatitis: Clinical study in consecutive patients. *British Medical Journal*, ***313***, 333-337; (e) Goldberg DM. (**2000**) Proteases in the evaluation of pancreatic function and pancreatic disease. *Clinica Chimica Acta*, ***291***, 201-221.

[16] Olsen JV, Ong SE, Mann M. (**2004**) Trypsin cleaves exclusively C-terminal to arginine and lysine residues. *Molecular & Cellular Proteomics*, ***3***, 608-614.

[17] (a) Taylor A. (**1993**) Aminopeptidases: structure and function. *FASEB Journal*, ***7***, 290-298; (b) Matsui M, Fowler JH, Walling LL. (**2006**) Leucine aminopeptidases: diversity in structure and function. *Biological Chemistry*, ***387***, 1535-1544.

[18] (a) Cascio P, Hilton C, Kisselev AF, Rock KL, Goldberg AL. (**2001**) 26S proteasomes and immunoproteasomes produce mainly N-extended versions of an antigenic peptide. *The EMBO Journal*, ***20***, 2357-2366; (b) Saric T, Graef CI, Goldberg AL. (**2004**) Pathway for degradation of peptides generated by proteasomes: a key role for thimet oligopeptidase and other metallopeptidases. *Journal of Biological Chemistry*, ***279***, 46723-46732; (c) Neefjes J, Dantuma NP. (**2004**) Fluorescent probes for proteolysis: tools for drug discovery. *Nature Review Drug Discovery*, ***3***, 58-69.

[19] Light A. (**1972**) Leucine aminopeptidase in sequence determination of peptides. In *Methods in Enzymology*. Vol. ***25***, Hirs CHW,Timasheff SN (Ed.). Academic Press, New York, 253-262.

[20] Smith LA, Caprioli RM. (**1983**) Following enzyme catalysis in real-time inside a fast atom bombardment mass-spectrometer. *Biomedical Mass Spectrometry*, ***10***, 98-102.

[21] (a) van den Heuvel RHH, Gato S, Versluis C, Gerbaux P, Kleanthous C, Heck AJR. (**2005**) Real-time monitoring of enzymatic DNA hydrolysis by electrospray ionization mass spectrometry. *Nucleic Acids Research*, ***33***, e96; (b) Dennhart N, Letzel T. (**2006**) Mass spectrometric real-time monitoring of enzymatic glycosidic hydrolysis, enzymatic inhibition and enzyme complexes. *Analytical and Bioanalytical Chemistry*, ***386***, 689-698.

[22] Reymond JL, Fluxà VS, Maillard N. (**2009**) Enzyme assays. *Chemical Communications*, 34-46.

[23] Logsdon LA, Schardon CL, Ramalingam V, Kwee SK, Urbach AR. (**2011**) Nanomolar Binding of Peptides Containing Noncanonical Amino Acids by a Synthetic Receptor. *Journal of the American Chemical Society*, ***133***, 17087–17092.

[24] Berg JM, Tymoczko JL, Stryer L. (**2002**) Biochemistry. W. H. Freeman and Company, New York. 41-76

[25] Labouess J, Gervais M. (**1967**) Preparation of Chemically Defined ε*N*-Acetylated Trypsin. *European Journal of Biochemistry*, ***2***, 215-223.

[26] Misselwitz R, Zirwer D, Frohne M, Hanson H. (**1975**) Bovine Lens Leucine Aminopeptidase Number and State of Tryptophyl Residues. *Febs Letters*, ***55***, 233-236.

Appendix 4.4 Publications

JACS
JOURNAL OF THE AMERICAN CHEMICAL SOCIETY

ARTICLE

pubs.acs.org/JACS

Determining Protease Substrate Selectivity and Inhibition by Label-Free Supramolecular Tandem Enzyme Assays

Garima Ghale,[§] Vijayakumar Ramalingam,[†] Adam R. Urbach,*[,†] and Werner M. Nau*[,§]

[§]School of Engineering and Science, Jacobs University Bremen, Campus Ring 1, D-28759 Bremen, Germany

[†]Department of Chemistry, Trinity University, San Antonio, Texas 78218, United States

Supporting Information

ABSTRACT:

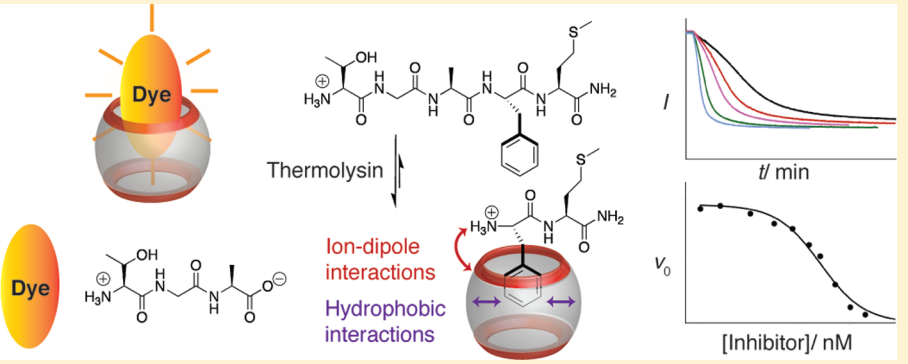

An analytical method has been developed for the continuous monitoring of protease activity on unlabeled peptides in real time by fluorescence spectroscopy. The assay is enabled by a reporter pair comprising the macrocycle cucurbit[7]uril (CB7) and the fluorescent dye acridine orange (AO). CB7 functions by selectively recognizing N-terminal phenylalanine residues as they are produced during the enzymatic cleavage of enkephalin-type peptides by the metalloendopeptidase thermolysin. The substrate peptides (e.g., Thr-Gly-Ala-Phe-Met-NH_2) bind to CB7 with moderately high affinity ($K \approx 10^4\ M^{-1}$), while their cleavage products (e.g., Phe-Met-NH_2) bind very tightly ($K > 10^6\ M^{-1}$). AO signals the reaction upon its selective displacement from the macrocycle by the high affinity product of proteolysis. The resulting supramolecular tandem enzyme assay effectively measures the kinetics of thermolysin, including the accurate determination of sequence specificity (Ser and Gly instead of Ala), stereospecificity (D-Ala instead of L-Ala), endo- versus exopeptidase activity (indicated by differences in absolute fluorescence response), and sensitivity to terminal charges ($-CONH_2$ vs $-COOH$). The capability of the tandem assay to measure protease inhibition constants was demonstrated on phosphoramidon as a known inhibitor to afford an inhibition constant of (17.8 ± 0.4) nM. This robust and label-free approach to the study of protease activity and inhibition should be transferable to other endo- and exopeptidases that afford products with N-terminal aromatic amino acids.

INTRODUCTION

As the enzymes that catalyze the hydrolytic degradation of proteins, proteases are ubiquitous in living systems and regulate a multitude of cellular processes including the cell cycle, hormone activation, angiogenesis, and apoptosis.[1−5] Aberrations in protease expression or function are therefore implicated in many pathological conditions such as cancer,[6] arthritis,[7] and Alzheimer's disease.[8] In addition, proteases play an essential role in viral replication and in the toxicity of bacteria.[9] Indeed, the potential of proteases as targets for drug development is enormous, as evidenced by the successful development of numerous therapeutics based on protease inhibition.[5]

The characterization of protease activity for the purpose of determining substrate activity and inhibitor potency is unfortunately slow and expensive. The vast majority of assays require labeled substrates,[10−17] which are costly and may not behave the same as their natural counterparts.[18] Label-free protease assays, on the other hand, rely on analytical instruments such as mass spectrometers[18] or employ synthetic/semisynthetic multifunctional pores,[19,20] which are difficult to scale up for high-throughput screening. Hence, the development of rapid and robust assays for protease activity greatly accelerates the characterization of protease targets and the discovery of drug candidates.[17,21]

This paper describes a robust and convenient approach for measuring protease kinetics using optical spectroscopy on label-free substrates and products. Our approach is based on a supramolecular tandem assay,[22−25] which incorporates an essential component of indicator-displacement assays.[26−28] Supramolecular tandem assay is a recently developed technique that

Received: February 12, 2011
Published: April 22, 2011

dx.doi.org/10.1021/ja2013467 | J. Am. Chem. Soc. 2011, 133, 7528–7535

provides real-time continuous monitoring of enzymatic activity by following a change in the concentration of substrate *or* product as it competitively displaces a fluorescent reporter dye from the cavity of a macrocyclic host. These assays therefore rely on the differential binding of the macrocycle with the fluorescent dye, the enzymatic substrate, and the corresponding product.

Supramolecular tandem assays have been implemented successfully for monitoring enzymatic transformations involving amino acids, biogenic amines, amino aldehydes, and nucleotide phosphates.[22−25] Until now, the technique was limited to substrates and products which, owing to their low molecular weight, could essentially be fully immersed in the macrocyclic host cavity, such that the entire analyte, e.g. arginine or cadaverine, served as recognition motif. Here, the utility of the tandem assay principle is transferred to peptides, which themselves are far too large to be fully included in the macrocyclic cavity. Rather, it is a *residue* of the peptide chain which complexes with differential affinity to the macrocycle in the substrate and the product. For the first time, we demonstrate the quantitative determination of absolute kinetic parameters (k_{cat}/K_M) for protease activity, the application of this analysis to the profiling of enzyme substrates for sequence selectivity, stereospecificity, and endo- vs exopeptidase activity, as well as the quantitative determination of inhibitory constants for protease inhibitors.

RESULTS AND DISCUSSION

Experimental Design. Cucurbit[7]uril (CB7, Figure 1) is a water-soluble macrocycle that has been investigated extensively in biological applications including drug delivery,[29−33] interactions with enzymes,[34,35] plasma membrane protein fishing,[36] and label-free enzyme assays.[22−25] The repeating glycoluril units produce a barrel-shaped container that has a hydrophobic cavity and negatively charged portals.[37] The latter are capable, not only for CB7 but also for its homologues, of binding inorganic cations as well as the cationic sites of organic guests, mostly ammonium groups; nonpolar groups are preferentially immersed in the inner cavity.[38−42] CB7 and its larger homologue CB8 have been shown to bind aromatic amino acids and sequence specifically to peptides and proteins containing phenylalanine (Phe), tryptophan (Trp), or tyrosine (Tyr) at the N-terminal positions.[43−47] Recognition at the N terminus is achieved via the cooperation of hydrophobic inclusion of the aromatic side chain and electrostatic stabilization of the proximal N-terminal ammonium group.

The differential binding of CB7 to an aromatic residue located at the N terminus versus other positions is exploited here in the design of an enzyme assay by choosing a protease (thermolysin) that efficiently hydrolyzes the peptide bond on the amino side of phenylalanine residues and thus generates an N-terminal phenylalanine as its product. The product binds to CB7 more tightly than the starting material and will, therefore, selectively displace a fluorescent indicator from CB7. This allows real-time monitoring of the thermolysin-mediated reaction by the pronounced change in fluorescence intensity. Thermolysin is a thermally resistant (thermophilic) enzyme produced by *Bacillus thermoproteolyticus*. It is selective for bulky, hydrophobic amino acids such as Phe and Leu,[48] and represents the family of thermolysin metalloendopeptidases as relevant therapeutic targets due to their high substrate specificity, their functional role in extracellular transformations of neuroendocrine as well as cardiovascular peptides, and in processes ranging from reproduction to cardiovascular homeostasis.[9,49,50]

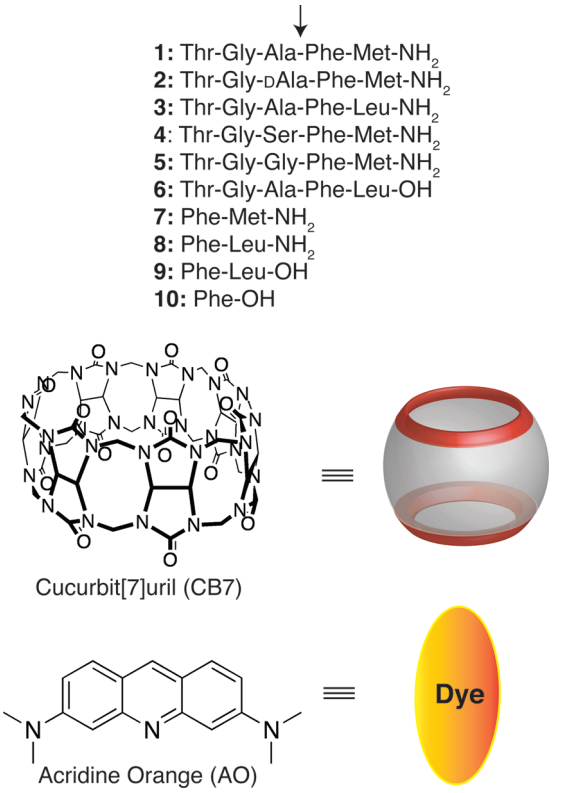

Figure 1. Amino acid sequences of the peptides used in this study; the N termini are unprotected primary amines, the C termini are designated as $-NH_2$ for a primary amide and $-OH$ for a carboxylic acid. The arrow indicates the cleavage site for thermolysin. Also shown are the chemical structures of the macrocycle and fluorescent dye constituting the employed reporter pair.

Scheme 1. CB7 Binds Selectively to N-Terminal Phe Residues Due to Cooperative Hydrophobic and Ion−Dipole Interactions

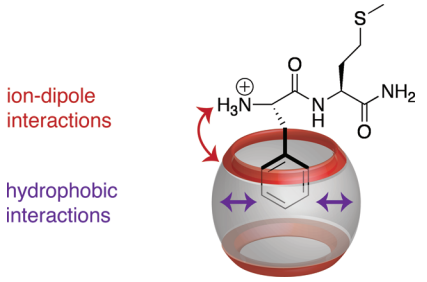

Enkephalin-based peptides were chosen as substrates to establish proof-of-principle for the protease assay. These neurological pentapeptides of sequence Tyr-Gly-Gly-Phe-Met-OH (natural amino and carboxy termini) or Tyr-Gly-Gly-Phe-Leu-OH are part of the endogenous opioid system involved in pain perception and emotional behavior, and they are implicated in the pathogenesis of Alzheimer's dementia.[51] Thermolysin hydrolyzes these peptides at the Gly-Phe peptide bond, producing Phe-Met-OH and Phe-Leu-OH products that contain an N-terminal Phe and, thus, should bind to CB7 selectively versus the substrates as well as the other peptide product fragments (Scheme 1).[52−54]

dx.doi.org/10.1021/ja2013467 |*J. Am. Chem. Soc.* 2011, 133, 7528–7535

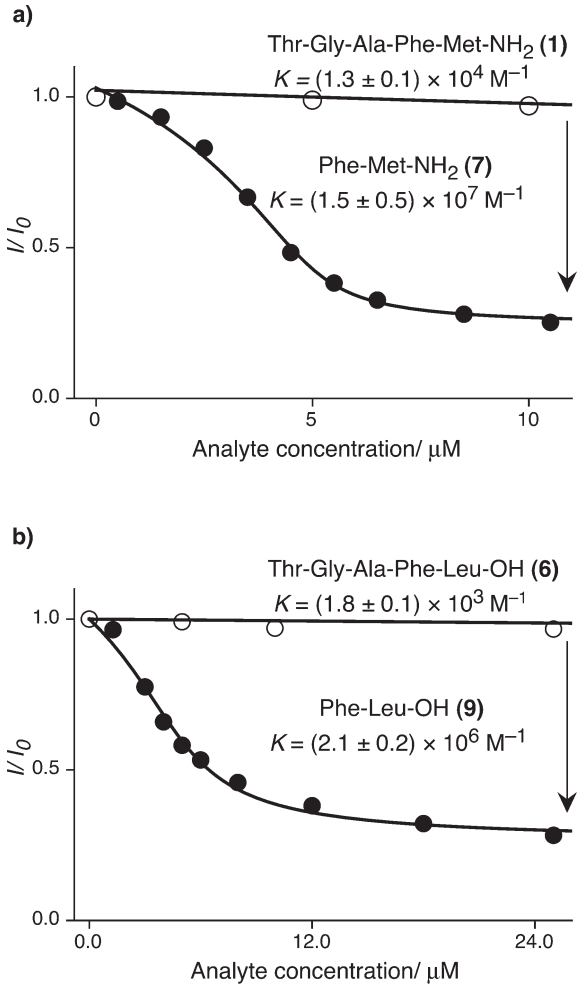

Figure 2. Fluorescence titrations (λ_{exc} = 485 nm, λ_{obs} = 510 nm) of substrates **1** and **6** and their proteolysis products (dipeptides **7** and **9**) by using competitive displacement of AO (0.5 μM) from CB7 (5 μM) in 10 mM ammonium phosphate buffer at pH 7.2, 37 °C. The titrations for the substrates are cut off for clarity, see Supporting Information for more data. I_0 and I are the fluorescence intensities in the absence and presence of competitor, respectively. The arrow indicates the expected fluorescence response in the course of the enzymatic reaction.

The choice of the fluorescent dye is critical to the design of a supramolecular tandem assay. Acridine orange (AO, Figure 1) and CB7 were selected as the "reporter pair" (i.e., the macrocycle and dye pair). AO is a weakly fluorescent dye in aqueous solution, which becomes strongly fluorescent upon encapsulation by CB7.[55] Upon the addition (or enzymatic formation) of a strongly binding analyte to the preformed CB7·AO complex, the fluorescence intensity drops again, leading to a "switch-off" fluorescence response. Important to note, the binding constant of CB7 with AO (2.9×10^5 M^{-1})[24,55] lies *in between* the binding strength of CB7 with the substrate and product of interest. This was demonstrated by simple titration experiments (Figure 2 and Supporting Information), from which the binding constants of peptides **1**−**9** were determined (Table 1). Peptides **1**−**6**, the candidates to potentially act as substrates for thermolysin, have invariably a low binding affinity to CB7, accounted by the presence of only hydrophobic interaction between the amino acid Phe and the host cavity. However, the corresponding proteolytic products (dipeptides **7**−**9**) have 3 orders of magnitude higher affinity for

Table 1. Binding Constants (K) of Peptides 1−9, Phenylalanine 10, and Phosphoramidon 11 with CB7 and Proteolytic Constants (k_{cat}/K_M) for Their Reaction with Thermolysin

entry	peptide sequence	K (10^4 M^{-1})[a]	k_{cat}/K_M (10^4 s^{-1} M^{-1})[b]
1	Thr-Gly-Ala-Phe-Met-NH_2	1.3	14
2	Thr-Gly-D-Ala-Phe-Met-NH_2	2.6	≤0.005[c]
3	Thr-Gly-Ala-Phe-Leu-NH_2	0.35	3.2 [7.0][d]
4	Thr-Gly-Ser-Phe-Met-NH_2	1.9	6.9
5	Thr-Gly-Gly-Phe-Met-NH_2	1.4	1.2
6	Thr-Gly-Ala-Phe-Leu-OH	0.18	2.3
7	Phe-Met-NH_2	1500 ± 500	*e*
8	Phe-Leu-NH_2	2700 ± 1500	*e*
9	Phe-Leu-OH	210	*e*
10	Phe-OH	2.0 [2.5] [f]	*e*
11	Phosphoramidon	0.12	*g*

[a] Determined by competitive fluorescence titrations, *cf.* Figure 2 and Supporting Information; 15% error unless explicitly stated. [b] Determined by supramolecular tandem assay at varying peptide concentrations (5−55 μM, n = 5−6), *cf.* Figure 3; kinetic parameters were determined by nonlinear regression (see Supporting Information); 20% estimated error. [c] Insignificant hydrolysis due to the presence of D-Ala. [d] Value in square brackets refers to exopeptidase activity, see text and Supporting Information. [e] No conversion detected due to Phe N terminus. [f] Value in square brackets in 0.1 M NaCl solution.[56] [g] Phosphoramidon was employed as inhibitor, cf. Figure 5.

CB7 due to the additional electrostatic interaction between the N-terminal ammonium group of Phe with the CB7 carbonyls. This high affinity disappears again for the simple amino acid Phe (**10**), for which the adjacent C-terminal carboxylate group entirely offsets the stabilizing interaction by the ammonium group. Note that the binding affinity of CB7 between the peptides **1** and **2** is slightly different. Nevertheless, it is not surprising due to the diastereomeric differentiation between L- and D-Ala by the achiral host CB7.[56]

When compared to highly selective antibodies, the molecular recognition of peptides by CB7 must be considered as rather unspecific. The synthetic macrocyclic host binds to all pentapeptides **1**-**6** with very similar affinity, and even the binding constant of the amino acid Phe (**10**) falls in the same range (Table 1). CB7 shows also little selectivity toward the dipeptides **7**−**9**. However, it *differentiates* the dipeptides **7**−**9** reliably from the pentapeptides **1**−**6**, and this substrate/product differentiation is sufficient to set up robust enzyme assays. When thermolysin is added to the peptide solution containing an enkephalin-based substrate and the CB7/AO reporter pair (Scheme 2), the enzymatic product, containing an N-terminal phenylalanine residue, should rapidly (relative to the enzymatic transformation itself) and competitively displace the AO dye from the CB7 cavity, thus yielding a decrease in fluorescence intensity that reports the protease activity continuously and in real time. The immediate response is due to the fast rates for the formation and dissociation of the supramolecular assemblies which, as previously discussed, constitutes an advantage of using macrocycles instead of antibodies.[24] As can be further seen from the actual titration plots (Figure 2), even working at relatively low substrate concentrations of 5−20 μM should produce a readily detectable change in fluorescence response upon conversion of a substrate to a product. This working concentration range is exactly desirable in protease assays, including those employed in high-throughput screening for pharmaceutical investigations.[14−17]

Enzyme Assays. To establish proof of principle for the use of a supramolecular tandem assay to monitor protease activity on unlabeled peptides, we first investigated a series of enkephalin-based peptides (Figure 1) with the sequences Thr-Gly-Ala-Phe-Met-NH_2 (**1**), Thr-Gly-D-Ala-Phe-Leu-NH_2 (**2**), Thr-Gly-Ala-Phe-Leu-NH_2 (**3**), as well as the dipeptide product from proteolysis of enkephalin **1**, Phe-Met-NH_2 (**7**).

As depicted in Figure 3a, peptides **1** and **3** were hydrolyzed rapidly, but peptide **2** showed insignificant hydrolysis. The stark contrast in the rate of cleavage at the Ala-Phe bond for peptides **1** and **2** was due to the substitution of L-Ala by its enantiomer.

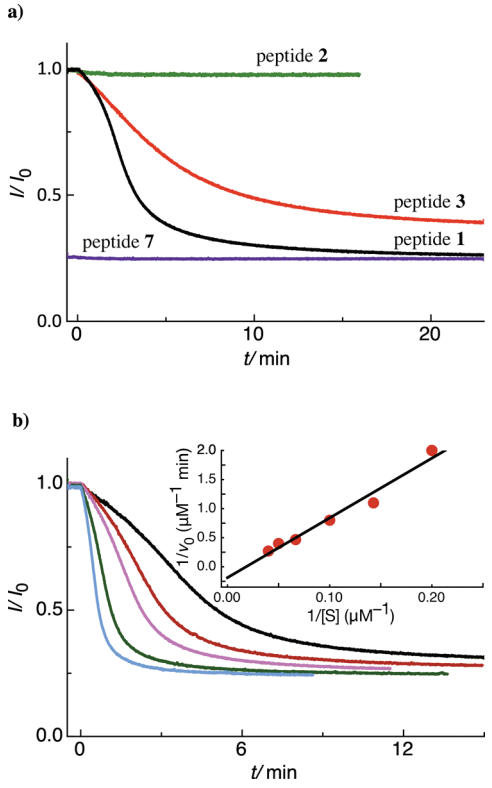

Figure 3. (a) Continuous fluorescence assays (λ_{exc} = 485 nm, λ_{obs} = 510 nm) with the CB7/AO reporter pair (8 μM/ 0.5 μM) upon addition of thermolysin (t = 0 min, 15 nM) to peptides **1**−**3** and **7** (30 μM), at 37 °C. (b) Determination of enzyme kinetic parameters by monitoring of thermolysin (15 nM) activity with varying concentration of enkephalin **1** (5−25 μM) in 10 mM ammonium phosphate buffer, pH 7.2, at 37 °C with the CB7/AO reporter pair (2.5 μM/0.5 μM). I_0 and I are the fluorescence intensities at time t = 0 and time t, respectively.

The tandem assay thus reflects the previously established substrate selectivity of thermolysin, including the remarkable stereospecificity of the P1 position.[48,57−60] As can be also seen from Figure 3a, the dipeptide **7** shows no fluorescence response. This signifies that the peptide bond between Phe and Met in this peptide is not cleaved by thermolysin (exopeptidase activity, see below). If it were cleaved, an increase in fluorescence would have been observed, because the product (free Phe, **10**) would again constitute a weak competitor (see binding constants in Table 1). Again, it was known that substrates lacking a peptide bond N-terminal to Phe (such as **7**) are not digested by thermolysin,[53] such that our result established a negative control experiment.

Substrate Selectivity. Given the high sensitivity of the tandem assay observed in the initial experiments, we decided to measure the kinetic behavior of thermolysin for substrates with varying amino acids at the P_1 position. With peptides **1** and **3** as parent compounds, the P_1 mutations of Ala to Ser (peptide **4**) and Ala to Gly (peptide **5**) examined the effects of adding a hydroxyl group to the β carbon, or removing the β carbon, respectively. Peptide **6** is an analogue of **3** with a carboxylate at the C terminus, which was designed to test the effect of C-terminal charge.

The enzyme-kinetic analysis required the determination of initial rates of reaction. For this purpose, the observed fluorescence decay needed to be related to changes in absolute concentration.[25] This relationship was achieved by recording the fluorescence response obtained by addition of a known quantity of an authentic sample of reaction product (see Supporting Information). Analysis of the initial reaction rates at varying substrate concentrations (Figure 3b) yielded the characteristic proteolytic constants (k_{cat}/K_M) for the different peptide sequences (inset of Figure 3b and Table 1).[61]

Note that our tandem assays allow kinetic measurements for unlabeled peptides, while previous assays were carried out with peptides carrying fluorescent labels such as 2-naphthylamide (2NA)[62] or dansyl.[63] The structural differences prevent a direct comparison of the absolute proteolytic constants. Nevertheless, peptides **1** ($k_{cat}/K_M = 14 \times 10^4$ M^{-1} s^{-1}) and **5** (1.2×10^4 M^{-1} s^{-1}) showed the same order of magnitude as well as the same trends of substrate selectivity as did the labeled derivatives Glt-Gly-Ala-Phe-2NA (5.2×10^4 M^{-1} s^{-1}) and Glt-Gly-Gly-Phe-2NA (0.15×10^4 M^{-1} s^{-1}),[62] which was gratifying to observe.

The data in Table 1 show that the identity of the amino acid residue at the P_1 position significantly affects the proteolytic coefficients of thermolysin activity. The values are moderately reduced for the peptides containing glycine and serine at P_1 compared to their parent compound **1** with alanine at the P1 position. The binding of the substrate at P_1 is governed by hydrophobic interactions, which accounts for the fact that, at P_1,

Scheme 2. Product-Selective Fluorescence Switch-Off Tandem Assay Using CB7 and AO as Reporter Pair[a]

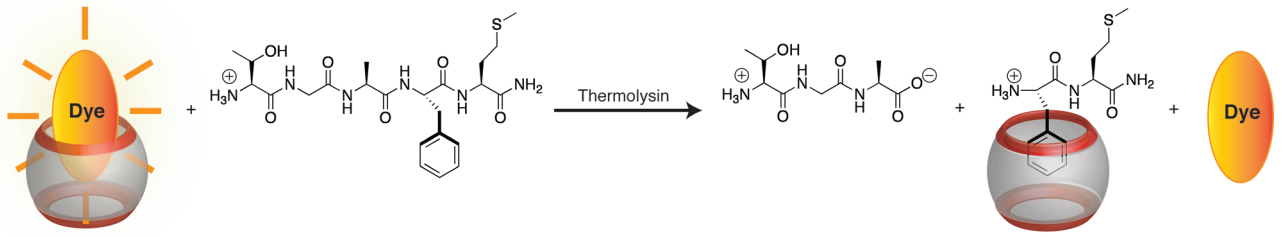

[a] It should be noted that the dye, substrate, and product are in rapid dynamic competitive equilibrium for encapsulation within the CB7 macrocycle.

dx.doi.org/10.1021/ja2013467 |J. Am. Chem. Soc. 2011, 133, 7528–7535

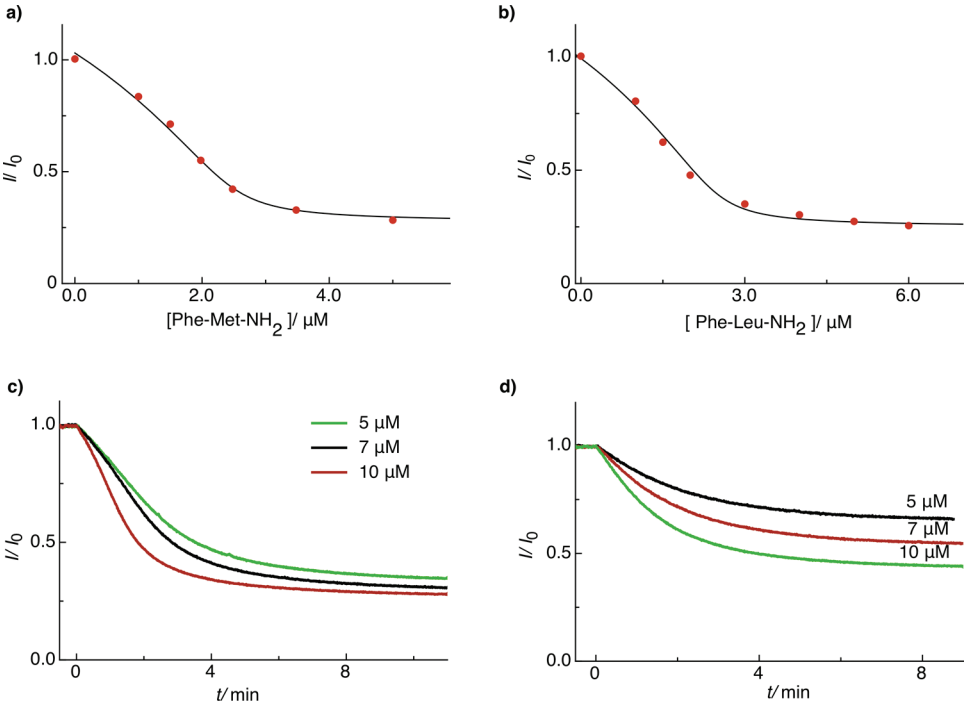

Figure 4. Fluorescence measurements using CB7/AO (2.5 μM CB7 and 0.5 μM AO, λ_{exc} = 485 nm, λ_{obs} = 510 nm) as a reporter pair in 10 mM ammonium phosphate buffer, pH 7.2, at 37 °C. Competitive fluorescence titration plots of (a) Phe-Met-NH_2 (**7**) and (b) Phe-Leu-NH_2 (**8**). Tandem protease assays for thermolysin (15 nM) with substrates (c) Thr-Gly-Ala-Phe-Met-NH_2 (**1**) and (d) Thr-Gly-Ala-Phe-Leu-NH_2 (**3**).

Gly, and Ser are cleaved more slowly than Ala.[62,64,65] The use of a carboxylate group leads to a slight reduction in enzymatic activity, as indicated by the k_{cat}/K_M value, presumably due to the known sensitivity of thermolysin toward adjacent charges (see the following section; note that most model substrates were amidated at the C terminus for the convenience of peptide synthesis).

Exo- and Endopeptidase Behavior. During the determination of the k_{cat}/K_M values for the peptides described above, we stumbled on the unexpected exopeptidase behavior of thermolysin that was specific to the substrate, Thr-Gly-Ala-Phe-Leu-NH_2 (**3**). The *expected* endopeptidase products of the cleavage of substrates Thr-Gly-Ala-Phe-Met-NH_2 (**1**) and Thr-Gly-Ala-Phe-Leu-NH_2 (**3**) are Phe-Met-NH_2 (**7**) and Phe-Leu-NH_2 (**8**), respectively. These products bind tightly to CB7 and are therefore responsible for the change in fluorescence intensity during the tandem assay. Therefore, the final steady-state fluorescence response (i.e., after quantitative enzymatic digestion of substrates **1** and **3**) was expected to be similar to the fluorescence response brought about by the same concentrations of their endopeptidase products **7** and **8**. This similarity was observed for substrate **1** but not for substrate **3**.

In detail, the enzymatic hydrolysis of 5 μM of the substrate Thr-Gly-Ala-Phe-Met-NH_2 (**1**) resulted in complete displacement of the dye from CB7, as observed by the similarity of the steady-state fluorescence response after complete enzymatic conversion and the response of the same concentration of Phe-Met-NH_2 (Figure 4a,c). In the case of the substrate Thr-Gly-Ala-Phe-Leu-NH_2 (**3**), however, the final steady-state fluorescence response upon enzymatic hydrolysis of 5 μM substrate was less than that of its endopeptidase product Phe-Leu-NH_2 (**8**) at the same concentration (see Figure 4b,d). In fact, even a concentration of 10 μM of substrate **3** was insufficient to produce the same fluorescence response as that produced by 5 μM of **8**. We concluded that the expected product was not quantitatively formed. To account for this result, and inspired by previous experimental observations,[48,66,67] we suspected the possibility of *exo*peptidase activity, i.e., enzymatic cleavage of the Phe-Leu peptide bond. We were exactly able to corroborate this unusual pathway for peptide **3** by mass spectrometry (see Supporting Information).

The observed exopeptidase cleavage leads to the formation of Thr-Gly-Ala-Phe-OH as (another) product, one that is not further converted by thermolysin. Therefore, the yield of the expected endopeptidase product (**8**) and the corresponding change in fluorescence response upon the displacement of AO by **8** fall below expectation. In fact, the incomplete conversion, signaled by the plateau being reached at higher fluorescence intensities, can be used to assess the ratio of exo- versus endopeptidase cleavage (2.2:1) which, with the endopeptidase kinetics being directly accessible (Figure 4 and Supporting Information), allows the projection of both rates. This analysis affords a k_{cat}/K_M value of 3.2×10^4 M^{-1} s^{-1} for the endopeptidase activity and a value of 7.0×10^4 M^{-1} s^{-1} for the exopeptidase activity. The higher proteolytic constant for the hydrolysis of the Phe-Leu *exo* bond (i.e., Leu at P1′ position) compared to the hydrolysis of the Ala-Phe *endo* bond (i.e., Phe at P1′) is consistent with the enzyme's preference for hydrophobic P1′ residues, whereby increasing the hydrophobic residue from Leu to Phe increases the interaction of the substrate with the active site of the enzyme, while decreasing the catalytic efficiency,[60,68,69] thereby accounting for the observed lower k_{cat}/K_M value for the *endo* cleavage.

It is interesting that we observed no exopeptidase activity for the nonamidated peptide Thr-Gly-Ala-Phe-Leu-OH (**6**), as confirmed by the plateau region of the fluorescence trace as well as by mass spectrometry (see Supporting Information).

dx.doi.org/10.1021/ja2013467 |*J. Am. Chem. Soc.* 2011, 133, 7528–7535

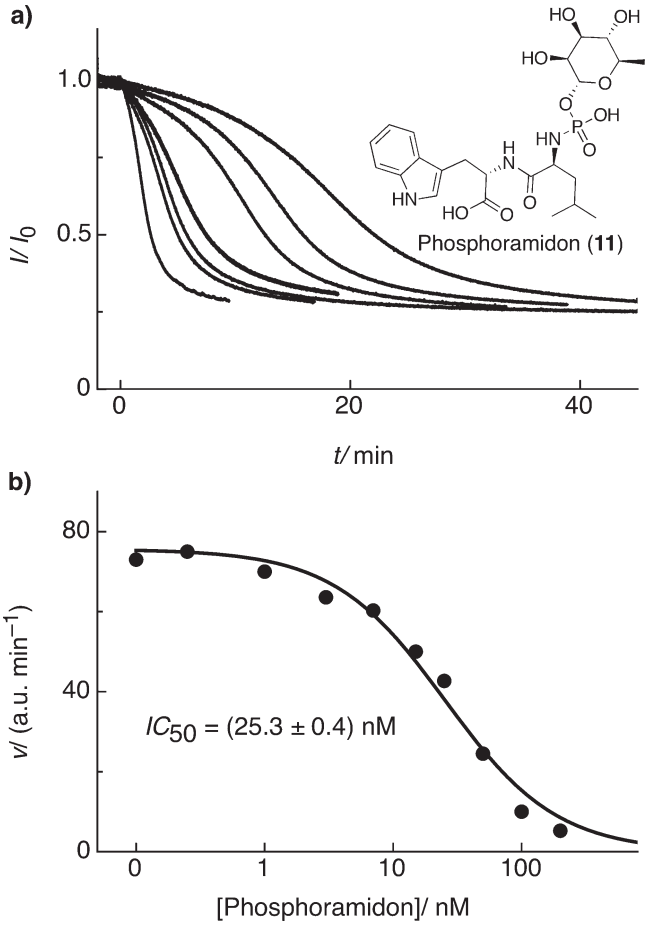

Figure 5. Determination of thermolysin (15 nM) inhibition by phosphoramidon (**11**, 0−100 nM) in the presence of 10 μM Thr-Gly-Ala-Phe-Met-NH_2 (**1**) by using the CB7/AO (0.5 μM/2.5 μM) reporter pair in 10 mM ammonium phosphate, pH 7.2, at 37 °C. (a) Continuous fluorescence traces (λ_{exc} = 485 nm, λ_{obs} = 510 nm) upon addition of 10 μM Thr-Gly-Ala-Phe-Met-NH_2 (**1**) for the determination of the initial rates. (b) Corresponding dose−response curve for inhibition of thermolysin by phosphoramidon (**11**).

This result reveals that the C-terminal charge of the peptide directs endo- versus exopeptidase activity, at least for substrates containing bulky hydrophobic residues (Phe and Leu) at the P_1' position. Conversely, a comparison of substrate **3** (exopeptidase cleavage observed) with its product **8**, for which no conversion by themolysin is observed (Figure 3a and Supporting Information), further exposes that an N-terminal charge directed at phenylalanine suppresses the exopeptidase activity of thermolysin. This observed sensitivity of thermolysin toward adjacent charges supports prior claims based on studies performed by alternative assays with labeled substrates.[48,66,67]

As can be seen from these studies, our label-free protease tandem assay provides information not only on the enzymatic activity, kinetics, and substrate selectivity but also on the chemoselectivity of the proteolytic cleavage, because the plateau region after quantitative conversion is a signature for the identity of the expected product and thus enables direct quantification of the extent of the expected reaction.

Protease Inhibition. Having established the capability of the assay to effectively measure the kinetics of thermolysin activity, we sought to apply the assay to the determination of enzyme inhibition, which is critical to the evaluation of drug candidates. Using Thr-Gly-Ala-Phe-Met-NH_2 (**1**) as the model substrate, inhibition studies for thermolysin were carried out using the product-selective tandem assay principle and the inhibitor phosphoramidon (**11**), a naturally occurring, potent inhibitor of thermolysin.[70−73] Inhibitors can hypothetically interfere with the assay principle by binding to the macrocycle.[24] Fortunately, this can be readily tested by competitive titrations, which afforded a low binding constant for **11** (1200 M^{-1}, Table 1). In the concentration range relevant for studies with potent inhibitors (up to 100 nM), binding of **11** to CB7 (<0.3%) can therefore be safely neglected.

We observed that, as is typical for competitive inhibitors, increasing the concentration of **11** decreases the *rate* of thermolysin hydrolysis via dynamic competition with the substrate for binding to the enzyme, and yet allows the irreversible peptidase reaction on the enzyme·substrate complex to proceed to completion, as observed by similar final steady-state fluorescence intensities at all concentrations of inhibitor (Figure 5a). The change in initial rates of decrease in fluorescence intensity was used to calculate a K_i value of (17.8 ± 0.4) nM,[74] which falls right into the reported range (3.5−60 nM), all determined under slightly varying experimental conditions and with different assay methods employing fluorescently labeled substrates.[70,71,75]

CONCLUSIONS

The addition of macrocyclic host molecules in combination with fluorescent dyes establishes a label-free method for the real-time, continuous monitoring of protease activity by fluorescence spectroscopy. Protease assays using unmodified substrates are important because they enable the detailed characterization of the natural substrate selectivity of a target protease as well as its activity in the presence of inhibitors. We have successfully applied the tandem assay principle to the continuous monitoring of the hydrolysis of enkephalin-based peptides by thermolysin. In doing so, we have established proof-of-principle for the use of cucurbituril-based fluorescent reporter pairs for proteases. The general selectivity of macrocycles (even if moderate in comparison to specific receptors) renders potentially broad transferability of this assay to other exo- and endopeptidases. Furthermore, for the first time, we have extended the applicability of tandem assays toward an in-depth profiling of enzyme activity for a wide range of substrates and toward sensing enzyme substrate stereospecificity, and have demonstrated the potential of this assay for the screening of inhibitors. These applications of tandem assays to monitor proteolytic activity have significant implications for drug design, as well as medical diagnostics, where proteases are important disease markers.

EXPERIMENTAL SECTION

Materials. Peptides **1**−**8** were synthesized by standard Fmoc solid-phase synthesis protocols on Rink amide MBHA resin (for C-terminal amides) or Wang acid resin (for peptide **6** containing a C-terminal carboxylic acid) and purified by reversed phase HPLC. Purity was verified by reversed phase analytical HPLC and ^{1}H NMR spectroscopy. Identity was verified by electrospray mass spectrometry.

Peptide Phe-Leu-OH (**9**) and amino acid Phe-OH (**10**) were used as received from Bachem and Applichem, respectively. Cucurbit[7]uril (CB7) was synthesized according to the literature.[76−78] Acridine orange

dx.doi.org/10.1021/ja2013467 |J. Am. Chem. Soc. 2011, 133, 7528–7535

(AO), thermolysin (lyophilized powder, 36.5 U/mg), and phosphoramidone (**11**) were used as received from Sigma-Aldrich.

Methods. Absorbance measurements were performed with a Varian Cary 4000 spectrophotometer. The concentrations of peptides **1**−**10** were determined assuming the extinction coefficient of free phenylalanine (**10**) at 257 nm, $\varepsilon_{257} = 195\ M^{-1}\ cm^{-1}$.[79] For thermolysin and phosphoramidon, $\varepsilon_{280} = 61100\ M^{-1}cm^{-1}$ and $\varepsilon_{280} = 5500\ M^{-1}\ cm^{-1}$, respectively, were used.[63,71] A Varian Eclipse spectrofluorimeter was used for steady-state fluorescence measurements and for the enzyme assays.

Continuous assays were performed with 0−55 μM peptide, 2.5 μM CB7, and 0.5 μM AO (λ_{exc} = 485 nm, λ_{obs} = 510 nm) in 10 mM ammonium buffer, pH 7.2, in a variable-temperature cell holder at 37.0 ± 0.1 °C, and the reaction was initiated by addition of thermolysin (15 nM). For the inhibition studies, the mixture of thermolysin (10 nM) and phosphoramidon (0−100 nM) was preincubated for 15 min at 37.0 ± 0.1 °C in the presence of the reporter pair, and the reaction was initiated by addition of 10 μM Thr-Gly-Ala-Phe-Met-NH_2 (**1**).

■ ASSOCIATED CONTENT

Supporting Information. Fluorescence titration plots of peptide substrates, details on the calculations of the enzymatic reaction rates, mass spectra, and supporting evidence for the exopeptidase activity. This material is available free of charge via the Internet at http://pubs.acs.org.

■ AUTHOR INFORMATION

Corresponding Author
w.nau@jacobs-university.de; aurbach@trinity.edu

■ ACKNOWLEDGMENT

Financial support from the Deutsche Forschungsgemeinschaft (DFG Grant NA-686/5-1, G.G. and W.M.N.), Fonds der Chemischen Industrie (W.M.N.), COST Action CM1005 "Supramolecular Chemistry in Water" (W.M.N.), National Science Foundation (CHE-0748483, V.R. and A.R.U.), and Welch Foundation (W-1640, A.R.U.) is gratefully acknowledged. G.G. thanks Prof. Dr. Nikolai Kuhnert and Ms. Anja Müller for help with the mass-spectrometric measurements. A.R.U. thanks Anita Chaudhari for preliminary contributions.

■ REFERENCES

(1) Carmeliet, P. *Nat. Med.* **2003**, *9*, 653–660.
(2) Koblinski, J. E.; Ahram, M.; Sloane, B. F. *Clin. Chim. Acta* **2000**, *291*, 113–135.
(3) Patel, T.; Gores, G. J.; Kaufmann, S. H. *FASEB J.* **1996**, *10*, 587–597.
(4) Puente, X. S.; Sanchez, L. M.; Overall, C. M.; Lopez-Otin, C. *Nat. Rev. Genet.* **2003**, *4*, 544–558.
(5) Turk, B. *Nat. Rev. Drug Discovery* **2006**, *5*, 785–799.
(6) Egeblad, M.; Werb, Z. *Nat. Rev. Cancer* **2002**, *2*, 161–174.
(7) Krane, S. M. *Arthritis Res. Ther.* **2003**, *5*, 2–4.
(8) Esler, W. P.; Wolfe, M. S. *Science* **2001**, *293*, 1449–1454.
(9) Adekoya, O. A.; Sylte, I. *Chem. Biol. Drug Des.* **2009**, *73*, 7–16.
(10) Goddard, J. P.; Reymond, J. L. *Curr. Opin. Biotechnol.* **2004**, *15*, 314–322.
(11) Goddard, J. P.; Reymond, J. L. *Trends Biotechnol.* **2004**, *22*, 363–370.
(12) Reymond, J. L.; Fluxa, V. S.; Maillard, N. *Chem. Commun.* **2009**, 34–46.
(13) Sittampalam, G. S.; Kahl, S. D.; Janzen, W. P. *Curr. Opin. Chem. Biol.* **1997**, *1*, 384–391.
(14) Hennig, A.; Roth, D.; Enderle, T.; Nau, W. M. *ChemBioChem* **2006**, *7*, 733–737.
(15) Hennig, A.; Florea, M.; Roth, D.; Enderle, T.; Nau, W. M. *Anal. Biochem.* **2007**, *360*, 255–265.
(16) Marguerre, A. K.; Kramer, R. *Bioorg. Med. Chem. Lett.* **2009**, *19*, 5757–5759.
(17) Yongzheng, Y.; Reymond, J. L. *Mol. BioSyst.* **2005**, *1*, 57–63.
(18) Su, J.; Rajapaksha, T. W.; Peter, M. E.; Mrksich, M. *Anal. Chem.* **2006**, *78*, 4945–4951.
(19) Macrae, M. X.; Blake, S.; Jiang, X. Y.; Capone, R.; Estes, D. J.; Mayer, M.; Yang, J. *ACS Nano* **2009**, *3*, 3567–3580.
(20) Sorde, N.; Das, G.; Matile, S. *Proc. Natl. Acad. Sci. U.S.A.* **2003**, *100*, 11964–11969.
(21) Pogson, M.; Georgiou, G.; Iverson, B. L. *Curr. Opin. Biotechnol.* **2009**, *20*, 390–397.
(22) Hennig, A.; Bakirci, H.; Nau, W. M. *Nat. Methods* **2007**, *4*, 629–632.
(23) Bailey, D. M.; Hennig, A.; Uzunova, V. D.; Nau, W. M. *Chem.—Eur. J.* **2008**, *14*, 6069–6077.
(24) Nau, W. M.; Ghale, G.; Hennig, A.; Bakirci, H.; Bailey, D. M. *J. Am. Chem. Soc.* **2009**, *131*, 11558–11570.
(25) Florea, M.; Nau, W. M. *Org. Biomol. Chem.* **2010**, *8*, 1033–1039.
(26) Niikura, K.; Bisson, A. P.; Anslyn, E. V. *J. Chem. Soc., Perkin Trans. 2* **1999**, 1111–1114.
(27) Nguyen, B. T.; Wiskur, S. L.; Anslyn, E. V. *Org. Lett.* **2004**, *6*, 2499–2501.
(28) Zhang, T. Z.; Anslyn, E. V. *Org. Lett.* **2007**, *9*, 1627–1629.
(29) Kemp, S.; Wheate, N. J.; Wang, S.; Collins, J. G.; Ralph, S. F.; Day, A. I.; Higgins, V. J.; Aldrich-Wright, J. R. *J. Biol. Inorg. Chem.* **2007**, *12*, 969–979.
(30) Saleh, N.; Koner, A. L.; Nau, W. M. *Angew. Chem., Int. Ed.* **2008**, *47*, 5398–5401.
(31) Kim, C.; Agasti, S. S.; Zhu, Z.; Isaacs, L.; Rotello, V. M. *Nature Chem.* **2010**, *2*, 962–966.
(32) Wyman, I. W.; Macartney, D. H. *Org. Biomol. Chem.* **2010**, *8*, 247–252.
(33) Koner, A. L.; Ghosh, I.; Saleh, N.; Nau, W. M. *Can. J. Chem.* **2011**, *89*, 139–147.
(34) Ghosh, S.; Isaacs, L. *J. Am. Chem. Soc.* **2010**, *132*, 4445–4454.
(35) Hennig, A.; Ghale, G.; Nau, W. M. *Chem. Commun.* **2007**, 1614–1616.
(36) Lee, D.-W.; Park, K. M.; Banerjee, M.; Ha, S. H.; Lee, T.; Suh, K.; Paul, S.; Jung, H.; Kim, J.; Selvapalam, N.; Ryu, S. H.; Kim, K. *Nature Chem.* **2011**, *3*, 154–159.
(37) Lagona, J.; Mukhopadhyay, P.; Chakrabarti, S.; Isaacs, L. *Angew. Chem., Int. Ed.* **2005**, *44*, 4844–4870.
(38) Buschmann, H. J.; Cleve, E.; Schollmeyer, E. *Inorg. Chim. Acta* **1992**, *193*, 93–97.
(39) Buschmann, H. J.; Cleve, E.; Jansen, K.; Wego, A.; Schollmeyer, E. *J. Inclusion Phenom. Macrocyclic Chem.* **2001**, *40*, 117–120.
(40) Isaacs, L. *Chem. Commun.* **2009**, 619–629.
(41) Jeon, W. S.; Moon, K.; Park, S. H.; Chun, H.; Ko, Y. H.; Lee, J. Y.; Lee, E. S.; Samal, S.; Selvapalam, N.; Rekharsky, M. V.; Sindelar, V.; Sobransingh, D.; Inoue, Y.; Kaifer, A. E.; Kim, K. *J. Am. Chem. Soc.* **2005**, *127*, 12984–12989.
(42) Marquez, C.; Hudgins, R. R.; Nau, W. M. *J. Am. Chem. Soc.* **2004**, *126*, 5806–5816.
(43) Bush, M. E.; Bouley, N. D.; Urbach, A. R. *J. Am. Chem. Soc.* **2005**, *127*, 14511–14517.
(44) Heitmann, L. M.; Taylor, A. B.; Hart, P. J.; Urbach, A. R. *J. Am. Chem. Soc.* **2006**, *128*, 12574–12581.
(45) Rekharsky, M. V.; Yamamura, H.; Ko, Y. H.; Selvapalam, N.; Kim, K.; Inoue, Y. *Chem. Commun.* **2008**, 2236–2238.
(46) Nguyen, H. D.; Dang, D. T.; van Dongen, J. L. J.; Brunsveld, L. *Angew. Chem., Int. Ed.* **2010**, *49*, 895–898.
(47) Chinai, J. M.; Taylor, A. B.; Ryno, L. M.; Hargreaves, N. D.; Morris, C. A.; Hart, P. J.; Urbach, A. R. *J. Am. Chem. Soc.* **2011** ASAP article.

(48) Matsubara, H. *Biochem. Biophys. Res. Commun.* **1966**, *24*, 427–430.
(49) Shrimpton, C. N.; Smith, A. I.; Lew, R. A. *Endocr. Rev.* **2002**, *23*, 647–664.
(50) Turner, A. J.; Isaac, R. E.; Coates, D. *BioEssays* **2001**, *23*, 261–269.
(51) Meilandt, W. J.; Yu, G. Q.; Chin, J.; Roberson, E. D.; Palop, J. J.; Wu, T.; Scearce-Levie, K.; Mucke, L. *J. Neurosci.* **2008**, *28*, 5007–5017.
(52) Antonczak, S.; Monard, G.; Lopez, M. R.; Rivail, J. L. *J. Mol. Model.* **2000**, *6*, 527–538.
(53) Malfroy, B.; Schwartz, J. C. *Biochem. Biophys. Res. Commun.* **1985**, *130*, 372–378.
(54) Rush, R. S.; Mitas, M.; Powers, J. C.; Tanaka, T.; Hersh, L. B. *Arch. Biochem. Biophys.* **1984**, *231*, 390–399.
(55) Shaikh, M.; Mohanty, J.; Singh, P. K.; Nau, W. M.; Pal, H. *Photochem. Photobiol. Sci.* **2008**, *7*, 408–414.
(56) Rekharsky, M. V.; Yamamura, H.; Inoue, C.; Kawai, M.; Osaka, I.; Arakawa, R.; Shiba, K.; Sato, A.; Ko, Y. H.; Selvapalam, N.; Kim, K.; Inoue, Y. *J. Am. Chem. Soc.* **2006**, *128*, 14871–14880.
(57) The substrate specificity of proteases is denoted using the Schechter and Berger nomenclature. The amino acids in peptide substrates are labeled as H-P_X...P_2-P_1-P_1'-P_2'...P_X'-OH where P_1 is the position of an amino acid at the N terminus of the cleavage site and P_1' is the position of an amino acid at the C terminus of the cleavage site.
(58) Schechter, I.; Berger, A. *Biochem. Biophys. Res. Commun.* **1967**, *27*, 157–162.
(59) Abramowi, N.; Schechter, I.; Berger, A. *Biochem. Biophys. Res. Commun.* **1967**, *29*, 862–867.
(60) Morihara, K.; Tsuzuki, H. *Eur. J. Biochem.* **1970**, *15*, 374–380.
(61) Under physiological conditions with very low substrate concentration, the k_{cat}/K_M value provides a direct measure for the catalytic efficacy and is therefore commonly employed to scale the substrate specificity of an enzyme. At $[S] \ll K_M$, most of the active sites are unoccupied, that is, the concentration of free enzyme, [E], is approximately equal to the total concentration of enzyme, $[E]_0$. The Michaelis–Menten equation then simplifies to $v_0 = k_{cat}/K_M \times [S] \times [E]_0$, and k_{cat}/K_M becomes the apparent bimolecular rate constant for the interaction between the substrate and the enzyme, *cf.* Berg, J. M.; Tymoczko, J. L.; Stryer, L. *Biochemistry*; 5th ed.; W. H. Freeman and Company: New York, 2002. Hennig, A.; Florea, M.; Roth, D.; Enderle, T.; Nau, W. M. *Anal. Biochem.* **2007**, *360*, 255–265. Koshland, D. E. *Bioorg. Chem.* **2002**, *30*, 211–213.
(62) Pozsgay, M.; Michaud, C.; Liebman, M.; Orlowski, M. *Biochemistry* **1986**, *25*, 1292–1299.
(63) Yang, J. J.; Vanwart, H. E. *Biochemistry* **1994**, *33*, 6508–6515.
(64) Hersh, L. B.; Morihara, K. *J. Biol. Chem.* **1986**, *261*, 6433–6437.
(65) Oda, K.; Takahashi, T.; Takada, K.; Tsunemi, M.; Ng, K. K. S.; Hiraga, K.; Harada, S. *FEBS Lett.* **2005**, *579*, 5013–5018.
(66) Ligne, T.; Pauthe, E.; Monti, J. P.; Gacel, G.; Larreta-Garde, V. *BBA-Protein Struct. M.* **1997**, *1337*, 143–148.
(67) Pauthe, E.; Dauchez, M.; Berry, H.; Berjot, M.; Monti, J.-P.; Alix, A. J. P.; Larreta-Garde, V. R. *Ann. N.Y. Acad. Sci.* **1998**, *864*, 458–462.
(68) de Kreij, A.; van den Burg, B.; Veltman, O. R.; Vriend, G.; Venema, G.; Eijsink, V. G. H. *Eur. J. Biochem.* **2001**, *268*, 4985–4991.
(69) Inouye, K.; Yasukawa, K. *BBA-Proteins Proteom.* **2007**, *1774*, 1281–1288.
(70) Inouye, K.; Kuzuya, K.; Tonomura, B. *J. Biochem.* **1994**, *116*, 530–535.
(71) Kitagishi, K.; Hiromi, K. *J. Biochem.* **1984**, *95*, 529–534.
(72) Komiyama, T.; Suda, H.; Aoyagi, T.; Takeuchi, T.; Umezawa, H. *Arch. Biochem. Biophys.* **1975**, *171*, 727–731.
(73) Tronrud, D. E.; Monzingo, A. F.; Matthews, B. W. *Eur. J. Biochem.* **1986**, *157*, 261–268.
(74) The equation $K_i = (IC_{50} - 0.5 \times [E]_0)/(1 + ([S]/K_M))$ was used for conditions of tight stoichiometric competitive inhibition for a monosubstrate reaction, with IC_{50} determined from the dose–response curve in Figure 5b and $[S]/K_M \approx 0$, due to $[S] \ll K_M$ (K_M = 108 mM for peptide **1**), *cf.* Copeland, R. A.; Lombardo, D.; Giannaras, J.; Decicco, C. P. *Bioorg. Med. Chem. Lett.* **1995**, *5*, 1947–1952.
(75) Marie Claire, C.; Ruffet, E.; Antonczak, S.; Beaumont, A.; O'Donohue, M.; Roques, B. P.; Fournie-Zaluski, M.-C. *Biochemistry* **1997**, *36*, 13938–13945.
(76) Day, A.; Arnold, A. P.; Blanch, R. J.; Snushall, B. *J. Org. Chem.* **2001**, *66*, 8094–8100.
(77) Kim, J.; Jung, I. S.; Kim, S. Y.; Lee, E.; Kang, J. K.; Sakamoto, S.; Yamaguchi, K.; Kim, K. *J. Am. Chem. Soc.* **2000**, *122*, 540–541.
(78) Marquez, C.; Huang, F.; Nau, W. M. *IEEE Trans. Nanosci.* **2004**, *3*, 39–45.
(79) Fasman, G. D. In *Handbook of Biochemistry and Molecular Biology, Proteins*, 3rd ed.; Fasman, G. D., Ed.; CRC Press: Boca Raton, FL, 1976; pp 183–203.

Appendix 4.5 Publications

Reprinted with permission from Nau, W. M.; Ghale, G.; Hennig, A.; Bakirci, H.; Bailey, D. M. Substrate-selective supramolecular tandem assays: monitoring enzyme inhibition of arginase and diamine oxidase by fluorescent dye displacement from calixarene and cucurbituril macrocycles. *J. Am. Chem. Soc.* **2009**, *131*, 11558-11570. Publisher's version can be found at:
http://pubs.acs.org/doi/abs/10.1021/ja904165c

J|A|C|S
ARTICLES

Published on Web 07/23/2009

Substrate-Selective Supramolecular Tandem Assays: Monitoring Enzyme Inhibition of Arginase and Diamine Oxidase by Fluorescent Dye Displacement from Calixarene and Cucurbituril Macrocycles

Werner M. Nau,* Garima Ghale, Andreas Hennig, Hüseyin Bakirci, and David M. Bailey

School of Engineering and Science, Jacobs University Bremen, Campus Ring 1, D-28759 Bremen, Germany

Received May 22, 2009; E-mail: w.nau@jacobs-university.de

Abstract: A combination of moderately selective host−guest binding with the impressive specificity of enzymatic transformations allows the real-time monitoring of enzymatic reactions in a homogeneous solution. The resulting enzyme assays ("supramolecular tandem assays") exploit the dynamic binding of a fluorescent dye with a macrocyclic host in competition with the binding of the substrate and product. Two examples of enzymatic reactions were investigated: the hydrolysis of arginine to ornithine catalyzed by arginase and the oxidation of cadaverine to 5-aminopentanal by diamine oxidase, in which the substrates have a higher affinity to the macrocycle than the products ("substrate-selective assays"). The depletion of the substrate allows the fluorescent dye to enter the macrocycle in the course of the enzymatic reaction, which leads to the desired fluorescence response. For arginase, *p*-sulfonatocalix[4]arene was used as the macrocycle, which displayed binding constants of 6400 M^{-1} with arginine, 550 M^{-1} with ornithine, and 60 000 M^{-1} with the selected fluorescent dye (1-aminomethyl-2,3-diazabicyclo[2.2.2]oct-2-ene); the dye shows a weaker fluorescence in its complexed state, which leads to a switch-off fluorescence response in the course of the enzymatic reaction. For diamine oxidase, cucurbit[7]uril (CB7) was used as the macrocycle, which showed binding constants of 4.5×10^6 M^{-1} with cadaverine, 1.1×10^5 M^{-1} with 1-aminopentane (as a model for the thermally unstable 1-aminopentanal), and 2.9×10^5 M^{-1} with the selected fluorescent dye (acridine orange, AO); AO shows a stronger fluorescence in its complexed state, which leads to a switch-on fluorescence response upon enzymatic oxidation. It is demonstrated that tandem assays can be successfully used to probe the inhibition of enzymes. Inhibition constants were estimated for the addition of known inhibitors, i.e., *S*-(2-boronoethyl)-L-cysteine and 2(*S*)-amino-6-boronohexanoic acid for arginase and potassium cyanide for diamine oxidase. Through the sequential coupling of a "product-selective" with a "substrate-selective" assay it was furthermore possible to monitor a multistep biochemical pathway, namely the decarboxylation of lysine to cadaverine by lysine decarboxylase followed by the oxidation of cadaverine by diamine oxidase. This "domino tandem assay" was performed in the same solution with a single reporter pair (CB7/AO).

Introduction

The monitoring of enzymatic processes is of fundamental importance for the understanding of biological phenomena.[1] Inspired by indicator displacement and synthetic pore strategies,[2−13] we have recently introduced a label-free method based on the competitive encapsulation of a fluorescent dye and an enzymatic product by macrocyclic hosts to monitor enzymatic reactions (Scheme 1).[14−16] In our previous examples, the investigated enzymes transformed a weak competitor (substrate) into a strong competitor (product) which displaced the fluores-

(1) Reymond, J.-L.; Fluxà, V. S.; Maillard, N. *Chem. Commun.* **2009**, 34–46.
(2) Inouye, M.; Hashimoto, K.; Isagawa, K. *J. Am. Chem. Soc.* **1994**, *116*, 5517–5518.
(3) Koh, K. N.; Araki, K.; Ikeda, A.; Otsuka, H.; Shinkai, S. *J. Am. Chem. Soc.* **1996**, *118*, 755–758.
(4) Niikura, K.; Anslyn, E. V. *J. Chem. Soc., Perkin Trans. 2* **1999**, 2769–2775.
(5) Wiskur, S. L.; Ait-Haddou, H.; Lavigne, J. J.; Anslyn, E. V. *Acc. Chem. Res.* **2001**, *34*, 963–972.
(6) Nguyen, B. T.; Anslyn, E. V. *Coord. Chem. Rev.* **2006**, *250*, 3118–3127.
(7) Zhang, T.; Anslyn, E. V. *Org. Lett.* **2007**, *9*, 1627–1629.
(8) Zhu, L.; Anslyn, E. V. *J. Am. Chem. Soc.* **2004**, *126*, 3676–3677.
(9) Das, G.; Talukdar, P.; Matile, S. *Science* **2002**, *298*, 1600–1602.
(10) Sorde, N.; Das, G.; Matile, S. *Proc. Natl. Acad. Sci. U.S.A.* **2003**, *100*, 11964–11969.
(11) Litvinchuk, S.; Tanaka, H.; Miyatake, T.; Pasini, D.; Tanaka, T.; Bollot, G.; Mareda, J.; Matile, S. *Nat. Mater.* **2007**, *6*, 576–580.
(12) Mora, F.; Tran, D.-H.; Oudry, N.; Hopfgartner, G.; Jeannerat, D.; Sakai, N.; Matile, S. *Chem.—Eur. J.* **2008**, *14*, 1947–1953.
(13) Sakai, N.; Mareda, J.; Matile, S. *Acc. Chem. Res.* **2008**, *41*, 1354–1365.
(14) Hennig, A.; Bakirci, H.; Nau, W. M. *Nat. Methods* **2007**, *4*, 629–632.
(15) Bailey, D. M.; Hennig, A.; Uzunova, V. D.; Nau, W. M. *Chem.—Eur. J.* **2008**, *14*, 6069–6077.
(16) Praetorius, A.; Bailey, D. M.; Schwarzlose, T.; Nau, W. M. *Org. Lett.* **2008**, *10*, 4089–4092.

 10.1021/ja904165c CCC: $40.75

Scheme 1. Product- *versus* Substrate-Selective Tandem Assays for Monitoring Enzymatic Activity

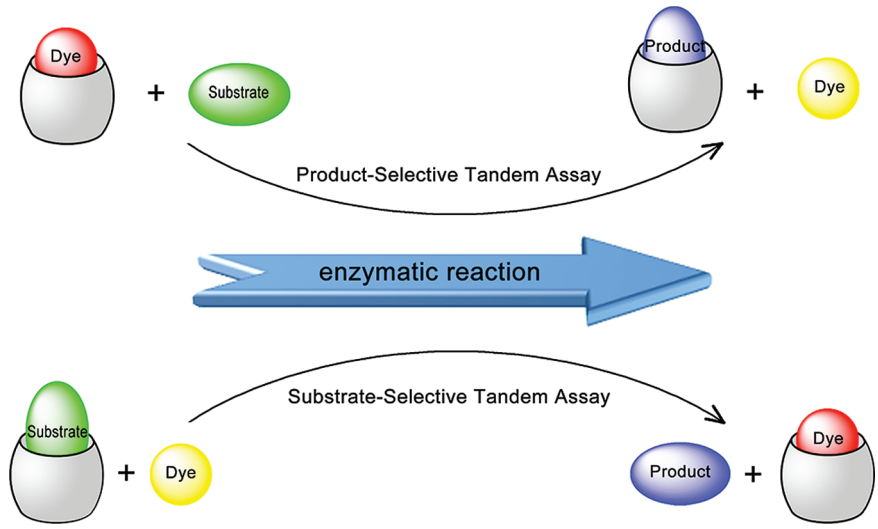

cent dye from the macrocycle and effected a concomitant change in its fluorescent properties. This method can be described as a "product-selective supramolecular tandem assay", because the enzymatic product acts as the analyte responsible for the stronger competitive binding and associated fluorescence response (Scheme 1, top). We have further suggested that the macrocyclic hosts in these types of continuous enzyme assays serve as cheap substitutes for antibodies, which have become indispensable in enzyme assays.[17−20] We also demonstrated that the lower selectivity of macrocycles[14,15] (as opposed to highly specific antibodies) toward the binding of different, structurally related products[21,22] can be used as an advantage in the development of enzyme assays, because it allows access to several enzymes affecting closely related functional group interconversions.

We now find that macrocycles in combination with simple fluorescent dyes not only can substitute antibodies in product-selective enzyme assays but also allow for a different line of enzyme assays in which the *substrate* binds more tightly to the receptor and competes with the fluorescent dye. This establishes the concept of a "substrate-selective tandem assay" (Scheme 1, bottom) in which the enzymatic reaction occurs with the uncomplexed substrate. The latter is in a rapid dynamic supramolecular equilibrium with the host−substrate complex, allowing for a continuous fluorescence signaling of the ongoing enzymatic reaction. The possibility of using substrate-selective macrocycles substantially broadens the applicability of tandem assays and opens new opportunities, because comparable enzyme assays with continuous monitoring based on substrate-specific antibodies are nonfeasible. Biological receptors bind analytes through antibody−antigen interactions which, while highly specific and exceedingly strong, suffer from an unfavorably strong binding and slow release kinetics,[23] which would prevent a real-time response in a substrate-specific enzyme assay. In contrast, macrocyclic receptors bind analytes more weakly and reversibly through supramolecular interactions, which is essential for substrate-selective tandem assays to be performed.

Besides the conceptual advancement, our present study is original in that we expand the range of tandem assays to two new enzymes (arginase and diamine oxidase versus the previously studied amino acid decarboxylases) and two additional enzyme classes (a hydrolase (EC3) and an oxidoreductase (EC1) versus the previously documented examples of several lyases (EC4)). Moreover, we apply an additional reporter pair, namely cucurbit[7]uril (CB7)/acridine orange (AO)[24] and demonstrate for the first time the potential of tandem assays for inhibitor screening. Finally, we show that the working principle of tandem assays is not limited to enzymatic reactions in which the charge status in substrate versus product is altered, and where several orders of magnitude difference in binding constants apply. Instead, it can be extended to more subtle structural variations, such as the size or shape of substrate and product, which are also associated with much smaller variations in affinity to the macrocycle (factor of 10).

Results

Conceptual Approach. Once an enzymatic reaction of interest has been identified for which a supramolecular tandem assay should be set up according to Scheme 1, a suitable reporter pair needs to be identified. The macrocyclic component of the reporter pair must necessarily display a sufficiently large binding differentiation between the substrate and the product of the enzymatic reaction. As will be seen herein, even a rather small variation in binding constants by 1 order of magnitude can be sufficient to conduct the assay. Furthermore, it should display a sizable binding with either the substrate (for a substrate-selective assay) or with the product (for a product-selective assay); i.e., the respective binding constant should be sufficiently

(17) Tawfik, D. S.; Green, B. S.; Chap, R.; Sela, M.; Eshhar, Z. *Proc. Natl. Acad. Sci. U.S.A.* **1993**, *90*, 373–377.
(18) MacBeath, G.; Hilvert, D. *J. Am. Chem. Soc.* **1994**, *116*, 6101–6106.
(19) Geymayer, P.; Bahr, N.; Reymond, J.-L. *Chem.—Eur. J.* **1999**, *5*, 1006–1012.
(20) Venn, R. F. In *Principles and Practice of Bioanalysis*, 2nd ed.; Venn, R. F., Ed.; CRC Press: Boca Raton, FL, 2008.
(21) Lagona, J.; Mukhopadhyay, P.; Chakrabarti, S.; Isaacs, L. *Angew. Chem.* **2005**, *117*, 4922–4949; *Angew. Chem., Int. Ed.* **2005**, *44*, 4844−4870.
(22) Rekharsky, M. V.; Inoue, Y. *Chem. Rev.* **1998**, *98*, 1875–1917.
(23) Houk, K. N.; Leach, A. G.; Kim, S. P.; Zhang, X. *Angew. Chem.* **2003**, *115*, 5020–5046; *Angew. Chem., Int. Ed.* **2003**, *42*, 4872−4897.
(24) Shaikh, M.; Mohanty, J.; Singh, P. K.; Nau, W. M.; Pal, H. *Photochem. Photobiol. Sci.* **2008**, *7*, 408–414.

large to effect a sizable complexation within the substrate concentration range appropriate for the particular enzymatic conversion. Additionally, the fluorescent dye must be selected such that it shows a large change in fluorescence properties upon complexation under the conditions, particularly the pH, required for the enzymatic reaction. Also important, its concentration must be adjusted such that the dye competes with the substrate or product in binding to the macrocycle. For example, when the fluorescent dye displays very strong binding, it can be used in a more dilute form, presuming that its fluorescence is still instrumentally detectable. In order for the reporter pair to produce a sufficiently large fluorescence response, a sizable fraction of dye must become complexed or uncomplexed in the course of the enzymatic reaction. This degree of dye uptake or displacement can be conveniently varied through the concentration of added macrocycle, and it can be predicted from direct fluorescence titrations of the dye with the respective macrocycle. The concentration of macrocycle should ideally lie within the titration range where the fluorescence intensity of the dye is most sensitive to the addition of macrocycle, i.e., not in the plateau region of nearly quantitative dye complexation. Once a reporter pair and the concentrations of the individual components have been set up, the robustness of the system for a potential enzyme assay can be tested in the absence of the actual enzyme by carrying out competitive fluorescence titrations with the substrate and product of the enzymatic reaction. As an additional control experiment, to assess interactions of the fluorescent dye with the enzyme, the fluorescence of the dye or of the reporter pair can be monitored upon addition of enzyme, in the absence of substrate. While the procedure just outlined may sound quite complex and involved, it is actually quite intuitive, as will be shown in the following.

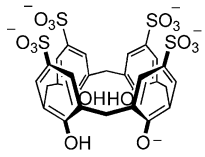

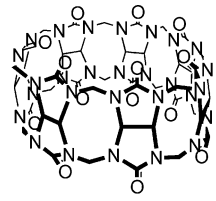

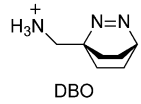

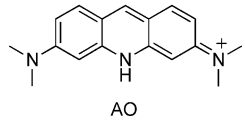

Binding Studies and Assay Working Principles. The first substrate-selective supramolecular tandem assay was developed for the enzyme arginase, which hydrolyzes the guanidinium group of arginine to yield the amino acid ornithine and urea as products. Arginase is involved in asthma,[25] immune response,[26] and sexual arousal,[27] such that arginase assays are presently of considerable current interest for use both in academic laboratory settings and in an industrial high-throughput screening format. Recall that the tandem assay principle requires a differential binding of the substrate and the product of the enzymatic reaction with the supramolecular receptor, in our case the macrocyclic host. From our previous study,[14] both *p*-sulfonatocalix[4]arene (CX4) and cucurbit[7]uril (CB7) were known to bind with poor to moderate selectivity to different amino acids at pH 6, but only the former showed the differentiation in binding between arginine [$K = (2800 \pm 100)$ M^{-1}] and ornithine [$K = (210 \pm 10)$ M^{-1}] required for a tandem assay for arginase. The preferential binding of arginine, the substrate, to CX4 is also the prerequisite for performing the tandem assay in the substrate-selective mode. Moreover, a suitable fluorescent dye (1-aminomethyl-2,3-diazabicyclo[2.2.2]oct-2-ene, DBO, $K = 60\,000 \pm 16\,000$ M^{-1}; see Supporting Information) was already known for this macrocycle,[28,29] thereby setting up the reporter pair for the desired tandem assay.[30]

In our present study, the CX4/DBO reporter pair was first employed to remeasure, by competitive fluorescence displacement titrations, the binding constants of the amino acids at the alkaline pH most suitable for the enzyme arginase.[31−33] The resulting values at pH 9.5 ($K = (6400 \pm 250)$ M^{-1}) for arginine and $K = (550 \pm 130)$ M^{-1} for ornithine) revealed essentially the same differentiation (a factor of 12 difference) as that at pH 6 (factor of 13)[14] with a slight increase in absolute binding constants by a factor of *ca.* 2.5. This can be accounted for by the different electrolyte concentrations employed previously for pH 6 (10 mM NH_4OAc)[14] and presently for pH 9.5 (no buffer), since inorganic cations are well-known to show a competitive binding to the calixarene, thereby lowering the observed binding constants with analytes.[34] It should be noted that the difference in binding constants for the arginine/ornithine pair is much smaller than that previously found for the amino acid/biogenic amine pairs because the binding with the calixarene macrocycle is based on a more subtle amino acid residue recognition (preferential binding of the larger arginine)[35−37] as opposed to the previously applicable recognition of charge status (largely favored binding of the bis-cationic diamines).[14] In general, CX4 is well-known to recognize positive charges but displays a poor, but for our purposes sufficient, selectivity toward other structural variations.[28,38,39]

The observed preferential binding for the substrate arginine should allow the setup of a substrate-selective tandem assay according to Scheme 2. Accordingly, arginase converts a

(25) Ricciardolo, F. L. M.; Zaagsma, J.; Meurs, H. *Expert Opin. Invest. Drugs* **2005**, *14*, 1221–1231.
(26) Bronte, V.; Zanovello, P. *Nat. Rev. Immunol.* **2005**, *5*, 641–654.
(27) Christianson, D. W. *Acc. Chem. Res.* **2005**, *38*, 191–201.
(28) Bakirci, H.; Nau, W. M. *Adv. Funct. Mater.* **2006**, *16*, 237–242.
(29) Bakirci, H.; Koner, A. L.; Dickman, M. H.; Kortz, U.; Nau, W. M. *Angew. Chem., Int. Ed.* **2006**, *45*, 7400–7404.
(30) The DBO chromophore has the additional advantage, owing to its exceedingly long fluorescence lifetime, of being amenable to detection by nanosecond time-resolved fluorescence (Nano-TRF), which can lead to an improved background suppression and increased robustness of enzyme assays; *cf.* Hennig, A.; Roth, D.; Enderle, T.; Nau, W. M. *ChemBioChem* **2006**, *7*, 733–737. Sahoo, H.; Hennig, A.; Florea, M.; Roth, D.; Enderle, T.; Nau, W. M. *J. Am. Chem. Soc.* **2007**, *129*, 15927–15934. Hennig, A.; Florea, M.; Roth, D.; Enderle, T.; Nau, W. M. *Anal. Biochem.* **2007**, *360*, 255–265.
(31) Baggio, R.; Cox, J. D.; Harper, S. L.; Speicher, D. W.; Christianson, D. W. *Anal. Biochem.* **1999**, *276*, 251–253.
(32) Kuchel, P. W.; Nichol, L. W.; Jeffrey, P. D. *J. Biol. Chem.* **1975**, *250*, 8222–8227.
(33) Greenberg, D. M. *Methods Enzymol.* **1955**, *2*, 368–374.
(34) Bakirci, H.; Koner, A. L.; Nau, W. M. *Chem. Commun.* **2005**, 5411–5413.
(35) Douteau-Guével, N.; Coleman, A. W.; Morel, J.-P.; Morel-Desrosiers, N. *J. Chem. Soc., Perkin Trans. 2* **1999**, 629–634.
(36) Kalchenko, O. I.; Perret, F.; Morel-Desrosiers, N.; Coleman, A. W. *J. Chem. Soc., Perkin Trans. 2* **2001**, 258–263.
(37) Perret, F.; Morel, J.-P.; Morel-Desrosiers, N. *Supramol. Chem.* **2003**, *15*, 199–206.
(38) Ballester, P.; Shivanyuk, A.; Far, A. R.; Rebek, J. *J. Am. Chem. Soc.* **2002**, *124*, 14014–14016.
(39) Bakirci, H.; Koner, A. L.; Nau, W. M. *J. Org. Chem.* **2005**, *70*, 9960–9966.

Scheme 2. Binding Equilibria in a Substrate-Selective Switch-Off Supramolecular Tandem Assay for Arginase[a]

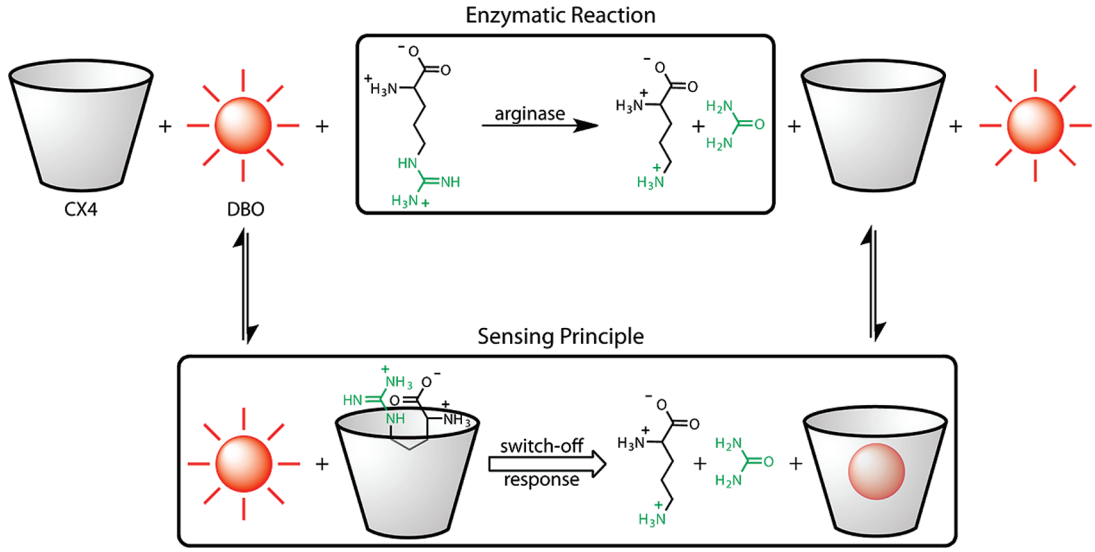

[a] It should be noted that the dye, substrate, and product are in a rapid dynamic competitive equilibrium for encapsulation within the CX4 macrocycle.

relatively stronger competitor (arginine) to relatively weaker competitors (ornithine and urea), thereby allowing the dye to compete more efficiently in forming a complex with the macrocycle as the enzymatic reaction proceeds and depletes the substrate. The concentration of uncomplexed substrate is rapidly replenished through its dynamic chemical equilibrium with its corresponding macrocycle−substrate complex.[40] Overall, because the fluorescence of the dye is lower in the inclusion complex, the fluorescence of the system should diminish as a stronger competitor is enzymatically converted into a weaker one ("switch-off" response, see Scheme 2 and Figure 1).

We next turned our attention to the enzyme diamine oxidase, which converts its substrate cadaverine to 5-aminopentanal. Diamine oxidase plays important roles in cancer, tumor growth, and apoptosis;[41−43] it also regulates cellular polyamine levels and, as such, is implicated in cell growth and proliferation processes.[44−46] We have previously studied the binding of cadaverine to the CB7 macrocycle in its capacity as a product of the enzymatic decarboxylation of lysine.[14−16] The primary driving force in the encapsulation of alkylamines is the attractive interaction between their cationic ammonium sites and the electronegative oxygen atoms of the cucurbituril portal carbonyls, as evidenced by the higher binding affinity of the biscationic cadaverine to CB7 [$K = (4.5 \pm 1.3) \times 10^6$ M^{-1}; lit.: $K = 1.4 \times 10^7$ M^{-1} in 10 mM NH_4OAc buffer, pH 6] than the monocationic 1-aminopentane [amylamine, $K = (1.1 \pm 0.1) \times 10^5$ M^{-1}; see Figure 1b]. Both binding constants were determined by competitive displacement titrations in 10 mM $(NH_4)_2PO_4$ buffer, pH 7.2 (using the CB7/AO reporter pair, see below), and the observed variation in binding proclivity was comparable to the differential binding of the same set of guests with the smaller CB6 (factor of 70).[47,48] Note that amylamine serves as a model for 5-aminopentanal, which is the primary enzymatic product of the diamine oxidase reaction but which is thermally unstable under the reaction conditions.[49−51]

Our previous product-selective tandem assay studies utilizing CB7 employed the fluorescent dye Dapoxyl to monitor the reaction.[14] The fluorescence response of this dye upon CB7 encapsulation stems primarily from a complexation-induced pK_a shift;[52] it is consequently strongly pH dependent, which precludes its use at neutral pH and above. Since the optimum pH for diamine oxidase lies at pH 7.2, an alternative dye had to be utilized. Recently,[24] the fluorescent dye AO has been shown to undergo significant changes to its fluorescence properties upon encapsulation by CB7. A direct fluorescence titration of this dye with CB7 under the recommended conditions (pH 7.2, 10 mM $(NH_4)_2PO_4$ buffer, see Supporting Information) led to an approximately 6.5-fold increase in its fluorescence intensity and afforded a binding constant of $(2.9 \pm 0.1) \times 10^5$ M^{-1} (lit. 2.0×10^5 M^{-1} at pH 7).[24] Application of the CB7/AO reporter pair in a substrate-selective tandem assay for monitoring the enzymatic oxidation of cadaverine (Scheme 3) should consequently lead to a "switch-on" response in fluorescence intensity over time, as a strong competitor (cadaverine) is transformed into a weaker one (initially 5-aminopentanal).

Enzymatic Assays. Enzymatic activity of arginase (available as partially purified enzyme) was investigated by adapting the conditions of Greenberg.[33] When the enzyme (140 nM) was added to an arginine (0.1−10 mM) solution containing the CX4/DBO reporter pair (200 μM/100 μM), the enzymatic activity was immediately signaled by a continuous decrease in fluorescence intensity, the absolute magnitude of which depended on the absolute concentrations of substrate (Figure 2a). According

(40) For the investigated macrocycles, a rapid complexation kinetics has been experimentally confirmed through NMR measurements. These established a fast guest exchange (milliseconds or faster) between arginine and CX4, as well as between cadaverine and CB7, ensuring a fast response to the much slower (minutes to hours, Figure 2) enzymatic conversion.

(41) Buffoni, F.; Ignesti, G. *Mol. Genet. Metab.* **2000**, *71*, 559–564.
(42) Pietrangeli, P.; Mondovì, B. *NeuroToxicology* **2004**, *25*, 317–324.
(43) Toninello, A.; Pietrangeli, P.; De Marchi, U.; Salvi, M.; Mondovì, B. *Biochim. Biophys. Acta, Rev. Cancer* **2006**, *1765*, 1–13.
(44) Tabor, C. W.; Tabor, H. *Annu. Rev. Biochem.* **1984**, *53*, 749–790.
(45) Walters, D. R. *Phytochemistry* **2003**, *64*, 97–107.
(46) Gerner, E. W.; Meyskens, F. L. *Nat. Rev. Cancer* **2004**, *4*, 781–792.
(47) Rekharsky, M. V.; Ko, Y. H.; Selvapalam, N.; Kim, K.; Inoue, Y. *Supramol. Chem.* **2007**, *19*, 39–46.
(48) Mock, W. L.; Shih, N. Y. *J. Org. Chem.* **1983**, *48*, 3618–3619.
(49) Mann, P. J. G.; Smithies, W. R. *Biochem. J.* **1955**, *61*, 101–105.
(50) Hill, J. M. *Biochem. J.* **1967**, *104*, 1048–1055.
(51) Medda, R.; Padiglia, A.; Floris, G. *Phytochemistry* **1995**, *39*, 1–9.
(52) Koner, A. L.; Nau, W. M. *Supramol. Chem.* **2007**, *19*, 55–66.

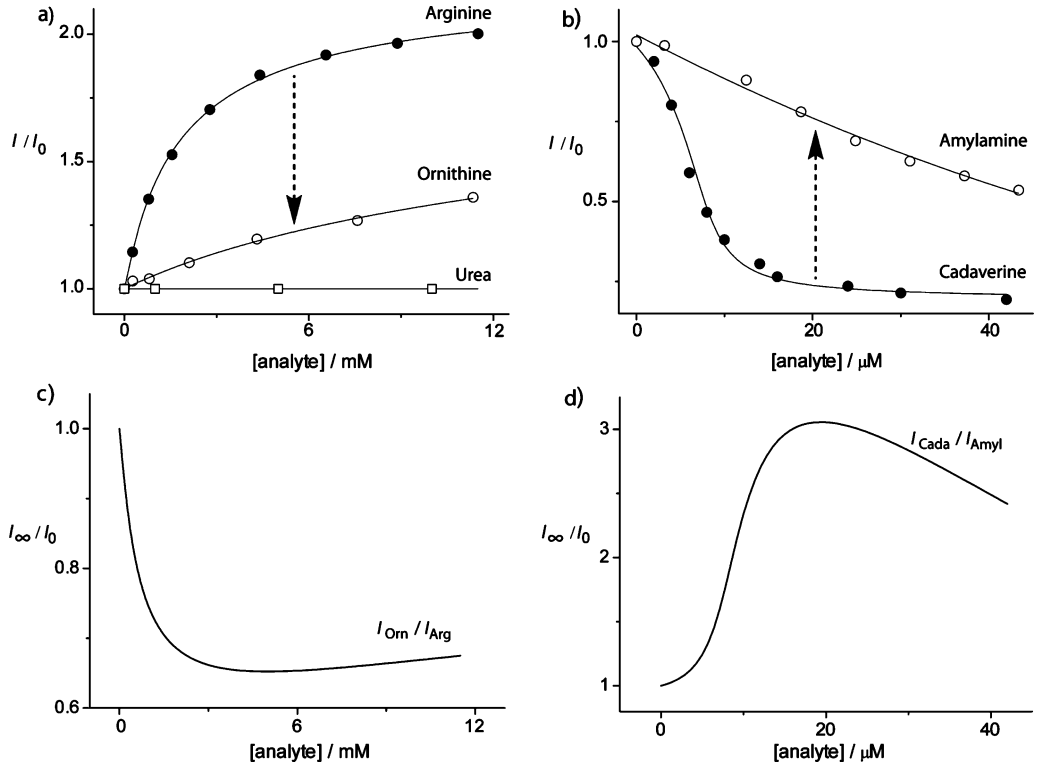

Figure 1. (a) Competitive fluorescence titration plots (λ_{ex} = 365 nm, λ_{em} = 450 nm) of L-arginine (●), L-ornithine (○), and urea (□) in H_2O, pH 9.5, with the CX4/DBO reporter pair (200 μM/100 μM). (b) Competitive fluorescence titration plots (λ_{ex} = 485 nm, λ_{em} = 510 nm) of cadaverine (●) and amylamine (○) in 10 mM $(NH_4)_2PO_4$ buffer, pH 7.2, with the CB7/AO reporter pair (8 μM/0.5 μM). The solid lines correspond to the fitted curves analyzed according to a competitive binding function; *cf.* Experimental Section. Plots (c) and (d) were obtained by dividing the fitted competitive binding curve of the substrate through that of the product, thus representing the expected fluorescence differentiation (I_∞/I_0) between substrate and product in a tandem assay. Values of I_∞/I_0 smaller and larger than 1 indicate a switch-off and switch-on fluorescence response, respectively, in the course of an enzyme assay, which is also qualitatively illustrated by the arrows in (a) and (b).

Scheme 3. Binding Equilibria in a Substrate-Selective Switch-On Supramolecular Tandem Assay for Diamine Oxidase[a]

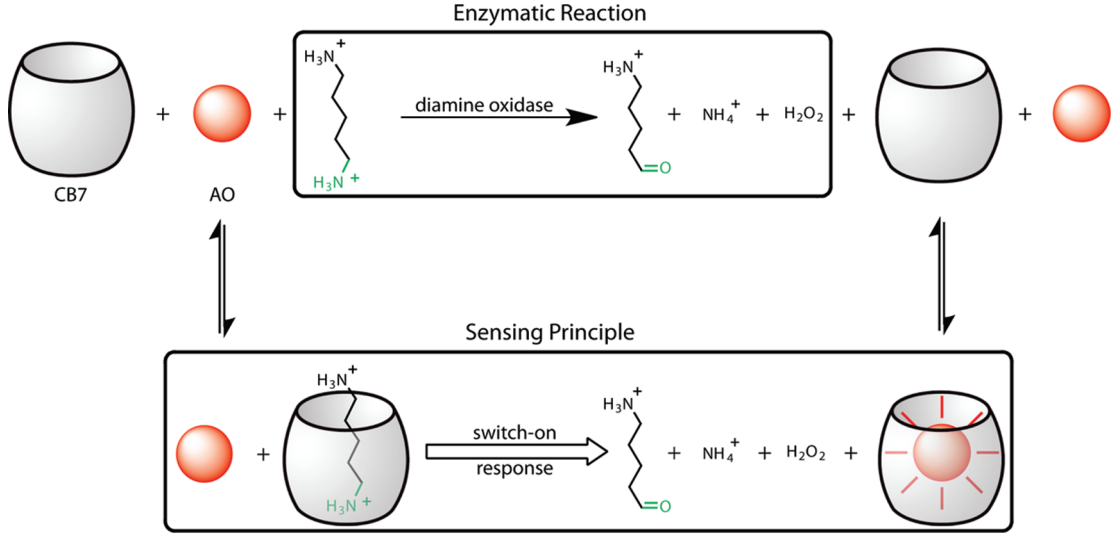

[a] It should be noted that the dye, substrate, and product are in a rapid dynamic competitive equilibrium for encapsulation within the CB7 macrocycle.

to Scheme 2, arginase transforms the "strong" competitor arginine into the weaker competitor ornithine, which allows a greater fraction of the fluorescent dye (DBO) to compete with the enzymatic product and therefore to bind to the macrocycle (CX4). Thus, a significant decrease in fluorescence was observed (switch-off fluorescence response), which approached a plateau region as the enzymatic reaction neared completion.

The enzymatic activity of diamine oxidase (available as crude enzyme extract) was followed with the CB7/AO reporter pair (8 μM/0.5 μM) under conditions (10 mM $(NH_4)_2PO_4$ buffer, pH 7.2,) similar to the ones used by Aarsen and Kemp.[53] Monitoring the enzymatic oxidation of cadaverine led to the

(53) Aarsen, P. N.; Kemp, A. *Nature* **1964**, *204*, 1195–1195.

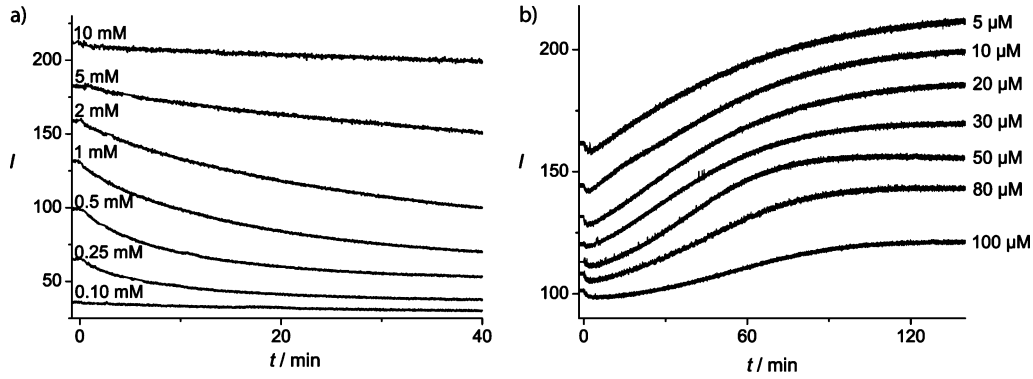

Figure 2. (a) Evolution of fluorescence intensity (λ_{ex} = 365 nm, λ_{em} = 450 nm) of the CX4/DBO (200 μM/100 μM) system during enzymatic hydrolysis of arginine by arginase at different substrate concentrations at 25 °C. The reaction was initiated by addition of arginase (140 nM) at t = 0 min. (b) Evolution of fluorescence intensity (λ_{ex} = 485 nm, λ_{em} = 510 nm) of the CB7/AO (8 μM/0.5 μM) system during enzymatic oxidation of cadaverine to 5-aminopentanal at different substrate concentrations at 37 °C. The reaction was initiated by addition of crude diamine oxidase extract (1 unit/ml) at t = 0 min. Note that the different initial fluorescence intensities are due to varying degrees of dye displacement at different substrate concentrations. Background fluorescence (in the absence of dye) accounts for not more than 10% of the total fluorescence intensity.

expected switch-on response in fluorescence intensity over time, as the strong competitor cadaverine is transformed into a weaker competitor, initially 5-aminopentanal and its cyclization product Δ^1-piperideine (2,3,4,5-tetrahydropyridine), and ultimately larger trimers.[49−51] Again, the appearance of a plateau region in the time-resolved fluorescence traces signaled the completion of the enzymatic reaction (notable at high substrate concentrations, Figure 2b).

Through comparison of the competitive titration plots of the substrates (in this case arginine and cadaverine) and products (ornithine and amylamine), it is possible to approximately predict the change in fluorescence response during the enzymatic transformations at various substrate concentrations (Figure 1) and to identify the substrate concentration range in which the largest fluorescence changes should occur. For this purpose, the *ratios* of fluorescence intensities observed at comparable substrate and product concentrations were plotted (Figure 1c and d). As can be seen, the titration plots predict a maximum fluorescence decrease by ca. 35% at 2 to 6 mM substrate concentration for the arginase assay (Figure 1c), which is even somewhat more pronounced in the actual enzyme assay (decrease by nearly 50%, Figure 2a), where it occurs in a similar concentration range (1−5 mM). For the diamine oxidase assay, the titration plots predict a maximum fluorescence enhancement of 3 near a 20 μM substrate concentration (Figure 1d), which in this case is not reached in the actual assay (maximum factor of 1.5 increase). Control experiments revealed that diamine oxidase, which was used as a crude hog kidney extract and consequently contained large amounts of unknown impurities,[54] caused a sizable reduction of the fluorescence enhancement of the CB7/AO reporter pair (see below), which is held responsible for this quantitative variation. Nevertheless, the concentration range in which the largest fluorescence differentiation is expected according to the competitive fluorescence titrations (15−30 μM, Figure 1d) agrees very well with the experimental results of the diamine oxidase assay runs (20−30 μM, Figure 2b).

The results for arginase and diamine oxidase confirm the viability of substrate-selective supramolecular tandem assays according to Schemes 2 and 3. The activity of both enzymes previously investigated by other assay methods[31−33,53,55−58] can now be sensitively detected and continuously monitored by fluorescence of an added dye in the presence of a suitable macrocycle. While the *qualitative* signaling of enzymatic activity is readily observable, its *quantification* from the recorded fluorescence traces is less straightforward, due to the complexity of the multiple and inter-related reaction equilibria and kinetics involved (see Schemes 2 and 3). In particular, the fluorescence traces (Figure 2) do not provide a direct measure of the absolute reaction rate. For example, the initial slopes of the fluorescence traces are steepest in an intermediary concentration range (around 0.5−2 mM for arginase and 20−30 μM for diamine oxidase) and are reached far below the respective K_M values of the enzymes (5.14 mM for arginase[59] and 1.28 mM for diamine oxidase[58]). This is a manifestation of the tandem assay principle, because at higher concentrations the excess substrate is still capable of displacing the fluorescent dye from the macrocycle, although the enzymatic reaction has already considerably progressed. However, the development of new enzyme assays is currently not driven by the challenge to extract *absolute* enzyme kinetics (which are already known for these two enzymes[27,58]) but to supply convenient tools for rapid screening of *relative* enzymatic activity in the presence of either a series of potentially pharmaceutically relevant inhibitors or a biotechnologically engineered library of enzyme mutants.[60] Therefore, we have investigated in further detail the utility of supramolecular tandem assays by studying the effects of inhibitors on the enzymatic transformations.

Monitoring of Inhibitory Activity. We have investigated known inhibitors of both enzymes in the corresponding substrate-selective tandem assays. For example, *S*-(2-boronoethyl)-L-cysteine (BEC) and 2-(*S*)-amino-6-boronohexanoic acid (ABH) are known inhibitors of arginase.[27] We studied arginase inhibition at substrate concentrations of 0.25−0.5 mM which presented a favorable balance between a rapid and sufficiently

(54) Note that purification of crude hog kidney diamine oxidase extracts can lead to more than a 1000-fold increase in its activity; *cf.* refs 55 and 56.

(55) Mondovi, B.; Rotilio, G.; Finazzi, A.; Scioscia-Santoro, A. *Biochem. J.* **1964**, *91*, 408–415.
(56) Tabor, H. *J. Biol. Chem.* **1951**, *188*, 125–136.
(57) Costa, M. T.; Rotilio, G.; Agro, A. F.; Vallogini, M. P.; Mondovi, B. *Arch. Biochem. Biophys.* **1971**, *147*, 8–13.
(58) He, Z.; Nadkarni, D. V.; Sayre, L. M.; Greenaway, F. T. *Biochim. Biophys. Acta, Protein Struct. Mol. Enzymol.* **1995**, *1253*, 117–127.
(59) Xie, X. Y.; Wang, C. X.; Wang, Z. Y. *J. Therm. Anal. Calorim.* **2004**, *76*, 275–284.
(60) Copeland, R. A. *Anal. Biochem.* **2003**, *320*, 1–12.

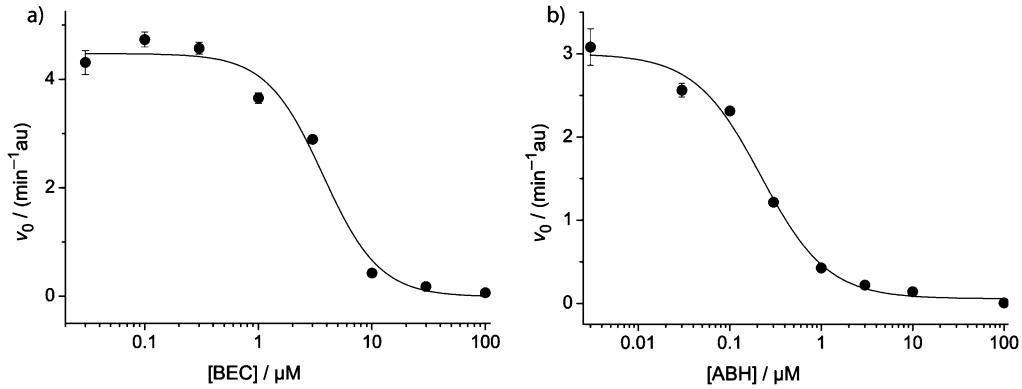

Figure 3. Determination of arginase inhibition by (a) BEC and (b) ABH at 25 °C and corresponding dose−response curves. The inhibition was determined in the presence of 140 nM arginase in H_2O (pH 9.5). 100 μM DBO and 200 μM CX4 were used as a reporter pair. Arginine concentrations were 0.5 mM for BEC and 0.25 mM for ABH.

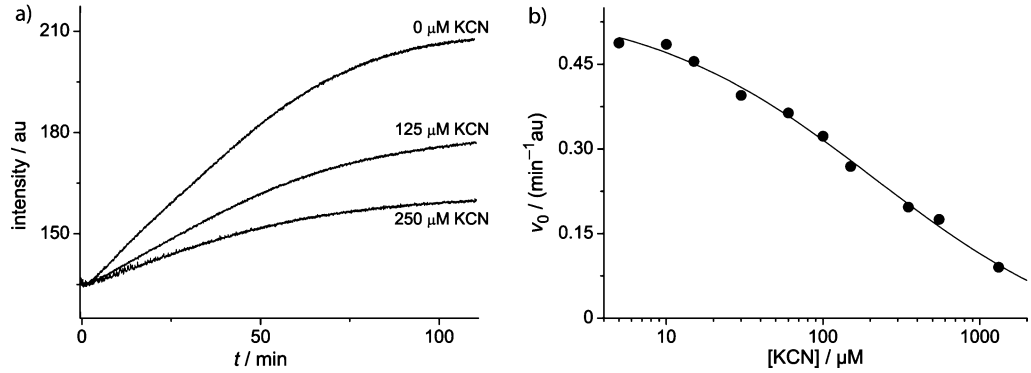

Figure 4. Determination of diamine oxidase inhibition by KCN (0−1320 μM) at 37 °C upon addition of 1 unit/mL diamine oxidase extract at $t = 0$ min. Monitored with the CB7/AO reporter pair (8 μM/0.5 μM) in 10 mM ammonium phosphate buffer at pH 7.2 with the cadaverine concentration held at 30 μM. (a) Selected continuous fluorescence traces ($\lambda_{ex} = 485$ nm, $\lambda_{em} = 510$ nm) upon addition of enzyme (raw data) for the determination of the initial rates. (b) Dose−response curve.

sensitive fluorescence response (see Figure 2a). In fact, addition of either inhibitor in high concentration (100 μM) completely suppressed the fluorescence response, signaling efficient inhibition. We additionally assessed the extent of inhibition by recording fluorescence decays at intermediary inhibitor concentrations. The initial decrease in fluorescence intensity versus time was taken as a *relative* reaction rate to allow the analysis of the resulting dose−response curves (Figure 3a and b) with the Hill equation.[60] The IC_{50} values were 3.7 ± 0.7 μM for BEC and 0.22 ± 0.04 μM for ABH, which can be readily converted into the inhibition constants K_I by considering the enzyme concentration ($IC_{50} = K_I^{app} + {}^1/_2[E]$.)[60] The resulting values for K_I (3.6 ± 0.7 μM for BEC and 0.15 ± 0.04 μM for ABH) are in good agreement with previously reported values of 2.2 and 0.11 μM, respectively,[27] and nicely reflect the approximately 20 times more potent inhibitory activity of ABH.

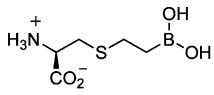

BEC

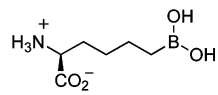

ABH

Inhibition of diamine oxidase by cyanide was studied similarly with the substrate-selective tandem assay involving the CB7/AO reporter pair. A substrate concentration of 30 μM was selected, which produced a strong fluorescence response in the absence of inhibitor (see Figure 2b). In this case, the initial *increase* in fluorescence intensity versus time (Figure 4a) was taken as a *relative* reaction rate for the dose−response curve over a cyanide concentration range of 0−1320 μM (Figure 4b).[60] The resulting IC_{50} value for cyanide was 210 ± 110 μM, which compares very well with literature reports of inhibition constants, which are in the range 80−380 μM.[61−63] Incidentally, as can be seen from Figure 4a, the fluorescence intensities reach a plateau at a lower level in the presence of inhibitor, which is fully in agreement with the fact that cyanide acts as a mixed noncompetitive inhibitor of diamine oxidase,[61] thereby irreversibly deactivating the enzyme and resulting in only partial conversion. More potent inhibitors of diamine oxidase were also investigated and found to have a similar inhibition potential as reported in the literature; e.g., the IC_{50} value of semicarbazide was estimated to lie below 10 μM.[62,63] However, due to the crude nature of the enzyme extract, no detailed quantification was performed.

It is worthwhile in this context to consider the potential undesirable effects which an inhibitor could have in a screening based on a substrate-selective supramolecular tandem assay. The most relevant aspect is that an inhibitor might itself bind significantly to the macrocyclic host, which would inevitably reduce its ability to inhibit the enzyme. Fortunately, a significant

(61) He, Z. W.; Zou, Y.; Greenaway, F. T. *Arch. Biochem. Biophys.* **1995**, *319*, 185–195.
(62) Mondoví, B.; Costa, M. T.; Agrò, A. F.; Rotilio, G. *Arch. Biochem. Biophys.* **1967**, *119*, 373–381.
(63) Mondovi, B.; Rotilio, G.; Costa, M. T. In *Methods in Enzymology*; Taylor, H., Tabor, C. W., Eds.; Academic Press: New York, 1971; Vol. 17B, pp 735−740.

binding of an inhibitor to the host would lead to immediate dye displacement, which would be readily identified by a sudden change in fluorescence intensities upon addition of the compound. In the case of the arginase assay, the fluorescence readout would be artificially *increased*, while, for the diamine oxidase assay, a *decreased* intensity would be observed. Such changes, which are in fact *opposite* to the fluorescence response expected for the enzymatic reactions themselves, were *not* observed for the presently investigated inhibitors,[64] such that this complication did not need to be further considered. Despite the potential interference of the macrocycle present in the assay mixture, a substrate-selective supramolecular tandem assay offers an intrinsic possibility to identify potential false negatives by considering all fluorescence intensity outliers, which show, upon addition of inhibitor, an immediate fluorescence change opposite to the expected direction.[67]

Effect of Macrocycle on the Enzymatic Reaction. The non-negligible binding of the enzymatic substrate with the macrocycle, which constitutes the working principle of any substrate-selective tandem assay, leads to a compulsory modulation of the enzyme kinetics because the free substrate concentration is effectively lowered due to partial complexation.[68] In fact, macrocycles,[69−71] including the presently employed CB7,[72] can even be used as (apparent) inhibitors of enzymatic reactions, e.g., of proteases, whenever they bind the substrate and their concentration is sufficiently high.[71−75] However, the required concentrations of macrocycles to successfully employ them in tandem assays (μM) are much lower than the concentrations previously employed to achieve sizable inhibition effects (mM), such that no large effect on the enzyme kinetics was *a priori* effected. To verify this conjecture, we have monitored the enzymatic transformations by alternative methods.

For arginase, owing to the high substrate concentrations employed in the assay, the reaction could be independently monitored by ^{1}H NMR (data not shown). Integration of the signals from the δ-CH_2 protons verified that the transformation in the absence of CX4 (by ^{1}H NMR) did indeed occur on the same time scale as in the supramolecular tandem assay in the presence of CX4 (by fluorescence). For diamine oxidase, an alternative, established enzyme-coupled assay was used which exploits the enzymatic (with peroxidase) oxidation of the dye *o*-dianisidine by hydrogen peroxide, the enzymatic byproduct (Scheme 3).[53] The depletion of the dye (which shows no detectable binding with CB7) was followed UV-spectrophotometrically at 440 nm to monitor the progress of the enzymatic reaction in the absence and presence of CB7 (see Supporting Information). While a strong retardation of the enzymatic reaction was observed at concentrations above 0.1 mM of CB7, lower concentrations such as those selected for the enzymatic assays (8 μM) displayed quite small effects, particularly on the initial rates relevant for inhibitor studies (see above). This can be rationalized by considering the percentage of bound substrate in each of these cases; for instance, when more than 30 μM, i.e., a large excess, of substrate is used with 8 μM CB7, a maximum of 26% of the substrate is complexed. However, when 0.1 mM of CB7 is utilized, the substrate is quantitatively (>99%) complexed which necessarily leads to a reduced conversion rate. Thus, although the presence of the macrocycle *does* affect the enzyme kinetics in a substrate-selective tandem assay, the conditions can be selected such that this interference becomes either insignificant or at least practically acceptable. Most important, applications in inhibitor screening are based on the effects of additives on *relative* enzyme kinetics, such that small, but constant, influences on the absolute rates are generally tolerable.

Monitoring Multistep Enzymatic Transformations by Domino Tandem Assays. We also tested the possibility whether the tandem assay principle would be suitable to monitor a multistep enzymatic reaction, namely the sequential transformation of lysine to cadaverine by lysine decarboxylase followed by the oxidation of cadaverine to 5-aminopentanal (*vide supra*) by diamine oxidase.

As a common reporter pair for such a "domino tandem assay" we selected CB7/AO, and as common working conditions for both enzymes we chose pH 7.2 and 37 °C. The initial decarboxylation of lysine to cadaverine results in a dramatic increase (ca. ×10 000) in affinity for the analyte toward the macrocycle (CB7).[14] This results in the dye (AO) being ejected from its macrocyclic host (CB7) as is shown in Scheme 4, accompanied by a drastic decrease of the overall fluorescence intensity of the system (Figure 5). The plateau region (~140 min) demonstrates the exhaustion of substrate as the conversion to cadaverine nears completion. After this point, addition of the second enzyme (second arrow), diamine oxidase, initiates the conversion of cadaverine to 5-aminopentanal and its cyclization products (*vide supra*). These products, in turn, have a lower binding affinity to CB7 than cadaverine resulting in an increase in the overall fluorescence intensity as the equilibrium shifts (Figure 5), allowing a greater amount of the dye (AO) to once again become encapsulated by CB7 (Scheme 4).

Noteworthy is that the fluorescence of the system does not fully recover to its initial intensity, which is ostensibly due to two factors: First, a non-negligible residual binding of the product 5-aminopentanal (Figure 1) or its cyclization products[49−51] applies, e.g., amylamine ($K = 1.1 \times 10^5$ M^{-1}, our model for 5-aminopentanal) competes with cadaverine ($K = 4.5 \times 10^6$ M^{-1}) more effectively for CB7 encapsulation than does lysine (870 M^{-1}),[14] thereby allowing a lower fraction of dye to re-enter the macrocyclic cavity. Second and more important, diamine oxidase is being added as a crude enzyme extract,

(64) KCN causes interferences at high millimolar concentrations due to competitive metal ion (K^+) binding to the carbonyl portals of CB7; *cf.* refs 65 and 66.
(65) Marquez, C.; Hudgins, R. R.; Nau, W. M. *J. Am. Chem. Soc.* **2004**, *126*, 5806–5816.
(66) Marquez, C.; Huang, F.; Nau, W. M. *IEEE Trans. Nanobiosci.* **2004**, *3*, 39–45.
(67) To further identify false negatives, a secondary screening is routinely performed in high-throughput applications. In the case of supramolecular tandem assays, this could be done in the simplest case by adding the reporter pair *after* incubation with the enzyme. Such an additional single-point determination would conveniently eliminate the influence of the inhibitor-macrocycle binding on the enzyme kinetics. Alternatively, a secondary screen with a different reporter pair could be performed.
(68) This establishes an important contrast to product-selective tandem assays, where a complexation of the enzymatic product would generally have no effect on the enzyme kinetics, or potentially a beneficial effect in cases where product inhibition applies.
(69) Uekama, K.; Hirayama, F.; Irie, T. *Chem. Rev.* **1998**, *98*, 2045–2076.
(70) McGarraghy, M.; Darcy, R. *J. Inclusion Phenom. Macrocyclic Chem.* **2000**, *37*, 259–264.
(71) Koralewska, A.; Augustyniak, W.; Temeriusz, A.; Kanska, M. *J. Inclusion Phenom. Macrocyclic Chem.* **2004**, *49*, 193–197.
(72) Hennig, A.; Ghale, G.; Nau, W. M. *Chem. Commun.* **2007**, 1614–1616.
(73) Irwin, W. J.; Dwivedi, A. K.; Holbrook, P. A.; Dey, M. J. *Pharm. Res.* **1994**, *11*, 1698–1703.
(74) Matsubara, K.; Ando, Y.; Irie, T.; Uekama, K. *Pharm. Res.* **1997**, *14*, 1401–1405.
(75) Monteiro, J. B.; Chiaradia, L. D.; Brandao, T. A. S.; Dal Magro, J.; Yunes, R. A. *Int. J. Pharm.* **2003**, *267*, 93–100.

Scheme 4. Binding Equilibria in a "Domino" Tandem Assay, Combining a "Switch-Off" and "Switch-On" Fluorescence Response As Well As Both Product- And Substrate-Selective Binding

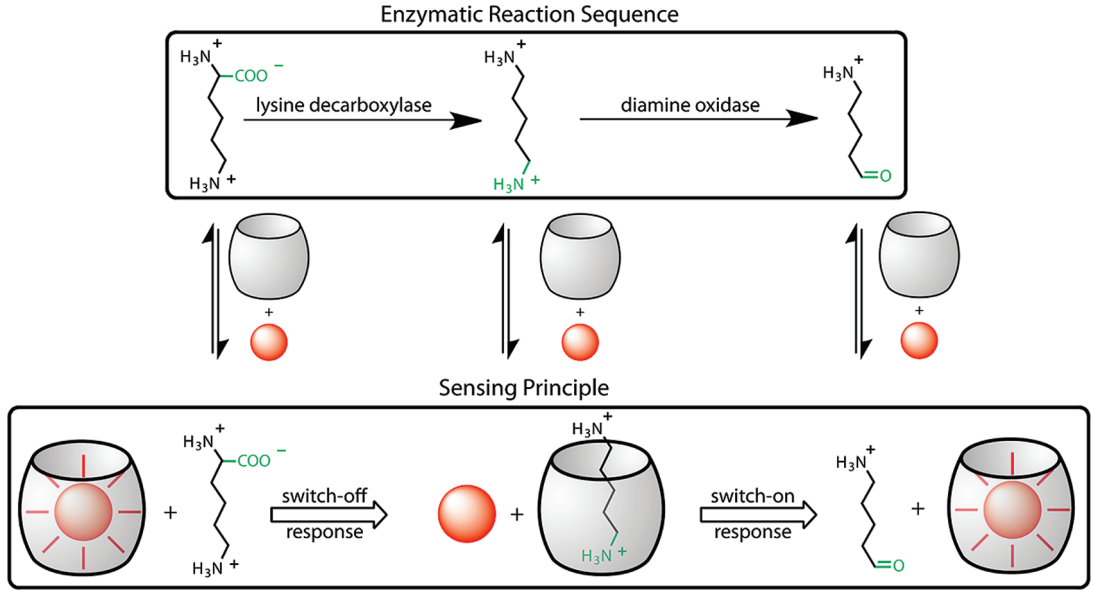

requiring the addition of a 140 times larger amount by weight than the partially purified lysine decarboxylase. This results in the addition of a large excess of unknown impurities[54] which lead to a reduction in fluorescence intensity, most likely by partial displacement of dye from the complex. In fact, we were independently able to estimate the extent of this second effect (dashed line in Figure 5) by adding the same amount of crude enzyme extract to a solution containing only the CB7/AO reporter pair (8 μM/0.5 μM) and lysine (30 μM) *without addition of lysine decarboxylase*, thereby mimicking the conditions after complete conversion (and assuming negligible binding of the product). Accordingly, impurities in the crude enzyme extract are largely responsible for the lower fluorescence intensity at the end of the domino tandem assay. Notwithstanding, both enzymatic reactions can be reliably followed by this unconventional approach.

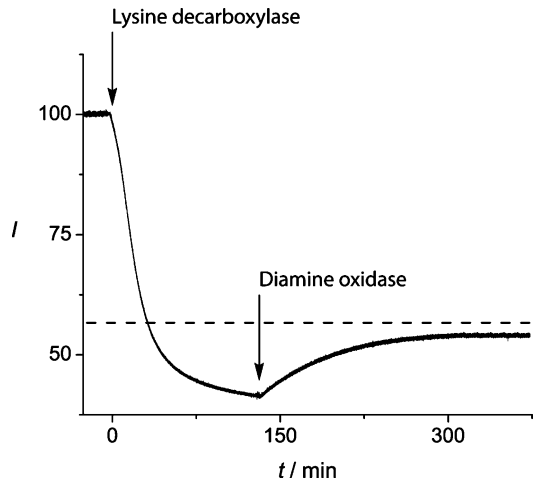

Figure 5. Evolution of fluorescence intensity (λ_{ex} = 485 nm, λ_{em} = 510 nm) of the CB7/AO (8 μM/0.5 μM) system during enzymatic decarboxylation of lysine (30 μM) initiated by lysine decarboxylase (40 μg/mL, t = 0 min), followed by oxidation of the intermediary cadaverine to 5-aminopentanal by diamine oxidase (5.6 mg/mL, $t \approx$ 140 min), at pH 7.2 and 37 °C. The dashed line represents the fluorescence intensity of the system when the crude diamine oxidase extract is added without addition of lysine decarboxylase.

Discussion

Enzymatic assays frequently require the use of fluorescently or radioactively labeled substrates or cofactors, or they depend on a recognition of the reaction products through subsequent binding to antibodies in competition with added fluorescently labeled antigens.[1,19] Also popular are assays in which the reaction products are converted into chromophoric or fluorescent secondary products, either catalyzed by another added enzyme (enzyme-coupled assays) or by chemical follow-up reactions with added (functional-group selective) reagents.[1] The various assay types require, in particular those involving radioactive labels, antibodies, and chemical follow-up reactions, multiple incubation steps or heterogeneous workup, which preclude, with few exceptions,[19] a direct and continuous monitoring of the reaction progress. For example, the established arginase assays require either multiple incubation steps, heating to 100 °C, a colorimetric detection of the enzymatic byproduct urea,[32,33] or the use of chromophoric derivatives like 1-nitro-3-guanidinobenzene.[31] The colorimetric enzyme-coupled assay[53] (see Results) and oxygen-consumption based assays[55,56] common for the determination of diamine oxidase concentration and activity are inherently less sensitive than fluorimetric assays, and only the latter allow for implementation into fluorescence microplate readers and up-scaling to high-throughput screening formats,[76,77] as well as the use of state-of-the-art detection techniques including time-resolved fluorescence.[77,78]

As documented by the kinetic traces in Figure 2 and the inhibition studies in Figures 3 and 4, the assays developed herein for arginase and diamine oxidase allow a real-time, direct, and sensitive monitoring of the progress and inhibition of the

(76) Goddard, J.-P.; Reymond, J.-L. *Trends Biotechnol.* **2004**, *22*, 363–370.
(77) Hennig, A.; Florea, M.; Roth, D.; Enderle, T.; Nau, W. M. *Anal. Biochem.* **2007**, *360*, 255–265.
(78) Hennig, A.; Roth, D.; Enderle, T.; Nau, W. M. *ChemBioChem* **2006**, *7*, 733–737.

enzymatic reaction in homogeneous solution by fluorescence. They entirely bypass the use of antibodies, radioactive labels, covalently attached fluorescent probes, chromogenic or fluorogenic substrates or cofactors,[1,31] chemical follow-up reactions, multiple incubation steps or heating, and heterogeneous workup. Instead, they operate by simple addition of two additives (a macrocycle and a dye), which are either commercially available (CX4, CB7, AO) or readily synthesized (DBO).

We have referred to assays which exploit indicator displacement from macrocycles according to the working principles illustrated in Schemes 1−3 as "tandem assays". Tandem assays exploit a differential, reversible, and competitive intermolecular binding of three potential guests (substrate, product, and dye) with a synthetic receptor and therefore present a genuinely supramolecular approach to the design of enzyme assays. Principles of supramolecular chemistry have been previously utilized in enzyme assays, including the vesicles with synthetic pores pioneered by Matile and co-workers,[9−13] and case studies of tailor-made fluorescent chemosensors, which chelate the substrate or product of an enzymatic reaction.[79−82] In contrast to the known supramolecular approaches, tandem assays allow a continuous monitoring of the enzymatic reaction and bypass the need for the construction of specific fluorescent chemosensors, respectively. Most importantly, they can be simply devised by screening a library of reporter pairs composed of different macrocycles and common fluorescent dyes and testing them for differential binding and a fluorescence response (these are the two prerequisites for the development of any tandem assay), under the enzymatic reaction conditions.

The development of tandem assays for arginase and diamine oxidase presents a very good example of how powerful this approach can be. Although our own "library" is presently still vanishingly small with only four reporter pairs employed until now (CX4/DBO,[14,28,29] CB7/Dapoxyl,[14,52] CB7/AO,[24] and CB6/3-amino-9-ethylcarbazole[16]), it was nevertheless sufficiently large to find at least one suitable reporter pair. For example, CB7 does not show the required differential binding toward arginine and ornithine, but CX4 does, such that the CX4/DBO reporter pair was selected for the arginase assay. Conversely, the fluorescent dye Dapoxyl does not show a sufficient fluorescence response at pH 7, the preferred condition for the diamine oxidase assay, but AO does, such that the CB7/AO reporter pair was preferred in this case.

The tandem assay approach was originally inspired by antibody-based indicator displacement assays and introduced for enzymatic reactions, which afford *products that bind strongly* to the macrocycle (product-selective assays, Scheme 1, top). The presently designed tandem assays are substrate-selective, i.e., based on competitive complexation of the substrate as the stronger competitor. This conceptual step from "product-selective" to "substrate-selective" is nontrivial, as can be seen from a comparison between the potential of *synthetic* receptors (macrocycles) and their *biological* counterparts (antibodies).[19] The latter would bind the substrate too tightly (in some cases irreversibly on the pertinent time scale) and moreover release it too slowly to result in a real-time fluorescence response to the enzymatic conversion.[23] To become specific, antibodies typically display binding constants in the range 10^7-10^9 M^{-1} and "on rates" in the range 10^3-10^6 M^{-1} s^{-1},[19,23] which corresponds to "off rates" in the range $10^{-1}-10^{-6}$ s^{-1}. The release of a complexed substrate, which would be relevant in a substrate-specific antibody assay, would consequently take seconds to days ($1/k_{off}$), far too slow for a continuous monitoring of enzymatic reactions. Note also that the complexation of the substrate would itself require an additional incubation step. In fact, while exceptions are known, it is good practice to equilibrate (incubate) antibodies for typically 5−20 min in homogeneous assays.[19] This limits enzyme assays involving substrate-specific antibodies to indirect examples, in which the function of the antibody is essentially to assess conversion through a single-point measurement[83,84] and not to replenish the free substrate through a dynamic equilibrium.

For comparison, common macrocyclic receptors like cyclodextrins and calixarenes typically show binding constants in the range 10^2-10^6 $M^{-1}$and "on rates" in the range 10^6-10^9 M^{-1} s^{-1},[85−91] which corresponds to "off rates" in the range $1-10^7$ s^{-1}. The release rates of a substrate bound to a macrocycle is consequently faster (seconds to microseconds) in relation to the typical times of enzymatic reactions in enzyme assays (minutes to hours).[40] The reversibility of the guest−macrocycle complexation, ensured by the mM to μM binding constants in combination with a rapid exchange dynamics,[23,88] are consequently critical parameters of supramolecular tandem assays, which ensure the reporter pair to respond sufficiently rapidly and precisely to the depletion of substrate as affected by the enzymatic conversion.

Any sequestration of the substrate by a receptor will inevitably lower its apparent concentration and consequently result in a lowering of the absolute enzymatic reaction rate. This peculiarity of substrate-selective tandem assays[68] is not a primary concern in inhibition studies, where hits are based on clear-cut relative effects in a large series of investigated compounds. Additionally, we could show that adverse effects on the reaction rate can be minimized by working under conditions in which only a small fraction of substrate is complexed, while still allowing the reporter pair to "observe" the enzymatic reaction through its response to the chemical equilibrium changes. This can be ensured, in particular, by working at low macrocycle concentrations with an excess of substrate. For example, the diamine oxidase assay functions quite well by using a macrocycle concentration of 8 μM and substrate concentrations above 30 μM, conditions under which less than 26% of the substrate are complexed. This results in comparably small and tolerable

(79) Vance, D. H.; Czarnik, A. W. *J. Am. Chem. Soc.* **1994**, *116*, 9397–9398.
(80) Mizukami, S.; Nagano, T.; Urano, Y.; Odani, A.; Kikuchi, K. *J. Am. Chem. Soc.* **2002**, *124*, 3920–3925.
(81) Wongkongkatep, J.; Miyahara, Y.; Ojida, A.; Hamachi, I. *Angew. Chem., Int. Ed.* **2006**, *45*, 665–668.
(82) Chen, X.; Jou, M. J.; Yoon, J. *Org. Lett.* **2009**, *11*, 2181–2184.
(83) Wong, R. C.; Burd, J. F.; Carrico, R. J.; Buckler, R. T.; Thoma, J.; Boguslaski, R. C. *Clin. Chem.* **1979**, *25*, 686–691.
(84) Karvinen, J.; Laitala, V.; Mäkinen, M.-L.; Mulari, O.; Tamminen, J.; Hermonen, J.; Hurskainen, P.; Hemmilä, I. *Anal. Chem.* **2004**, *76*, 1429–1436.
(85) Monti, S.; Flamigni, L.; Martelli, A.; Bortolus, P. *J. Phys. Chem.* **1988**, *92*, 4447–4451.
(86) Petrucci, S.; Eyring, E. M.; Konya, G. In *Comprehensive Supramolecular Chemistry*; Atwood, J. L., Ed.; Pergamon: New York, 1996; Vol. 8, pp 483−497.
(87) Franchi, P.; Lucarini, M.; Pedulli, G. F.; Sciotto, D. *Angew. Chem., Int. Ed.* **2000**, *39*, 263–266.
(88) Zhang, X.; Gramlich, G.; Wang, X.; Nau, W. M. *J. Am. Chem. Soc.* **2002**, *124*, 254–263.
(89) Bakirci, H.; Nau, W. M. *J. Photochem. Photobiol. A: Chem.* **2005**, *173*, 340–348.
(90) Bohne, C. *Langmuir* **2006**, *22*, 9100–9111.
(91) Pace, T. C. S.; Bohne, C. *Adv. Phys. Org. Chem.* **2008**, *42*, 167–223.

effects on the absolute reaction rate, as was demonstrated through control experiments with an alternative assay.

The substrate/product differentiation in the previously reported tandem assays for decarboxylase assays[14−16] was due to an increase in the net positive charge of the competitor during enzymatic transformation, which resulted in a 100−10000-fold difference in binding constants of substrate and product with cation-receptor macrocycles (CX4, CB6, and CB7). The working principle for the diamine oxidase tandem assay is similar (charge-selective binding), except that in this case the substrate binds only ca. 40 times more strongly than the product. As demonstrated for arginase, however, the application of supramolecular tandem assays is not restricted to enzymatic reactions, in which the charge status of the substrate is changed. Note that arginine and ornithine are expected to have a very similar charge status between pH 6 and 9.5. Enzymatic reactions in which the size (or shape) of the competitor changes can be similarly explored, owing to the fact that binding to any macrocycle is also significantly size selective (hole-size selectivity) as well as functional-group selective.[28,38,39] Although in this case the differentiation with respect to the binding constants of substrate and product can be frequently quite small (factor of only 12 for the arginine/ornithine couple), the fluorescence response in the arginase tandem assay is sufficiently robust to reliably monitor the effects of added inhibitors and varying substrate concentration.

The results for arginase thus demonstrate that the assay principle can also be expanded to enzymatic reactions, which affect more subtle structural variations than a change in charge status, and even a factor of 10 difference in binding constants between substrate and product can be sufficient to ensure a sizable fluorescence response through the tandem assay working principle. In other words, even poorly selective macrocycles[28,38,39] can be successfully employed, which presents another illustrative example of the shift toward differential as opposed to highly selective receptors in the research area of molecular recognition.[92,93] As shown for the arginase assay, even a *high affinity* of the macrocycle is no principal requirement. The binding constant of CX4 with arginine, for example, is only on the order of 10^3 M^{-1}, that is, a weak or at best moderate binding. The binding constant does, however, determine the concentration range in which substrate conversion can be reliably monitored, and the latter also depends on the investigated enzyme.

In the course of our investigations on the enzymatic reactions involving amino acids, we became aware of the interrelationship of the various enzymes as well as the intermediary polyamines in fundamental biochemical reaction pathways during cell growth and differentiation.[44−46] Elevated levels of arginase and diamine oxidase activity, for example, are found in cancerous tissues. Enzymatic conversion of arginine by arginase yields ornithine which in turn undergoes decarboxylation to putrescine, which is finally oxidized by diamine oxidase.[58,94] Cadaverine adapts a similarly central position in a metabolic pathway involving decarboxylation of lysine as precursor and deamination of 1-aminopentanal as product.[95,96]

It was our idea to apply the supramolecular tandem assay principle to such a cascade of enzymatic reactions and monitor a multistep enzymatic reaction sequence by coupling product- with substrate-selective sensing. In essence, the first reaction could be signaled through the binding of a product with the macrocycle, which could then serve as the substrate for a second reaction. In an extreme situation, an analyte could go through a series of enzymatic transformations (or an entire metabolic pathway) that all affect its binding affinity to the macrocycle, and by combining the tandem assay principle with a sequential addition of the different enzymes, it should be possible to continually monitor these transformations in real time and in a "one-pot" fashion, potentially by using a single reporter pair. This "domino" tandem assay technique should be especially powerful when a metabolite undergoes transformations that alternate its affinity to the macrocycle, e.g., from weak to strong and back to weak.

The enzymatic reaction sequence from arginine (strong competitor) to ornithine (weak competitor) to putrescine (very strong competitor) to 1-aminobutanal (weaker competitor) fulfills this requirement, as well as the reaction sequence from lysine (weak competitor) to cadaverine (very strong competitor) to 1-aminopentanal (weaker competitor). Unfortunately, we lacked access to the enzyme ornithine decarboxylase and could therefore not examine the associated three-step enzymatic process, but the two enzymes involved in the reaction sequence involving cadaverine were available: lysine decarboxylase (in partially purified form) and diamine oxidase (as crude extract). The working principle of the corresponding domino tandem assay is illustrated in Scheme 4. As can be seen from Figure 5, the two assays can indeed be sequentially combined to afford first a fluorescence decrease due to decarboxylation and then, upon addition of diamine oxidase, a fluorescence increase due to oxidative deamination (on−off−on response). The fact that the fluorescence does not fully recover after the enzymatic conversion by diamine oxidase is attributed to the use of this enzyme as a crude enzyme extract, which results in partial dye displacement due to large amounts of biological "impurities" (dashed line in Figure 5). But regardless of this interference caused by the lack of selectivity, tandem assays are sufficiently robust to function also in more complex biological mixtures, as was previously demonstrated through comparative experiments with purified enzymes, crude extracts, and whole cells expressing a particular enzyme. This may be quite surprising, but the concentration of biological impurities contained in a certain enzyme preparation is expected to remain constant as the enzymatic reaction proceeds. The interference is consequently "static" in nature and does not influence the time-resolved change in fluorescence intensity, which presents the optical read-out of the assay and which is diagnostic and specific for the enzymatic reaction.

The domino tandem assay shows that it is possible to monitor, in real time, quite complex, but biologically highly relevant, metabolic pathways by a very simple method. Additionally and very interesting to note, similar enzymatic reaction cascades with alternating on−off−on optical signaling have been proposed to be promising for biocatalyst-stimulated logic gate operations in the context of biocomputing.[97,98] In any case, our results present a proof-of-principle; they demonstrate nicely the

(92) Lavigne, J. J.; Anslyn, E. V. *Angew. Chem., Int. Ed.* **2001**, *40*, 3118–3130.
(93) Das, G.; Matile, S. *Chem.—Eur. J.* **2006**, *12*, 2936–2944.
(94) Nikolic, J.; Stojanovic, I.; Pavlovic, R.; Sokolovic, D.; Bjelakovic, G.; Beninati, S. *Amino Acids* **2007**, *32*, 127–131.
(95) Watson, A. B.; Brown, A. M.; Colquhoun, I. J.; Walton, N. J.; Robins, D. J. *J. Chem. Soc., Perkin Trans. 1* **1990**, 2607–2610.
(96) Shoji, T.; Hashimoto, T. *Plant Cell Physiol.* **2008**, *49*, 1209–1216.
(97) Niazov, T.; Baron, R.; Katz, E.; Lioubashevski, O.; Willner, I. *Proc. Natl. Acad. Sci. U.S.A.* **2006**, *103*, 17160–17163.
(98) Freeman, R.; Sharon, E.; Tel-Vered, R.; Willner, I. *J. Am. Chem. Soc.* **2009**, *131*, 5028–5029.

potential of the tandem assay principle and reveal the inherent advantage of employing differentially selective as opposed to highly specific receptors.

Conclusions

We have expanded the range of supramolecular tandem assays from product- to substrate-selective variants. We demonstrated that even small differences in binding constants of substrate and product are sufficient not only to monitor the activity of two important enzymes in real time in a homogeneous solution but also to study inhibition effects. Tandem assays are exceptionally adaptable and flexible, which is attractive in view of the ever-expanding range of substrates and enzymes. Instead of designing a specific chemosensor or raising a specific antibody, generally for the product of an enzymatic reaction, tandem assays can be simply devised by screening a library of reporter pairs. Even by combining all commercially available macrocycles and fluorescent dyes, or focusing on the large diversity of host−dye complexes already investigated,[2−4,14,16,24,28,29,52,99−113] a very large library could readily be built up. This approach has enormous potential for enzyme assay development, and the effort, time, and resources related to testing such a library should compete well with alternative strategies in assay development. Owing to the moderate but known selectivity-of different macrocycles, the search can also be rationally limited (e.g., to cation-receptor macrocycles for reactions involving positively charged substrates and products) and a once identified reporter pair can be with high probability transferred to enzymes affecting similar functional group interconversions; e.g., the CB7/Dapoxyl reporter pair was previously employed for not less than six amino acid decarboxylases.[14,15]

Experimental Section

DBO was synthesized according to a literature procedure[114] and purified by precipitation as the sulfate salt from diethyl ether. Acridine orange, cadaverine, putrescine, ornithine, and CX4 (all Fluka) as well as ornithine, dianisidine, urea, and potassium cyanide (all Sigma-Aldrich) were obtained in the highest purity available and used as received. Cucurbit[7]uril was synthesized in >95% purity, following established synthetic protocols.[66,115,116] The arginase inhibitors ABH and BEC were received as ammonium salts from Alexis Biochemicals (Lausen, Switzerland). Diamine oxidase (crude extract from hog kidney, 0.18 units/mg solid), peroxidase (type II from horseradish, 181 purpurogallin units/mg), and lysine decarboxylase (partially purified, 1.6 U/mg) were from Sigma-Aldrich. Arginase (partially purified, from cow liver, 100−200 units/mg solid) was from Fluka.

Absorption measurements were performed with a Varian Cary 4000 spectrophotometer. For bovine liver arginase an extinction coefficient of $1.1 \times 10^5\ M^{-1}\ cm^{-1}$ at 278 nm was used.[117] For fluorescence measurements, a Varian Eclipse fluorimeter (arginase assays: $\lambda_{ex} = 365$ nm, $\lambda_{em} = 450$ nm, diamine oxidase assays: $\lambda_{ex} = 485$ nm, $\lambda_{em} = 510$ nm) was used. Continuous assays for arginase (16 μg/mL, 140 nM) were performed unbuffered at pH 9.5 in the presence of 100 μM DBO and 200 μM CX4 in a variable-temperature cell holder at 25.0 ± 0.1 °C. Continuous assays for diamine oxidase (1 unit/ml) were measured in 10 mM $(NH_4)_2PO_4$ buffer, pH 7.2, with a mixture of 0.5 μM acridine orange, 8 μM CB7, and 30 μM of cadaverine in a variable-temperature cell holder at 37.0 ± 0.1 °C. Dose−response curves of the inhibitors BEC and ABH were obtained in a similar manner using 0.5 mM and 0.25 mM of arginine. Inhibition kinetic traces for KCN were obtained with 30 μM cadaverine for a series of KCN concentrations (0−1320 μM).

For analytical analysis of the titrations, we define $[D]_0$, $[C]_0$, and $[H]_0$ as the total concentrations of dye, competitor (substrate or product), and host (macrocycle). [D], [C], and [H] are the concentrations of uncomplexed dye, uncomplexed competitor, and uncomplexed host. [H•D] and [H•C] are the concentrations of the host−dye and host−competitor complex, and K_C and K_D are the association constants of the competitor and dye with the host.

The fluorescence intensity (I) in the course of the titration can be expressed as a linear combination of the fluorescence intensity of the uncomplexed dye (I_D) and that of the host−dye complex ($I_{H•D}$), weighted by their molar fractions according to eq 1. $I_{H•D}$ was extrapolated from host−guest titrations (in the absence of competitor) fitted according to a 1:1 binding model.[28,52,118]

$$I = \frac{[D]}{[D]_0} I_D + \frac{[H•D]}{[D]_0} I_{H•D} \quad (1)$$

Upon appropriate substitution one obtains eq 2, with the concentration of uncomplexed host as variable; the latter is defined by a cubic equation (eq 3).[119]

$$I = I_D + (I_{H•D} - I_D)\frac{K_D[H]}{1 + K_D[H]} \quad (2)$$

$$0 = a[H]^3 + b[H]^2 + c[H] - d, \text{ where}$$
$$a = K_C K_D,\ b = K_C + K_D + K_C K_D([D]_0 + [C]_0 - [H]_0),$$
$$c = K_C([C]_0 - [H]_0) + K_D([D]_0 - [H]_0) + 1, \text{ and } d = -[H]_0 \quad (3)$$

The fitting was implemented in OriginPro 7.5 (OriginLab Corporation, Northampton, MA), by using a subroutine to solve

(99) Miskolczy, Z.; Biczok, L.; Megyesi, M.; Jablonkai, I. *J. Phys. Chem. B* **2009**, *113*, 1645–1651.
(100) Bhasikuttan, A. C.; Mohanty, J.; Nau, W. M.; Pal, H. *Angew. Chem., Int. Ed.* **2007**, *46*, 4120–4122.
(101) Liu, Y.; Han, B. H.; Chen, Y. T. *J. Phys. Chem. B* **2002**, *106*, 4678–4687.
(102) Wagner, B. D.; Stojanovic, N.; Day, A. I.; Blanch, R. J. *J. Phys. Chem. B* **2003**, *107*, 10741–10746.
(103) Nau, W. M.; Mohanty, J. *Int. J. Photoenergy* **2005**, *7*, 133–141.
(104) Baglole, K. N.; Boland, P. G.; Wagner, B. D. *J. Photochem. Photobiol. A: Chem.* **2005**, *173*, 230–237.
(105) Arunkumar, E.; Forbes, C. C.; Smith, B. D. *Eur. J. Org. Chem.* **2005**, *2005*, 4051–4059.
(106) Wang, R.; Yuan, L.; Macartney, D. H. *Chem. Commun.* **2005**, 5867–5869.
(107) Mohanty, J.; Bhasikuttan, A. C.; Nau, W. M.; Pal, H. *J. Phys. Chem. B* **2006**, *110*, 5132–5138.
(108) Liu, Y.; Li, C. J.; Guo, D. S.; Pan, Z. H.; Li, Z. *Supramol. Chem.* **2007**, *19*, 517–523.
(109) Wang, R.; Yuan, L.; Ihmels, H.; Macartney, D. H. *Chem.—Eur. J.* **2007**, *13*, 6468–6473.
(110) Megyesi, M.; Biczok, L.; Jablonkai, I. *J. Phys. Chem. C* **2008**, *112*, 3410–3416.
(111) Halterman, R. L.; Moore, J. L.; Mannel, L. M. *J. Org. Chem.* **2008**, *73*, 3266–3269.
(112) Montes-Navajas, P.; Corma, A.; Garcia, H. *ChemPhysChem* **2008**, *9*, 713–720.
(113) Neelakandan, P. P.; Hariharan, M.; Ramaiah, D. *J. Am. Chem. Soc.* **2006**, *128*, 11334–11335.
(114) Hudgins, R. R.; Huang, F.; Gramlich, G.; Nau, W. M. *J. Am. Chem. Soc.* **2002**, *124*, 556–564.
(115) Kim, J.; Jung, I.-S.; Kim, S.-Y.; Lee, E.; Kang, J.-K.; Sakamoto, S.; Yamaguchi, K.; Kim, K. *J. Am. Chem. Soc.* **2000**, *122*, 540–541.
(116) Day, A.; Arnold, A. P.; Blanch, R. J.; Snushall, B. *J. Org. Chem.* **2001**, *66*, 8094–8100.
(117) Harell, D.; Sokolovsky, M. *Eur. J. Biochem.* **1972**, *25*, 102–108.
(118) Nau, W. M.; Zhang, X. *J. Am. Chem. Soc.* **1999**, *121*, 8022–8032.
(119) Wang, Z.-X. *FEBS Lett.* **1995**, *360*, 111–114.

the cubic eq 3 with the Newton−Raphson method. The module is available from the authors upon request.

Acknowledgment. This work was supported by the Deutsche Forschungsgemeinschaft (DFG Grant NA-686/5-1 "Supramolecular Tandem Assays for Monitoring Enzymatic Activity") and by the Fonds der Chemischen Industrie.

Supporting Information Available: Host−dye titrations and spectrophotometric assays of diamine oxidase to study the effect of added macrocycle. This material is available free of charge via the Internet at http://pubs.acs.org.

JA904165C

Appendix 4.6 Publications

Hennig, A.; Ghale, G.; Nau, W. M. "Effects of cucurbit[7]uril on enzymatic activity." *Chem. Commun.* **2007**, 1614-1616. Reproduced by permission of the Royal Society of Chemistry. Publisher's version can be found at:
http://pubs.rsc.org/en/content/articlepdf/2007/cc/b618703j

Effects of cucurbit[7]uril on enzymatic activity†

Andreas Hennig, Garima Ghale and Werner M. Nau*

Received (in Cambridge, UK) 22nd December 2006, Accepted 1st February 2007
First published as an Advance Article on the web 22nd February 2007
DOI: 10.1039/b618703j

The macrocyclic host cucurbit[7]uril exhibits highly specific inhibitory effects on the activity of proteases, which can be analyzed by a host–substrate complexation model.

Interactions of biomolecules (*e.g.*, peptides and proteins) with macrocyclic receptors are of current interest for sensor[1] and therapeutic applications[2–4] as well as enzyme-assisted synthesis.[5,6] While calixarenes[1,2] and cyclodextrins[3–5] have been frequently used in this context, studies with cucurbiturils are scarce,[7–11] although interesting differences between these classes of macrocyclic receptors have frequently been found. Herein, we compare the activity of a set of peptide model substrates (Scheme 1) towards the proteases chymotrypsin (CT), trypsin, and leucine aminopeptidase (LAP) in the absence and presence of cucurbit[7]uril (CB7). We demonstrate that the supramolecular complexation affords a highly efficient inhibition of several substrates, which has a direct bearing on drug delivery systems and potential biological effects.

Substrate hydrolysis was monitored by fluorescence (**1–3**) or absorbance (**4–6**) (see ESI†). In the absence of CB7, all proteases cleaved the model substrates with the expected rates (*cf.* Fig. 1 and Table 1). Addition of CB7 had an inhibitory effect on the activity

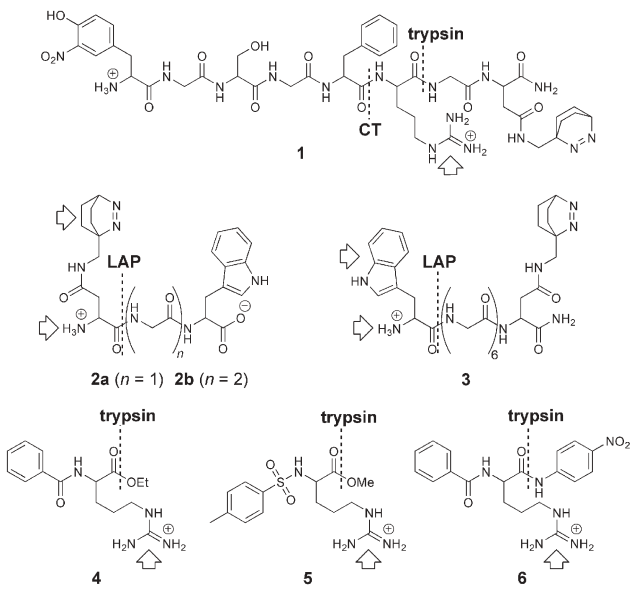

Scheme 1 Substrates for CT, trypsin, and LAP; dashed lines indicate cleavage sites, arrows indicate the presumed interaction sites with CB7.

School of Engineering and Science, Jacobs University Bremen, Campus Ring 1, D-28759, Bremen, Germany. E-mail: w.nau@iu-bremen.de; Fax: +494212003229; Tel: +494212003233

† Electronic supplementary information (ESI) available: Details on assay procedures and NMR. See DOI: 10.1039/b618703j

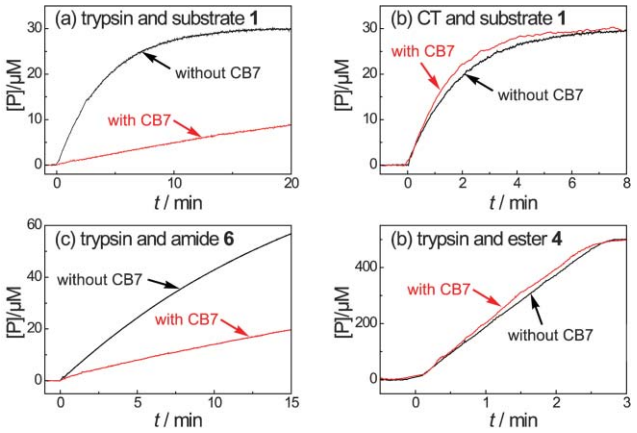

Fig. 1 Enzyme kinetic traces in the absence (black) and presence (red) of CB7 for the activity of (a) trypsin towards 30 μM peptide **1** (red: with 100 μM CB7), (b) CT towards 30 μM peptide **1** (red: with 1 mM CB7), (c) trypsin towards 500 μM amide **6** (red: with 1 mM CB7), and (d) trypsin towards 500 μM ester **4** (red: with 5 mM CB7).

of trypsin towards **1** and **6** and the activity of LAP towards **2–3**. In contrast, the activity of trypsin towards **4** and **5** as well as the activity of CT towards **1** was not significantly affected. The conservation of enzymatic activity for several protease/substrate combinations (*e.g.*, **4** and **5** with trypsin) and pronounced substrate-dependent variations (*e.g.*, **2** *vs.* **3** with LAP) revealed immediately that a complexation of the substrate and not an interaction with the enzyme was responsible for the inhibitory effect.

Naturally, CB7 will bind to several sites of the large and polyfunctional substrates with different affinity. For example, control experiments by ^{1}H NMR, UV-Vis absorption, and fluorescence spectroscopy confirmed that also those substrates, whose activity was not influenced, were complexed by CB7 under the employed conditions. In addition, the exchange kinetics of CB7 is fast on the timescale of the enzymatic digestion.[10] We therefore introduced an *apparent* binding constant K_a (eqn (1)), assuming a 1 : 1 host–guest binding model for simplicity, as a measure of the complexation-induced inhibition. Accordingly (eqn (2)), the initial hydrolysis rate k_0 under equilibrium conditions is given by a linear combination of the cleavage rates for the uncomplexed (k_S) and complexed ($k_{S\cdot CB7}$) substrate, weighted by their molar fractions (x_S and $x_{S\cdot CB7}$). A plot of the initial rate *vs.* CB7 concentration provided K_a and $k_{S\cdot CB7}$ (Table 1).[12]

$$[S\cdot CB7] = \left([CB7]_0 - [S]_0 - 1/K_a\right)/2 + \sqrt{\frac{1}{4}\left([CB7]_0 - [S]_0 - 1/K_a\right)^2 - [CB7]_0[S]_0} \quad (1)$$

Table 1 Effect of cucurbit[7]uril on the activity of proteases

Enzyme	Substrate	k_S[a]/μM min^{-1}	$k_{S\cdot CB7}$[b]/μM min^{-1}	K_a/10^3 M^{-1}
CT[c]	**1**	5.3	6.5[d]	<0.5
Trypsin[e]	**1**	6.0	<0.5	>50
LAP[f]	**2a**	1.8	<0.1	50 ± 20
	2b	5.3	<0.5	78 ± 35
	3	6.3	<0.9	2.8 ± 0.5
Trypsin[g]	**4**	210	240[h]	<0.5
	5	84	68[i]	<0.5
	6	5.5	<0.5	3.8 ± 0.6

[a] k_S was directly determined in the absence of CB7, error 10%. [b] $k_{S\cdot CB7}$ was fitted according to eqn (1) and (2) (10% error). [c] 10 μM **1**, 250 nM CT. [d] 1 mM CB7. [e] 30 μM **1**, 300 nM trypsin. [f] 10 μM **2–3**, 20 nM LAP for **2**, 150 nM LAP for **3**. [g] 500 μM **4**, 150 nM trypsin; 500 μM **5**, 30 nM trypsin; 100 μM **6**, 900 nM trypsin. [h] 5 mM CB7. [i] 3 mM CB7.

$$k_0 = x_S k_S + x_{S\cdot CB7} k_{S\cdot CB7} = k_S + (k_{S\cdot CB7}/[S]_0 - k_S/[S]_0)[S\cdot CB7] \quad (2)$$

Interestingly, in those cases where inhibition was observed, the fitted $k_{S\cdot CB7}$ values (the cleavage rates of the complexed substrates) became vanishingly small, such that only an upper limit is provided in Table 1. This suggests that complexation by CB7 leads to an efficient protection against enzymatic cleavage.

The inhibitory effect of CB7 on proteases needs to be considered in the context of its biological activity (*e.g.*, by suppression of proteolytic metabolic pathways) and for potential drug delivery applications.[8] For example, the inhibition by CB7 can be viewed as a stabilizing effect on the substrate against enzymatic degradation which could be of great interest for the delivery of peptide-based drugs.[3,4] Cyclodextrins, for example, are utilized as such drug stabilizing additives.[3,4] However, concentrations of up to 80 mM cyclodextrin, well above the presently used concentrations of CB7, are required to afford similarly stabilizing effects.[3b] In addition, the action of cyclodextrins is attributed to complexation of *hydrophobic* amino acid residues (Phe, Tyr, Trp) which serve as recognition sites for several hydrolytic enzymes. CB7, in its role as a cation receptor, is complementary because it has a high affinity for *positively charged* residues (Arg, Lys).

The latter conjecture was nicely confirmed by the contrasting effects of CB7 on substrate **1**, which contains well-known recognition sites for both, trypsin and CT. Trypsin recognizes the positively charged arginine, and its activity was efficiently suppressed at high CB7 concentrations (Fig. 1(a)), as would be expected from a complexation of the arginine residue. In contrast, cleavage of peptide **1** by CT, which specifically recognizes the hydrophobic phenyl residue of phenylalanine, was not inhibited (Fig. 1(b)), presumably because phenylalanine has only a very low affinity to CB7.[11]

In addition, cucurbiturils are known for their preferential complexation of positively charged *N*-terminal amino acids.[10,11] LAP cleaves off such *N*-terminal residues and we therefore trace the inhibition of substrates **2–3** back to a complexation of the *N*-terminal amino acid residues. Most likely, CB7 causes steric hindrance towards binding of the enzyme to the *N* terminus and "masks" (through ion–dipole interactions with the ureido carbonyl groups of the CB7 portal) the positively charged ammonium group, which are both critical for enzyme–substrate recognition.[13] The more than one order of magnitude difference between the K_a values for **2** and **3** (with exchanged terminal amino acids) supports this model. CB7 binds more strongly with the spherical 2,3-diazabicyclo[2.2.2]oct-2-ene residue (4×10^5 M^{-1})[7c] than with the Trp indole ring (2400 M^{-1} for Trp-OMe in Tris buffer at pH 7.8, this work), which results in an improved "protection" of the *N* terminus of substrates **2** towards cleavage by LAP compared to substrate **3**.

Surprisingly, the activity of trypsin towards the *esters* **4** and **5** was unaffected even with 3 mM CB7 (Fig. 1(b)), while hydrolysis of the *amides* **1** and **6** was inhibited as expected. Such a clear-cut differential reactivity of esters and amides has long been sought for when using proteases for organic synthesis, namely to increase the selectivity of their kinetically controlled hydrolysis reactions.[15] The observed selectivity of trypsin was the more surprising since NMR measurements (*cf.* ESI†) confirmed similar complexation patterns with CB7, *i.e.*, we observed strong upfield shifts of the aromatic protons, consistent with binding inside the cavity, and downfield shifts of the arginine side chain protons, suggesting portal binding.[14] The investigation of the underlying reasons for the contrasting inhibitory effects on ester and amide hydrolysis will consequently require the design of additional peptide model substrates in future studies.

In summary, cucurbiturils can inhibit the hydrolysis of substrates (and potentially drugs) towards LAP, trypsin, and other enzymes recognizing positively charged residues. This complements the use of cyclodextrins, which are used as stabilizers of drugs towards CT and other enzymes recognizing hydrophobic residues. Additionally, the observed effects of cucurbituril on protease activity are directly relevant for potential medicinal applications.

This work was performed within the graduate program "Nanomolecular Science". A. H. thanks Hoffmann-La Roche for a doctoral stipend.

Notes and references

1 R. Zadmard and T. Schrader, *J. Am. Chem. Soc.*, 2005, **127**, 904.
2 (*a*) Y. Hamuro, M. C. Calama, H. S. Park and A. D. Hamilton, *Angew. Chem., Int. Ed. Engl.*, 1997, **36**, 2680; (*b*) L. Memmi, A. Lazar, A. Brioude, V. Ball and A. W. Coleman, *Chem. Commun.*, 2001, 2474.
3 (*a*) W. J. Irwin, A. K. Dwivedi, P. A. Holbrook and M. J. Dey, *Pharm. Res.*, 1994, **11**, 1698; (*b*) K. Matsubara, Y. Ando, T. Irie and K. Uekama, *Pharm. Res.*, 1997, **14**, 1401; (*c*) J. B. Monteiro, L. D. Chiaradia, T. A. S. Brandão, J. Dal Magro and R. A. Yunes, *Int. J. Pharm.*, 2003, **267**, 93.
4 K. Uekama, F. Hirayama and T. Irie, *Chem. Rev.*, 1998, **98**, 2045.
5 (*a*) J. B. Harper, C. J. Easton and S. F. Lincoln, *Curr. Org. Chem.*, 2000, **4**, 429; (*b*) A. Koralewska, W. Augustyniak, A. Temeriusz and M. Kanska, *J. Inclusion Phenom. Macrocycl. Chem.*, 2004, **49**, 193.
6 J. Broos, R. Arends, G. B. van Dijk, W. Verboom, J. F. J. Engbersen and D. N. Reinhoudt, *J. Chem. Soc., Perkin Trans. 1*, 1996, 1415.
7 (*a*) J. Kim, I.-S. Jung, S.-Y. Kim, E. Lee, J.-K. Kang, S. Sakamoto, K. Yamaguchi and K. Kim, *J. Am. Chem. Soc.*, 2000, **122**, 540; (*b*) A. Day, A. P. Arnold, R. J. Blanch and B. Snushall, *J. Org. Chem.*, 2001, **66**, 8094; (*c*) C. Marquez, F. Huang and W. M. Nau, *IEEE Trans. Nanobiosci.*, 2004, **3**, 39.
8 (*a*) N. J. Wheate, A. I. Day, R. J. Blanch, A. P. Arnold, C. Cullinane and J. G. Collins, *Chem. Commun.*, 2004, 1424; (*b*) N. J. Wheate, D. P. Buck, A. I. Day and J. G. Collins, *Dalton Trans.*, 2006, 451.
9 H. Isobe, S. Sato, J. W. Lee, H.-J. Kim, K. Kim and E. Nakamura, *Chem. Commun.*, 2005, 1549.
10 M. E. Bush, N. D. Bouley and A. R. Urbach, *J. Am. Chem. Soc.*, 2005, **127**, 14511.

11 L. M. Heitmann, A. B. Taylor, P. J. Hart and A. R. Urbach, *J. Am. Chem. Soc.*, 2006, **128**, 12574.
12 M. McGarraghy and R. Darcy, *J. Inclusion Phenom. Macrocycl. Chem.*, 2000, **37**, 259.
13 W. T. Lowther and B. W. Matthews, *Chem. Rev.*, 2002, **102**, 4581.
14 W. L. Mock and N.-Y. Shih, *J. Org. Chem.*, 1986, **51**, 4440.
15 (*a*) S. Rival, J. Saulnier and J. Wallach, *Biocatal. Biotransform.*, 2000, **17**, 417; (*b*) F. Bordusa, *Chem. Rev.*, 2002, **102**, 4817.

– Curriculum Vitae –

Garima Ghale

Contact Address
Jacobs University Bremen
Res. III, Campus Ring 1
28759 Bremen, Germany
Email: g.ghale@jacobs-university.de

Personal Information
Date of Birth: 28/08/1986
Nationality: Nepalese
Phone: +49 151 4632 9286

Scientific Interest: Supramolecular Chemistry • Fluorescence • Host/Guest Complexes• Enzyme Assays• Proteases • Arginine-rich Peptides • Membrane Proteins • Biomembrane Transport.

EDUCATION

September 2010 – expected April 2014	Jacobs University, Bremen, Germany **PhD in Chemistry**, Supervisor: Prof. Werner M. Nau Thesis: Analyte-responsive macrocyclic host–fluorophore systems to monitor biological processes.
August 2008 – August 2010	Jacobs University, Bremen, Germany **MSc. Nanomolecular Sciences**, GPA: 1.36/5.0 Master's Thesis: Development of novel fluorescence-based proteases assays.
August 2005 – June 2008	Jacobs University, Bremen, Germany **BSc. Chemistry**, GPA: 1.63/5.0 Bachelor's thesis: Substrate-selective supramolecular tandem assay for diamine oxidase.

RESEARCH EXPERIENCES

September 2010 – to date	**Research Associate**, Jacobs University Bremen Designing and developing a novel label–free method for real-time monitoring of biomembrane transport processes using supramolecular receptors and fluorophores.

- Examined the translocation of arginine-rich peptides through bacterial channel — Prof. Mathias Winterhalter.
- Assay development for Bayer Corp.
- Derived and programmed fitting functions to determine binding constants from fluorescence titrations, available at http://www.jacobs-university.de/fitting

August 2008 – August 2010 **Graduate Student**, Jacobs University Bremen

- Use of macrocyclic host/guest to probe stepwise degradation of peptides by exopeptidases via sequential change in fluorescence.
- Mass spectrometry to monitor protease catalysed reactions — Prof. Nikolai Kuhnert.
- Development of label free fluorescent protease assay for determining substrate selectivity, screening of inhibitors, and protease–resistant peptides — Prof. Adam R. Urbach, Trinity University, USA.

February 2006 – June 2008 **Undergraduate Student Assistant**, Jacobs University Bremen

- Interaction of biomolecules with macrocyclic receptors.
- Designing substrate-selective and domino tandem assay to monitor enzymatic conversions in real-time using fluorescence.

February 2006 – June 2008 Summer Internship, University of Basel, Switzerland
Synthesis of organocatalyst mimicking the active site of polyketide synthase — Prof. Helma Wennemers.

TEACHING EXPERIENCES

August 2011 – To date **Research Supervisor**
Supervised and mentored students for their Master's and Bachelor's thesis.

August 2006 – June 2010 **Teaching Assistant for Physical and Organic Chemistry**

- Designed experimental protocols for Advanced Physical Chemistry Lab Course.
- Conducted lectures and tutorials for Advanced Physical Chemistry and Organic Chemistry.
- Assisted students with experimental setups, trained students in scientific techniques – organic synthesis, NMR, fluorescence spectroscopy, and retrieving scientific information.

August 2010 **Impact-The Student Competition in Social Entrepreneurship**
Assisted coaches from "Team Akademia" for helping student teams during team building, idea generation, project planning and development.

PUBLICATIONS

1. Ghale, G., Nau, W. M. Dynamically Analyte-Responsive Macrocyclic Host–Fluorophore Systems. *Acc. Chem. Res.* (2014) DOI: 10.1021/ar500116d.

2. Ghale, G., Lanctôt A.G., Kreissl, H.T., Jacob, M.H., Weingart, H., Winterhalter, M., & Nau, W.M., Chemosensing ensembles for monitoring biomembrane transport in real time. *Angew. Chem. Int. Ed.* **53**, 2762-2765 (2014).

3. Ghale, G., Kuhnert, N., Nau, W. M. Monitoring stepwise proteolytic degradation of peptides by supramolecular domino tandem assays and mass spectrometry for trypsin and leucine aminopeptidase, *Nat. Prod. Commun*. **7**, 343-348 (2012).

4. Ghale, G., Ramalingam, V., Urbach, A. R. & Nau, W. M. Determining protease substrate selectivity and inhibition by label-free supramolecular tandem enzyme assays. *J. Am. Chem. Soc.* **133**, 7528-7535 (2011).

5. Nau, W. M., Ghale, G., Hennig, A., Bakirci, H. & Bailey, D. M. Substrate-selective supramolecular tandem assays: Monitoring enzyme inhibition of arginase and diamine oxidase by fluorescent dye displacement from calixarene and cucurbituril macrocycles. *J. Am. Chem. Soc.* **131**, 11558-11570 (2009).

6. Hennig, A., Ghale, G., & Nau, W. M. Effects of cucurbit[7]uril on enzymatic activity. *Chem. Commun.*, 1614-1616 (2007).

Manuscripts in Preparation

7. Biedermann, F., Ghale, G., & Nau, W.M., A Supramolecular Fluorescence-based Method to Quantify Lipid-bilayer Membrane Permeability of Organic Compounds by Real-time Kinetics. *Manuscript in Preparation*.

PARTICIPATION IN SCIENTIFIC CONFERENCES

Oral Contributions

July 2011	"Enzyme Assays: The Domino and Tandem Game", **2nd International Conference on Cucurbiturils**, Cambridge, UK.
July 2011	"Supramolecular Tandem Membrane Assays to Monitor Porin Mediated Translocation of Cationic Peptides", **International WE-Heraeus Workshop "Nanofluidics in Biology"**, Bremen, Germany.
May 2011	"A Chemosensing Ensemble to Monitor Porin Mediated Permeation of Arginine-rich Peptides into Liposomes'', **Molecular Life Sciences Graduate Retreat**, Seefeld, Germany.
January 2011	"Supramolecular Tandem Assays for Cross–membrane Transport of Arginine–rich Peptides", **4th Meeting of the North German Biophysicists, Borstel, Germany.**
January 2011	"Molecular Spies for Monitoring Biological Transformations", **Nanofun Workshop**, Clausthal (Harz), Germany.

Poster Contributions

August 2013	**Transport Through Nanopores: From Understanding to Engineering**, Bremen, Germany. G. Ghale, A.G. Lanctôt, H. T. Kreissl, M. H. Jacob, H. Weingart, M. Winterhalter and W.M. Nau, "Having an Eye on Who's Passing the Biomembrane".
August 2012	**4th EuCheMS Chemistry Congress**, Prague, Czech Republic. G.Ghale, H. Weingart, M. Winterhalter and W. M. Nau, "Monitoring Channel Protein–mediated Translocation of Arginine–rich Peptides by a Supramolecular Sensing Ensemble".

September 2010	**22nd Lecture Conference of the GDCh-Division Photochemistry**, Erlangen, Germany. G.Ghale, W. M. Nau, "Development of Tandem Assays For Proteases".
August 2010	**3rd EuCheMS Chemistry Congress**, Nürnberg, Germany. G.Ghale and W. M. Nau, "Development of Novel Fluorescent Protease Assays".
June 2009	**4th joint International Symposium on Macrocyclic & Supramolecular Chemistry**, Maastricht, Netherlands. G.Ghale and W. M. Nau, "Substrate-selective Tandem Assay for Diamine Oxidase".

Additional Workshops and Seminars

November 2010	**1st Hamburger MicroCal Andwendertag**, Germany
October 2010	**International Workshop on Frontiers of Supramolecular Chemistry**, 2009, Tianjin, China.

AWARDS AND FELLOWSHIPS

- Best oral presentation at the NANOFUN workshop, Clausthal-Zellefield, Germany, 2011.
- Selected for the 59th Meeting of Nobel Laureates dedicated to Chemistry, Germany, 2009.
- Merit scholarship from Jacobs University for graduate studies in Nanomolecular Science, 2008.
- Merit Scholarship from Jacobs University for Bachelor's studies, 2005.

SKILLS

Software

Publishing: MS Office, Adobe illustrator, Photoshop, Endnote. *Scientific*: proFit and Origin (data analysis and programming), ChemDraw, SciFinder, Hyperchem.

Scientific

Proficient in: Quantitative analysis of biophysical parameters biomembrane transport and enzyme kinetics, UV– and fluorescence spectroscopy, ^{1}H and ^{13}C NMR, stopped-flow fluorescence spectroscopy, multiplate reader, liposome preparation and channel protein reconstitution. *Working knowledge in*: Circular Dichorism, mass spectrometry (ESI and MALDI), confocal microscopy and organic synthesis.